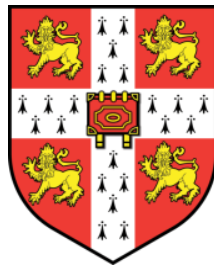


Modulation of neutrophil degranulation by hypoxia

Kim Hoenderdos

Submitted towards the degree of Doctor of Philosophy

UNIVERSITY OF CAMBRIDGE



Hughes Hall

Department of Medicine

2014

Declaration

This thesis is the result of my own work and includes nothing which is the outcome of work done in collaboration except where specifically indicated in the text. This thesis was composed on the basis of work carried out under the supervision of Professor Edwin Chilvers and Dr. Alison Condliffe in the Division of Respiratory Medicine, Department of Medicine, University of Cambridge.

This thesis (excluding figures, tables, appendices and bibliography) does not exceed the word limit imposed by the Clinical Medicine and Clinical Veterinary Medicine degree committee.

Kim Hoenderdos

September 2014, Cambridge

Acknowledgements

First and foremost I would like to thank my supervisors Alison Condliffe and Edwin Chilvers for giving a crazy Dutch girl a chance to come and study in Cambridge and for their support and enthusiasm throughout the course of my Ph.D. studies. Their doors were always open if I needed advice and I could not have asked for better supervisors!

Next I would like to thank my colleagues from the Morrell and Chilvers group and especially my “office mates” for their help along the way! Your enthusiasm, scientific discussions and banter made the lab a joy to work in! A special thanks to Linsey, Ross and Jatinder for all their help and to Jo for all our fun coffee breaks and chats.

During my Ph.D. I supervised 2 students; Charlotte and Cheng and I would like to thank both of them for all the hard work they put in. Even if it was a bit chaotic at times, I really enjoyed working with both of you and it sometime felt more like a very chatty “tea party” than work!

Away from the lab I spend most of my time in a dance studio and I made some amazing friends there and in Cambridge in general. Fil, Tanya, Zara, Michael, Sylvie, Lukasz, Melanie, Sanna and of course my dance partner Chris, thank you so much for your support (in the form of a willing ear, cards/presents or alcohol), and providing me with a place where I could forget about everything but dance, during the inevitable ups and downs of doing research.

I would like to express my gratitude to the British Lung Foundation for funding me and to all the blood donors that made this work possible.

Finally a very special thanks goes out to my family for their continuous love and support. You were always there for me and provided me with a place where I could recharge and relax. I could not have done this without any of you!

Table of Contents

Declaration.....	i
Acknowledgements	ii
Table of Contents	iii
List of Figures.....	viii
List of Tables	xi
List of Abbreviations	xii
Abstract.....	xv
1. Introduction.....	17
1.1 The immune system	17
1.2 Neutrophils	17
1.2.1 Neutrophil recruitment	19
1.2.2 Neutrophil intracellular bacterial killing	23
1.2.3 Neutrophil extracellular traps	25
1.2.4 Role of neutrophils in disease: a double-edged sword	27
1.3 Neutrophil granules: development and function	28
1.3.1 Secretory vesicles	32
1.3.2 Gelatinase granules.....	32
1.3.3 Specific granules.....	33
1.3.4 Azurophilic granules.....	34
1.4 Lung epithelial dysfunction and damage.....	37
1.4.1 Structure of the respiratory tract.....	37
1.5 The airway epithelium.....	38
1.5.1 Role of neutrophil proteases in airway epithelial injury and lung disease	39
1.6 Mechanisms of neutrophil degranulation.....	44
1.6.1 Receptors regulating degranulation	46
1.6.2 Phospholipid and kinase signalling in degranulation	47
1.6.3 Calcium signalling in degranulation.....	47
1.6.4 Src family kinases in degranulation	48
1.6.5 GTPase signalling in degranulation.....	50

1.6.6 SNAP/SNARE proteins in degranulation.....	52
1.7 Effects of cigarette smoke on neutrophils.....	53
1.8 Hypoxia.....	54
1.8.1 Physiological and pathological hypoxia.....	54
1.8.2 Cellular requirements for oxygen.....	57
1.8.3 Mechanism of oxygen sensing.....	58
1.8.4 Neutrophil function under hypoxic conditions.....	63
1.8.5 Neutrophil degranulation under hypoxic conditions.....	64
1.9 Summary.....	65
2. Hypothesis & Aims.....	66
2.1 Hypothesis.....	66
2.2 Specific aims.....	66
3. Materials and Methods.....	68
3.1 Materials.....	68
3.2 Neutrophil isolation.....	70
3.3 Working under hypoxic conditions.....	72
3.3.1 The hypoxic incubator.....	72
3.3.2 Analysis of media pH, pO ₂ and pCO ₂	74
3.4 Preparation of cigarette smoke medium.....	74
3.5 Neutrophil extracellular reactive oxygen species production.....	75
3.6 Measurement of intracellular reactive oxygen species (ROS) production.....	76
3.7 Apoptosis assays.....	76
3.8 Assessment of degranulation.....	78
3.8.1 Assessment of the effect of hypoxia on secreted NE activity.....	78
3.8.2 Quantification of NE.....	78
3.8.3 Optimisation of the NE activity assay.....	81
3.8.4 Investigation of the mechanism of hypoxia-induced augmented neutrophil degranulation.....	83
3.8.5 Quantification of myeloperoxidase.....	83
3.8.6 Quantification of lactoferrin release by ELISA.....	83
3.8.7 Quantification of MMP-9 (gelatinase) release by ELISA.....	85
3.8.8 Quantification of secreted MMP-9 activity by gelatin zymography.....	86
3.9 Western blot analysis of neutrophil granule protein content.....	86

3.9.1 Preparation of cell lysates and protein extraction.....	86
3.9.2 Bicinchonnic Acid (BCA) protein assay	87
3.9.3 SDS-polyacrylamide gel electrophoresis.....	87
3.9.4 Western blotting for MMP-9	88
3.10 Real-time PCR.....	90
3.11 Assessment of the effect of hypoxia on kinase signaling.....	90
3.12 Assessment of hypoxia induced morphological changes	92
3.12.1 Assessment of neutrophil morphology by electron microscopy	92
3.12.2 Assessment of neutrophil cytoskeletal remodeling by immuno-histochemistry	93
3.13 Human airway epithelial cell culture systems	95
3.13.1 A549 cells	95
3.13.2 Immortalised human bronchial epithelial (iHBE) cells.....	95
3.13.3 Normal human bronchial epithelial (NHBE) cells	96
3.14 Assessment of damage to epithelial cell layers	96
3.14.1 Poly-L-lysine coating of tissue culture plates	96
3.14.2 MTT assay	98
3.14.3 Immuno-histochemistry of cell layers	98
3.14.4 Preparation of NHBE cells for electron microscopy analysis	99
3.14.5 Assessment of cellular leakage by LDH assay	99
3.14.6 Analysis of ciliary function	101
3.15 Statistical Analysis	103
4. Hypoxia induces a more activated neutrophil phenotype.....	105
4.1 Introduction.....	105
4.2 Confirmation of the neutrophil hypoxic response	106
4.3 The effects of hypoxia on neutrophil degranulation	109
4.3.1 The effects of hypoxia on azurophil granule protein release.....	109
4.3.2 The effects of hypoxia on specific granule protein release	111
4.3.3 The effects of hypoxia on gelatinase granule release	111
4.4 The effects of cigarette smoke medium (CSM) on NE release.....	115
4.5 The effects of hypoxia on neutrophil morphology	118
4.5.1 TEM analysis of neutrophils morphology	118
4.5.2 Cytoskeletal changes under hypoxic conditions.....	120

4.6 Discussion	123
5. The effect of hypoxia on neutrophil-induced damage to lung epithelial cells	128
5.1 Introduction.....	128
5.2 The effect of hypoxia on neutrophil-induced damage to A549 cells.....	129
5.2.1 The effects of hypoxia on neutrophil induced toxicity to A549 cells	130
5.2.2 The effect of hypoxia on neutrophil-induced detachment of A549 cells	132
5.2.3 Nature of the damaging agent in hypoxic neutrophil supernatants	134
5.3 The effect of hypoxia on neutrophil induced damage to immortalized primary bronchial epithelial cells.....	136
5.4 The effect of hypoxia on neutrophil induced damage ALI-cultures.	139
5.4.1 The effect of hypoxia on neutrophil induced cell damage in ALI cultures.	141
5.4.2 The effect of hypoxia on neutrophil induced ciliary dysfunction	145
5.5 Discussion	148
6. The mechanism of augmented neutrophil degranulation under hypoxic conditions.....	154
6.1 Introduction.....	154
6.1.1 Hypoxia and hypoxia-mimetics delay neutrophil apoptosis.....	155
6.1.2 The effects of hypoxia-mimetics on neutrophil degranulation.....	157
6.1.3 The effects of hypoxia on de-novo granule protein production	159
6.1.4 The effects of re-oxygenation on the hypoxic up-regulation of neutrophil degranulation	163
6.2 The effects of hypoxia on degranulation signalling pathways	163
6.2.1 The effects of peptidylglycine-monooxygenase on neutrophil degranulation ..	165
6.2.2 The effects of hypoxia on kinase signalling	165
6.2.3 The effects of phospholipase C (PLC) inhibition on the hypoxic uplift of neutrophil degranulation.....	168
6.2.4 The effects of modulating intracellular Ca ²⁺ transients on the hypoxic uplift of neutrophil degranulation.....	169
6.2.5 The effects of PI3K inhibition on the hypoxic uplift of neutrophil degranulation	173
6.3 Discussion	177
7. Discussion	183

7.1 Overview	183
7.2 Experimental challenges.....	184
7.3 Discussion of results.....	185
7.4 Future research avenues	192
7.4.1 Elucidating the mechanism of augmented degranulation under hypoxia.....	193
7.4.2 The effects of hypoxia on neutrophil function in an epithelial cell system.....	194
7.4.3 Translational studies	194
7.5 Final summary and conclusions	195
8. Appendixes	199
8.1 : Elastase targets	199
8.2 : HIF targets	200
8.3 Hypoxic neutrophil supernatants induce A549 cell detachment and apoptosis.	201
8.4 Ciliary function	202
8.4.1 Ciliary beat frequency	202
8.4.2 Standard Operating Procedure for the determination of ciliary dyskinesia.....	203
8.5 HRE's in the promoter regions of neutrophil granule proteins	204
8.6 Primer sequences of primers used in section 5.1.3.1.....	209
8.7 Phospho-kinase array	210
8.8 Publications arising from this thesis	211
8.8.1 Papers	211
8.8.2 Abstracts	211
9. References.....	213

List of Figures

Chapter 1

Figure 1.1 The neutrophil structure and phagocytic capacity.....	18
Figure 1.2: Neutrophil recruitment and function	20
Figure 1.3: Leading edge formation in the neutrophil	22
Figure 1.4: Neutrophil oxygen-dependent bacterial killing.....	24
Figure 1.5: NETs.....	26
Figure 1.6: The lung epithelium in health and disease	40
Figure 1.7 Neutrophil signalling pathways involved in degranulation.....	45
Figure 1.8: Hypoxia is present in physiological and pathological circumstances.	55
Figure 1.9: Hypoxia inducible factor regulates most cell responses to hypoxia	60

Chapter 3

Figure 3.1: Neutrophil isolation using discontinuous plasma-Percoll® gradients	71
Figure 3.2: Working with the Invivo ₂ 400 workstation	73
Figure 3.3: Different stages of neutrophil apoptosis.....	77
Figure 3.4: Flow chart of typical neutrophil incubation, priming and stimulation protocol	79
Figure 3.5: Cytospins of resting and activated neutrophils incubated under normoxic and hypoxic conditions.....	80
Figure 3.6: Optimising the neutrophil elastase activity assay	82
Figure 3.7: Scoring system of neutrophil images made by transmission electron microscopy (TEM).....	94
Figure 3.8: NHBE cell culture	97
Figure 3.9: Immunocytochemistry of A549, iHBEC and NHBE epithelial cells.....	100
Figure 3.10: Analysis of ciliary function	102

Chapter 4

Figure 4.1: Hypoxia alters neutrophil function.....	108
Figure 4.2: Hypoxia augments the exocytosis of azurophil granules	110
Figure 4.3: Hypoxia up-regulates the exocytosis of specific granules	112
Figure 4.4: Hypoxia up-regulates the exocytosis of gelatinase granules.....	114
Figure 4.5: CSM induces ROS generation but does not affect NE release	116
Figure 4.6: High concentrations of CSM are toxic to neutrophils.....	117
Figure 4.7: Effect of hypoxia on neutrophil morphology: TEM images	119

Figure 4.8: Effect of hypoxia neutrophil morphology: TEM quantification	121
Figure 4.9: Activation and hypoxia induce actin cytoskeletal remodelling.....	122
Chapter 5	
Figure 5.1: Hypoxic neutrophil supernatants compromise A549 cells survival.....	131
Figure 5.2: Hypoxic neutrophil supernatants induce A549 cell detachment and apoptosis	133
Figure 5.3: Porcine pancreatic elastase recapitulates the damage caused by neutrophil supernatants	135
Figure 5.4: A549 cell damage caused by neutrophil supernatants is protein-dependent.	137
Figure 5.5: A549 cell damage caused by neutrophil supernatants is protease-dependent	138
Figure 5.6: Hypoxic neutrophil supernatants damage iHBE cells layers	140
Figure 5.7: Scanning electron microscopy of primary HBECs grown in ALI culture	142
Figure 5.8: Hypoxic neutrophil supernatants induce apoptosis in ALI cultures.....	144
Figure 5.9: Hypoxic neutrophil supernatants induce LDH release from ALI cultures....	146
Figure 5.10: Neutrophil supernatants do not affect ciliary beat frequency.....	147
Figure 5.11: Neutrophil supernatants induce ciliary dysfunction in ALI cultures	149
Chapter 6	
Figure 6.1: Hypoxia and HIF stabilizers delay neutrophil apoptosis	156
Figure 6.2: HIF-1 α stabilizers do not recapitulate the hypoxic upregulation of NE release	158
Figure 6.3: Hypoxia does not increase transcription or translation of granule proteins ..	160
Figure 6.4: Granule MMP-9 protein content decreases under hypoxic conditions	162
Figure 6.5: Re-oxygenation does not affect the augmented degranulation response seen under hypoxia	164
Figure 6.6: PAM does not influence neutrophil degranulation.....	166
Figure 6.7: Phospho-kinase array performed under normoxia and hypoxia.....	167
Figure 6.8: Role of phospholipase C activation in the hypoxic augmentation of degranulation	170
Figure 6.9: Role of calcium influx in the hypoxic augmentation of neutrophil degranulation	172
Figure 6.10: Role of calcium release from intracellular stores in the hypoxic augmentation of neutrophil degranulation.....	174
Figure 6.11: Role of PI3K signalling in the hypoxic augmentation of NE release	176

Chapter 7

Figure 7.1: Supernatants from normoxic and hypoxic neutrophils contain cytoplasmic proteins.....	187
Figure 7.2: BMP-9 is cleaved following exposure to hypoxic neutrophil supernatants..	188
Figure 7.3: Neutrophil function in healthy and chronic obstructive pulmonary disease (COPD) airways.....	196
Figure 7.4: Neutrophil signalling pathways involved in the augmented degranulation under hypoxic conditions.....	198

List of Tables

Table 1.1: Contents of neutrophil granules.....	29
Table 1.2: Neutrophil granules develop at different stages during neutrophil maturation	31
Table 3.1: Compounds used in neutrophil elastase activity assay.....	84
Table 3.2: Composition of SDS gels	89
Table 3.3: Kinase array targets and phosphorylation sites	91

List of Abbreviations

α 1-AT	alpha-1-antitrypsin
ALI	Acute Lung Injury
ATP	Adenosine triphosphate
ARDS	Acute Respiratory Distress Syndrome
BC	Band cell
BLC	B-lymphocyte chemoattractant
BSA	Bovine serum albumin
BMP-9	bone morphogenetic protein
Ca ²⁺	Calcium ion
CaCl ₂	Calcium chloride
CM-H2-DCFDA	5-(and-6)-chloromethyl-2',7'- dichlorodihydrofluorescein diacetate, acetyl ester
CoCl ₂	Cobalt chloride
COPD	Chronic obstructive pulmonary disorder
CSE	Cigarette smoke extract
CSM	Cigarette smoke medium
DFO	Deferrioxamine mesylate
DMOG	Dimethyloxalyglycine
DMSO	Dimethyl sulfoxide
DPX	Distyrene, a plasticizer, and xylene
EDTA	Ethylenediamine tetraacetic acid
ELISA	Enzyme-linked immunosorbent assay
EMC	Extracellular matrix
ER	Endoplasmic reticulum
FIH	Factor inhibiting HIF
FITC	Fluorescein isothiocyanate
fMLP	N-formly-methionyl-leucyl-phenylalanine
G-CSF	Granulocyte colony stimulating factor
GM-CSF	Ganulocyte-macrophage colony-stimulating factor
GPCR	G-protein coupled receptors
GTP	Guanine triphosphate
H ₂ O ₂	Hydrogen peroxide
HBSS	Hanks balanced salt solution

HIF	Hypoxia-inducible factor
HRE	Hypoxia response elements
HRP	Horseradish peroxidase
ICAM-1	Intracellular adhesion molecule-1
IFN- γ	Interferon- γ
IL	Interleukin
IMDM	Iscove's modified dulbecco's medium
InsP3	Inositol 1,4,5-triphosphate
kDa	Kilodalton
kPa	Kilopascal
LPS	Lipopolysaccharide
LTB4	Leukotriene B4
MAPK	Mitogen-activated protein kinases
MB	Myeloblast
MC	Myelocyte
MCP-1	Monocyte chemotactic protein-1
Mg ²⁺	Magnesium ion
MMC	Metamyelocyte
MMP	Matrix metalloproteinases
MPO	Myeloperoxidase
NADP	Nicotinamide adenine dinucleotide phosphate
NE	Neutrophil elastase
NET	Neutrophil extracellular trap
NF- κ B	Nuclear factor- κ B
O ₂ ⁻	Superoxide anion
PAF	Platelet-activating factor
PAGE	Polyacrylamide gel electrophoresis
PBS +	Phosphate-buffered saline with calcium chloride and magnesium chloride
PBS- and	Phosphate-buffered saline without calcium chloride magnesium chloride.
PHD	proly hydroxylase domain protein
PI3K	Phosphoinositide 3-kinase
PIP	Phosphatidylinositol 4,5-bisphosphate

PKC	Protein kinase C
PLC	Phospholipase C
PLD	Phospholipase D
PMC	Promyelocyte
PMA	Phorbol myristate acetate
PMN	Polymorphonuclear leukocyte
PPP	Platelet-poor plasma
PRP	Platelet-rich plasma
ROS	Reactive oxygen species
SDS	Sodium dodecyl sulphate
Segm	Segmented cell
SNARE	SNAP receptor
SOD	Superoxide dismutase
TGF	Transforming growth factor
TNF α	Tumour necrosis factor- α
VAMP	Vesicle-associated membrane protein.
VHL	Von Hippel-Lindau factor
vW-factor	Von Willebrand factor
WP-bodies	Weibel-Palade bodies

Abstract

Modulation of neutrophil degranulation by hypoxia

Kim Hoenderdos

Neutrophils are key effector cells of the innate immune system. They employ a number of powerful ‘weapons’ to eliminate pathogens, including an array of destructive proteins packaged into distinctive granule subsets. In addition to their microbicidal activity, these granule proteins are capable of causing substantial tissue damage if inappropriately deployed. To mitigate against this possibility, most physiological stimuli induce minimal extracellular degranulation. Sites of inflammation and infection are usually hypoxic, and it has been shown that oxygen depletion compromises neutrophil function by impairing the generation of reactive oxygen species and hence bacterial killing.

The key finding reported in this thesis is that hypoxia substantially increases the release of all neutrophil granule subsets, as measured by the release of (active) hallmark proteins (elastase, myeloperoxidase, lactoferrin and matrix metalloproteinase-9). In consequence, supernatants from hypoxic neutrophils induced substantially more damage to lung epithelial cell layers than supernatants from neutrophils cultured under normoxic conditions; this damage was protein- and protease-dependent. This pattern of damage was seen consistently across lung adenocarcinoma-derived epithelial cells, primary immortalised lung epithelial cells, and primary human bronchial epithelial cells grown in physiological air-liquid interface culture. Surprisingly, the mechanism of hypoxia-augmented degranulation was found to be independent of protein synthesis and specifically, of the transcription factor HIF-1 α (the ‘master-regulator’ of hypoxic responses); thus, hypoxia did not affect mRNA transcript or protein abundance of the major granule components, and hypoxia mimetics failed to recapitulate the phenotype. Inhibition of the key pathways known to be involved in neutrophil degranulation, including, phosphatidylinositol 3-kinase and phospholipase C, but not calcium flux prevented augmented granule release under hypoxia

In conclusion, hypoxia induces a destructive neutrophil phenotype, with increased release of multiple histotoxic proteases. This may contribute to tissue injury and disease pathogenesis in a range of clinically important conditions.

Chapter 1

Introduction

1. Introduction

1.1 The immune system

The immune system protects the body from invading pathogens and consists of a range of physical barriers and cellular components. These barriers are provided by the skin, the low pH of the stomach, the mucous membranes of the gut and the muco-ciliary escalator in the lungs. Besides comprising a physical barrier, the skin and epithelial surfaces of the gut and lungs also secrete a range of anti-microbial peptides. The second component of the immune system is comprised of two constituent parts, namely the innate and the adaptive immune systems. To function effectively these systems need to distinguish between harmful pathogens ('non-self') and the body's own tissues and proteins ('self'). The innate immune system provides an immediate, but non-specific response through the recognition of non-self proteins called pathogen-associated molecular patterns (PAMPS), which leads to the activation of range of immune cells through Toll-like receptors (TLRs). Immune cells that play an important role in the innate immune system include phagocytic cells like macrophages and neutrophils, which ingest and kill invading pathogens, and natural killer (NK) cells, whose main role is to identify and destroy infected host cells. Dendritic cells reside in the physical barriers exposed to the external environment such as skin, gut and lung epithelial surfaces; they are the interface between the innate and adaptive immunity, and process foreign antigen to present to adaptive B and T lymphocytes. The adaptive immune system is capable of mounting a very specific response through this precise and tailored recognition of pathogens, leading to antibody production and cytotoxic T cell responses. This is a slower process than the innate response, but the specific generation of immunological memory results in a faster response when the same pathogen is subsequently encountered¹.

1.2 Neutrophils

Neutrophils (Figure 1.1) play a key role in the innate immune response as "first responders" in instances of pathogen invasion or damage. They are the most abundant white blood cell present in the circulation (54-62% of the leukocyte differential count²) and have two important roles in the defence against microbial invasion; immune surveillance and the elimination of micro-organisms. This is reflected in their development, abilities and lifespan.

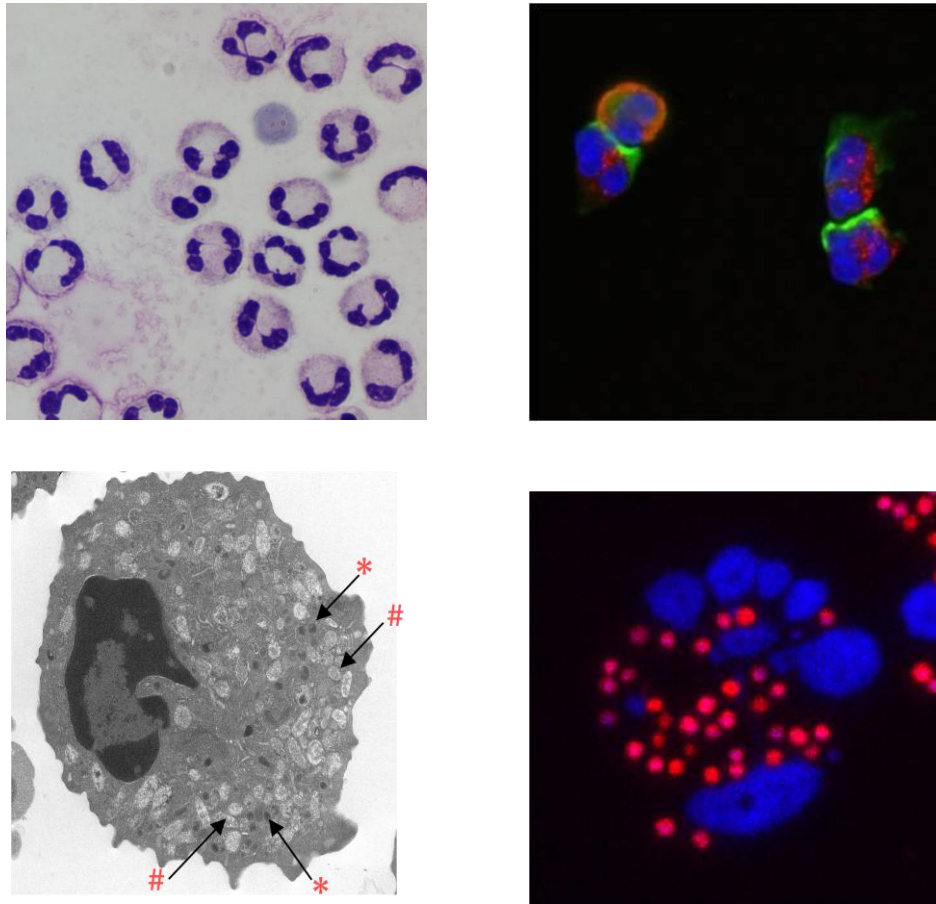


Figure 1.1 The neutrophil structure and phagocytic capacity

A. Cytospin of isolated human neutrophils stained with May/Grünwald/Giemsa (x40 magnification). B. Confocal immunofluorescence image (x63) of neutrophils stained for the nucleus (blue, DAPI) the azurophilic granules (red: goat IgG antibody and Alexa Fluor 488 – donkey anti-goat IgG) and actin (green: rhodamine-phalloidin). C. Electron microscope image of a neutrophil, highlighting the many intracellular granules; * indicate electron dense (Myeloperoxidase (MPO) positive) granule # indicate the electron light (MPO negative) granules (x3500). D. Confocal immunofluorescence image of a neutrophil that has phagocytosed Ph-Rhodo-labelled *S. Aureus* (red), (nucleus blue, DAPI) x63 with 6x zoom (images taken from my own experiments).

Neutrophils are one of the three types of granulocytes (with eosinophils and basophils) that develop in the bone marrow, with $1-2 \times 10^{11}$ cells generated per day³. Under normal conditions only a small percentage of the total neutrophils resident in the bone marrow are released into the circulation, where they have a very short half-life and are rapidly cleared by macrophages in the reticulo-endothelial system^{4,5}. During inflammation, the production of neutrophils increases and both mature and immature neutrophils are released into the circulation to boost the available circulating pool. Their role in immune surveillance requires neutrophils to move quickly; they are the most motile cells in the body⁶ and purposeful or directional motion (chemotaxis) enables them to home in on their prey. To enable these responses they express a large range of cell surface receptors involved in the reaction to microbial invasion; these include receptors for the recognition of microbial structures, those allowing the detection of soluble chemoattractants, those responsible for recognising an inflammatory environment and those involved in activation of the adaptive immune system⁷.

To avoid non-specific activation, circulating neutrophils are relatively quiescent cells. However, neutrophils can be converted to a substantially more aggressive phenotype by a process called priming, as shown by Forehand et al.⁸. Neutrophil priming has been studied extensively and it has been shown that a range of inflammatory mediators, including TNF- α ⁹, GM-CSF¹⁰, platelet activating factor (PAF)¹¹ and lipopolysaccharide (LPS)¹² can induce this state of pre-activation. Besides having a direct effect on cell polarisation, deformability¹³ and integrin/selectin expression¹⁴, priming enables an increased activation-mediated oxidative burst (up to 20 fold¹²), degranulation response¹⁵ and lipid mediator (e.g. leukotriene B4 and arachidonic acid) release^{16,17}. Priming is a relatively quick process, which occurs within seconds to minutes, depending on the ligand¹⁴. It has been suggested that neutrophil priming occurs in the circulation as a first step in neutrophil recruitment and precedes extravasation and activation at the site of infection¹⁸.

1.2.1 Neutrophil recruitment

Neutrophils are recruited rapidly to sites of infection or inflammation, through a number of steps (Figure 1.2), guided by signals generated by microbes and host cells such as tissue macrophages. Neutrophils are present in the circulation in two pools; a freshly circulating vascular pool and a marginating pool that consists of granulocytes

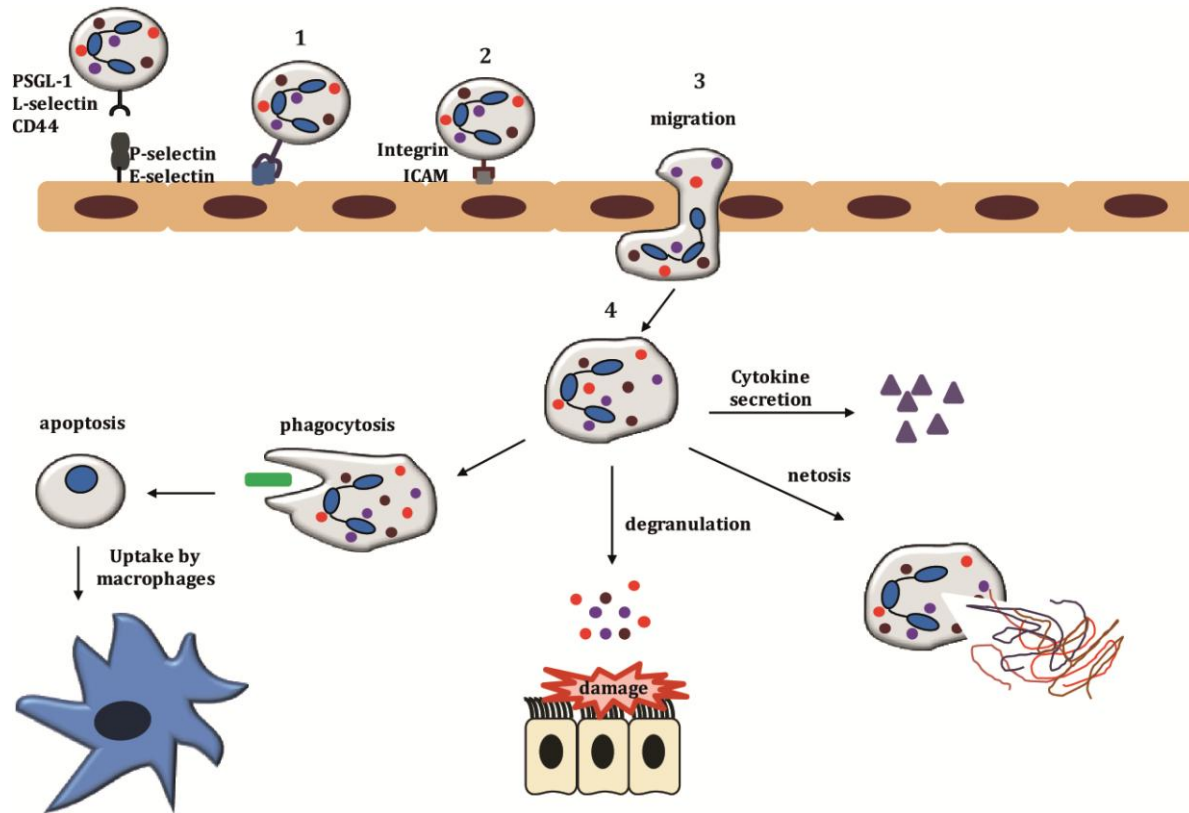


Figure 1.2: Neutrophil recruitment and function

Upon pathogen recognition, neutrophils are recruited rapidly to sites of infection, guided by signals generated by the microbes and resident tissue macrophages. Circulating, un-activated neutrophils “roll” along the endothelial cells surface (1), patrolling for signs of damage/infection. The rolling, transient contact with the endothelial cells involves P-selectin and E-selectin interactions with L-selectin and P-selectin ligand-1 (PSGL-1) on the surface of neutrophils. After “capture” of the neutrophil the next step is firm adhesion (2); β 2-integrins interact with intracellular adhesion molecule (ICAM)-1 and ICAM-2. The final step in neutrophil recruitment is migration towards the site of inflammation following a chemo-attractant gradient. Neutrophils cross the endothelial cell layer (3) and then migrate through the basal membrane. Neutrophil granule proteases play an important role in the latter process as they are capable of breaking down components of the basal membrane such as collagen and laminins. When the neutrophils reach the site of infection (4) they phagocytose pathogens, degranulate and undergo apoptosis or netosis. Apoptotic neutrophils are taken up by macrophages. (Adapted from Borregaard et al.¹⁹)

transiently arrested in sinusoids of the liver and spleen²⁰. Circulating, non-activated neutrophils “roll” along the endothelial cell surface, patrolling for signs of damage/infection. The transient, rolling contact with endothelial cells involves the interaction of P- and E-selectins with L-selectin (CD62L) and P-selectin ligand-1 (PSGL-1) on the surface of neutrophils^{21,22}. Upon contact with inflammatory stimuli, many cell surface receptors involved in neutrophil recruitment are up-regulated; P-selectin expression increases within minutes after stimulation with thrombin or reactive oxygen species (ROS)²³ and E-selectin expression increases after 1 to 2 hours of stimulation with IL-1, TNF- α or LPS. If the interactions between the selectins and their ligands are sufficient, the rolling neutrophil becomes ‘captured’.

After capture of the neutrophil, the next step is firm adhesion. In this step β_2 -integrins play an important role, particularly CD11a/CD18 (LFA-1) and CD11b/CD18 (Mac-1)²¹. CD11a/CD18 interacts with intracellular adhesion molecules ICAM-1 and ICAM-2, while CD11b/CD18 interacts with a larger range of receptors including ICAM-1, ICAM-2, fibrinogen and complement fragment iC3b. Further activation is mediated through neutrophil chemokine receptors²⁴, which bind ligands secreted or presented by endothelial cells^{25,26}, such as IL-8, and platelet activating factor (PAF). Upon activation by these chemo-attractants or contact with activated epithelium, neutrophils switch from a rounded to a polarised morphology, forming cells with a clear leading edge and a distinct rear (uropod). The establishment of a leading edge is controlled by G-protein coupled receptors through a complex signalling cascade; phosphoinositide 3-kinase (PI3K) generates the second messenger phosphatidylinositol (3,4,5)-trisphosphate (PIP₃) from phosphatidylinositol (4,5)-bisphosphate (PIP₂); PIP₃ accumulates at the leading edge and induces the activation of Rho GTPases and the polarisation of F-actin^{27,28}.

The constant generation of an F-actin mesh pushes the neutrophil forwards, while the uropod detaches following degradation of PIP₃ (by the phosphatases PTEN and SHIP), and the engagement of RhoA/Rock dependent signalling, leading to actin-myosin contraction (Figure 1.3). The final step in neutrophil recruitment is migration towards the focus of inflammation following a chemo-attractant gradient. Neutrophils can cross the endothelial cell layer by passing directly through an individual endothelial cell or by paracellular migration, squeezing between cells. Migration is mediated by the integrins CD11a/CD18 and CD11b/CD18 on the neutrophil cell surface, and their ligands ICAM-1 and ICAM-2 on the endothelium (reviewed by *Pick et al.*²⁹).

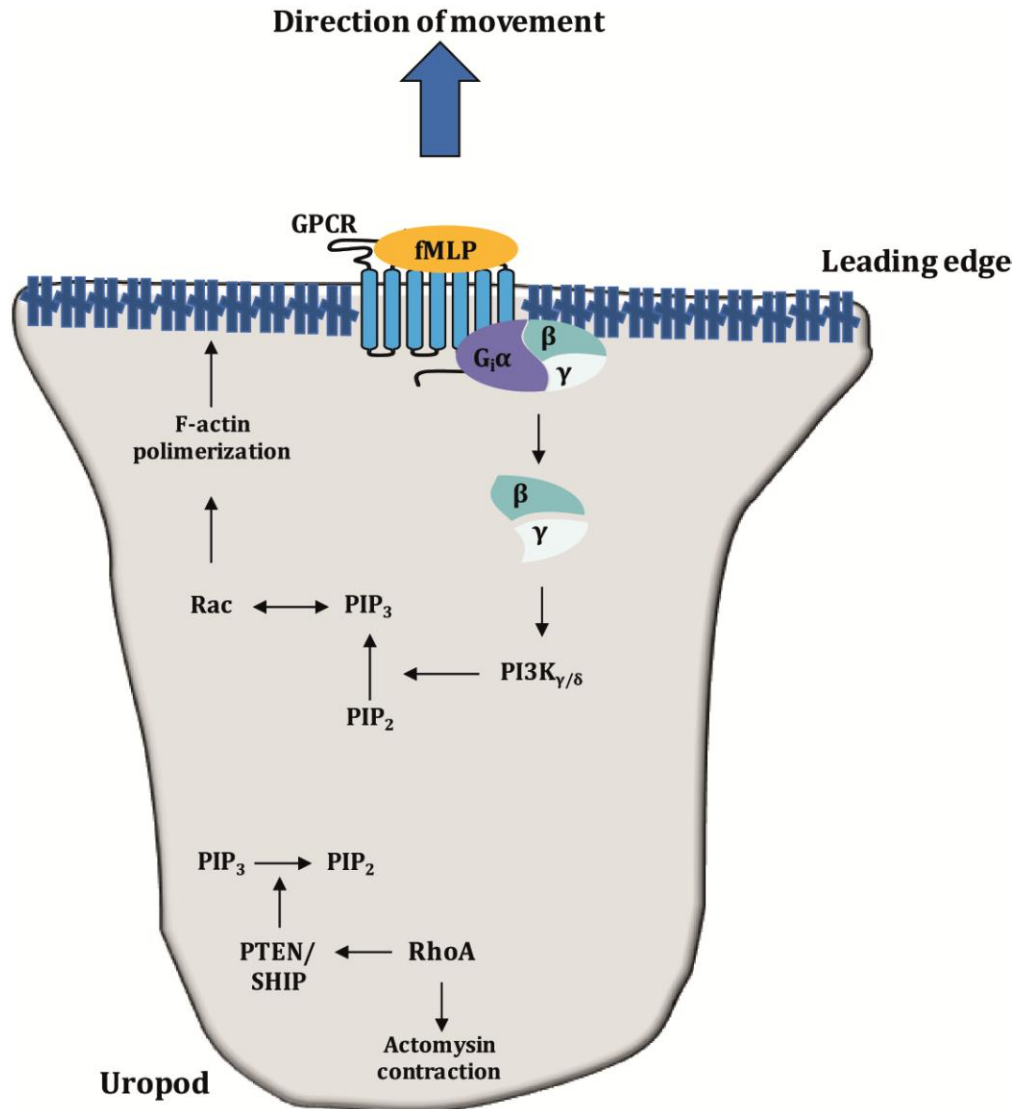


Figure 1.3: Leading edge formation in the neutrophil

Upon activation by chemoattractants or by contact with activated epithelium, neutrophils change from a rounded morphology to a polarised “activated” state. Activated neutrophils undergo shape change to generate more elongated cells with a clear leading edge and a distinct rear end (uropod). Activation of the cognate GPCR by fMLP leads to the dissociation of the G protein into α - and $\beta\gamma$ -subunits, which activate $PI3K_{\gamma}$. $PI3K_{\gamma}$ generates the second messenger phosphatidylinositol (3,4,5)-trisphosphate (PIP_3) from phosphatidylinositol (4,5)-biphosphate (PIP_2), and PIP_3 accumulates at the leading edge to induce the local activation of Rho GTPases (particularly Rac) and polarisation of F-actin^{27,28}. The constant generation of an F-actin mesh pushes the neutrophil forward, while the uropod detaches due to PTEN/SHIP degradation of the second messengers PIP_3 and RhoA/Rock dependent signalling leading to actomyosin contraction, again pushing the neutrophil forward.

Once they have crossed the endothelium, neutrophils must migrate through the basal membrane. Neutrophil granule proteins play an important role in this process as they contain proteases capable of breaking down components of the basal membrane such as collagen and laminins³⁰. Both MMP-9 and neutrophil elastase (NE) have been shown to play a role in migration through basement membranes and ECM breakdown; *in vitro* work has shown that MMP-9 is needed for migration through Matrigel and amnion membranes³¹ and Llewellyn-Jones et al.³² showed that connective tissue degradation can be reduced by the serine protease inhibitor α_1 AT, suggesting a possible role for NE. Despite the presence of abundant protease inhibitors in the extra-cellular space, NE is still capable of degrading ECM for two main reasons. Firstly, secreted NE has been shown to bind to the neutrophil plasma membrane locally via a charge-dependent mechanism³³, making it inaccessible to the tissue inhibitors. Secondly, the formation of shielded pericellular micro-environments, in which NE molecules greatly outnumber the opposing protease inhibitors, can protect NE and allow substantial but localised tissue breakdown ('quantum proteolysis'^{34,35})

1.2.2 Neutrophil intracellular bacterial killing

Once at the site of infection, neutrophils fulfill their second role, namely the elimination of micro-organisms (Figure 1.4). Neutrophils have a large arsenal of "weapons" they can employ against pathogens. They are extremely effective phagocytes, being able to ingest an opsonized particle within 20 seconds³⁶. After pathogen engulfment, the phagosome matures through fusion with a range of vesicles present in the cytosol, acquiring machinery to kill the ingested pathogen. Inside the phagosome, the environment is rendered hostile to the pathogen by the secretion of bactericidal proteins and proteases and by a series of redox reactions including the production of reactive oxygen species (ROS) by the NADPH oxidase complex. Upon neutrophil activation, the cytosolic components of the NADPH complex (p40^{phox}, p47^{phox}, p67^{phox} and p21^{rac}) translocate to the plasma or phagosome membrane and interact with the membrane-associated cytochrome b₅₅₈. The assembled NADPH oxidase complex then catalyses a sequence of reactions, culminating in the formation of hydrogen peroxide (H₂O₂). Catalysed by myeloperoxidase (MPO) from the azurophilic granules, and in the presence of halide ions, H₂O₂ is then converted into hypohalous acids. These and other products of the oxidative burst are effective anti-microbial agents but can also cause tissue damage; they

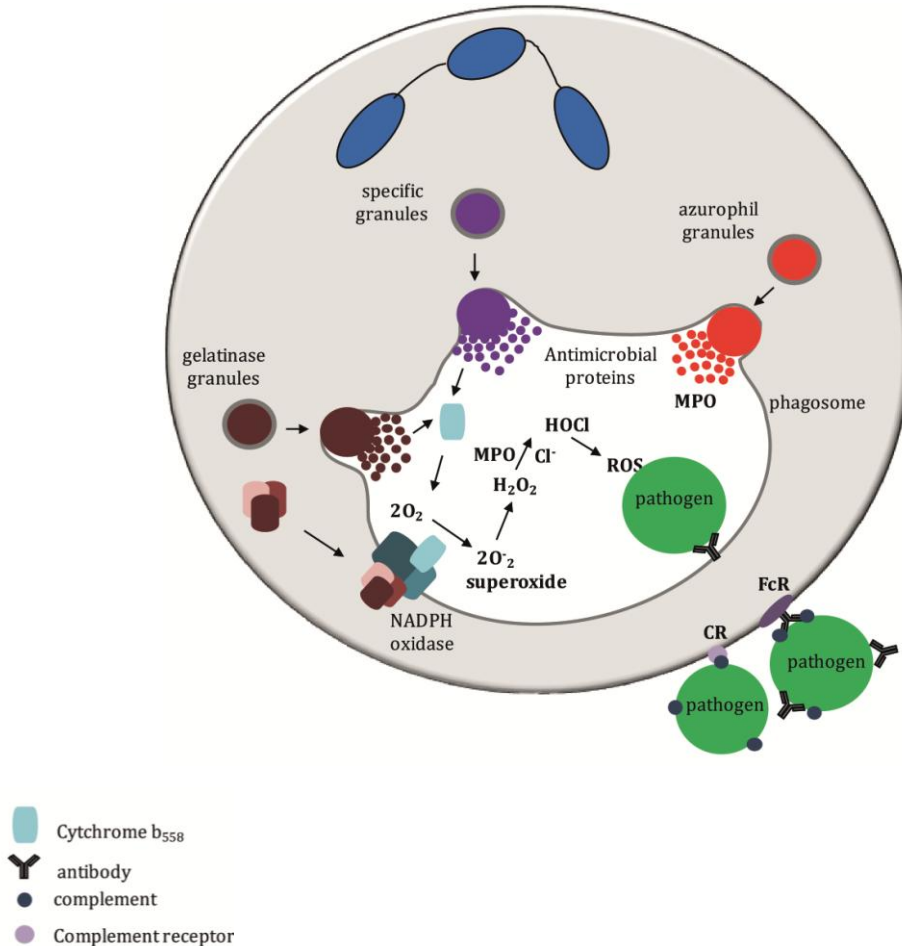


Figure 1.4: Neutrophil oxygen-dependent bacterial killing

After Fc receptor or complement receptor-assisted phagocytosis of pathogens, the phagosome matures through fusion with a range of vesicles present in the cytosol, acquiring the machinery to kill the ingested pathogen. Upon phagocytosis, the cytosolic components of the NADPH complex (p40^{phox}, p47^{phox}, p67^{phox} and p21^{rac}) translocate to the phagosomal membrane and assemble with cytochrome b₅₅₈. The resulting activated NADPH oxidase complex catalyzes a sequence of reactions through which hydrogen peroxide is formed. Hydrogen peroxide, catalysed by myeloperoxidase (MPO) from the azurophilic granules and in the presence of halide ions, is then converted into hypochlorous acids, which are highly effective anti-microbial agents. The neutrophil granules also play a role in ROS-independent bacterial killing as they contain a range of bactericidal proteins.

activate pro-collagenases, pro-gelatinases³⁷ and induce the production of cholesterol chlorohydrins^{38,39}. The importance of the respiratory burst is epitomised by patients with chronic granulomatous disease (CGD). Neutrophils from these patients migrate and phagocytose normally but fail to mount a respiratory burst due to a defect in one of the components of the NADPH oxidase. This impairs intracellular bacterial and fungal killing, especially of *Staphylococcus spp* and *Aspergillus spp*, leading to recurrent infections and early death⁴⁰.

In addition to the NADPH oxidase, the neutrophil possess several granule populations which contain a range of bactericidal proteins (Table 1.1) that play a key role in bacterial killing, as discussed in detail in section 1.3. Segal et al.³⁶ postulate that instead of MPO and ROS production being the primary killing systems they have been thought to be, they help create conditions in the phagosome conducive to microbial killing and digestion by enzymes released into the phagosome from the cytoplasmic granules.

1.2.3 Neutrophil extracellular traps

An additional, recently discovered mechanism of bacterial killing is the formation of neutrophil extracellular traps (NETs, Figure 1.5^{41,42}). NETs consist of de-condensed strands of DNA coated with proteins from the nucleus, cytosol and granules. Urban et al.⁴³ identified 24 different proteins present on NETs including histones, defensins, elastase, lactoferrin and cathepsin G. NET formation is characterised by the loss of intracellular membranes before the integrity of the plasma membrane is compromised and ruptures, ejecting chromatin and attached proteins into the extracellular space as NETs. The main functions of NETs are to trap microbes, prevent dissemination of infection, and inactivate virulence factors. NETs capture microbes via a charge reaction, although some pathogens have evolved either a capsule structure or an alteration of surface charge that prevents binding to NETs⁴⁴. Proteases presented by NETs such as elastase and cathepsin G can inactivate bacterial virulence factors⁴¹. NETs also contain anti-microbial proteins including defensins and lactoferrin, which can kill or inhibit bacteria. The importance of NETs is illustrated by Li et al.⁴⁵, who showed that mice deficient in NET formation were more susceptible to necrotising fasciitis induced by group A *streptococci* than wild type (WT) mice. However, like many components of the immune system, aberrant activation can cause damage. For example, NETs have been implicated in auto-immunity; Systemic Lupus Erythematosus (SLE) patients make antibodies against histones and neutrophil

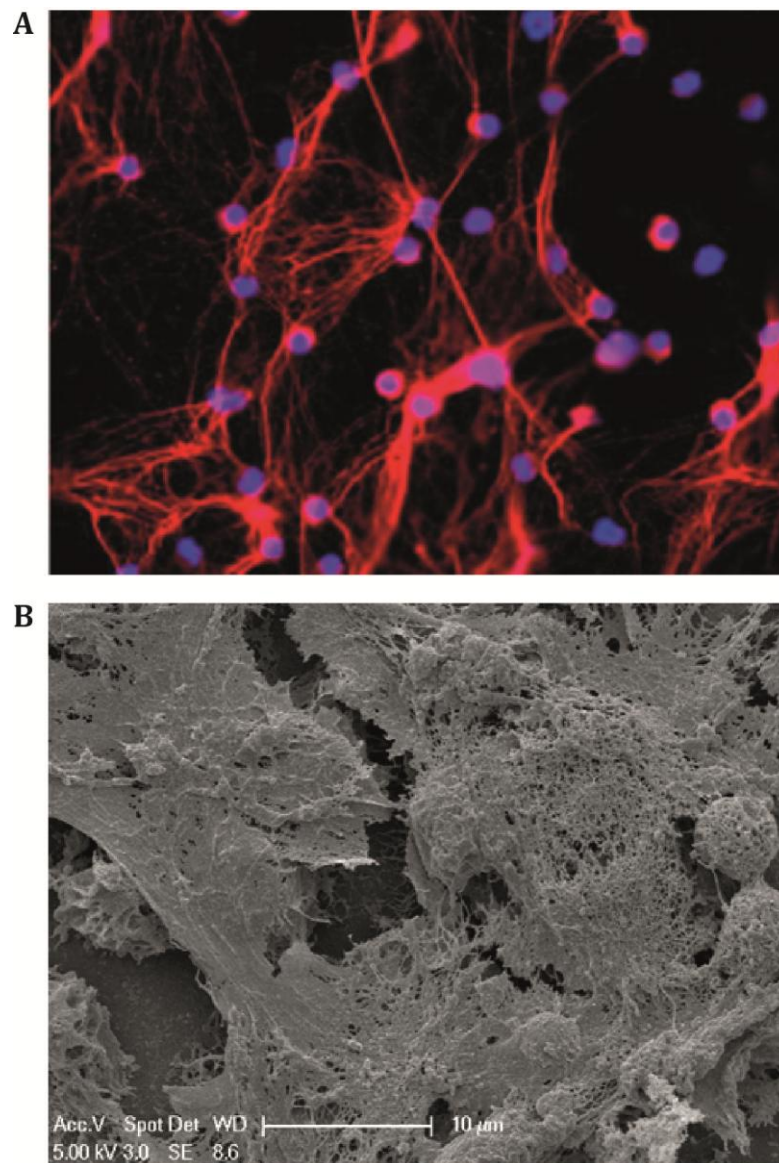


Figure 1.5: NETs

A. Neutrophil extracellular traps (NETs) are characterised by long strands of DNA (blue) decorated with the granular protein, neutrophil elastase (red). Immunofluorescence image, Magnification= 40x. Adapted from Carmona-Rivera⁴⁶. B. Scanning electron microscope image showing blankets of NETs after 4 hours of PMA (200 nM) treatment (B :This imags was prepared and is shown by courtesy of Daniel Storisteanu).

proteins, and their neutrophils have been shown to be more prone to forming NETs⁴⁷. NETs have also been suggested to play a role in cystic fibrosis (CF); Manzenreiter et al.⁴⁸ found that NETs are present in sputum from CF patients and their presence can contribute to the viscosity of CF sputum.

1.2.4 Role of neutrophils in disease: a double-edged sword

Neutrophils are expertly equipped to carry out their role, as illustrated by the susceptibility of patients with neutrophil defects such as congenital neutropenia or chronic granulomatous disease to severe and recurrent infections^{36,49}. Neutropenia is more commonly due to chemotherapy, and these patients are likewise highly susceptible to sepsis⁵⁰. Neutrophils are professional phagocytes designed to phagocytose and eliminate pathogens rapidly, however in the context of adhesion or integrin activation, if they do not encounter pathogens within a short time frame (*in vitro* this is 15-45 minutes), they may release large amounts of reactive oxygen species into the extracellular space⁵¹.

This, combined with the release of granule proteins, causes localised tissue damage which again can be beneficial: it leads to the trapping of pathogens in a 'toxic soup' (pus), collagen disassembly which improves neutrophil-pathogen contact, and the collapse of lymphatics and capillaries therefore cutting off pathogen escape routes^{37,51,52,53}.

Besides fighting infection, neutrophils have been shown to play an important role in wound healing; patients with neutropenia⁵⁴ or those with defective neutrophil adhesion experience poor wound healing⁵⁵. However, neutrophil function must be tightly controlled to prevent inappropriate or excessive damage. Aberrant or over-activation of neutrophils has been related to a range of inflammatory diseases such as rheumatoid arthritis (RA), where neutrophils have been implicated in joint damage. A mouse model of RA shows a correlation between the earliest signs of ankle joint inflammation and the presence of neutrophils in the synovial tissue⁵⁶ and neutrophils have been found in high numbers in the synovium during the initial stages of RA⁵⁷.

Another example of a disease process in which neutrophils have a detrimental effect is cancer. Several mouse models have shown that neutrophils modulate the tumour micro-environment to promote tumour progression, through promoting angiogenesis via the release of vascular endothelial growth factor, and by promoting tumour cell motility, migration and invasion⁵⁸. Fridlender et al.⁵⁹ show that tumour associated neutrophils (TANs) can acquire a pro-tumour phenotype (similar to M2 macrophes), largely driven

by TGF- β . Upon TGF- β blockade, neutrophils acquire an antitumor phenotype to become “N1” TANs (similar to M1). This paradigm suggests that TANs are a double-edged sword, capable of being pro- or anti-tumourigenic, depending on the tumor microenvironment. N2 neutrophils express higher levels of CXCR4, VEGF, MMP-9 and arginase, supporting carcinogenesis, angiogenesis and immune suppression.⁶⁰ Tumour invasion requires the degradation of extracellular matrix (ECM), which neutrophils are capable of either directly by the release of granule proteins including elastase, cathepsin G, MMP-8 and MMP-9, or indirectly by activating MMP-2 and thereby promoting the invasion of tumour cells^{61,62}

Additionally, neutrophils have been implicated in a range of inflammatory lung diseases such as chronic obstructive pulmonary disease (COPD). This disease is characterised by aberrant and persistent inflammation leading to severe damage both to the airways and the lung parenchyma. Neutrophils are the most abundant cells found in the bronchial wall and lumen of COPD patients^{63,64} and their presence correlates with the decline in lung function characteristic of this relentlessly progressive disease⁶⁵. Neutrophil granule proteins, otherwise important in fighting infection, have been heavily implicated in causing tissue damage in COPD; circulating levels of NE have been shown to increase during exacerbations⁶⁶ and alveolar NE (as measured in bronchoalveolar lavage fluid (BALF)) is related to disease severity⁶⁷.

Thus while the neutrophil plays an essential role in host defence, it also plays a pathogenic role in many diseases. In the next section neutrophil degranulation, which has many important physiological functions but also the capacity to cause substantial tissue injury, will be discussed.

1.3 Neutrophil granules: development and function

Granule contents play a role in almost every step of the neutrophil inflammatory response, from the initial endothelial capture and extravasation to bacterial killing and modulating the inflammatory response at the site of infection. Thus neutrophil granules not only contain anti-microbial proteins and proteases, but are also a store of NADPH oxidase components, receptors for endothelial adhesion molecules, extra-cellular matrix proteins and soluble inflammatory mediators, as summarised in Table 1.1. Degranulation can be induced by a range of ligands, including fMLP and PAF⁶⁸⁻⁷⁰; the degranulation response is very rapid, starting 30-40 seconds after stimulation with fMLP⁷¹.

Secretory vesicles	Gelatinase granules	Specific granules	Azurophil granules
Membrane	Membrane	Membrane	Membrane
<ul style="list-style-type: none"> Alkaline phosphatase C1q-R CR1 Cytochrome b₅₅₈ CD10, CD11b, CD13, CD14, CD16, CD45 DAF fMLP-R SCAMP U.kinase-type plasmasminogen activator R. V-type H⁺-ATPase VAMP-2 	<ul style="list-style-type: none"> CD11b, CD15 Cytochrome b₅₅₈ Diacylglycerol-deacylating enzyme fMLP-R SCAMP U.kinase-type plasmasminogen activator R. VAMP-2 V-type H⁺-ATPase 	<ul style="list-style-type: none"> CD11b, CD15, CD66, CD67 Cytochrome b₅₅₈ fMLP-R Fibronectin-R G-protein_q-subunit Laminin-R NB 1 antigen 19-kD 155 protein Rap1, Rap2 SCAMP Thrombospondin-R TNF-receptor Urokinase-type plasminogen activator R VAMP-2 	<ul style="list-style-type: none"> CD63, CD69 V- type H⁺-ATPase
Matrix	Matrix	Matrix	Matrix
<ul style="list-style-type: none"> Plasma binding proteins 	<ul style="list-style-type: none"> Acetyltransferase β_2Microglobulin Gelatinase Lysozyme 	<ul style="list-style-type: none"> β_2 Microglobulin Collagenase Gelatinase hCap-18 Histaminase Heparanase Lactoferrin Lysozyme NGAL Urokinase-type plasminogen activator R Sialidase SGP28 Vitamin B₁₂ -binding protein 	<ul style="list-style-type: none"> Acid β-glycerophosphatase Acid muco polysaccharide α_1-antitrypsin α-Mannosidase Azurocidin/CAP37/ Bacterial perm. increasing protein β/Glycerophosphatase β/Glucuronidase Cathepsins Elastase Lysosyme Myeloperoxidase Proteinase-3 Ubiquitin-protein

Table 1.1: Contents of neutrophil granules

This table summarises the major contents of each granule type, divided into membrane and intracellular components. The granule membranes contain essential components for neutrophil activation and recruitment (CD11b and fMLP-R), ROS dependent intracellular bacterial killing (cytochrome b₅₅₈) and lysosome acidification (ATP-pump), which are highlighted in blue. The granule matrix contains many key components for extravasation (gelatinases) and bacterial killing (lactoferrin, MPO and NE) highlighted in red. (Adapted from Borregaard et al.¹⁹).

Neutrophil granules are bounded by a phospholipid bilayer membrane and possess an intracellular matrix incorporating proteins destined for delivery to the phagosome or for exocytosis⁷². There are four granule subsets that can be classified according to their contents: primary (azurophil) granules, secondary (specific) granules, tertiary (gelatinase) granules and secretory vesicles. However, this classification is not precise, as granules are formed continuously from the early promyelocyte stage until nuclear segmentation (Table 1.2). Granulopoiesis involves budding of vesicles from the Golgi network and their fusion to form early stage granules^{73,74}. Borregaard et al.⁷⁵ and others^{76,77} showed that the granule content depends on the changing transcriptional profile as neutrophil development proceeds, and if the bio-synthetic window of a granule protein is changed it will be incorporated into a different granule types⁷⁸. Since the expression of granule proteins occurs as a continuum rather than in a distinct quantal fashion, there is some overlap in protein content⁷². The azurophil granules are formed first, in the promyelocyte stage⁷⁹, the specific granules in the myelocyte and metamyelocyte stages, and gelatinase granules in the band cell and segmented cell stage^{70,74}. The secretory vesicles are last to be formed and appear in segmented neutrophils⁸⁰ (Table 1.2). Once maturation is complete, it is thought that no further granule proteins are produced; Fouret et al. showed that mature neutrophils do not contain mRNA transcripts for myeloperoxidase (MPO), lactoferrin or NE.

Granule subsets differ not only in their protein content but also in the timing of their release; the secretory vesicles, which play a role in the earliest phases of the neutrophil response, are released first. Tertiary, secondary and primary granules are progressively less prone to mobilise to the cell surface (a control mechanism, which reduces the likelihood of extra-cellular release of the potentially destructive serine proteases). This hierarchical mobilisation of neutrophil granule populations can be reproduced *in vitro* by inducing progressive elevations of intracellular calcium⁸¹, suggesting that activation of phospholipase C may be important in controlling this response. The primary (azurophil) granule is preferentially targeted to the emerging phagosome, a process dependent on the microtubule network⁸² and on the small GTPase Rac⁸³. The precise molecular mechanisms providing this fine control of granule deployment are not fully understood, but are likely to involve differential granule expression of soluble N-ethylmaleimide-sensitive attachment protein receptor (SNARE) proteins and differences in SNARE complex

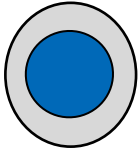
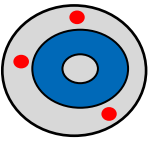
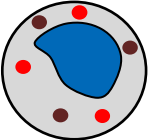
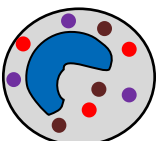
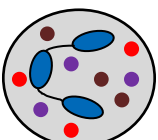
	Developmental stage	Granule population
	Myeloblast	
	Promyelocyte	Azuropilic granules
	Myelocyte	Specific granules
	Meta myelocyte	
	Band cell	Gelatinase granules
	Mature neutrophil	Secretory vesicles

Table 1.2: Neutrophil granules develop at different stages during neutrophil maturation

The formation of granules occurs sequentially, during neutrophil maturation in the bone marrow. Granulopoiesis starts in early promyelocytes; the azurophilic granules are formed first, in this promyelocyte stage. The peroxidase-negative granules, which include the specific and gelatinase granules, are formed next. The specific granules are formed in the myelocyte and metamyelocyte stages and the gelatinase in the band cell and segmented cell stages. The secretory vesicles are the last to be formed and appear in segmented, mature neutrophils.

formation⁸⁴. This targeted and timed release profile is essential for optimal neutrophil function and to minimise tissue damage^{72,52}.

1.3.1 Secretory vesicles

The secretory vesicles are the last to be formed during neutrophil development and are the most readily exocytosed, for example following contact with inflamed endothelial surfaces or exposure to priming agents. They contain a reservoir of membrane-associated receptors such as integrins (CD11b/CD18) and fMLP receptors (table 1.1), which facilitate the earliest phases of the neutrophil-mediated inflammatory response, in particular the recruitment of these cells to the inflammatory focus^{85,86}. The mobilisation of secretory vesicles is accompanied by L-selectin shedding on the surface of neutrophils and this allows the neutrophil to establish firm contact with the activated vascular endothelium. Secretory vesicles only contain a few intra-vesicular components, which are mostly plasma proteins, suggesting that they are formed by endocytosis⁸⁷.

1.3.2 Gelatinase granules

The gelatinase granules are the next most readily exocytosed granule population after the secretory vesicles. This reflects their function as a reservoir of matrix degrading enzymes (gelatinases) and membrane receptors (CD11b/CD18) required for neutrophil extravasation and migration through the tissues. *In vitro* experiments have shown that gelatinase activity is essential for neutrophil migration through Matrigel and amniotic membranes⁸⁸. Matrix metalloproteinase 9 (MMP-9 or gelatinase B) is the predominant component of gelatinase granules. MMP's are stored as inactive pro-forms and undergo proteolytic activation after exocytosis. Together with other MMP's, MMP-9 is capable of degrading major structural components of the extracellular matrix, including collagen, laminin and gelatin, thereby facilitating neutrophil extravasation and migration, but also conferring the potential for tissue injury^{30,89,90}. In a recent study into the role of intravenous salbutamol in the treatment of ARDS, an increase in BALF MMP-9 level at day 4 correlated with reduced extravascular lung water⁹¹, suggesting a possible role for MMP-9 in injury repair. However, excessive release of MMP-9 (or other metalloproteases) in most settings is associated with tissue damage. Increased expression of MMP-2 and MMP-9 in tumours has been associated with the progression of ovarian

cancer⁹² and has been shown to play a role in breast tumour growth. Additionally MMP-9 has been shown to disrupt vascular integrity and to induce leukocyte migration in an ischaemia/reperfusion liver injury model; MMP-9 knockout mice are protected from liver injury with reduced leukocyte infiltration, pro-inflammatory cytokine expression and liver necrosis⁹³. Furthermore increased MMP-9 levels have been associated with tissue damage in a range of inflammatory lung disease such as COPD⁹⁴ and acute lung injury (ALI)^{95,96}, as discussed in more detail in Section 1.4. In tissues such as the lung, tissue inhibitors of metalloprotease (TIMPs) 1-4 are present, and can limit the damage caused by these MMPs; an imbalance between TIMPs and neutrophil proteases is a feature of several inflammatory lung diseases, including ARDS⁹⁷.

The gelatinase granules also contain cytochrome b₅₅₈⁹⁸, the major membrane component of the NADPH oxidase, responsible for most of the proton pump activity of the assembled complex⁹⁹. Thus fusion of tertiary granules with the phagosome is essential for phagosome acidification and intracellular ROS production. The gelatinase granules contain another ion-transporter: natural resistance-associated macrophage protein 1 (Nramp 1), which also locates to the phagosome membrane and transports divalent cations so as to deprive micro-organisms of metals such as Fe²⁺, Mn²⁺ and Zn²⁺¹⁰⁰.

A rare disease called Specific Granule Deficiency (SGD) illustrates the importance of the gelatinase and specific granules. Neutrophils from these patients have abnormal bi-lobed nuclei, and lack expression of both specific and gelatinase granule proteins. This leads to an inability to infiltrate tissues, and defects in chemotaxis, receptor upregulation and impaired bactericidal activity¹⁰¹. SGD is an inherited disorder, which causes patients to suffer severe and recurrent infections^{54,102,103} and at least in some patients, reflects loss-of-function mutations in the C/EBP factor gene which regulates the transcription of the relevant granule proteins.

1.3.3 Specific granules

The specific granules have some overlap in granule contents with the gelatinase granules (for example, both contain cytochrome b₅₅₈) but have a different function; in particular, they play an important antimicrobial role^{104–106}. Lactoferrin is the principal constituent of specific granules^{107,108}. It is a member of the transferrin family of iron-binding proteins and impairs bacterial growth by the sequestration of iron¹⁰⁹. It is also capable of binding

to bacterial cell membranes via an N-terminal amphipathic α -helical region, causing irreversible membrane damage and cell lysis¹¹⁰. It has anti-microbial activity against a broad spectrum of gram-positive and gram-negative bacteria. Lactoferrin has recently been suggested to be a specific biomarker of cystic fibrosis pulmonary exacerbations¹¹¹; however, as other granule proteins including NE are also implicated in these episodes, this probably reflects neutrophil activation and degranulation in general rather than a process specific to lactoferrin.

Besides lactoferrin, the specific granules contain other bactericidal components including hCAP-18, a cathelicidin peptide that exerts antimicrobial effects against both gram-negative and gram-positive bacteria and can induce chemotaxis of neutrophils, monocytes and T-cells. Another antimicrobial peptide present in the specific granules is neutrophil gelatinase-associated lipocalin (NGAL)^{70,112}. This peptide can bind MMP-9, protecting it from degradation, but also plays a role in iron-depletion by means of its ability to sequester ferric-siderophore complexes¹¹³. In addition to its presence in neutrophil granules, NGAL is also produced by a variety of normal, inflamed and neoplastic tissues^{114,115}. Urinary NGAL has been shown to be a sensitive and specific biomarker of a range of renal diseases such as acute renal injury¹¹⁶ and the interstitial nephritis associated with IgA nephropathy¹¹⁷. NGAL has also been suggested to be a key player in a range of different cancer types; its proposed functions range from inhibiting apoptosis (of thyroid cancer cells), invasion and angiogenesis (of pancreatic cancer) to increasing proliferation and metastasis (of breast and colon cancer) as reviewed in Chakraborty et al.¹¹⁸

1.3.4 Azurophilic granules

Azurophil granules are the last granules to be released and require the most potent stimuli (such as cytochalasin B, which is not a physiological compound) to induce major degranulation into the external milieu, although less potent stimuli may trigger a more limited release. Instead they are directed preferentially to fuse with phagosomes that contain engulfed pathogens^{68,81}.

Azurophil granules are defined by the presence of MPO, a 150 kDa microbicidal haemoprotein. MPO reacts with H₂O₂, a product of the neutrophil respiratory burst, to increase its toxic potential. Through oxidation of chloride, tyrosine and nitrite, the H₂O₂-MPO system induces formation of hypochlorous acid and a number of other reactive intermediates, which can attack the surface membranes of microorganisms¹¹⁹. Besides

playing a role in bacterial killing, MPO has also been shown to modulate the immune response; El Kebir et al.¹²⁰ have shown that MPO rescues human neutrophils from constitutive apoptosis and prolongs their lifespan, potentially delaying the resolution of inflammation. Furthermore it has been shown that MPO can disrupt endothelial cell (EC) function through β_2 -integrin-dependent neutrophil-EC contact, which mediates MPO transfer from neutrophils to ECs¹²¹; this process has been shown to play a role in atherosclerosis and vasculitis. MPO has also been associated with oxidative damage in a range of diseases including Parkinson's disease¹²², diabetes mellitus¹²³ and COPD^{124,125}. In contrast to its pro-inflammatory functions, MPO can also dampen the inflammatory response by suppressing dendritic cell activation, function and migration¹²⁶.

Azurophil granules also contain serine proteases including NE, cathepsin G and proteinase 3. These proteases play an important role in the non-oxidative pathway of intracellular and extracellular pathogen destruction¹²⁷. In the phagolysosome they contribute to microbial killing together with the NADPH oxidase system, which produces abundant reactive oxygen species to optimise protease activity³⁶. Whilst redundancy of the serine proteases offers some protection from individual deficiencies, mice lacking NE and/or cathepsin G show enhanced susceptibility to bacterial infection^{128,129}, fungal infection¹³⁰, and mycobacterial infection¹³¹. Of particular relevance to the work described in this thesis, Reece and colleagues showed that serine protease activity plays an important role in the control of *Mycobacterium tuberculosis* in hypoxic lung granulomas in mice. Finally, mutations in the human elastase gene (*ELANE*) cause cyclical or severe congenital neutropenia syndromes, but the mechanism seems to relate to defective protein folding or processing¹³².

Recently it has been shown that serine proteases, especially NE, also have regulatory functions during inflammation. Demonstrated functions include the release of active cytokines from their inactive precursors, the proteolytic cleavage/inactivation of active cytokines, proteolysis of cell surface bound cytokines and the activation of specific cell surface receptors, including Proteinase-activated receptors (PARs) and Toll-Like Receptor 4 (TLR4)¹³³ (full list of NE targets can be found in the appendixes, section 8.1). Mihara et al.¹³⁴ have shown that both NE and Proteinase-3 can cleave the endothelial proteinase-activated receptor (PAR)-1 leading to impaired endothelial barrier integrity, and promoting neutrophil infiltration. Furthermore, NE has been shown to modulate the expression and activity of important inflammatory cytokines such as TNF α and G-CSF¹³⁵

in the context of *Pseudomonas aeruginosa*-induced pneumonia. However, it is important to note that most of our knowledge of how NE regulates these targets comes from *in vitro* studies, and further studies are needed to assess the role of NE in the modulation of inflammation *in vivo*.

Mice lacking NE are protected from lung injury in some models¹³⁶, but the efficacy of neutrophil elastase inhibitors in human disease has been disappointing¹³⁷. Neutrophil-derived proteases have been implicated in the pathogenesis of CF (reviewed by *Griese et al.*¹³⁸) and 90% of the elastolytic activity in CF sputum has been attributed to NE¹³⁹, but again targeted therapeutic intervention has been unsuccessful¹⁴⁰. Perhaps as a safety measure against over-activity of the serine proteases, the azurophil granules also contain a powerful endogenous anti-protease, alpha 1-antitrypsin (α_1 AT). This promiscuous inhibitor can bind and inhibit not only elastase, but also a range of other serine proteases. The majority of circulating α_1 AT is released by the hepatocyte; it is present in circulation at 1.5-3.5 g/L¹⁴¹. In patients with α_1 AT- deficiency low circulating serum levels of α_1 AT, leads to early onset and severe smoking-related pulmonary emphysema¹⁴². This is partly due to damage caused by over-activity of NE in the absence of an inhibitor as discussed further in section 1.5.1.

Besides α_1 AT, other important endogenous serine protease inhibitors include secretory leukocyte protease inhibitor (SLPI) and elafin. SLPI can inhibit the serine proteases cathepsin G and NE, but not PR3. It can be found in all body fluids including bronchial secretions but the highest concentrations of SLPI are present in the upper airways. It is also produced by phagocytes including monocytes and neutrophils¹⁴³ and, due its low molecular weight, it has unique access to the space between adherent neutrophils and the ECM, protecting it from degradation¹⁴⁴. Elafin inhibits serine proteases PR3 and NE, but not Cathepsin G. It is mainly present in the skin, but like SLPI can also be found in bronchial secretions, produced by Clara cells and type II pneumocytes¹⁴³.

Further constituents of the azurophil granules include the α -defensins, which are small antimicrobial peptides with activity against a range of bacteria, fungi, enveloped viruses and protozoa^{145,146}. They function by forming transmembrane pores¹⁴⁷, and upon release into the extracellular matrix are able to induce chemotaxis of monocytes, CD4⁺ and CD8⁺ T-cells¹⁴⁸. Thus in summary, azurophil granule contents are essential for killing a range of pathogens but also contribute to tissue injury, with a particular predilection for lung damage.

1.4 Lung epithelial dysfunction and damage

Neutrophil granule proteins have been strongly associated with lung epithelial cell damage and dysfunction. An example of the severe damage that can be caused by neutrophil degranulation is supplied by Soehnlein et al.¹⁴⁹; they shown that a protein (M1) released by *Streptococcus pyogenes* induces degranulation of all neutrophil granule subsets by forming complexes with fibrinogen that bind to β_2 -integrins, resulting in acute lung injury in mice. Thus the respiratory epithelial surface is a highly relevant model in which to study the damaging effects of neutrophil granule proteins.

1.4.1 Structure of the respiratory tract

The lung epithelium is a complex system lining the airway spaces, which changes composition along the lungs to fulfil its functions including gas exchange, hydration, muco-ciliary clearance and host defence. The respiratory system extends from the nasal cavities to distal bronchia and alveoli structures and can be divided into two sections; the “Upper Respiratory Tract” and the “Lower Respiratory Tract”. The upper respiratory tract includes the nostrils, nasal cavities, pharynx, epiglottis and larynx¹⁵⁰. The lower respiratory tract consists of the trachea, bronchi bronchioles and alveoli. The upper respiratory tract, trachea and large bronchi are lined with respiratory epithelium consisting of pseudo-stratified columnar, ciliated epithelium with mucus-secreting goblet cells (discussed in more detail below). As bronchi progressively decrease in size, there is a gradual transition to ciliated simple columnar and finally simple cuboidal epithelium and an accompanying decrease in the number of goblet cells. In areas subjected to abrasion (eg. pharynx), respiratory epithelium is replaced by stratified squamous epithelium. Gas exchange occurs in the alveolus which consists of 3 cell types; type I pneumocytes which are simple squamous cells covering most of the alveolar wall, and type II pneumocytes which are cuboidal cells that produce surfactant¹⁵¹. By acting to reduce the surface tension of the fluid lining the alveolar surface, surfactant helps to prevent collapse of the alveoli; surfactants are also responsible in part for the regulation of gas exchange¹⁵². The third cell type in this compartment is the alveolar macrophage, which is a resident phagocyte and scavenges particulates and micro-organisms. Adjacent alveoli form sandwich-like inter-alveolar septa consisting of the epithelial lining of the alveoli on each side and a thin layer of loose connective tissue between. This connective

tissue layer contains the extensive network of pulmonary capillaries, a few fibroblasts, some reticular fibres and numerous elastic fibres. This part of the lung is also known as the interstitium, and is affected in a number of inflammatory and fibrosing conditions^{153,154}. Due to the lack of supporting cartilage and their small size, bronchioles are vulnerable to blockage and collapse. For example; in chronic bronchitis hypersecretion of mucus may lead to bronchiolar blockage¹⁵⁵.

1.5 The airway epithelium

The airway epithelium contains a number of morphologically different cell types, which can be divided into three categories according to their function; basal cells, secretory cells and ciliated cells¹⁵⁶. Basal cells are present throughout the large (50%) and small airways (81%) and can differentiate into secretory or ciliated cells¹⁵⁷. Within the epithelium, basal cells are the only cells attached to the basement membrane, forming a scaffold for the other cells. They are able to release a number of bioactive molecules including neutral endopeptidase, 15-lipoxygenase products and cytokines¹⁵⁷. Goblet cells are the main secretory cells present in the lung epithelium. They secrete mucin granules to form a mucus layer covering the epithelium, which traps foreign particles in the airway lumen^{158,159}. This mucous layer is present in the airway from the trachea to the bronchioles. In normal, “healthy” airways there is a perfect balance between mucus production and clearance; in contrast, goblet cell hyperplasia can lead to excessive mucus production and has been associated with diseases like chronic bronchitis and asthma¹⁶⁰.

Another type of secretory cells found in the small airway, Clara cells, contain electron dense granules and play a role in the regulation of bronchial epithelial integrity and immunity¹⁶¹. Clara cells produce protease inhibitors such as the SLPI¹⁶² and have been shown to produce p450 mono-oxygenases, which can metabolise xenobiotic compounds such as the aromatic hydrocarbons present in cigarette smoke¹⁶³. Ciliated cells differentiate from basal cells, and are the most prominent cell type present in the upper airway epithelium accounting for approximately 50% of all epithelial cells in this region. They have around 300 cilia per cell and contain many mitochondria to supply the energy for their main function, namely muco-ciliary clearance¹⁵⁶.

The muco-ciliary escalator provides a semi-permeable barrier that prevents most pathogens from penetrating the airway surface but still allows for the exchange of

nutrients and gas. It is highly effective as around 90% of inhaled particles including bacteria and viruses are cleared of the lungs via this route¹⁶⁴.

The main components of the secreted mucous are the large, highly charged mucin molecules MUC5B and MUC5AC, which cross-link to form a viscoelastic gel to contribute to airway defence¹⁶⁵. The mucus contains approximately 200 other proteins including antimicrobial compounds such as defensins, lactoferrin, lysozyme, nitric oxide, cytokines and anti-oxidants¹⁶⁶. All inhaled particles interact with the lung epithelium and it is normally very effective in eliminating any “threats”. However, if this layer of defence is breached the epithelium is able to signal efficiently to immune cells as a variety of them reside within this layer, including mast cells, macrophages, dendritic cells and neutrophils¹⁶⁷ (Figure 1.6).

1.5.1 Role of neutrophil proteases in airway epithelial injury and lung disease

The lung epithelium responds to infectious or inflammatory insults via stimulation of pattern recognition receptors (PRRs) such as Toll-like receptors (TLRs), leading to the release a range of inflammatory mediators including IL-1 β and IL-8, which are both neutrophil chemo-attractants. The presence and actions of a range of immune cells present in, or adjacent to, the delicate epithelial cell lining can be either beneficial or detrimental; although they can respond quickly to limit infection, aberrant activation and/or function can cause substantial damage.

In chronic inflammatory lung diseases such as COPD, CF and asthma, goblet cell hyperplasia is a common finding and is thought to contribute to the productive cough associated with these diseases¹⁶⁰; NE is the archetypal neutrophil protease that has been shown to induce goblet cell hyperplasia¹⁶⁸ and also to increase the expression of MUC5 and other mucins^{169,170}. Whilst other aspects of neutrophil biology such as ROS may contribute to epithelial damage and dysfunction, the following discussion focuses on the role of neutrophil-derived proteases in this setting.

1.5.1.1 Role of NE in airway epithelial injury and lung disease

Although NE and other neutrophil proteases have an important role in neutrophil-mediated bacterial and fungal killing, they can also directly damage the ECM; NE and MMP-9 are capable of degrading almost every ECM component including collagen,

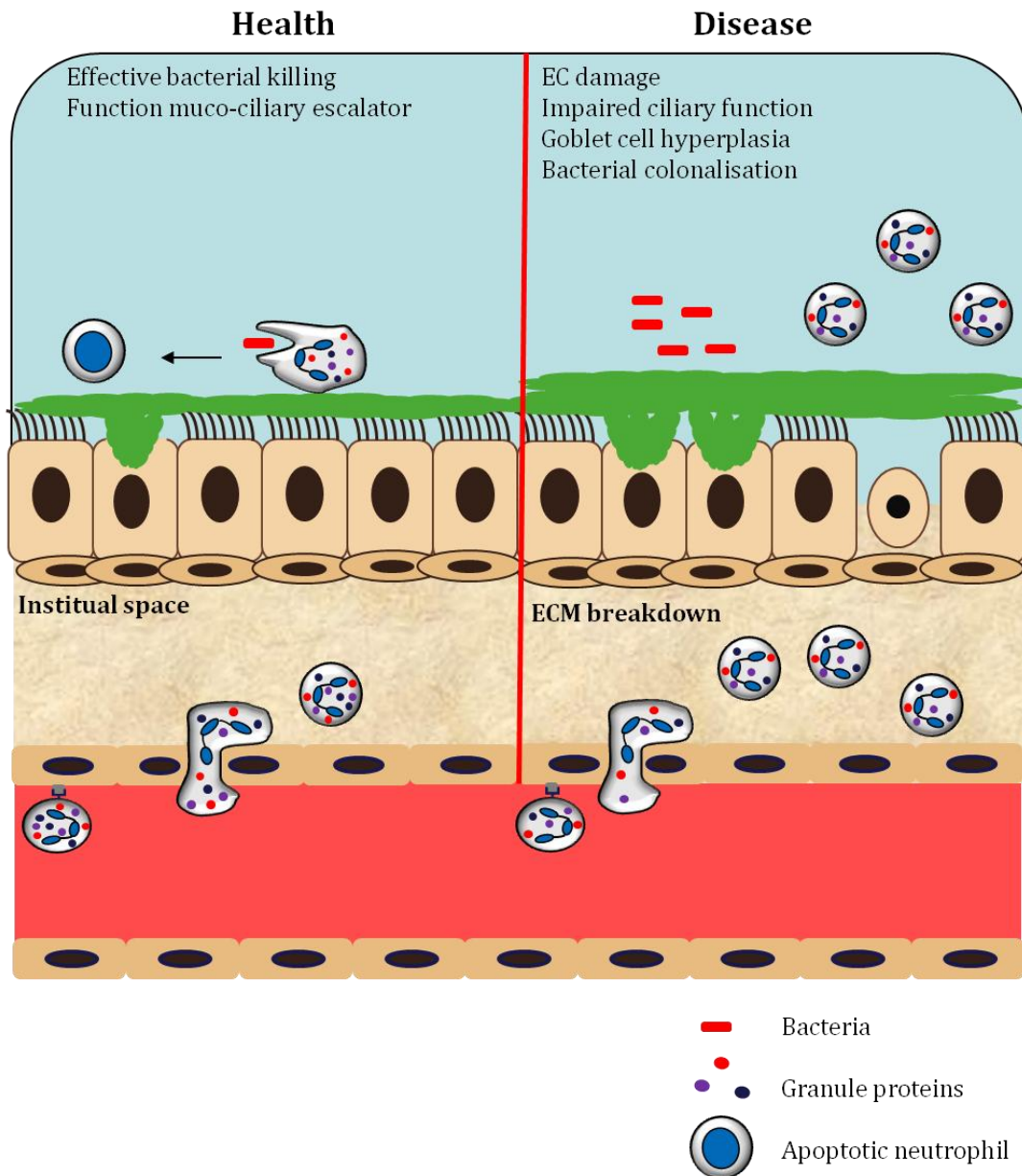


Figure 1.6: The lung epithelium in health and disease

Healthy airways are protected from infection by the innate immune system; bacteria are cleared by the muco-ciliary escalator, by the action of anti-bacterial peptides, and by resident phagocytes. Pathogens which evade these first-line defences are ingested and killed by recruited neutrophils, which then undergo apoptosis and efferocytosis, controlling infection and limiting inflammation. In the inflamed airway ('disease'), pathogens trigger the release of chemo-attractants, promoting the recruitment of neutrophils and other inflammatory cells. Although there is increased neutrophil infiltration, local or systemic hypoxia impairs bacterial killing and increases the release of proteases, resulting in muco-ciliary dysfunction and cellular and tissue injury. Finally, the pro-inflammatory state is perpetuated by increased neutrophil lifespan secondary to hypoxia and inflammatory cytokines. ECM: extra cellular matrix, EC: epithelial cell.

fibronectin, proteoglycans, heparin, and cross-linked fibrin¹⁷¹. Stockley et al.¹⁷² have shown that neutrophils moving in close proximity to ECM degrade it *en passant*, and that this degradation can be reduced but not abolished by α_1 -antitrypsin³². The inability of naturally occurring protease inhibitors to prevent NE-dependent damage completely has been attributed to a number of factors. One such factor is the phenomenon of quantum proteolysis, which refers to the fact that NE molecules vastly outnumber inhibitor molecules in the immediate peri-cellular zones³⁴. Another suggested mechanism is that upon degranulation, serine proteases bind to the neutrophil cell surface, and these bound proteases are remarkably resistant to protease inhibitors, a finding that has been attributed to steric hindrance^{33,173}.

The installation of elastase in the lungs of experimental animals (usually porcine pancreatic elastase, but the model is phenocopied when human NE is used) induces emphysema in a dose-dependent fashion^{174,175}. Likewise, transgenic mice lacking NE are protected from cigarette smoke-induced emphysema¹³⁶. This evidence, together with the observation that in humans, α_1 -AT deficiency predisposes to early onset emphysema¹⁷⁶ led to the protease:antiprotease imbalance hypothesis of COPD¹⁷⁷, which proposes that alveolar and interstitial tissue destruction is driven by excessive proteolysis. In healthy individuals α_1 -AT is produced in abundance by hepatocytes; in individuals with α_1 -AT 'deficiency', α_1 -AT polymers accumulate in the ER of hepatocytes and secretion is impaired, which leads to the observed reduction in circulating protein; when this is combined with the recruitment of neutrophils into the bronchi and interstitium by cigarette smoke, failure of local pulmonary elastase inhibition results in smoking-induced lung tissue destruction and early emphysema¹⁷⁸. Therapeutic replacement (or 'augmentation') of α_1 -AT in this disease has been shown to improve some parameters such as radiological disease progression; however to date, robust evidence of clinical benefit from augmentation therapy is lacking. This may reflect under-powering of trials, the initiation of augmentation therapy at too late in the disease process, or it may indicate that the pulmonary disease seen in α_1 -AT deficiency is not caused by a lack of functional α_1 -AT alone.

In addition to its elastolytic activity, NE has a range of immune-modulatory effects. It has been shown to cleave critical components of the bronchial defences, such as the C3Bi opsono-phagocytic receptor CR1¹⁷⁹ and immunoglobulins¹⁸⁰, reducing the ability of the airway tissue to retain sterility in diseases such as cystic fibrosis. Additionally, NE has

been shown to degrade short palate, lung, and nasal epithelial clone 1 (SPLUNC1), which destroys its natural antimicrobial activity. NE-dependent SPLUNC1 degradation increased the non-typeable *haemophilus influenza* (NTHi) load in human airway epithelial cells, and SPLUNC1 KO mice had a higher bacterial load in the lungs than WT mice. Furthermore, SPLUNC1 is reduced in the lungs of COPD patients, potentially increasing airway susceptibility to infection¹⁸¹.

Perhaps as a consequence of its immune-modulatory functions and its ability to degrade ECM components, NE has been implicated in a range of inflammatory diseases. For example, inhibition or lack of NE has been shown to reduce neutrophilic infiltration in neutrophil-mediated injury models such as ischaemia-reperfusion injury¹⁸², endotoxin-induced lung injury¹⁸³ and ventilator-induced lung injury¹⁸⁴. Lack of NE significantly reduced airway neutrophilia, mucin expression, goblet cell metaplasia, and distal airspace enlargement in a mouse model of cystic fibrosis¹⁸⁵. NE contributes to the progression of a range of cancers by enhancing tumour invasion and metastasis^{186,187}. Together, these data indicate that the modulation of NE secretion and function may be a promising target for therapeutic intervention. A recent Phase II study of AZD9668, a newly developed oral NE inhibitor, in patients with bronchiectasis, reported some improvement in lung function, with a trend towards a reduction in sputum inflammatory biomarkers¹⁸⁸. However the improvements were small, indicating that inhibition of NE alone might not be enough to prevent inflammation and further damage, and that other neutrophil-derived products may contribute to disease pathogenesis.

1.5.1.2 Role of MPO in airway epithelial injury and lung disease

The presence of MPO defines the azurophil granule population, and its heme moiety is responsible for the green colour of secretions rich in neutrophils, such as pus and sputum. It is also expressed (to a lesser degree) by monocytes and macrophages. Like NE, MPO has been associated with tissue damage in a range of diseases and disease processes; for example, elevated leukocyte and blood MPO levels have been associated with the presence of coronary artery disease¹⁸⁹, and MPO-directed autoantibodies are associated with a range of vasculitis¹⁹⁰, in particular granulomatosis with polyangiitis (formerly known as Wegener's granulomatosis). MPO, together with other circulating neutrophil degranulation products, has been suggested to be a possible biomarker in CF¹¹¹, and MPO presented on the surface of NETS has been associated with *Pseudomonas*-induced airway

damage¹⁹¹. Serum MPO levels are associated with rapid lung function decline and poorer cardiovascular outcomes in COPD patients¹⁹² and 3-Chlorotyrosine, a specific product of MPO oxidative activity, was shown to be upregulated in COPD sputum¹⁹³. Late intervention with the MPO inhibitor AZ1 in a guinea pig cigarette smoke exposure model of COPD stopped the progression of emphysema and small airway remodelling and was partially protective against pulmonary hypertension¹²⁵. These studies suggest that the role of MPO in COPD warrants further investigation; however, as the authors note, positive findings in animal models of COPD have a disappointing record of failure in human disease¹⁹⁴.

Like NE, MPO has been shown to upregulate the inflammatory response directly; MPO internalised by endothelial cells leads to IL-6, IL-8, and ROS release^{195,196} (although others have shown that MPO can also inhibit IL-8 release by bronchial cells¹⁹⁷). MPO is capable of inducing oxidative stress in inflammatory states, especially in the presence of cigarette smoke^{38,198}, and neutrophil MPO content is increased in smokers¹⁹⁹.

1.5.1.3 Role of MMP-9 airway epithelial injury and lung disease

MMP-9 is a component of the gelatinase granules and is capable of degrading major structural components of the ECM, including collagen, laminin, and gelatin, allowing neutrophil extravasation and migration^{30,89,90}. However, indiscriminate MMP-9 release can also cause substantial damage. MMP-9 has been related to parenchymal destruction and lung function decline in both subclinical and established emphysema^{200,201}. Other studies have shown MMP-9 to be elevated in the sputum of patients with COPD in comparison to healthy control subjects, and MMP-9 sputum levels were found to correlate with decreased lung function^{94,202,203}. Because neutrophils do not synthesise the MMP-9 anti-protease TIMP-1, substantial and unrestrained release of this enzyme can occur²⁰⁴. Vlahos and colleagues⁶⁷ demonstrated a major up-regulation of MMP-9 in the BAL fluid of patients with COPD and noted a striking correlation with disease severity (21-fold increase in MMP-9 activity in GOLD II versus GOLD IV disease); upregulation of NE was noted in the same samples, and it is noteworthy that NE can degrade TIMP-1, further promoting the action of MMP-9²⁰⁵.

Thus there is abundant evidence that a range of neutrophil-derived proteases contribute to the pathogenesis of COPD and other inflammatory lung diseases and to the persistence of the inflammatory phenotype in these conditions.^{94,199–202,206–210} Therapeutic strategies to

control this aspect of neutrophil function may need to be directed at the broader spectrum of neutrophil-derived proteases rather than an individual target, and could be more beneficial if administered early in the course of disease before major irreversible tissue destruction occurs. Interventions aimed at limiting neutrophil degranulation would ideally target extracellular protease release and not inhibit the delivery of granules to the phagosome.

1.6 Mechanisms of neutrophil degranulation

The mechanisms of neutrophil degranulation are complex and only partially delineated (Figure 1.7). Different ligands have been shown to have different effects on degranulation; for example, stimulation with low nanomolar concentrations of the bacterial-derived tripeptide fMLP alone results in a rapid and almost complete discharge of secretory vesicles without significant release of the other granule populations⁸¹, whilst priming with agents such as TNF α augments granule release including the liberation of MPO from the azurophilic granules; stimulation with the pharmacological agent PMA (phorbol myristate acetate) alone leads to extensive release of gelatinase granules, moderate release of specific granules and low grade release of azurophil granules^{68,70}.

In general, exocytosis of the granules occurs in 4 steps; upon receptor stimulation granules are recruited from the cytoplasm to the target membrane (phagosome membrane or cell membrane). This process is dependent on actin cytoskeletal- and microtubule-remodelling²¹¹. The next step is vesicle tethering and docking, followed by granule “priming” (ensuring rapid fusion) in which a reversible fusion pore structure develops between the granule on the target membrane, and the final step is the rapid fusion between the granule and target membrane²¹².

Resting neutrophils contain a cortical actin ring that forms a barrier against granule docking and fusion; this is rapidly disassembled upon receptor ligation and exocytosis²¹². Jog et al.²¹³ demonstrated that actin is associated with all granule subsets and that disruption of the actin cytoskeleton by latrunculin A or cytochalasin D led to enhanced basal and fMLP dependent degranulation, implying an active role for actin in granule exocytosis. Conversely tetracaine, which causes enhanced accumulation of F-actin in the periphery of fMLP-stimulated cells, inhibits degranulation²¹⁴. It was postulated by Lacy et al.²¹² that cytoplasmic filamentous (F)-actin formation is required for primary granule exocytosis and that, as granules co-localise with polarised

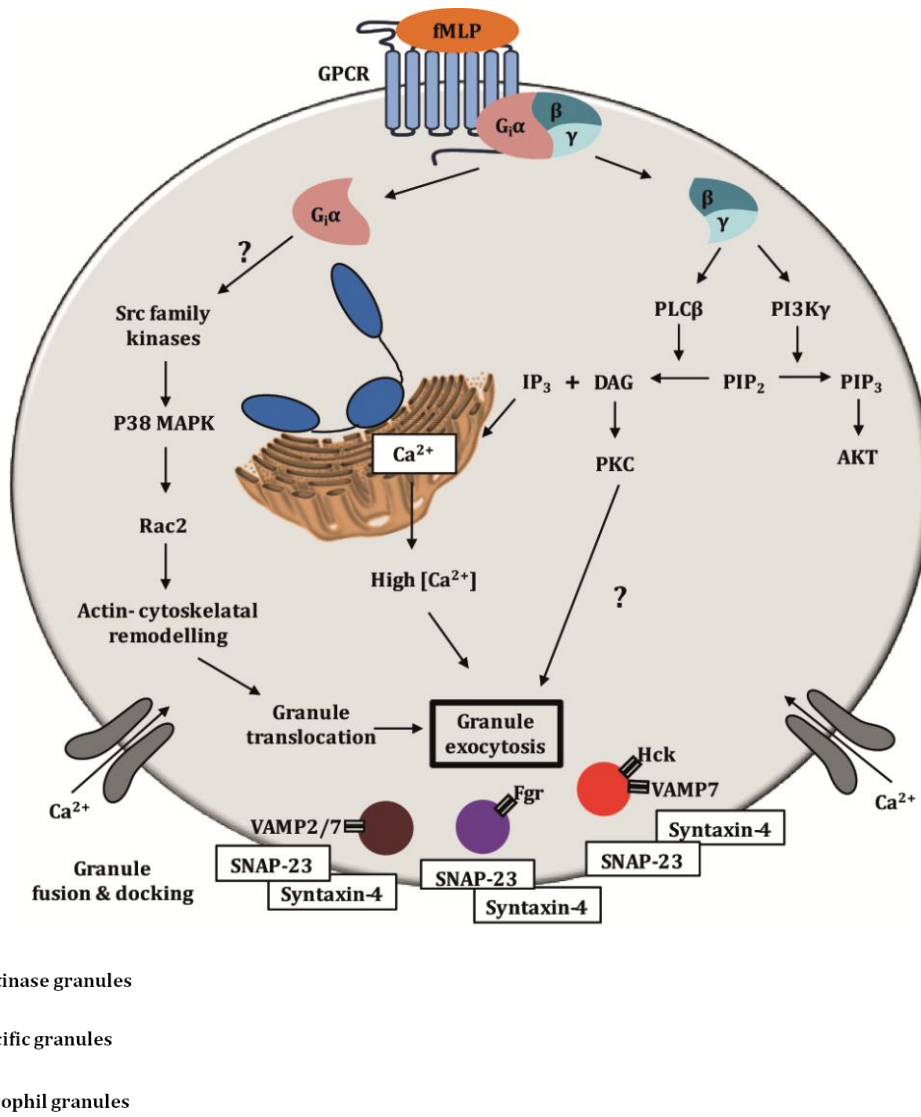


Figure 1.7 Neutrophil signalling pathways involved in degranulation

GPCR ligation results in signalling through the heterotrimeric G-proteins of the G $_{i/o}$ family; activation leads to the dissociation of the GPCR-specific G α subunit from the shared G $\beta\gamma$ dimer which triggers the activation of two signalling events: 1. Activation of PLC β leads to diacylglycerol formation and hence activation of PKC, and to the hydrolysis of PIP $_2$, generating IP $_3$. Elevation of intracellular IP $_3$ leads to an increase in intracellular Ca $^{2+}$ release from the endoplasmic reticulum. 2. Activation of PI3K γ induces the production of PIP $_3$ by phosphorylation of PIP $_2$. Ligation of integrins and of cytokine receptors induces activation of tyrosine kinases, leading to the activation of PLC and eventually to a rise in Ca $^{2+}$ levels. PI3K activation is also mediated by integrin and cytokine receptor binding.

F-actin during activation, cytoskeletal remodelling triggers the formation of actin “tracks” to guide granules to the target membrane for exocytosis. As actin polymerisation/reorganisation plays an important role in not only degranulation but in many features of neutrophil function, including migration and the ROS response, signalling pathways regulating these functions may overlap.

1.6.1 Receptors regulating degranulation

Neutrophils express a large range of cell surface receptors to sense damage or danger, including receptors for the recognition of microbial structures, receptors involved in activation of the adaptive immune system, and receptors involved in recognising an inflammatory environment (as summarised in Futosi et al.⁷). These receptors initiate a range of complex intracellular signalling pathways that lead to the induction of an appropriate spectrum of responses, including neutrophil chemotaxis, activation, phagocytosis, ROS production, degranulation, NET release, and cytokine release.

The receptors present on the neutrophil surface can be divided into a number of classes; G-protein-coupled seven-transmembrane domain receptors (GPCRs), Fc-receptors, adhesion molecule ‘receptors’ such as integrins, cytokine receptors and pattern recognition receptors (Toll-like receptors and C-type lectins). Of these receptor classes, Fc receptors, integrins and GPCRs have been shown to induce neutrophil degranulation^{215,216}. Fc-mediated neutrophil interaction with immune complexes has been shown to induce degranulation²¹⁷ through Src family kinase signalling leading to a rise in intracellular calcium levels²¹⁵. The combination of integrin-dependent neutrophil adhesion plus stimulation with inflammatory mediators also results in degranulation^{218,219}. However, most of the research into the signalling pathways involved in degranulation has focussed on GPCR signalling. Neutrophils express a range of different GPCRs, including those that recognise chemokines and chemoattractants such as IL-8, platelet activating factor (PAF) and leukotriene B₄, and those that recognise bacterial products (formyl-peptide receptors).

The archetypal ligand for the latter is the formylated tri-peptide fMLP, which is often used to interrogate neutrophil functional responses such as degranulation. GPCR ligation results in signalling through the pertussis toxin-sensitive heterotrimeric G-proteins of the G_{i/o} family; activation leads to the dissociation of the GPCR-specific G α subunit from the shared G $\beta\gamma$ dimer and subsequent activation of various signal transduction pathways⁷.

It is currently thought that the majority of signal transduction in neutrophils occurs through the G $\beta\gamma$ dimer and not the G α subunit^{220,221}.

1.6.2 Phospholipid and kinase signalling in degranulation

Stimulation of GPCRs by IL-8 or fMLP leads to the dissociation of the G $\beta\gamma$ dimer from the G α subunit, triggering activation of two phospholipid-based signalling cascades relevant to degranulation: firstly, the phosphoinositide 3-kinase (PI3K) pathway, which induces the production of phosphatidylinositol (3,4,5)-trisphosphate (PIP₃) from phosphatidylinositol (4,5)-bisphosphate (PIP₂)²²² and secondly phospholipase C- β (PLC β), which leads to both the activation of Protein Kinase C (PKC) isoforms (via the generation of diacylglycerol) and also to the hydrolysis of PIP₂, generating inositol 1,4,5-trisphosphate (IP₃) and hence regulating calcium signalling^{223,221}.

That PI3K plays a fundamental role in degranulation is illustrated by a number of studies including that of Kampe et al.²²⁴, who showed that neutrophil degranulation *in vitro* can be inhibited by the PI3K-inhibitor Wortmannin, and also Fensome et al.²²⁵, who showed that PI3K γ is required for granule exocytosis from permeabilised HL-60 cells, a neutrophil-like cell line. However, little data has been published regarding the precise PI3K-isoform controlling neutrophil degranulation, although of note PI3K γ is known to specifically regulate mast cell degranulation²²⁶. Phospholipase D (PLD) has also been shown to influence neutrophil degranulation via the generation of phosphatidic acid (PA)^{216,227}, although recently others have shown that PLD is entirely dispensable for neutrophil degranulation in mice²²⁸. Elevation of intracellular IP₃ leads to an increase in intracellular Ca²⁺ by release of stores from the endoplasmic reticulum (ER)²²⁹. The important role of IP₃ and the resultant rise in intracellular Ca²⁺ in degranulation was supported by the work of Reeves et al.²³⁰ who found that recombinant SLPI inhibited fMLP-induced degranulation populations, and that this was restored by the incorporation of exogenous IP₃ into electro-permeabilised cells. Ligation of integrins and of cytokine receptors activates tyrosine kinases leading to the subsequent activation of PLC and thence to a rise in Ca²⁺ levels^{231,232}.

1.6.3 Calcium signalling in degranulation

Translocation and exocytosis of neutrophil granules requires an increase in intracellular Ca²⁺^{233,234}. Receptor ligation induces a rise in intracellular Ca²⁺ levels that is biphasic;

the first phase is secondary to Ca^{2+} release from IP_3 -sensitive intracellular stores such as the ER, and the second phase is due to Ca^{2+} influx from the extracellular space²³⁵. It has been found that the hierarchy of granule exocytosis is linked to the magnitude of increase in intracellular Ca^{2+} levels, with secretory vesicle release triggered by a minor increase, and a far more significant elevation being required to stimulate azurophil granule exocytosis^{233,236}. A rise in Ca^{2+} can be induced by a number of stimuli, including ligation of GPCRs (e.g. those for fMLP/IL-8) and L-selectin and integrin engagement^{233,237,238}.

The specific target molecules influenced by Ca^{2+} transients in neutrophils are unknown, but potential candidates include annexins^{239,240}, PKC²⁴¹ and calmodulin²⁴², all of which bind Ca^{2+} to modulate their activities and are involved in the degranulation process. The role of calmodulin is supported by data from Nagaji et al.²⁴³, showing that a Ca^{2+} /calmodulin-coupling inhibitor prevents MPO release. Annexins are a group of phospholipid-binding proteins that mediate vesicle aggregation and membrane fusion when exposed to high concentrations of Ca^{2+} ²⁴⁴. Several annexins have been identified in neutrophils and appear to promote a calcium-dependent fusion event *in vitro*, including annexin I²⁴⁵, annexin XI²⁴⁶ and lipocortin III²⁴⁴. Furthermore, Zou et al.²⁴⁷ show that stored-operated Ca^{2+} entry plays a role in neutrophil polarisation by the downstream regulation of Akt and Src family kinases and Rho-family small GTPases including Rac. As actin polymerisation plays an important role in polarisation and in degranulation, cytoskeletal reorganisation may represent another route by which Ca^{2+} modulates neutrophil function.

1.6.4 Src family kinases in degranulation

Tyrosine kinases, especially the Src family of non-receptor tyrosine kinases, have also been implicated in neutrophil degranulation, although the mechanism of tyrosine activation through GPCRs is poorly understood.

Neutrophils express 3 members of the src tyrosine kinase family - Hck, Fgr and Lyn – all of which are activated by fMLP-GPCR ligation²⁴⁸; their inhibition (by Src family kinase inhibitor PP1) prevents the release of all granule subsets²⁴⁹. Research performed with Hck^{-/-}Fgr^{-/-} double and Hck^{-/-}Fgr^{-/-}Lyn^{-/-} triple knockout neutrophils showed that deficiency in these kinases leads to a failure of granule release and also impaired ROS production in response to fMLP^{249,249–251}. Src kinase deficiency also resulted in reduced activation of JNK (c-Jun N-terminal kinase) and p38 MAPK (mitogen-activated protein

kinase) and impaired activation of Rac, but did not affect Ca²⁺ signalling, suggesting that these pathways may mediate parallel non-Ca²⁺-dependent events required for degranulation and/or the downstream effects of Ca²⁺. Further studies have shown that the different Src tyrosine kinases have a particular affinity for certain granule populations suggesting separate and regulated release of different granule populations; for example Fgr associates with the specific granules²⁵², whereas Hck associates with the azurophil granules²⁵³.

The Src family of tyrosine kinases has a number of known downstream targets, which affect degranulation; Hck and Fgr have been shown to regulate the activation of the Rho guanine exchange factor (GEF) Vav1 to signal through Rac, inducing actin polymerisation and ROS release²⁵¹. Additionally, the Src family kinases have been shown to work upstream of p38 MAPK as Hck^{-/-}Fgr^{-/-}Lyn^{-/-} triple knockout neutrophils show reduced p38 MAPK activity and the p38 MAPK inhibitor SB203580 led to reduced azurophil and specific granule release^{249,254}.

Data from Simard et al.²⁵⁵ also support a role for p38 MAPK, but not ERK (extracellular signal-regulated kinase)1/2 in neutrophil degranulation. They showed that S100A9, a pro-inflammatory protein present in the neutrophil cytosol (and also expressed by activated endothelial and epithelial cells), induced degranulation via a p38 MAPK-dependent pathway. Other cytoplasmic tyrosine kinases that are expressed in neutrophils and have been implicated in degranulation are Syk and PyK2 (proline rich kinase2). Syk works downstream of integrin signalling and is involved in actin and microtubulin polymerisation; Syk deficiency impairs integrin- and Fc-mediated receptor-mediated neutrophil activation resulting in defective adhesion, ROS production and degranulation²⁵⁶ and impaired neutrophil-dependent host defence *in vivo*²⁵⁷. Pyk2 is activated upon integrin ligation and subsequent association with Src family kinases²⁵⁸. Kamen et al.²⁵⁹ showed that Pyk2 participates in cell migration and degranulation, as Pyk2 deficient mouse neutrophils display impaired adhesion- dependent degranulation.

Recently proteomic approaches have been employed to help identify the downstream targets of protein kinases including Hck and Fgr. Luerman et al.²⁶⁰, identified phosphoproteins that were associated with the gelatinase and specific granules after fMLP stimulation, supplying new candidates that may potentially play a role in degranulation including known regulators of vesicle trafficking. Several potential regulators of

membrane trafficking and exocytosis were identified in this screen, including *N*-ethylmaleimide sensitive factor (NSF), small molecular weight GTPases, GTPase regulators and effectors, and proteins known to regulate cytoskeletal re-arrangement and stability.

1.6.5 GTPase signalling in degranulation

GTP-binding proteins act as molecular switches in processes such as cell survival, transcriptional regulation and vesicle trafficking, cycling between active (GTP-bound) and inactive (GDP-bound) states²²⁹, with their activity regulated by GEFs. Two GTP-binding proteins (Rho and Rac) have emerged as major players in cytoskeletal re-organisation, directed migration of neutrophils (chemotaxis) and degranulation^{261,262}. Rac is present as 3 isoforms; Rac1, Rac2 and Rac3. Although both Rac1 and Rac2 are expressed in neutrophils, Rac2 predominates in human cells²⁶³, while mouse neutrophils also express Rac1 in addition to Rac 2. It has been shown that Rac2 plays an essential role in neutrophil degranulation; genetic deletion of Rac2 in mice affects cytoskeletal re-organisation and leads to complete loss of azurophil granule release from murine bone marrow neutrophils^{83,264}.

However, specific and gelatinase granule release is not altered in Rac2^{-/-} neutrophils; this suggests a non-redundant role for Rac2 in azurophil granule release only. It is possible that Rac1, which is present in mouse but not human neutrophils, supports specific and gelatinase granule release in this context, whilst Rac2 might still support such a function in human cells. A recent paper from Baier et al.²⁶⁵ investigated the role of Rac1 and Rac2 antigen-stimulated exocytosis in mast cells. Their data suggest that Rac isoforms play distinct roles in mast cell exocytosis, with Rac1 mediating membrane ruffling and Rac2 signalling calcium influx. Rac2^{-/-} neutrophils have also been shown to exhibit impaired adhesion²⁶⁶, likely due to impaired Rac2-mediated actin re-organisation. Data produced by Mitchell et al.²⁶⁷ showed that fMLP-mediated azurophil granule release was enhanced by compounds such as Latrunculin B and Cytochalasin B, which mediate actin-depolymerisation, but the opposite effect (reduced degranulation) occurred on F-actin stabilisation by Jasplakinolide or on inhibition of actin remodelling by the small molecule Rac inhibitor NSC23766.

The exact signalling pathway(s) mediating Rac-dependent degranulation are still under investigation, but a number of possible downstream targets have recently been

identified^{268,269}. For example, the GEF P-Rex-I is activated by PIP₃ and regulates Rac directly²⁶⁸ and also indirectly by acting as a GEF for the upstream GTPase RhoG²⁶⁹. Although this pathway might link PI3K signalling to actin polymerisation via Rac, Welch et al.²⁷⁰ have also shown that P-Rex1 is not an essential regulator of neutrophil degranulation. p21-activated kinase (PAK) is a well-established Rac binding protein that is known to regulate the conformation of the actin cytoskeleton and hence motility of mammalian cells²⁷¹. PAK is activated upon fMLP stimulation of neutrophils and accumulates at the actin-rich leading edge, thus implicating this serine/threonine kinase in Rac-dependent actin remodelling in this setting. PAK inhibition impaired neutrophil polarisation and directional migration towards an fMLP gradient, and was associated with dysregulated Ca²⁺ signalling²⁷². A similar role for PAK in mast cells was found by Allen et al.²⁷³ who demonstrated importantly that PAK plays a role in mast cell degranulation through its effects on Ca²⁺ signalling and cytoskeletal remodelling.

Together these data suggest a possible role for PAK in neutrophil degranulation, as mast cell signalling pathways has been shown to have some parallels with the analagous neutrophil pathways^{274,275}. More recent proteomic studies (eg *Eitzen et al.*²⁷⁶) have identified further novel proteins that may play a role in Rac-mediated degranulation including actin remodelling proteins such as HSP60, the F-actin binding protein coronin-1A, and the F-actin capping protein (CapZ-β); as yet however the relevance of these findings is unclear. Rho-family kinases such as Rac are mainly involved in the early phase of exocytosis that is dependent on actin cytoskeletal remodelling. Another family of GTPases - the Rab family - have been implicated in the more downstream aspects of exocytosis including vesicle transport and docking^{277,278}. Chaudhuri et al.²⁷⁹ identified 3 Rab GTPases that co-purify with neutrophil granules, namely Rab3, Rab4 and Rab5. The role for Rab3 and Rab4 in neutrophil degranulation is currently unknown, but Rab5a directs intracellular fusion of granules with pathogen-containing phagosomes²⁸⁰. Additional Rab isoforms mediate vesicle docking in other cell types including neural and endocrine cells (Rab3)^{281,282} and cytotoxic T-cells (Rab27)²⁸³. Thus a range of GTPases are involved in various steps of the degranulation signalling pathway, but more information is needed to elucidate their exact function(s) in the neutrophil.

1.6.6 SNAP/SNARE proteins in degranulation

The pathways linking intracellular Ca^{2+} transients and degranulation are not fully understood, but are thought to involve SNAP receptor (SNARE) proteins, which are important in vesicle docking and fusion²⁸⁴. This system consists of the recognition of a membrane-bound ligand present in the granule membrane by a membrane-bound receptor on the target membrane²⁸⁵. A range of SNARE proteins have been identified in neutrophils, including vesicle-associated membrane protein-2 (VAMP-2), which is located on the membrane of secretory vesicles, gelatinase and specific granules²⁸⁶, syntaxin-4 and -6, which can be found at the plasma membrane^{286,287}, and synaptosome-associated proteins (SNAPs)-23 and 25, which are present mainly on the peroxidase negative granules (specific and gelatinase granules)^{286,288,289}.

Another SNARE protein found in neutrophils, syntaxin-11, is located predominantly on the azurophil granule membrane with some expression on the selective and gelatinase granules. The density of VAMP-2 corresponds to the hierarchy of degranulation, and antibodies against SNAP-23 and syntaxin-6 inhibit Ca^{2+} -induced secretion of the specific granules and the azurophil granules respectively²⁸⁹. SNARE proteins have shown to interact with other proteins to regulate degranulation including SNARE-interacting Sec1/Munc18 family members. Brochetta et al.²⁹⁰ show that Munc18-2 and Munc18-3 are expressed by neutrophils, interact with SNARE proteins syntaxin-3 (Munc18-2) and syntaxin-4 (Munc18-3), and are associated with neutrophil granules. Both Munc18-2 and Munc18-3 can also be found in plasma membrane fractions and in the cytoplasm, where they associate with cytoskeletal elements. Upon stimulation both isoforms are redistributed to the granule and plasma membrane and Munc18-2 inhibition by antibodies blocks primary granule release²⁹⁰. Zhao et al.²⁹¹ provided further evidence to support a role for Munc18-2 in neutrophil degranulation; they found that mutations in the Munc18-2 gene cause the rare genetic disorder familial haemophagocytic lymphohistiocytosis (FHL) type 5, and lead to a profound defect of neutrophil granule mobilisation and consequently impaired bacterial killing.

Thus there are still many gaps in our knowledge of the signalling pathways regulating the key neutrophil function of degranulation. There is evidence that both separate and overlapping pathways exist to control the release of the differing granule populations, and greater understanding of these details could provide ways to inhibit or promote the release of individual granule populations without affecting other neutrophil functions.

This could allow either novel investigative techniques and reveal new therapeutic avenues.

1.7 Effects of cigarette smoke on neutrophils

COPD is characterised by persistent local and systemic inflammation, leading to a progressive decline in lung function. Cigarette smoke (CS) is the main risk factor for the development of COPD, although the majority of smokers do not develop this disease. Even after smoking cessation patients with established COPD exhibit a continuous cycle of airway inflammation leading to ongoing decline in lung function²⁹², indicating persistent activation of inflammatory cells. CS is a multicomponent mixture of gas-phase and particle-phase toxins with known immunomodulatory function, carcinogenic activity, and addictive activities. Components of CS include metals, volatile hydrocarbons, gas-phase components such as carbon monoxide, polycyclic aromatic hydrocarbons (PAHs), acrolein, and reactive oxygen species. Since exposure of submerged culture cells to CS is difficult to achieve in the laboratory setting, cells are usually exposed to either CS extract (CSE, obtained by condensing CS in a cold trap) or CS medium (CSM), which is prepared by bubbling CS through a tissue culture medium; the content and properties of CSM and CSE may differ, perhaps giving rise to the rather surprising variability of results in the reported literature.

As with the direct installation of NE, exposure of mice to CS recapitulates emphysema, and neutrophil recruitment is a key component of this model^{293–295}. Since neutrophils are thought to play a key role in COPD pathogenesis, the direct effects of cigarette smoke on neutrophils has been investigated *in vitro*, albeit to a somewhat limited extent. Koethe et al.²⁹⁶ detected a priming effect of CSE on neutrophils, leading to increased NE release and ROS generation on stimulation with fMLP. They also suggested that CSE induced an increase in fMLP receptor and integrin expression on the neutrophil membrane. In contrast to these results, Zappacosta et al.²⁹⁷ and Matthews et al.²⁹⁸ found a reduction in stimulated neutrophil ROS formation following CSM pre-incubation, whilst Mortaz et al.²⁹⁹ and Overbeek et al.³⁰⁰ found that CSM induced the production of reactive oxygen species, IL-8, NE, MMP-2 and MMP-9 directly. The variability in these results may reflect significant inconsistencies in the methodology used, for example differing pre-treatment times and the use of CSM or CSE; overall however the results suggest that cigarette smoke may induce a neutrophil phenotype that is detrimental to defence from

infection but which promotes tissue injury. These effects are similar to the effects of hypoxia; however the synergistic effects of hypoxia and cigarette smoke have not been previously investigated.

1.8 Hypoxia

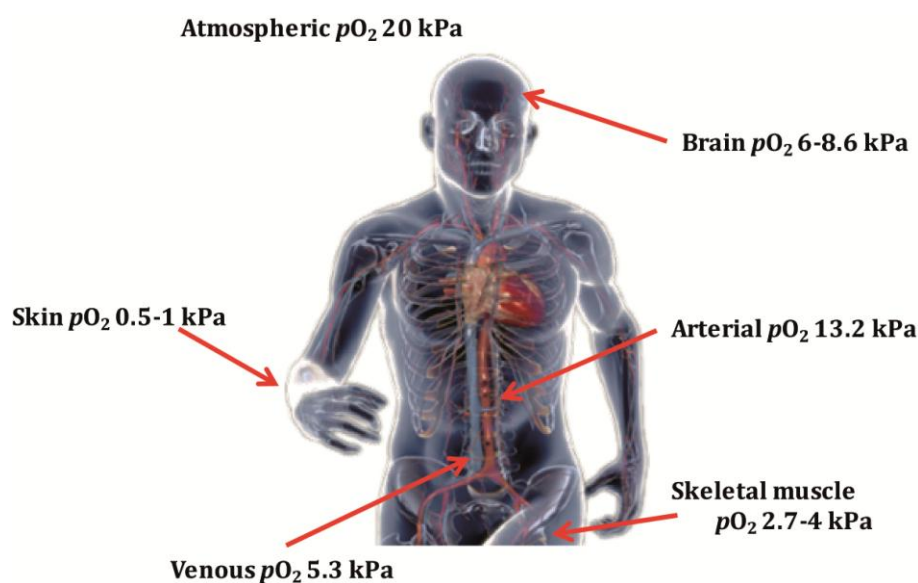
1.8.1 Physiological and pathological hypoxia

A range of oxygen tensions exist throughout the body even under physiological circumstances, ranging from 13 kPa in the arterial blood to 2.3 kPa in the spleen³⁰¹, with even lower oxygen tensions of around 0.5-1 kPa in the skin³⁰², skeletal muscle³⁰³ and gut wall³⁰⁴ (Figure 1.8A). Different oxygen tensions exist even within a single organ such as the liver, from 0.13 kPa in the venous sinusoid to 8 kPa in the portal regions^{305,306}. Cells present in the circulation such as leukocytes are exposed to oxygen tensions varying from around 13 kPa in the alveolar capillaries to approximately 5 kPa in mixed venous blood and venous capillaries. Upon migration to the lymphoid organs leukocytes may be exposed to oxygen tensions as low as 0.5 kPa³⁰⁷. Although these oxygen tensions are extremely low, this cannot be called hypoxia as this is a normal physiological state for these cells and or organs. Generally hypoxia exists because there is an insufficient supply of oxygen in relation to demand. Physiological hypoxia occurs when there is an inadequate supply of oxygen to the body as a whole as for example at high altitude.

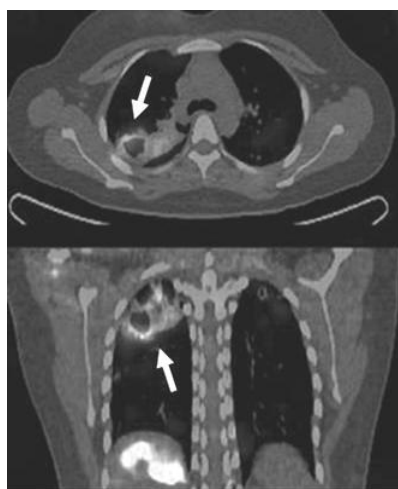
Pathological hypoxia occurs often at sites of infection and injury. Hypoxia in this setting can be caused by impaired blood flow, leading to a disruption of oxygen delivery, and/or by influx of inflammatory cells creating a situation where oxygen demand exceeds supply. Pathological tissue hypoxia (and in some situations systemic hypoxia) is a prominent feature in many disease states, and has been reported to have both positive and detrimental effects. Campbell and colleagues³⁰⁸ have shown that neutrophil-dependent depletion of oxygen is integral to and promotes the resolution of inflammation in a mouse colitis model. Additionally, there are data demonstrating that hypoxia with subsequent HIF-1 α stabilisation (section 1.8.3.1) plays an important role in wound healing^{309, 310,311}. Whereas HIF-1 α stabilisation promotes wound healing, HIF-2 α deletion induced an accelerated rate of wound closure³¹¹

In the setting of liver transplantation, ischaemic pre-conditioning (10 min vascular clamping) prior to organ harvest improved biochemical markers of liver function and reduced liver donor cell apoptosis and transplant non-function³¹². Such ischaemic pre-

A



B



C

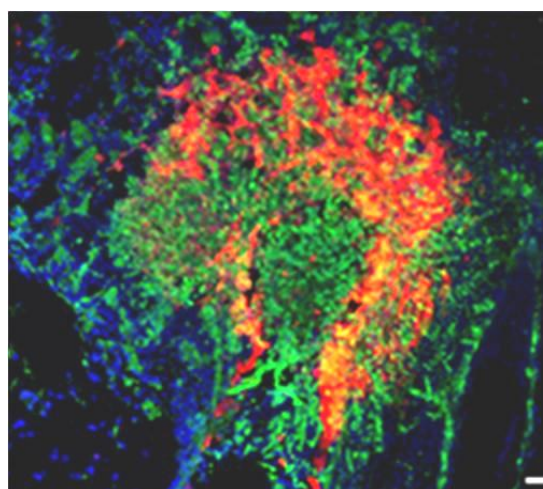


Figure 1.8: Hypoxia is present in physiological and pathological circumstances.

A. A range of different oxygen tensions exist throughout the body under physiological circumstances; ranging from 13 kPa in the arterial blood to 6 kPa in the brain and substantially lower oxygen tensions of around 0.5-3 kPa in the skin, muscle and gut. B. Axial and coronal PET-CT images of a human patient with pulmonary tuberculosis. The presence of hypoxic areas (white areas, see arrows) is shown using the hypoxia tracer [^{18}F] F-MISO (adapted from Belton et al.³¹³) C. Local tissue hypoxia is present in inflammation as demonstrated in this image which shows a section of mouse lung infected with *Aspergillus spp* and stained for the pathogen (green), inflammatory cells (blue) and for hypoxic areas with hypoxyprobe-1 (red, adapted from Grahl et al.³¹⁴).

conditioning has been tested in other clinical settings and is thought to work by pre-adapting the organ or tissue to hypoxia and hence reducing subsequent ischaemia-reperfusion injury (reviewed by Brooks and Andrews³¹⁵). Even more remarkably, brief cycles of ischemia and reperfusion in the arm or leg may protect the heart against injury following coronary artery occlusion and reperfusion, a phenomenon known as remote ischemic pre-conditioning. The mechanism by which this technique confers benefit is uncertain; whilst one group found that the value of remote ischaemia was dependent on HIF-mediated IL-10 transcription³¹⁶, another group found that HIF up-regulation was not required³¹⁷. In contrast, the physiological responses to hypoxia have been shown to be detrimental in other pathological settings. An example of this is tumour formation. Tumours are often hypoxic³¹⁸ due to rapid cell proliferation and insufficient or disorganized neovascularisation and tumour hypoxia is associated with resistance to chemotherapy and tumour metastasis. HIF-1 regulates glycolysis and the pentose phosphate pathway, and these cellular metabolic pathways increase the antioxidant capacity of tumours, thereby countering the oxidative stress caused by irradiation. HIF-1 upregulation further stimulates tumour cells to produce VEGF and other pro-angiogenic factors, which induce angiogenesis and protect the microvasculature from radiation-induced endothelial apoptosis.

Hypoxia has also been shown to play a role in a range of other diseases; it up-regulates RAGE receptor expression in murine and human cystic fibrosis and its expression is associated with infection related, lung disease severity³¹⁹. Belton et al.³¹³ show the presence of hypoxic areas in patients with *Mycobacterium tuberculosis* (MTB); this was demonstrated using PET-CT scanning and the hypoxia tracer [¹⁸F] F-MISO (Figure 18B); hypoxia potently upregulated MMP-1 in MTB-stimulated primary human monocyte-derived macrophages and in respiratory epithelial cells, and these proteases may contribute to the tissue damage (cavitation) that is so characteristic of this infection.

Others have shown that hypoxia induces an endothelial cell response similar to that seen in systemic inflammation, with upregulation of IL-1³²⁰, IL-6³²¹, IL-8³²², PAF and ICAM-1 expression^{323,324}. Changes in oxygen tension and HIF activation have a profound effect on cell function as described below. However, hypoxia may also exert HIF-independent effects, and there is limited knowledge about primary human cell function under hypoxia, especially in relation to the immune system. This is of significance, since sites of infection and injury can be profoundly hypoxic. Hypoxia in this setting can be caused by

impaired blood flow, leading to a disruption of oxygen delivery, and/or by influx of inflammatory cells creating a situation where oxygen demand exceeds supply. An illustration of local hypoxia in the setting of inflammation is shown in Figure 1.8C; in this image³¹⁴ a section of mouse lung infected with *Aspergillus spp.* has been stained for hypoxia with hypoxyprobe-1 (red); hypoxyprobe or pimonidazole is a commercial research tool that forms adducts within a cell at oxygen tensions lower than 1.3 kPa and labelled secondary antibodies to hypoxyprobe can then be used as a counter stain. Work by Niinikoski et al.³²⁵ further showed that the presence of bacterial infection causes additional wound hypoxia; whilst in uninfected wounds the oxygen tension rose from 0.9 to 3.9 kPa during healing, in the infected wounds the oxygen tension dropped even further to near anoxic levels. Tissue hypoxia has also been demonstrated directly in humans in head and neck tumours by Rademakers et al.³²⁶, who injected subjects with pimonidazole prior to biopsy and showed co-localization of pimonidazole staining with HIF-1 α stabilisation and a number of metabolic markers of hypoxia.

Above examples are ways to measure the presence of “pathological hypoxia” *in-vivo*. The term hypoxia (*In-vitro* hypoxia or “experimental hypoxia”) as used in the literature generally indicates the use of oxygen levels of approximately 1% O₂ (\pm 3 kPa) in the case of cell based work³²⁷ and around 15% O₂ in case human volunteers³²⁸. However, as mentioned above these are oxygen tensions that immune cells like neutrophils encounter in physiological situations, so whether “experimental hypoxia” mimics “pathological hypoxia” is an important question.

1.8.2 Cellular requirements for oxygen

Oxygen is vital for cellular energy production and is utilised mainly through a metabolic pathway called oxidative phosphorylation, in which ATP is formed as a result of the transfer of electrons from NADH or FADH₂ to O₂ by a series of electron carriers in the mitochondria. Oxidative phosphorylation is highly efficient and generates 26 of the 30 molecules of ATP that are formed when a single glucose moiety is completely oxidized to CO₂ and H₂O, and is the major source of ATP in aerobic organisms³²⁹. However, neutrophils contain relatively few mitochondria^{330,331} and due to the need to function at very low oxygen tensions have adapted to function predominantly (although not exclusively) by anaerobic metabolism³³² in the form of glycolysis. During glycolysis, glucose or glycogen is converted into pyruvate by a range of enzyme-catalysed reactions.

This pathway is less efficient as the net gain is only 2 molecules of ATP. Key enzymes that play a role in glycolysis have shown to be upregulated under hypoxic conditions including glyceraldehyde-3-phosphate dehydrogenase^{333,334} and triose-phosphate isomerase-1³³⁵.

1.8.3 Mechanism of oxygen sensing

Due to the importance of oxygenation of tissues and the wide range of effects hypoxia has on cellular function, the human body has sensitive mechanisms in place to monitor oxygen tensions and induce appropriate responses at both systemic and cellular levels. An organ that plays an important role in oxygen tension in the body is the carotid body. This is a neural crest-derived, highly vascularised organ, located at the bifurcation of the carotid arteries, whose major function is to detect changes in blood oxygen tension. In the carotid body, low arterial blood oxygen tensions lead to inhibition of the K⁺ channels and hence glomus cell membrane depolarisation, resulting in Ca²⁺ channel opening, increased cytosolic Ca²⁺ concentration and the release of transmitters such as catecholamines³³⁶; this results in respiratory and cardiovascular reflexes that attempt to restore oxygenation in the vital organs³³⁷. On a cellular level the HIF signalling pathway fulfils the role of oxygen sensing.

1.8.3.1 Oxygen sensing—the prolyl-4-hydroxylase-HIF signalling pathway

HIF transcription factors are crucial mediators of the cellular hypoxic response. They are heterodimers consisting of one of three major oxygen-sensitive HIF- α subunits (HIF-1 α , HIF-2 α or HIF-3 α) and a constitutively expressed subunit HIF-1 β (also known as aryl hydrocarbon receptor nuclear translocator or ARNT). Of the HIF- α subunits HIF-1 α and HIF-2 α are the most studied. Under normoxic conditions, *HIF1/2A* is continuously transcribed and translated to HIF-1/2 α protein, which is rapidly hydroxylated and degraded by the ubiquitin-proteasome pathway, and hence normally present at very low levels. HIF-1 α stability is regulated by the activity of a class of oxygen-, 2-oxoglutarate-, and iron-dependent enzymes known as the prolyl-4-hydroxylases or PHDs³³⁸. PHDs hydroxylate the two specific proline residues pro402 and pro564 within the oxygen degradation domain (ODD) of HIF-1 α ^{338,339}. Hydroxylation of HIF-1/2 α allows it to bind to the VHL (Von Hippel Lindau) tumour suppressor protein, that acts as a recognition component of the E3 ubiquitin ligase complex. Hydroxylated HIF-1/2 α becomes

polyubiquitinated at three lysines in the central ODD domain and is hence directed to the 26S proteasome for degradation³⁴⁰. The half-life of HIF-1 α is <5 minutes in normoxic conditions³⁴¹. As intracellular oxygen levels drop below 200 $\mu\text{mol/L}$, or if iron levels become limiting, PHDs fail to hydroxylate the proline residues within ODD of HIF-1/2 α . The un-hydroxylated protein is not a substrate for the ubiquitin ligase, and thus becomes stabilised and translocates to the nucleus. This oxygen-sensing mechanism is ubiquitous and, allows cells such as neutrophils to function effectively over a range of pathophysiological oxygen tensions³⁴² (Figure 1.9).

A second protein regulating HIF-1/2 α activity is Factor inhibiting HIF (FIH), which renders HIF-1 α transcriptionally inactive by hydroxylation of asparagine 803, thereby inhibiting its interaction with co-activators p300 and CREB binding protein (CBP). Following hypoxic stabilisation, HIF-1/2 α migrates to the nucleus, where it forms a heterodimer with HIF-1 β . This heterodimer binds to specific DNA binding sites (A/(G)CGTG) called hypoxic response elements (HREs) located in the promoter regions of a large number of genes (a list of HIF targets is given in Appendix 2), inducing their transcription and modulating cell functions including cell migration, growth and apoptosis, energy metabolism, matrix and barrier function, and angiogenic signalling³⁴³.

1.8.3.2 Effects of hypoxia and HIF on cell signalling

The biology of HIF signalling has been investigated by both transgenic knockout (KO) and over-expression mouse models. Targeted homozygous inactivation of HIF-1/2 α ^{344,345} or HIF-1 β ³⁴⁶ in the mouse is embryonically lethal, due to abnormal vascular development. Mice with heterozygous defects of HIF-1 α have a reduced protective effect of hypoxic preconditioning in a model of cardiac ischemia³⁴⁷ (see above) and display very different carotid body neural activity and ventilatory adaptation to chronic hypoxia³⁴⁸. The role of HIF-1 α in individual cell lineages has been explored using Cre-transgenics, and this approach has demonstrated that in addition to hypoxia adaption, HIF-1 α is required for normal physiological functions in a range of settings, in particular in the immune system^{349,350}. Both of these studies show that HIF-1 α deficient myeloid cells have profound defects in key effector functions including; adhesion, migration, chemotaxis, matrix invasion and bactericidal capacity. Peyssonnaud et al.³⁵⁰ also found that HIF-1 α -null neutrophils showed decreased enzymatic activity and protease content in comparison to WT neutrophils, while vHL-null neutrophils exhibited increased protease activity; this

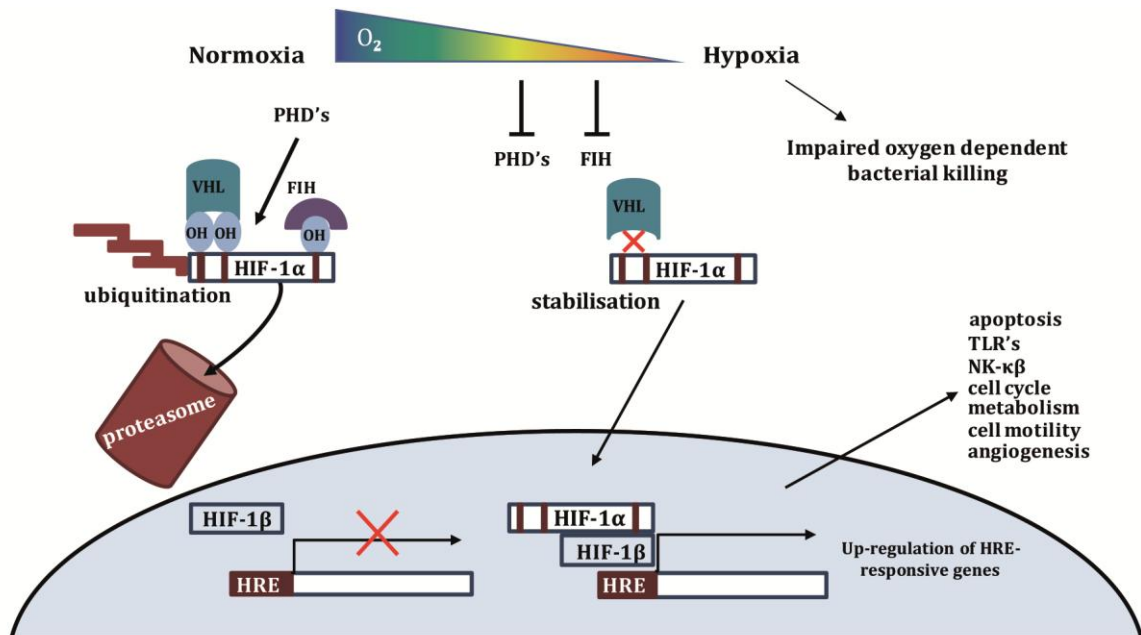


Figure 1.9: Hypoxia inducible factor regulates most cell responses to hypoxia

Classically, cells respond to changes in oxygen levels by means of hypoxia inducible factor (HIF)-mediated signalling. Under normal conditions the HIF-1 α subunit is hydroxylated by the prolyl hydroxylases (PHD's). This allows von Hippel-Lindau factor (VHL) to bind to HIF-1 α , targeting it for degradation by the proteasome. The PHDs exhibit reduced activity under hypoxic conditions, impairing VHL binding to HIF-1 α . This allows HIF-1 α to stabilize and migrate to the nucleus, where it forms a heterodimer with HIF-1 β . This heterodimer binds to hypoxic response elements (HREs) on a number of genes inducing their transcription.

is discussed in more detail below (section 1.8.5). The role of the HIF oxygen-sensing pathway in inflammation is supported further by a study of Walmsley et al.³⁵¹ showing that PHD3-deficient mice subjected to acute lung injury have increased levels of neutrophil apoptosis and clearance. However, PHD deficiency affected neutrophil apoptosis in the presence of preserved HIF transcriptional activity, indicating a likely specific function for PHD3 in regulating neutrophil apoptosis under hypoxic conditions.

Pharmacological approaches can also be used to interrogate the HIF signalling pathway, in particular the use of HIF-1 α stabilizers. There are 3 compounds that are widely employed; dimethyloxalylglycine (DMOG), desferrioxamine mesylate (DFO) and cobalt chloride (CoCl₂). These compounds each work in a slightly different way but all lead to the stabilisation of HIF. DMOG is a 2-oxoglutarate analogue that acts as a competitive inhibitor of PHDs and FIH. DFO is an iron chelator, and chelation of Fe²⁺ bound to the active site of PHD inhibits its enzymatic activity. CoCl₂ also works as an iron chelator, but has also been reported to bind to the PAS domain, blocking HIF-1 α -pVHL binding and thereby increasing HIF-1 α stability³⁵². Work with these HIF-1 α stabilizers and with transgenic mice has helped identify many HIF targets and functions, although much remains to be discovered. There are data, mainly in immune cells, linking some of the effects of HIF-1 α to the NF κ B pathway. NF κ B is a family of dimeric transcription factors that play an important role in regulating cytokine production, cell proliferation, differentiation, adhesion, survival and apoptosis (as reviewed by Baeuerle et al.³⁵³). In resting cells NF κ B is present in an inactive, I κ B-bound form. NF κ B activation is induced by ligands such as TNF α , which prompt the activation of the I κ k complex and induce a phosphorylation-dependent degradation of I κ B, allowing NF κ B to migrate to the nucleus and activate target genes. Walmsley et al.³⁵⁴ have shown that the hypoxia-induced survival of neutrophils is mediated by HIF-1 α dependent NF κ B activation. Additional support for crosstalk between these pathways comes from Cockman et al.³⁵⁵ who showed that FIH can hydroxylate ankyrin repeats in p105 (NF κ B1) and I κ B α in an oxygen-dependent manner, and Dyugovskaya et al.³⁵⁶, who show that NF κ B plays an essential role in neutrophil survival after intermittent hypoxic exposure. Interestingly, Culver et al.³⁵⁷ demonstrated a HIF-independent mechanism of hypoxic NF κ B activation, with hypoxic stress leading to I κ B kinase activity through a calcium/calmodulin kinase dependent pathway. Hypoxia has also been shown to modulate a number of other key cell signalling molecules *in vitro* including p38 MAPK³⁵⁸, PKC, and Src family kinases³⁵⁹,

indicating that hypoxia can activate multiple stress-activated signalling pathways; much of this data is derived from studies on rat neural cells or rat cardiac myocytes. Of possible relevance to neutrophil degranulation, the GTPase Rac and the actin-binding protein Filamin A (FLNA) have recently been identified as hypoxia targets. Misra et al.³⁶⁰ demonstrated that hypoxia increased localisation of Rac1 to the plasma membrane, leading to increased cell motility indicating a role in tumour metastasis. Although human neutrophils preferentially express Rac2, these GTPases have a high degree of sequence homology and many overlapping functions, hence this could be relevant to human neutrophil degranulation in the hypoxic setting. Filamin A (FLNA) is a large actin-binding protein that is widely expressed, and stabilises 3-dimensional (3D) actin webs and links them to cellular membranes³⁶¹. Zheng et al.³⁶² showed that FLNA interacts with HIF-1 α but not HIF-2 α in melanoma cell lines, increasing nuclear localisation of HIF-1 α . HIF-1 α can also be activated in a hypoxia-independent manner, as shown by Peyssonnaud et al.³⁵⁰ using exposure of WT mouse monocytes to a range of pathogens and inflammatory agents such as LPS³⁶³. On phagocytosis of group A *Streptococcus*, *Staphylococcus* or *Salmonella* spp, macrophages upregulated HIF-1 α expression to levels similar to those found under hypoxia. In addition, LPS induced HIF-stabilisation and downregulated PHD2 and PHD3 mRNA. These experiments indicate that HIF-1 α regulates myeloid cell function in inflammation, not solely in the context of hypoxia.

1.8.3.3 The roles of HIF-1 α and HIF-2 α in neutrophil function

HIF-2 α was identified in 1997^{364–366} and HIF-1 α and HIF-2 α can regulate the expression of many hypoxia-induced genes, although each HIF- α isoform has unique targets. Their stabilisation kinetics are also different; HIF-2 α stabilisation is delayed, but more sustained in comparison to HIF-1 α stabilisation. The biological actions of HIF-2 α in response to hypoxia are distinct from those of HIF-1 α (reviewed by Loboda et al.³⁶⁷). HIF-2 α -mediated signalling is of particular importance in erythropoiesis³⁶⁸, iron homeostasis³⁰⁹, metabolism^{369,370–372}, vascular permeability³⁷³, and tumour biology and angiogenesis (reviewed by Keith et al.³⁷⁴). The role of HIF-2 α in immunity has been less extensively investigated than that of HIF-1 α . However, Elks et al.³⁷⁵ showed that in a zebrafish model of TB, HIF-1 α and HIF-2 α in neutrophils have opposing effects on host susceptibility to mycobacterial infection via modulation of inducible nitric oxide synthase (iNOS) signalling at early stages of infection; stabilisation of HIF-1 α or deletion of HIF-

2 α lead to increased levels of reactive nitrogen species and reduced the mycobacterial burden in this model. Thompson et al.³⁷⁶ have recently also delineated a role for HIF-2 α in human neutrophil longevity. Neutrophils derived from 3 patients with gain-of-function mutations in HIF-2 α , display a reduction in constitutive apoptosis, although HIF stabilizers were able to further delay apoptosis in these cells. Neutrophils from these patients showed increased HIF-2 α target gene expression (VEGF, PAI1 and PHD3), but chemotaxis, respiratory burst and phagocytosis were unaffected. Finally, Thompson and colleagues showed that HIF-2 α deficiency reduced neutrophilic inflammation, lung damage and vascular leak in a mouse model of LPS-mediated lung injury. These studies indicate that HIF-2 α is emerging as an important regulator of neutrophil function and inflammation. Due to the temporal differences in expression of the two isoforms it is possible that HIF-1 α plays a major role in the initial stages of infection where as HIF-2 α mainly plays a role modulating neutrophil function in the resolution phase of the inflammation

1.8.4 Neutrophil function under hypoxic conditions

Neutrophils play an important function in the inflammatory response and their function is profoundly affected by hypoxia. Using a Cre-targeted myeloid HIF-1 α knockout mouse, Cramer et al.³⁴⁹ removed the myeloid cells' capacity to adapt to hypoxia, leading to a drop in the glycolytic capacity of these cells; this resulted in a substantial impairment of myeloid cell adhesion, migration and bacterial killing. Hypoxia has been shown to alter the phenotype and function of human neutrophils *in vitro*. Work by Mecklenburgh et al.³⁷⁷ demonstrated that neutrophil apoptosis was delayed by exposure to hypoxia or by iron chelation, suggesting an important role for HIF in determining neutrophil lifespan. Further work by Walmsley et al.³⁵⁴ confirmed a role for HIF-1 α in this effect, since neutrophils derived from the HIF-1 α conditional knockout mice described above showed increased apoptosis under conditions of hypoxia.

McGovern et al.³²⁷ demonstrated that hypoxia affects neutrophil function as well as lifespan; hypoxia compromised the neutrophil's ability to mount a respiratory burst in response to "primed stimulation" (GM-CSF/fMLP), stimulation (PMA), and even ingested particles (zymosan). As a consequence bactericidal capacity to *S. aureus* was also impaired. The impairment of bacterial killing was postulated to be due to a lack of molecular oxygen as a substrate for ROS production, since re-oxygenation of the cells

rapidly restored both the oxidative burst and killing of *S. aureus*. Of note, hypoxia did not prevent phagocytosis or shape change in response to IL-8, hence many neutrophil functions appear to be preserved or even augmented at low oxygen tensions. A recent paper from Shuang Ma et al.³⁷⁸ reported that hypoxia increased cell polarisation in response to fMLP in HL-60 cells (a neutrophil-like cell line) and that store-operated calcium entry plays a role in this process.

1.8.5 Neutrophil degranulation under hypoxic conditions

Knowledge of how hypoxia affects neutrophil degranulation is lacking. Published data from our laboratory³⁷⁹ suggested that NE release is increased under hypoxic conditions. Peyssonnaud et al.³⁵⁰ found a role for HIF-1 α in the production of neutrophil granule proteases; HIF-1 α -null neutrophils showed decreased enzymatic activity and protease content in comparison to WT neutrophils, while vHL-null neutrophils exhibited increased protease activity. However this might be caused by developmental differences, as neutrophil granules form during maturation in the profoundly hypoxic environment of the bone marrow, and others^{380,381} have shown that mature circulating neutrophils do not transcribe or translate mRNA for NE or other granule proteins. This probable developmental effect complicates the use of HIF-1 α -null mouse neutrophils to study the role of HIF-1 α in hypoxic degranulation.

The effects of hypoxia on degranulation in other cell types have been studied in a little more depth. There is some evidence that hypoxia can induce mast cell granule release^{382,383}, although others have suggested that this is an indirect effect, mediated by MCP-1 released from hypoxic alveolar macrophages³⁸⁴. Others, like Pinsky et al.³⁸⁵ and Goerge et al.³⁸⁶ have shown that hypoxia induces rapid endothelial cell degranulation. Hypoxic exposure led to exocytosis of endothelial cell Weibel-Palade (WP) bodies, releasing von Willebrand factor (vWF) and increasing expression of the adhesion molecule, P-selectin on the cell surface; Pinsky et al.³⁸⁵ postulated that endothelial WP-body exocytosis occurs during hypothermic/hypoxic cardiac preservation, priming the vasculature to recruit PMNs during reperfusion.

Thus the induction or augmentation of degranulation in other cell types under hypoxia, plus the preliminary data from McGovern et al.³⁷⁹ indicate that hypoxia may modulate neutrophil degranulation. The potential significance of such an effect to a range of disease processes including common and debilitating conditions such as COPD, led me to

hypothesise that hypoxia upregulates neutrophil degranulation, and that this is detrimental to the host in disease settings.

1.9 Summary

Neutrophils are key effectors of the innate immune system and have an array of “weapons” to eliminate pathogens, including abundant granules. These neutrophil granules contain proteins capable of causing substantial tissue damage. Neutrophil degranulation has been shown to be detrimental in a range of disease states, for example the smoking-related lung disease COPD. Neutrophil proteases such as NE, MPO and MMP-9 can degrade extracellular matrix proteins, and are implicated in the pathogenesis of emphysema. However, most physiological stimuli induce minimal extracellular degranulation. Signalling pathways regulating neutrophil degranulation are poorly understood, but include PI3K, PLC and calcium transients. Many tissues such as the skin and gut are hypoxic under physiological circumstances (physiological hypoxia), but sites of inflammation and infection can also be profoundly hypoxic (pathological hypoxia). Hypoxia affects neutrophil function, impairing the generation of reactive oxygen species and reducing bacterial killing. However, little is known about neutrophil degranulation under hypoxic conditions, and this will be the focus of my thesis.

2. Hypothesis & Aims

2.1 Hypothesis

Hypoxia induces a highly destructive neutrophil phenotype with an increased lifespan, a substantial reduction in oxidase-dependent bacterial killing and an increase in their ability to release granule proteins. These effects are exacerbated by cigarette smoke.

2.2 Specific aims

1. To determine whether hypoxia up-regulates the secretion of NE either in isolation, or as part of a more generalised up-regulation of the neutrophil secretory repertoire.
2. To investigate whether cigarette smoke and hypoxia act synergistically to modulate neutrophil degranulation.
3. To explore the effects of hypoxia on neutrophil-mediated tissue injury.
4. To determine the mechanism(s) whereby hypoxia modulates degranulation.

Chapter 3

Materials and Methods

3. Materials and Methods

3.1 Materials

Amersham Biosciences (Buckinghamshire, UK): Percoll®, dextran 500 (mw 500,000, dissolved in sterile 0.9% saline (6% w/v) and stored at 4°C)

AnaSpec EGT group: EGTA (tetrasodium salt, 10 mM)

Baxter Healthcare (Berkshire, UK): Sterile 0.9% sodium chloride

BD Biosciences (Embodegen, Belgium): Falcon polypropylene tubes (50 ml and 15 ml), 50 ml syringes, Falcon flexible 96-well plates, Cellfix™

Cal Biochem: Pan PI3Kinhibitor (LY294002)

Cell Signaling Technology®: cleaved caspase 3 rabbit monoclonal antibody, β-actin polyclonal antibody

Dako: goat anti-mouse horse radish peroxidase (HRP)-conjugated IgG

Fisher Scientific (UK): Keratinocyte serum-free media (VX17005075) + 25 µg/ml bovine pituitary extract, 0.2 ng/ml rEGF, 250 ng/ml puromycin and 25 µg/ml G418.

GE Healthcare (Little Chalfont, UK): ECL (Enhanced Chemiluminescence) system

Hycult Biotechnology (Cambridgeshire, UK): lactoferrin ELISA

Hospira Venisystems : sterile 19 gauge Butterfly needles

Invitrogen: (Paisley, Scotland, UK): Hanks balanced salt solution (HBSS), 5-(and-6)-chloro-methyl-2',7'-dichloro-dihydro-fluorescein-diacetate-acetyl-ester (CM-H2-DC-FDA), secondary antibody (Alexa Fluor 488 – donkey anti-goat IgG), F-actin stain (rhodamine phalloidin), DAPI containing mountant (Gold anti-fade)

Kentucky Tobacco Research & Development centre: 3R4F cigarettes

Life Technologies (Paisley, UK): Iscove's Modified Dulbecco's Medium (IMDM), Enzcheck Elastase assay kit, F-12K medium with 100 U/ml penicillin, 10 µg/ml streptomycin, 25 µg/ml amphotericin B (Invitrogen) and 10% fetal calf serum (GIBCO).

Lonza (Berkshire, UK): human bronchial epithelial cells, bronchial epithelial growth media (BEGM)

Martindale Pharmaceuticals Ltd (Essex, UK): sterile calcium chloride, sterile sodium citrate

Merck Ltd.(Nottingham UK): May/Grünwald/Giemsa stain

National Diagnostics (UK): Protogel (40%), stacking buffer, resolving buffer.

Radiometer (Copenhagen, Denmark): ABL80 Basic automated blood gas machine and calibration reagents

R&D Systems (Oxfordshire, UK): human recombinant granulocyte macrophage colony-stimulating factor (GM-CSF), MMP-9 ELISA DuoSet kit, goat anti rabbit IgG-APC, phospho-kinase antibody array

Ruskin Technologies, (Yorkshire, UK): Ruskin Invivo2 400 hypoxic chamber

Santa Cruz Technology (Germany): neutrophil elastase goat polyclonal antibody, donkey anti-goat HRP-conjugated IgG

Sigma-Aldrich, (Dorset, UK): cytochrome C from equine heart, phorbol 12-myristate 13-acetate (PMA), superoxide dismutase (SOD) from bovine erythrocytes, phosphate buffered saline (PBS) with (PBS⁺) or without (PBS⁻) calcium chloride and magnesium chloride, dimethyl sulfoxide (DMSO), Trypan blue solution (0.4%), cytochalasin B, N-formyl-methionyl-leucyl-phenylalanine (fMLP), tissue culture grade bovine serum albumin (BSA), Tween-20, Tri-reagent, U-73122 (phospholipase C and A₂ inhibitor), trans-styrylacetic acid (PAM inhibitor), poly-L-lysine solution, DMOG, DFO, hydrogen peroxide (30%), o-dianisidine dihydrochloride, TRI reagent[®], PAM inhibitor (4-phenyl 3 butenoic acid), PLC inhibitor (U-73122), PI3K γ inhibitor (AS605240), PI3K δ inhibitor (IC87114), Thapsigargin, Cyclohexamide, Poly-L-lysine solution, glycerol-gelatin, lactate dehydrogenase (LDH), o-dianisidine dihydrochloride (DMB), Triton X-100, polyvinylidene fluoride (PVDF) membrane, 3-[4,5-dimethylthiazol-2-yl]-2,5-diphenyl tetrazolium bromide (MTT)

Qiagen (Manchester, UK): primers for housekeeping genes B2M, 18S, granule proteins NE, MMP-9 and lactoferrin and for hypoxia targets BNIP and GLUT1

VWR International (Leicestershire, UK): DPX mountant, methanol, Eppendorfs (Safe-Lock micro test tube, PCR clean, 2 ml).

3.2 Neutrophil isolation

Ethical permission for taking peripheral blood from healthy volunteers was obtained from the Cambridge Local Research Ethics Committee (REC reference 06/Q0108/281). Neutrophil isolations were performed under sterile conditions in a laminar flow cell culture hood (Microflow Class II cabinet). Sterile polypropylene tubes (Falcon) and reagents were used throughout.

Neutrophils were isolated using dextran sedimentation followed by centrifugation over discontinuous plasma-Percoll® gradients. Blood was taken by venepuncture, performed by a qualified operator using a sterile 19 gauge Butterfly needle (Hospira Venisystems) and 50 ml Plastipak disposable syringes. The blood was carefully transferred into 50 ml tubes (Falcon) containing 4 ml of 3.8% sodium citrate, to a total volume of 40 ml. All subsequent steps were performed at 22°C, unless otherwise stated. The tubes were centrifuged at 310 g for 20 min, to yield platelet rich plasma (PRP) and pellets comprising red cells and leukocytes. The pellets were dextran-sedimented by the addition of 6% dextran-500 (2.5 ml/10 ml of cell pellet). The volume was made up to 50 ml with pre-warmed (37°C) sterile 0.9% saline (Baxter), carefully but thoroughly mixed, and allowed to stand for 30 min to allow erythrocyte sedimentation to occur. The PRP from the initial spin was used to make platelet poor plasma (PPP) and autologous serum; autologous serum was prepared by the addition of 220 µl of 10 mM CaCl₂ to 10 ml of PRP and incubation at 37°C, whilst PPP was prepared by centrifuging the remaining PRP at 1400 g for 20 min. The pellet from this spin (containing the platelets) was discarded and the PPP retained.

After erythrocyte sedimentation, the leukocyte-rich plasma (upper layer) was carefully aspirated from the red cell lower layer and centrifuged at 256 g for 5 min. The pellet (containing mixed leukocytes) was gently re-suspended in 2 ml PPP and transferred to a 15 ml tube (Falcon), where it was under-layered with 2 ml freshly prepared 42% Percoll® in the autologous PPP, which was then further under-layered with 2 ml of freshly prepared 51% Percoll® in PPP. Under-layering was performed using a glass pipette, which had been sterilised by autoclaving (240°C for 4 h). The gradients were centrifuged for 10 min at 150 g, with the brake and acceleration speed set to zero. The mononuclear cells remained at the top interface between the plasma and 42% Percoll® layer, with granulocytes cells ($\geq 95\%$ neutrophils) at the interface of the 42% and 51% layer Percoll® layers (Figure 3.1).

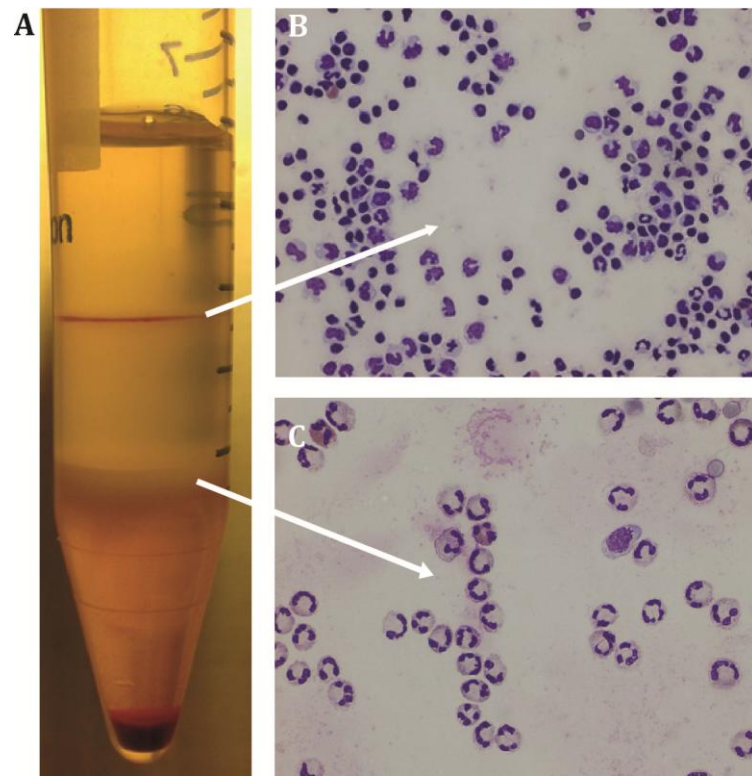


Figure 3.1: Neutrophil isolation using discontinuous plasma-Percoll® gradients

Neutrophils were isolated from healthy volunteers using discontinuous Plasma-Percoll® gradients. A. Photograph of plasma-Percoll® gradients following centrifugation. Mononuclear cells comprise the top interface between the plasma and 42% Percoll® layer, with neutrophils at the interface of the 42% and 51% layer Percoll® layers. B. & C. are representative photomicrographs of cytopins from the upper mononuclear and lower neutrophil layers respectively (x40 magnification).

Each band was aspirated with a Pasteur pipette (Appleton Woods). The granulocyte pellet was washed once in PPP, once in phosphate buffered saline without $\text{Ca}^{2+}/\text{Mg}^{2+}$ (PBS^-) and once in phosphate buffered saline with $\text{Ca}^{2+}/\text{Mg}^{2+}$ (PBS^+), each time by spinning at 256 g for 5 min. Using this method, the neutrophil isolate is >95% pure with less than 1% monocyte contamination. Cytospins were made by centrifugation in a Shandon Cytospin 3 centrifuge (3 min, 300 rpm). To assess purity, the cells were fixed in methanol and subsequently stained with May/Grünwald/Giemsa (Figure 3.1). Cells were counted using light microscopy (Olympus CX31).

3.3 Working under hypoxic conditions

3.3.1 The hypoxic incubator

An In-vivo 400 hypoxic incubator (Ruskin Technology, Figure 3.2A) was used to analyse the effects of hypoxia on neutrophil function. The gas levels in the hood are controlled by the Gas Mixer Q, which calibrates the O_2 sensor automatically through a touch screen control. It controls O_2 levels from 0.0% to 20.9% and CO_2 from 0.0% to 30.0%; O_2 and CO_2 levels are programmable in 0.1% increments. The chamber is supplied with separate feeds of compressed air, nitrogen, carbon dioxide and 10% hydrogen/90% nitrogen. A palladium catalyst can be employed to create anoxic conditions. Thermostatic monitoring controls the temperature, and maximum humidity is limited by controlled condensation. Items can be placed in the chamber via a small mailbox on the side, which is flushed with nitrogen upon closure, thereby preventing re-oxygenation of the hypoxic chamber when adding or removing materials. The chamber contains standard electrical supply points for equipment (such as a micro-centrifuge and thermo-mixer) and the front is removable, thereby allowing equipment to be placed into the chamber when needed. The chamber is maintained at positive pressure above ambient levels and the control unit supplies an appropriate gas mix when the pressure falls. An important general issue is that it is the oxygen tension in the chamber that is being controlled directly, not the oxygen tension experienced by the cells placed within it, which are bathed in tissue culture media. All media to be used in any experimental setting were therefore placed in the hypoxic workstation to equilibrate for at least 3 h prior to use and analysed as documented below (section 3.3.2).

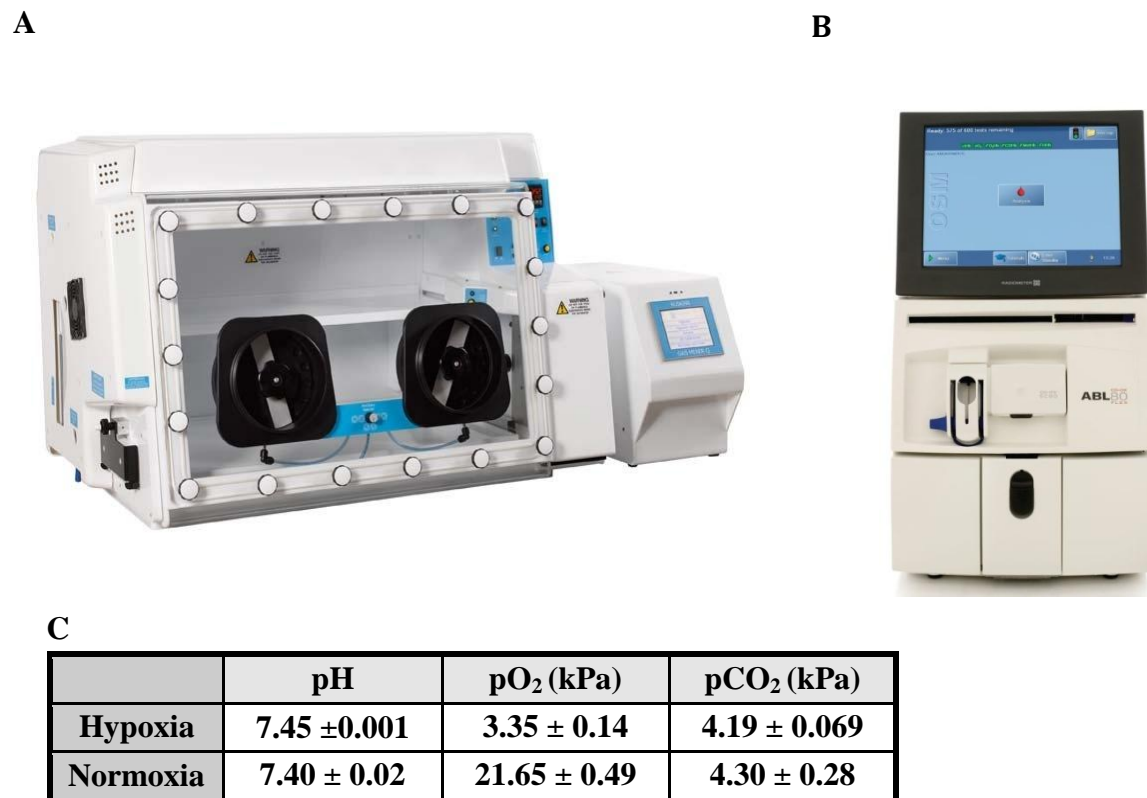


Figure 3.2: Working with the Invivo₂ 400 workstation

A. Ruskin Invivo₂ 400 workstation used to conduct all work under hypoxic conditions. B. Blood gas analyser from Radiometer used to check the pH, pO₂ and pCO₂. C. Blood gas analyser readings (pH, pO₂ and pCO₂) of normoxic and hypoxic media from n>20 experiments. Results represent mean ± SEM. (A. Adapted from <http://www.bioquip.com>. B. Adapted from <http://francais.radiometer.ch>).

3.3.2 Analysis of media pH, pO₂ and pCO₂

An ABL80 Basic blood gas analyser (Radiometer, Figure 3.2B) was used to measure the gaseous partial pressures (pO₂ and pCO₂) and pH of the media encountered by cells. The ABL80 Basic measures pH, pCO₂ and pO₂ through a multi-use disposable sensor cassette containing a low volume, flow-through cell. The ABL80 basic has disposable solution packs, containing precision tonometered electrolyte solutions packaged in gas tight disposable pouches, to enable calibration. Quality control solutions (QC's) were used before each experiment to ensure accurate function.

Because of the expense and limited lifespan of the calibration and QC solutions, I analysed the media used in my experiments for periods of 2 months at regular intervals to ensure that the hypoxic chamber was delivering media with partial pressures of O₂ of 3 kPa and pH of 7.2-7.4. The optimum settings for the hypoxic hood to achieve the desired level of hypoxia in the tissue culture media were determined previously by Dr Naomi McGovern. Bicarbonate-buffered media, such as Iscove's modified Dulbecco's medium (IMDM) required settings 5% CO₂ and 0.8% O₂, which, after a 3 h equilibration, gave media with a pH of 7.4 and an O₂ partial pressure of approximately 2.92±0.29 kPa (Figure 3.2C). For phosphate-buffered media such as PBS the optimal hypoxic chamber settings were found to be 0.5% CO₂ and 0.8% O₂, which delivered a pH of 7.16±0.03 and an O₂ partial pressure of 3.07±0.09 kPa. All solutions for use in the hypoxic hood were pre-equilibrated to hypoxia for 3 h.

Care was taken to prevent access of oxygen to the hood during experimental procedures, by ensuring that adequate flushing of the access mailbox or hand ports with the appropriate hypoxic gas mixture was performed. All reactions were fully stopped (by centrifugation and aspiration of supernatants) prior to removal of any samples from the hood, to ensure that the results were not confounded by re-oxygenation. All experimental procedures were performed in parallel in the hypoxic hood and outside the hood (ambient oxygen = 'normoxia') on the same neutrophil preparation.

3.4 Preparation of cigarette smoke medium

Research grade 3R4F cigarettes (Kentucky Tobacco Research Institute) were used to prepare the cigarette smoke medium (CSM). CSM was made by bubbling the smoke from 3 cigarettes through 25 ml of IMDM in a 50 ml conical tube. The CSM was filtered through a 0.22 µm filter to remove large particles and to ensure sterility, and the pH

measured and adjusted when necessary (to pH 7.5). This solution was designated as 100% CSM, and 500 μ l aliquots were stored at -20°C . Aliquots were defrosted and diluted in culture medium to yield concentrations specified for each experiment.

3.5 Neutrophil extracellular reactive oxygen species production

The superoxide dismutase (SOD)-inhibitable reduction of cytochrome C was used to measure extracellular superoxide anion (O_2^-) production. Cytochrome C is an electron-transferring protein that contains a haem prosthetic group. The iron in the cytochrome alternates between a reduced ferrous (2^+) state and an oxidized ferric (3^+) state during electron transport. The color change induced by the reduction is quantified by measuring the optical density of the solution at 550 nm. The concentration of superoxide anion released was calculated by the Beer-Lambert Law:

$$A = \epsilon cl, \text{ where}$$

A = absorbance, l = path length (1 cm, the width of the cuvettes used), c = concentration of the substance in mol^{-1} , and ϵ = the molar absorption (or extinction) coefficient.

Freshly isolated neutrophils were suspended in PBS^+ at $11.1 \times 10^6/\text{ml}$ at 37°C under normoxic or hypoxic (0.8% O_2 and 5% CO_2) conditions, in a thermo-mixer shaking at 450 rpm. Neutrophil aliquots of 90 μ l in 2 ml Eppendorf tubes were primed with granulocyte macrophage colony stimulating factor (GM-CSF, R&D) 10 ng/ml, or treated with vehicle for 1 h. Next, pre-warmed cytochrome C (prepared with hypoxic or normoxic medium and kept at 37°C under hypoxic or normoxic conditions) was added (750 μ l, 1.2 mg/ml final concentration). The cells were subsequently stimulated with either fMLP (100 nM, Sigma), or PMA (200 nM, Sigma) or vehicle for 10 min. Each reaction was performed in quadruplicate, and superoxide dismutase (SOD) 375 U (50 μ l) included in one of each set of quadruplicates. Cells were pelleted and the supernatants transferred to fresh tubes before removal from the hypoxic hood. The supernatants were placed in cuvettes (200-1600 nm, Uvette, Eppendorf). The superoxide dismutase-inhibitable reduction of cytochrome C was measured by assessing the optical density (OD) of the supernatants at 550 nm using a scanning spectrophotometer. The OD at 550 nm was converted to nmol superoxide/ml using the extinction coefficient of cytochrome C ($21 \times 10^3 \text{M}^{-1} \text{cm}^{-1}$). The values for the tube incorporating SOD (which converts O_2^- to hydrogen peroxide) were subtracted from the corresponding triplicates.

3.6 Measurement of intracellular reactive oxygen species (ROS) production

To determine the effects of CSM on intracellular ROS production the probe 5-(and-6)-chloromethyl-2',7'-dichlorodihydrofluorescein diacetate, acetyl ester (CM-H₂DC-FDA), abbreviated henceforth as DC-FDA, was used. This compound is non-fluorescent until the acetate groups are removed by intracellular esterases and oxidation occurs within the cell. Esterase cleavage of the lipophilic blocking groups yields a charged form of the dye that is much better retained by cells than is the parent compound. Once the probe is taken up into the cell, the cells can be fixed and oxidation of the probe can be detected by monitoring the increase in fluorescence using flow cytometry. As DC-FDA is susceptible to photo-oxidation, low-light conditions were used and the reaction tubes wrapped in foil. Freshly isolated neutrophils were re-suspended in HBSS (10⁷/ml) and 500 µl aliquots transferred to Eppendorf tubes. DC-FDA (0.2 µM, 500 µl) was then added to cell suspension for 10 min (final volume 1 ml). The DC-FDA-loaded cells were spun down and the supernatant removed. Cells were re-suspended in 500 µl of HBSS and incubated for 10 min to allow for esterase cleavage of the acetate groups, rendering the dye sensitive to oxidation. The cells were spun down and re-suspended in HBSS (500 µl) with or without a range of CSM concentrations and incubated for 30 minutes. PMA (200 nM, 10 min) was used as positive control. Aliquots (200 µl) of the cell suspension were added to a mix of 250 µl ice-cold optimised Cell FixTM and 250 µl PBS⁻. Samples were analysed immediately by flow cytometry (CANTOII, BD bioscience), using the FL-1 channel, gating on granulocytes by forward- and side-scatter properties, and the mean fluorescence of the individual samples was measured.

3.7 Apoptosis assays

To assess the effects of hypoxia/hypoxia mimetics on neutrophil apoptosis, purified cells were re-suspended at 5*10⁶ cells/ml in IMDM supplemented with 10% autologous serum and cultured at 37°C under normoxic conditions (with or without hypoxia mimetics) or hypoxic conditions, in Falcon Flexiwell 96-well low attachment plate inserts (135 µl cell suspension and 15 µl hypoxia mimetic). For morphologic assessment, neutrophils were harvested at 20 h by gently pipetting up and down 3 times, using cell saver tips. Cytospins were made by centrifugation of the samples in a Shandon 3 Cytocentrifuge, 3 min at 300 rpm, and the resulting slides fixed in methanol (4 min) and stained with May/Grünwald/Giemsa (DiffQuick reagents, Reagen).

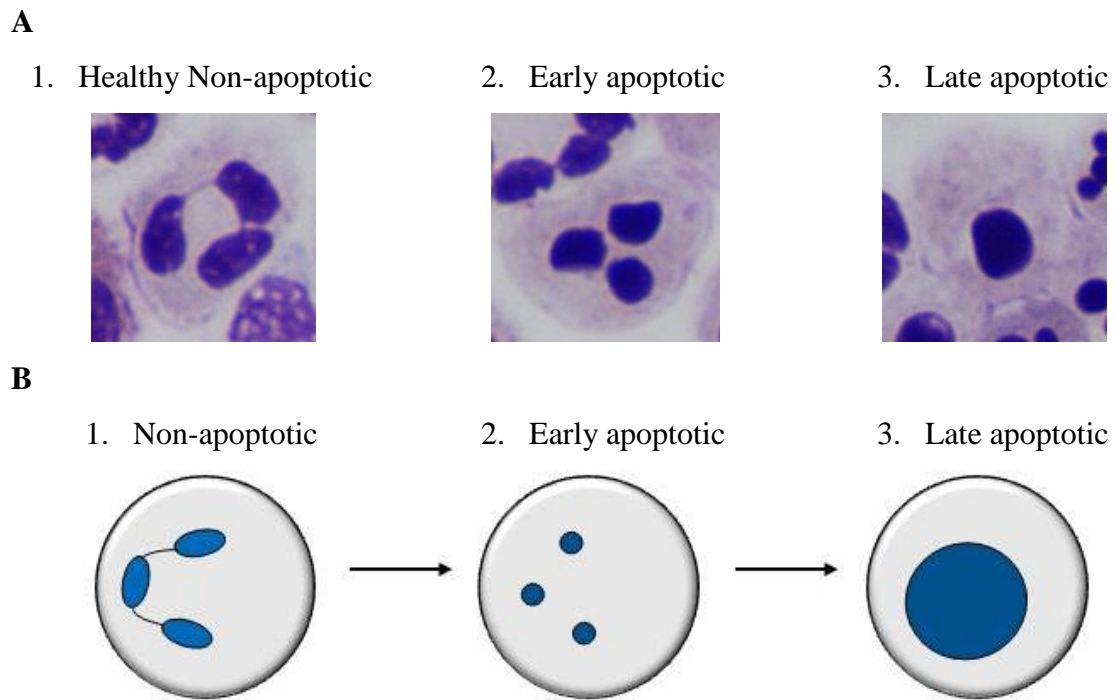


Figure 3.3: Different stages of neutrophil apoptosis

Morphology of non-apoptotic, early apoptotic and late apoptotic neutrophils. A. Photomicrographs illustrating the different stages of neutrophils apoptosis. The cells were stained with May/Grünwald/Giemsa (100x magnification) B. Cartoons illustrating the nuclear morphological changes used in scoring slides.

Morphology was examined by oil-immersion light microscopy (100 x magnification, Olympus CX31) with. 300 cells per cytopsin were counted. Apoptotic neutrophils have a distinct morphologic appearance with cell shrinkage, cytoplasmic vacuolation, and condensation of chromatin, leading to the loss of the normal multi-lobed nucleus (Figure 3.3).

3.8 Assessment of degranulation

3.8.1 Assessment of the effect of hypoxia on secreted NE activity

Freshly isolated neutrophils were re-suspended in normoxic or hypoxic IMDM ($11.1 \times 10^6/\text{ml}$). 270 μl aliquots were transferred to 2 ml Eppendorf tubes and incubated at 37°C for 4 h under normoxic or hypoxic conditions. After 4 h the cells were primed with cytochalasin B (5 $\mu\text{g}/\text{ml}$, Sigma) for 5 min, GM-CSF (10 ng/ml) or vehicle for 30 min. The cells were subsequently stimulated with fMLP (100 nM) or vehicle for 10 min (Figure 3.4). Cells were pelleted and the supernatants were transferred to fresh tubes before removal from the hypoxic hood. Samples were frozen and stored at -80°C until further analysis. To check that the neutrophils were intact (and that extracellular NE had not been released by degranulation rather than by necrosis), aliquots (90 μl) were taken to make cytopsin after stimulation. The cells were subsequently stained with May/Grünwald/Giemsa. Figure 3.5 shows representative photomicrographs of cytopsin from 3 independent experiments (40x magnification). The viability of the cells was also checked using trypan blue staining and was routinely $>99\%$.

3.8.2 Quantification of NE

Assays available to quantify NE fall into 2 categories: those that measure the total amount of elastase released (including NE complexed with inhibitors such as alpha 1-antitrypsin ($\alpha_1\text{-AT}$), plus free NE) and those that quantify the amount of active elastase, based on enzymatic cleavage of a substrate. Total elastase is usually measured by ELISA-based assays, however such assays may not reflect accurately the capacity for tissue damage. Measurement of NE activity was hence performed using the EnChek® activity assay (Molecular Probes), which is based on the cleavage of DQ-Elastin. The non-fluorescent substrate is digested by NE to yield fluorescent fragments. The resulting increase in fluorescence can be monitored by a fluorescence multiwell plate reader. This assay was

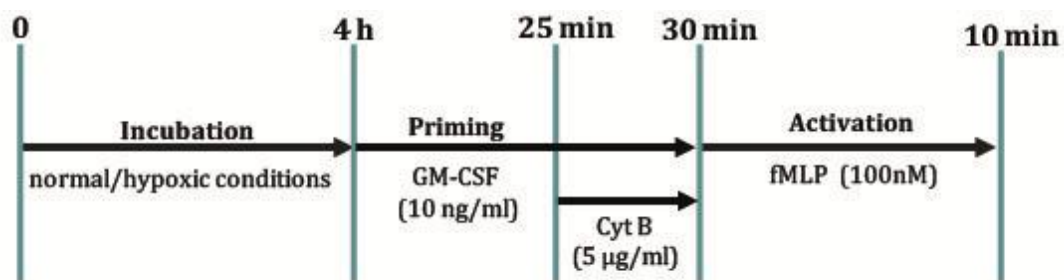


Figure 3.4: Flow chart of typical neutrophil incubation, priming and stimulation protocol

Freshly isolated neutrophils were suspended in normoxic or hypoxic IMDM ($11.1 \times 10^6/\text{ml}$). 270 μl aliquots were transferred to 2 ml Eppendorf tubes and incubated at 37°C for 4 h under normoxic or hypoxic conditions (3 kPa O_2 5% CO_2). After 4 h the cells were primed with cytochalasin B (5 $\mu\text{g}/\text{ml}$) for 5 minutes, or GM-CSF (10 ng/ml) or vehicle for 30 minutes. The cells were subsequently stimulated with fMLP (100 nM) or vehicle for 10 min. Cells were pelleted and the supernatant transferred to fresh tubes before removal from the hypoxic hood and further analysis.

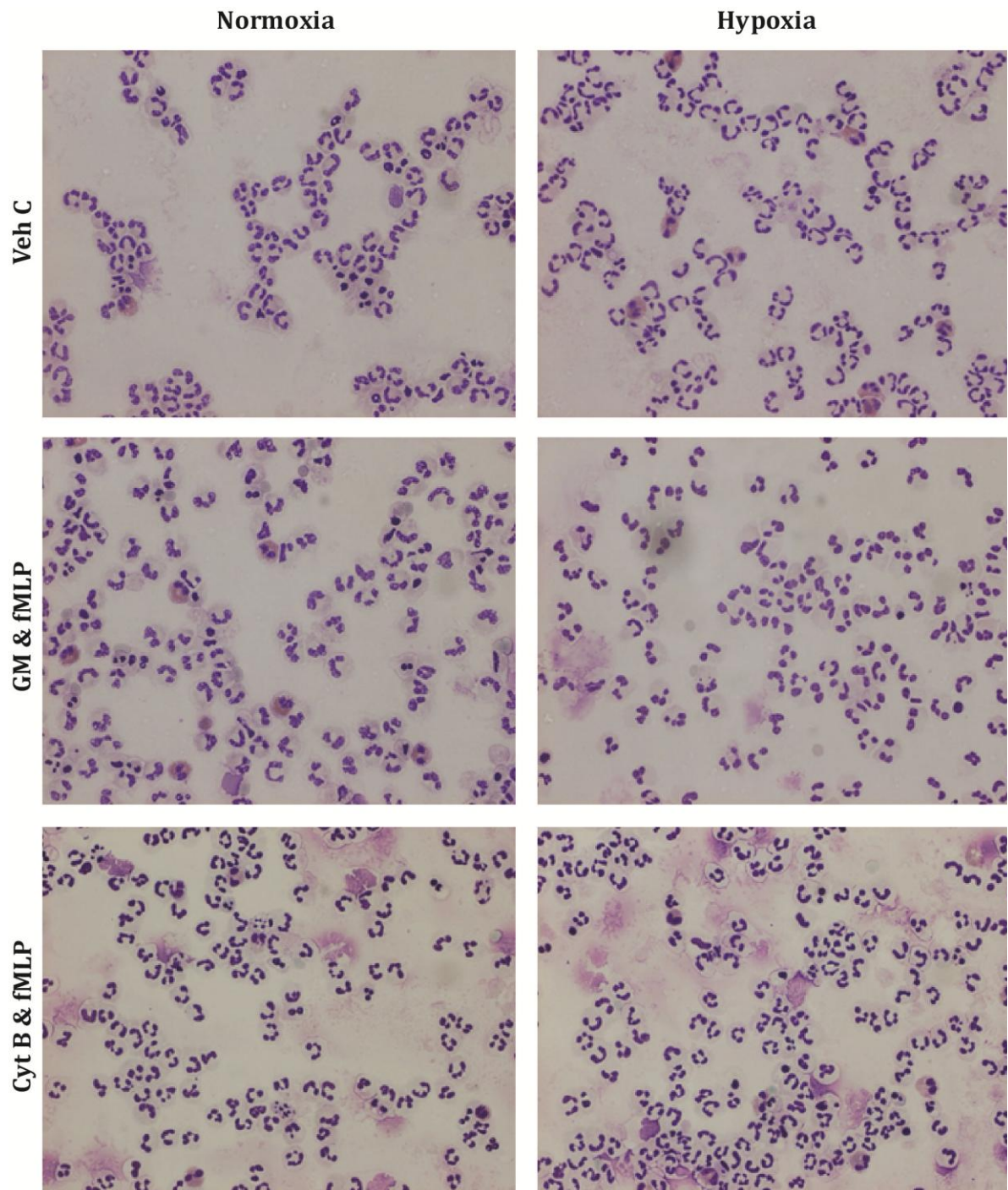


Figure 3.5: Cytopins of resting and activated neutrophils incubated under normoxic and hypoxic conditions

Neutrophils were re-suspended in hypoxic or normoxic IMDM at $11.1 \times 10^6/\text{ml}$ and incubated under normoxia or hypoxia (0.8% O_2 and 5% CO_2) at 37°C for 4 h. The cells were then primed (GM-CSF 10 ng/ml, 30 min or CB $5\mu\text{g}/\text{ml}$, 5 min) and then activated (fMLP 100 nM, 10 min). Cytopins were stained with May/Grünwald/Giemsa. Images are representative of 3 independent experiments (x40 magnification).

chosen because it is able to quantify active NE in supernatants, is sensitive and quick to perform, and can be used to measure multiple samples at low cost. For this assay, 100 μ l of neutrophil supernatant (with 100 μ L of 1x Reaction Buffer as a negative control, or 100 μ L of diluted porcine pancreatic elastase (0.2 U/mL) as a positive control) was combined with DQ elastin substrate diluted in 1x Reaction Buffer (final concentration of DQ elastin 25 μ g/ml). The plate was then incubated in the dark, at room temperature (RT) for 30 min (optimal time point determined in pilot experiments), after which the absorption at 485/535 nm was read by a multi-well plate reader (PerkinElmer). The value derived from the no-enzyme control was subtracted from each sample to correct for background.

3.8.3 Optimisation of the NE activity assay

The number of cells per sample was titrated to optimise the signal-to-noise. As shown in Figure 3.6A, 3×10^6 cells gave a near-maximal response, and this concentration was used therefore used in all subsequent studies (10^7 cells per sample gave the maximum response, but adoption of this as standard would have limited the number of conditions that could be analysed in a single experiment). To study degranulation I used a priming agent GM-CSF (10 ng/ml) and subsequently an activating agent (fMLP 100 nM), as stimulation with GM-CSF or fMLP alone did not reliably induce any detectable degranulation. Cytochalasin B (Cyt B, 5 μ g/ml), which disrupts actin filaments, is the most effective agent known to augment neutrophil degranulation, but I wished to assess and employ more physiological agonists; hence Cyt B was used as a positive control. Under conditions of hypoxia (but not ambient oxygen) GM-CSF (and also other priming agents such as PAF (1 μ M)) augmented the fMLP-induced release of enzymatically active NE, although they were somewhat less effective than Cyt B (Figure 3.6B). GM-CSF priming was used in further experiments. This assay was performed using IMDM as the culture medium, because incubation in HBSS resulted in a high background signal in unstimulated negative controls; this was speculated to be secondary to the stress induced by lack of nutrients over the 4 h incubation period. Additionally, it was found that freezing the supernatants at -80°C and subsequent thawing had no significant effect on NE activity (Figure 3.6C), enabling samples to be stored and run in batches.

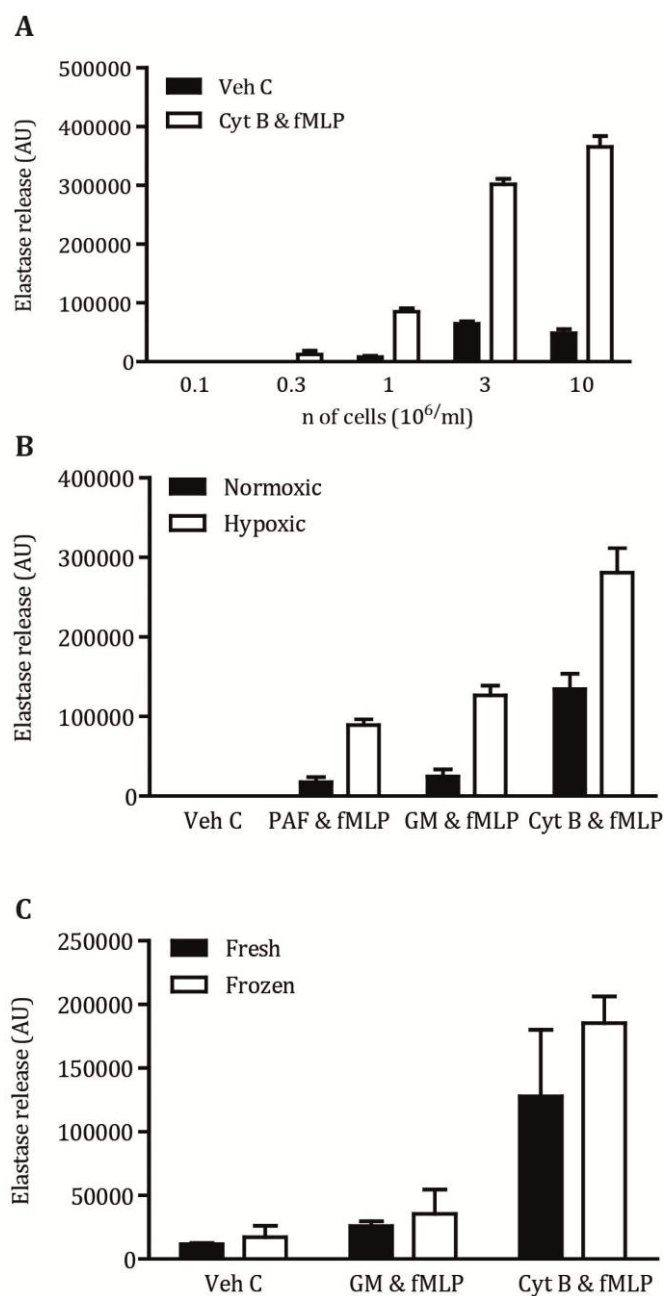


Figure 3.6: Optimising the neutrophil elastase activity assay

Neutrophils were subject to normoxic or hypoxic incubation for 4 h and primed with cytochalasin B (5 μ g/ml) or PAF (1 μ M) for 5 min, or GM-CSF (10 ng/ml) or vehicle for 30 min; they were then stimulated with fMLP (100 nM) or vehicle for 10 min. NE activity was quantified by the increased fluorescence caused by cleavage of DQ-Elastin. A. Effect of cell density on basal and stimulated (cytochalasin B and fMLP) NE production. B. Comparison of different priming agents C. Comparison of NE activity of fresh versus frozen supernatants from the same experiment. For A-C, results represent mean \pm SEM, samples were run in triplicate, n=3.

3.8.4 Investigation of the mechanism of hypoxia-induced augmented neutrophil degranulation

To investigate the specific role of hypoxia in neutrophil degranulation, a range of different inhibitors were used. The NE assay was used as a read-out of the effect of these compounds. Details regarding the compounds, and the concentrations used, are given in the relevant results sections and are summarised in Table 3.1.

3.8.5 Quantification of myeloperoxidase

This assay is based on the H₂O₂-dependent oxidation of o-dianisidine dihydrochloride (DMB) by MPO, leading to a colour change and hence a change of absorption at 460 nm. Freshly isolated neutrophils (11.1*10⁶/ml) in IMDM (270 µl aliquots) were subjected to normoxia or hypoxia at 37°C for 4 h and stimulated exactly as documented in section 3.8.1. Cells were pelleted, and the supernatants were transferred to fresh tubes before removal from the hypoxic hood. In addition, 3*10⁶ cells in 200 µl PBS⁻ were lysed with 10% Triton X-100 (for assessment of total cellular MPO content). Lysed cells were spun down, and the supernatants transferred to a new tube. Supernatants were frozen at -80°C for subsequent analysis. Supernatants and lysates were de-frosted, and 50 µl aliquots transferred 1.25 µg/ml DMB in dH₂O (50 µl) were added to each aliquot. The reaction mixtures were then incubated for exactly 15 min at 37°C. The reaction was stopped with 50 µl of 0.1% sodium azide in dH₂O, and the samples were placed on ice. 200 µl of each sample was transferred to a 96-well plate and absorption was read at 460 nm by a multi-well plate reader (Biorad 680). MPO release (mean of triplicates) was expressed as a percentage of the total MPO present in Triton X-100-lysed cells.

3.8.6 Quantification of lactoferrin release by ELISA

Freshly isolated neutrophils (11.1*10⁶/ml) in IMDM (270 µl aliquots) were subjected to normoxia/hypoxia at 37°C for 4 h and stimulated exactly as documented in section 3.8.1. Cells were pelleted and the supernatants transferred to fresh tubes before removal from the hypoxic hood and freezing at -80°C. Pilot experiments demonstrated that a 500-fold dilution of the thawed supernatants was appropriate to bring the samples into the range measurable by a commercial solid-phase ELISA (enzyme-linked immunosorbent assay: Hycult). The plates supplied with the kit were pre-coated with capture antibody against human lactoferrin.

Compound	Function	Final concentration	Company
DMOG	Competitive inhibitor of PHD enzymes	1 μ M	Sigma
DFO	Iron chelator	1 μ M	Sigma
Cobalt chloride	Inhibits interaction between HIF1- α and VHL	100 nM	Sigma
Cycloheximide	Inhibits eukaryotic protein synthesis	1 μ g/ml	Sigma
EGTA	Calcium chelator (1:1 stoichiometry)	2 mM	AnaSpec EGT group
Thapsigargin	Non competitive inhibitor of sarco/endoplasmic reticulum Ca ²⁺ ATPases	10-100 nM	Sigma
LY294002	Pan PI3Kinhibitor	10 μ M	CalBiochem
IC87114	Selective PI3K δ inhibitor	3 μ M	Sigma
AS605240	Selective PI3K γ inhibitor	3 μ M	Sigma
U-73122	Inhibits the hydrolysis of PIP ₂	2 μ M	Sigma
4-phenyl 3 butenoic acid	Inhibits PAM, an oxygen sensor	1-500 μ M	Sigma

Table 3.1: Compounds used in neutrophil elastase activity assay

The compounds shown in the table were obtained and used at the concentrations indicated; incubation times specified in the individual experiments.

Samples (1:500 dilution, 100µl) and standards (0-100 ng/ml) were incubated in a 96-well plate. After an 1 h incubation at 37°C, the wells were washed 4 times with wash buffer (supplied with kit), and a biotinylated tracer antibody added (1:11 dilution, 100 µl, 1 h, 22°C) which binds to the captured human lactoferrin, was added. After a further 4 washes with the wash buffer, streptavidin-peroxidase conjugate (which binds to the biotinylated tracer antibody; 1:23 dilution, 100 µl, 1 h, 22°C) was added. The peroxidase reacts with the subsequently added substrate, tetramethylbenzidine (TMB, 1:11 dilution, 100 µl, 30 min in the dark, 22°C). This reaction was stopped by the addition of a stop solution (supplied by kit, contains 2% oxalic acid, 100 µl) and the absorbance at 450 nm measured with a spectrophotometer. A standard curve was obtained by plotting the absorbance (linear) versus the corresponding concentrations of the human lactoferrin standards (log). The concentration of lactoferrin present in the samples (which were run concurrently with the standards) was determined from the standard curve.

3.8.7 Quantification of MMP-9 (gelatinase) release by ELISA

To quantify the total amount of MMP-9 in the neutrophil supernatants, a DuoSet ELISA (R&D) kit was used according to the supplied protocol, with minor modifications to optimise detection of MMP-9 in neutrophil supernatants. Supernatants were prepared exactly as documented in section 3.8.1 were defrosted and serially diluted 500-fold. Instead of overnight coating of the plate with the capture antibody (mouse anti-human MMP-9, 2 µg/ml), the plate was coated for 2 h at 22°C. After 3 washes with PBS-Tween, non-specific binding was blocked by 2 h incubation with PBS⁻ BSA (1% BSA), and the plates were then washed thrice. Subsequently, the samples (1:500 dilution, 100 µl) and calibration curve standards (0-300 pg/ml, 100 µl) were added and incubated overnight to maximise binding of MMP-9 to the capture antibody. The supplied detection antibody (goat anti-human MMP-9, 100 ng/ml) was used (100 µl), but instead of streptavidin-HRP, extravidin alkaline phosphatase (1:400 dilution in the supplied diluent, Sigma) was used and the plate was incubated for 2 h, to improve the binding of the detection antibody to the captured MMP-9. This antibody reacts with 4-nitrophenyl phosphate disodium salt; using 4-nitrophenyl phosphate disodium salt (hexahydrate tablet, Sigma) in diethyanolamine buffer as substrate solution (100µl) eliminated the need for a stop solution and enabled the absorption to be read continuously at 405 nm by a multi-well plate reader (Biorad 680). This allowed me to determine the optimal “measurement time”.

The effect of these changes was assessed by repeated and comparative measurement of the calibration curve. To quantify MMP-9 in neutrophil derived samples, a standard curve was obtained by plotting the absorbance (linear) versus the corresponding concentrations of the human lactoferrin standards (log). The concentration of lactoferrin in the samples, which were run concurrently with the standards, was determined from the standard curve.

3.8.8 Quantification of secreted MMP-9 activity by gelatin zymography

Supernatants were prepared exactly as documented above (section 3.8.1). For this experiment a 10% polyacrylamide gel was cast, using 30% acrylamide/ bisacrylamide 37.5:1 in 375 mM Tris pH 8.8, 0.1 % sodium dodecyl sulphate (SDS) and incorporating 2 mg/ml of gelatin (Sigma). Polymerisation was accelerated by the addition of 0.05% freshly prepared ammonium persulphate (APS) and 0.1% Temed (N,n,n,n-tetramethylethylenediamine). Water-saturated butanol was layered on top of the resolving mixture to ensure a flat surface and exclude air. After the resolving gels had set (approximately 30 min) the butanol was washed away and the stacking gel (5% acrylamide, 125 mM Tris pH 6.8, 0.1 % SDS with APS and Temed (to accelerate polymerisation as above) was poured. A 10-well comb was inserted carefully into each stacking gel. Supernatants were defrosted and loaded (10 µl) onto the gel in a 1:1 dilution (in loading buffer). The gel was run at 150 V for 120 min in 1 x Tris Glycine SDS. Following electrophoresis, the proteins were re-natured by rinsing the gel in 2.5 % Triton X-100 (3 x 20 min) at RT. After rinsing, the gel was washed with MMP-9 incubation buffer (50 mM Tris-HCl (pH 7.6), 150 mM NaCl and 5 mM CaCl₂) made fresh on the day of the experiment (2 x 20 min) to remove the Triton-X. Subsequently MMP-9 incubation buffer was added and the gel incubated for 16 h at 37⁰C allowing the MMP-9 to digest the gelatin. Finally, the gel was stained with 0.4% Coomassie Blue R250 in 45% methanol, 10% acetic acid for 1 h prior to de-staining with 30% methanol/10% acetic acid until the bands were clearly visible (Figure 4.4B). The gel was photographed with a *G:BOX* gel imaging system (SynGene) and densitometry analysis of the bands performed with ImageJ.

3.9 Western blot analysis of neutrophil granule protein content

3.9.1 Preparation of cell lysates and protein extraction

Western blot lysates were prepared by incubating freshly isolated neutrophils under normoxic or hypoxic conditions for 4 h in 6 well ultra-low attachment plates (Costar) at

37 °C, or by putting freshly isolated neutrophils on ice immediately. After 4 h the cells were collected in 15 ml Falcon tubes with the aid of a cell scraper (Corning). The cells were spun down at 310 *g* for 5 min at 4°C, washed with ice-cold PBS⁻, and resuspended in hypotonic lysis buffer (TRIS (pH 7.8, 10 mM), EDTA (1.5 mM), KCL (10 mM), DTT (500 µM), Na-orthovanadate (1 mM), tetramisole (2mM) in H₂O) with protease inhibitors (1 tablet, Roche, 200 µl of lysis buffer per 20*10⁶ cells). Following vigorous vortexing for 15 sec, cells were placed on ice for 5 min, sonicated for 10 sec and returned to ice for 15 min. Finally the insoluble fraction was spun down at 310 *g* for 5 min at 4°C and the supernatants transferred to new tubes

3.9.2 Bicinchonic Acid (BCA) protein assay

The BCA assay³⁸⁷ was used to determine the protein concentration of the lysates. This assay is based on the ability of proteins to reduce Cu²⁺ to Cu⁺ and on BCA to then chelate the Cu⁺, giving a purple coloration that can be quantified by spectrophotometry (at 550 nm). 10 µl of each sample was incubated with 200 µl of BCA solution (BCA 10 ml + 250 µl copper (II) sulphate (40:1)) for 30 min at 37°C in a 96-well plate, prior to analysis using an automated plate reader (Biorad 680). Samples were assayed in duplicate, and compared against standard curves prepared using pre-prepared BSA standards (0-1 mg/ml).

3.9.3 SDS-polyacrylamide gel electrophoresis

SDS-polyacrylamide gel electrophoresis (SDS-PAGE) was carried out using the Biorad Protean II system. Resolving gels were cast using Protogel (37.5:1 Acrylamide:Bisacrylamide Stabilised Solution, National Diagnostics, Table 3.2). Polymerisation was accelerated by the addition of 0.05% freshly prepared APS and 0.1% Temed. Ethanol was layered on top of the resolving gel to ensure a flat surface and exclude air. After these gels had set (approximately 30 min) the ethanol was washed away and the stacking gels (Protogel with APS and Temed to accelerate polymerisation as above, Table 3.2) were poured. A 10-well comb was inserted carefully into each stacking gel. Samples (15 µg protein per sample, volume required determined by BCA protein assay as described above) were mixed in proportion with 6x sample buffer (60 mM Tris-HCL, pH 6.8, 2% (v/w) SDS, 10% (v/v) glycerol, 5% (v/v) β-mercaptoethanol, 0.01% (w/v) bromophenol blue), heated for 5 min at 99°C, and allowed to cool to room

temperature before being loaded onto the gels, together with one lane for molecular weight markers (Precision Plus Protein™ Dual Color Standards, Biorad, CA, USA). The gel was run at 100 V through the stacking gel and at 150 V through the separation gel in 1x running buffer (Tris-Glycine-SDS PAGE Buffer, National Diagnostics).

3.9.4 Western blotting for MMP-9

Following electrophoresis (dye front run to the bottom of the gel), the proteins were transferred to methanol pre-soaked polyvinylidene fluoride (PVDF) membrane using the Trans-blot system. Care was taken to ensure the membrane was moist at all times. Gel and membranes were sandwiched between 2 layers of Whatman 3M paper and placed in the tank containing transfer buffer (24 mM Trizma base, 193 mM glycine, 10% methanol) with a constant voltage of 75 V for 2 h. Following transfer, the two membranes were cut in two, determined by molecular weight markers, and blocked in freshly prepared in 5% Marvel dry milk powder (Nestle, France) in PBS-Tween (PBS-T: PBS⁻ with 0.1% Tween-20, Sigma), for 1 h at room temperature, with constant agitation. The upper membranes were then incubated with a final concentration of 200 ng/ml anti-MMP-9 (rabbit polyclonal, Abcam), in freshly prepared 2.5% Marvel/PBS-T. The lower membrane portions were incubated with anti- β -actin (rabbit polyclonal, Cell Signaling, 1 in 5000) in freshly prepared 2.5% Marvel/PBS-T. Membranes were incubated overnight in primary antibody as indicated above at 4°C on a rocking platform. Membranes were washed thrice with PBS-T (10 min) and incubated with goat anti-mouse horseradish peroxidase (HRP)-conjugated IgG (Dako, 1 in 10,000) or donkey anti-goat HRP-conjugated IgG (Santa Cruz, 1 in 5,000) in 2.5% Marvel/PBS-T. After a 1 h RT incubation, the membranes were finally washed thrice with PBS-T. HRP-tagged proteins were detected using the ECL (Enhanced Chemiluminescence) system (GE Healthcare). This detection method is based on the HRP-catalysed oxidation of luminol, resulting in light emission. Detection reagents 1 and 2 were mixed (in equal volumes) and used to coat the membranes for 4 min. Membranes were then blotted dry, wrapped in clingfilm, and the resulting light was emission quantified by exposing to auto radiographic film in the dark for times ranging from 1 sec to 10 min. The films were scanned and densitometry analysis of the bands was performed using ImageJ.

Solutions	Contents	7.5 % gel (separation)	10% gel (separation)	4.5% gel (Stacking)
Separation gel buffer	see text	3.9 ml	3.9 ml	-
Stacking gel buffer	see text	-	-	1.95 ml
Proto gel (30%)	37.5:1 Acrylamide to Bisacrylamide Stabilized Solution	3.75 ml	5 ml	1 ml
De-ionised water	-	7.19 ml	5.74 ml	4.47 ml
APS [#]	10% (w/v) APS	150 µl	150 µl	75 µl
TEMED [#]	Tetra-methyl-ethyl-enediamine	15 µl	15 µl	8 µl

Table 3.2: Composition of SDS gels

The table shows the reagents used for the SDS gels. Reagents indicated * were obtained from National Diagnostics, reagents designated # were obtained from Sigma.

3.10 Real-time PCR

Real-time PCR (RT-PCR) experiments for assessment of BNIP3, MMP-9 and NE mRNA abundance were performed. Neutrophils were cultured at 5×10^6 cells/ml in IMDM for 4 h under hypoxia or normoxia. Cells were gently scraped off the plates and pelleted by centrifugation (325 g, 10 min). Supernatants were discarded and the cell pellets transferred to 2 ml Eppendorf tubes, spun at 15,000 g for 5 sec, and the excess medium removed. Total RNA (1 μ g), isolated with TRI-reagent (Sigma), was used for cDNA generation according to the manufacturer's instructions (high capacity cDNA kit, Applied Biosystems). Relative gene expression was determined by qPCR (iCycler, Bio-Rad) using Sybr-green master-mix (Sigma) and relevant primers obtained from Qiagen. Relative gene expression was determined by correcting cycle threshold for the target gene against two housekeeping genes (Beta-2-microglobulin (β 2M) and 18S ribosomal RNA (18S)). Relative gene expression (fold change) was expressed as $2^{-\Delta\Delta CT}$.

3.11 Assessment of the effect of hypoxia on kinase signaling

To screen for kinases that might play a role in modulating degranulation, a human phospho-kinase antibody array (R&D systems) was used. It detects the relative site-specific phosphorylation of 43 different kinases and related total proteins (Table 3.3). A nitrocellulose membrane is supplied with each capture antibody spotted on in duplicate, and the levels of phosphorylated protein in applied lysates can be assessed by the binding of phospho-specific antibodies and chemiluminescence detection. Neutrophils were incubated under normoxic or hypoxic conditions in ultra-low attachment 6 well plates (Costar) (to accommodate the large number of cells needed per condition) and activated as described previously, (section 3.8.1). After activation, the cells were collected in 15 ml Falcon tubes by gently scraping the cells off the plates with a cell scraper (Corning). The cells were spun down at 310 g for 5 min at 4°C. The cells were washed with ice cold PBS⁻ and resuspended at 1×10^6 /ml in the lysis buffer provided with the kit. The lysates were titrated to resuspend, rocked gently at 2-8°C for 30 minutes, clarified (14,000 g, 5 min, 4°C), and the supernatants transferred to clean eppendorf tubes. Protein content was quantified using the BCA protein assay described in section 3.9.2.

All kit reagents were brought to RT before use. Array buffer 1 (1 ml, Blocking Buffer) was added to each well of the supplied 8-well multi-dish. The membranes were placed in the array buffer, and incubated for 1 h on a rocking platform shaker. The lysates were

Kinase (phosphorylation site)		
Akt (S4873)	Hck (Y411)	PRAS40 (T246)
Akt (T308)	HSP27 (S78/S82)	Pyk2 (Y402)
AMPK alpha1 (T174)	HSP60	RSK1/2/3 (S380/S386/S377)
AMPK alpha2 (T172)	JNK pan (T183/Y185, T221/Y223)	Src (Y419)
Beta-Catenin	Lck (Y394)	STAT2 (Y689)
Chk-2 (T68)	Lyn (Y397)	STAT3 (S727)
c-Jun (S63)	MSK1/2 (S376/S360)	STAT3 (Y705)
CREB (S133)	P27 (T198)	STAT5a (Y694)
EGF-R (Y1086)	p38 alpha (T180/Y182)	STAT5a/b (Y694/Y699)
eNOS (S1177)	p53 (S15)	STAT5b (Y699)
ERK 1/2 (T202/Y204, T185/Y187)	p53 (S392)	STAT6 (Y641)
FAK (Y397)	p53 (S46)	TOR (S2448)
Fgr (Y412)	p70 S6 kinase (T421/S424)	WNK-1 (T60)
Fyn (Y420)	PDGF R beta (Y751)	Yes (Y426)
GSK-3 alpha/beta (S21/S9)	PLC gamma-1 (Y783)	

Table 3.3: Kinase array targets and phosphorylation sites

Adapted from R&D website.

diluted with array buffer 1 to a final volume of 2 ml and 1 ml of diluted lysate was added per well; the membranes were incubated with the lysates overnight on a rocking platform at 2-8°C. The membranes were transferred to plastic containers with 20 ml of wash buffer (provided with the kit) and washed for 10 minutes (repeated for a total of three washes). After the wash steps the membranes were returned to the wells of the (cleaned) 8-well plate, containing 1 ml of the supplied antibody detection cocktail (diluted 1 in 5 in array buffer) and incubated on a rocking platform for 2 h at RT. Membranes were washed thrice and returned to the wells of the (freshly-cleaned) 8-well plate, containing 1 ml of diluted streptavidin-HRP (in array buffer, diluted according to dilution factor given on vial). Following a 30 min incubation with streptavidin-HRP, another three wash steps were performed. Excess wash buffer was allowed to drain from the membrane by blotting the lower edge onto paper towels. The membranes were placed on the bottom sheet of the plastic sheet protector with the identification number facing up, with corresponding part A and B membranes end-to-end. Chemi-reagent mix supplied with the kit was used to coat the membranes for 1 minute. Membranes were then blotted dry, wrapped in cling film, and the resulting light emission quantified by exposing to auto-radiographic film in the dark for times ranging from 1 sec to 10 min. The films were scanned and densitometric analysis of the signal was performed using ImageJ.

3.12 Assessment of hypoxia induced morphological changes

3.12.1 Assessment of neutrophil morphology by electron microscopy

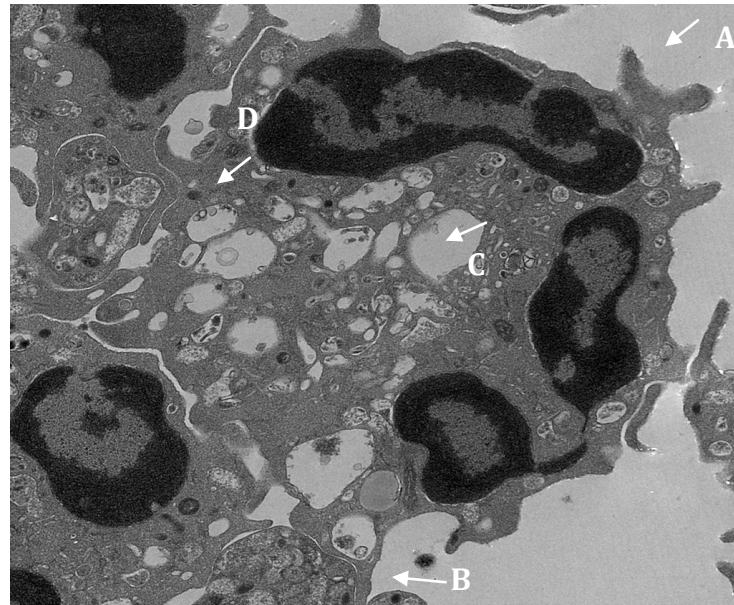
Freshly isolated neutrophils were suspended in normoxic or hypoxic IMDM (11.1×10^6 /ml, 270 μ l aliquots) and incubated at 37°C for 4 h under normoxic or hypoxic conditions. After 4 h the cells were primed with cytochalasin B (5 μ g/ml, Sigma) for 5 min, GM-CSF (10 ng/ml) or vehicle for 30 min. The cells were subsequently stimulated with fMLP (100 nM) or vehicle for 10 min (Figure 2.4). Cells were pelleted, washed with 1 ml of sterile 0.9% saline (Baxter) and fixed in 500 μ l of 4% glutaraldehyde (containing 0.1% (v/v) hydrogen peroxide and osmium tetroxide) for 2 h at 4°C. The cells were washed 4 times and finally suspended in 1 ml 0.9% saline. Cells were embedded in Spurr's resin. Dr Jeremy Skepper (Department of Physiology, Development and Neuroscience, University of Cambridge) completed sample preparation and took images (magnifications specified in the individual figures) of the cells using a CM 100 transmission electron microscope (TEM: Philips). The images were scored for a range of

morphological changes, including shape (rounded, irregular or elongated), membrane ruffling (small microvilli, small/medium extensions, long extensions), clustering, presence of “empty vacuoles” (none, low or high) and granule density (low, medium or high). The result was an “activity score”, with a score of 6-8 indicating a quiescent cell, 9-12 an activated cell and 13-17 a highly activated cell. The scoring system adapted from that of Mitchell et al.³⁸⁸, and is fully depicted in Figure 3.7.

3.12.2 Assessment of neutrophil cytoskeletal remodeling by immuno-histochemistry

Freshly isolated neutrophils were re-suspended in normoxic or hypoxic IMDM (3.5×10^6 /ml) and 270 μ l aliquots transferred to 2 ml Eppendorf tubes to be incubated at 37°C for 1 h under normoxic or hypoxic conditions. After 4 h the cells were stimulated with 30 μ l fMLP (100 nM final concentration) or vehicle for 5 min. All subsequent steps were performed at RT (22°C) unless otherwise stated. The neutrophils were pelleted and the pellets were fixed by re-suspension in 200 μ l of 4% paraformaldehyde (PFA), prior to removing samples from the hypoxic hood. Fixed neutrophils were washed thrice with PBS⁻, resuspended in 200 μ l PBS⁺, and cytopins prepared. Before staining the neutrophils were permeabilised with 0.5% Triton X-100 in PBS for 10 min and washed 3 times with PBS⁻. Non-specific staining was blocked with PBS-BSA (0.5% BSA, 30 min), after which the slides were washed 3 times with PBS⁻. The cells were stained with anti-NE (goat polyclonal, Santa Cruz, 1:1,000) for 1 h, washed 3 times with PBS⁻ and incubated with the secondary antibody (Alexa Fluor 488 – donkey anti-goat IgG, 1:1,000, Invitrogen) for 1 h in the dark, after which a further wash step was performed. Next the cells were stained for F-actin using rhodamine phalloidin (a high-affinity F-actin probe conjugated to the red-orange fluorescent dye, tetramethylrhodamine, Invitrogen) 1:200, 30 min, in the dark, and washed thrice with PBS⁻. Finally, to prepare slides for microscopy, a DAPI containing mountant (Invitrogen) was dropped on to each sample, and cover slips were applied. The slides were kept on ice and in the dark prior to imaging with a Leica Sp5 confocal microscope. Representative images were taken in different areas of the well with the observer unblinded to the treatments.

This protocol was developed by Cheng Chen, a Part 2 Medical Student at the University of Cambridge, who worked under my direct supervision during a 12-week lab project.



Feature	Score
Shape	rounded (1), irregular (2), elongated (3)
Membrane ruffling	small extensions(1), small/medium extensions (2), long extensions(3)
Cell clustering	no (1), yes (2)
Intracellular Vacuoles	0-2 (1), 2-5 (2), 5> (3)
Granule number	high (1), medium (2), low(3)

Figure 3.7: Scoring system of neutrophil images made by transmission electron microscopy (TEM)

The images obtained by TEM were scored on a number of morphological criteria; including shape (rounded, irregular or elongated), membrane ruffling (A, small microvilli, small/medium extensions, long extensions), clustering (B), presence of “empty vacuoles” (C, none, low or high) and granule density (D, low, medium or high). The result was an “activity score”, with a score of 6-8 indicating a quiescent cell, 9-12 an activated cell and 13-17 a highly activated cell.

3.13 Human airway epithelial cell culture systems

3.13.1 A549 cells

A549 cells (a human lung adenocarcinoma cell line, ATCC) were initially used as a model cell-line to quantify neutrophil-mediated lung “epithelial” cell injury. The A549 cells were cultured in 75 cm² cell culture flasks in F-12K medium with 100 U/ml penicillin, 10 µg/ml streptomycin, 25 µg/ml amphotericin B (Invitrogen) and 10% fetal calf serum (FCS: GIBCO, Life Sciences). Cell aliquots were taken from nitrogen storage, defrosted and put into a flask with 15 ml F-12K medium. After 24 h the medium was replaced to remove any DMSO (dimethyl sulfoxide) present in the freezing solution. When the cell monolayers were confluent, the medium was removed and the cell layer washed with 10 ml of sterile PBS. The cells were then detached from the flask by incubation with 0.25% (v/v) trypsin/EDTA (Gibco) for 5 min at 37°C. Cells were viewed under an inverted microscope to ensure that they had rounded up and detached. Trypsin was inactivated by the addition of FCS-containing medium and the cells transferred into a 15 ml Falcon tube, and spun at 1000 g, 5 min at 22^oC. The pellet was re-suspended in fresh medium prior to counting on a haemocytometer. To maintain cell stocks, the cell suspension was diluted at a ratio of 1:10 or 1:20 and aliquotted into 75 cm³ tissue culture flasks and further stocks were frozen down.

3.13.2 Immortalised human bronchial epithelial (iHBE) cells

Immortalised human bronchial epithelial cells were a gift from Professor Gisli Jenkins (University of Nottingham). These cells were originally derived from normal human primary epithelial cells by Professor Jerry Shay, by transfection with cyclin-dependent kinase (Cdk) 4 and hTERT³⁸⁹. The iHBE cells were cultured in 75 cm² cell culture flasks in keratinocyte serum-free media (500 ml, Fisher Scientific VX17005075) + 25 µg/ml bovine pituitary extract, 0.2 ng/ml rEGF, 250 ng/ml puromycin and 25 µg/ml G418. Puromycin and G418 are used for positive selection of the immortalised cells. Cell aliquots were taken from nitrogen storage, defrosted and put into a flask with 15 ml keratinocyte serum-free medium. After 1 day the medium was replaced to remove any DMSO present in the freezing solution. iHBE cells grew as a monolayer, adherent to the culture flask. When the cells were confluent, the medium was removed and the cell layer washed with 10 ml of sterile PBS. The cells were then detached from the flask by incubation with 10 ml 0.25% trypsin/EDTA solution for 5 min at 37 °C as above. Trypsin

was inactivated by the addition of 5 ml filter-sterilised FCS and the cells collected in a 15 ml Falcon tube, and spun at 1000 g, 5 min at 22°C. The pellet was re-suspended in fresh medium prior to counting on a haemocytometer, the cell suspension (diluted 1:10 - 1:20 and aliquotted) into 75 cm³ tissue culture flasks and further stocks frozen down.

3.13.3 Normal human bronchial epithelial (NHBE) cells

Primary normal human bronchial epithelial (NHBE) cells were purchased from Lonza and cultured by Dr Robert A. Hirst (Senior Scientist, University of Leicester) as previously described³⁹⁰; Dr Hirst has extensive experience in culturing and working with these cells, and his input was vital as these cells are both expensive and extremely difficult to differentiate to ciliation. NHBE cells were grown on collagen-coated (0.1%; Nutacon; Leimuiden, The Netherlands) 12-well tissue culture trays using bronchial epithelial growth media (BEGM; Lonza; Berkshire, England) for 2 to 7 days. The confluent non-ciliated basal cells were expanded into collagen-coated 80 cm² flasks and the BEGM was replaced every 2 to 3 days. The basal cells were then seeded at approximately 10⁵ cells/cm², on collagen-coated, 1.2 cm diameter, Transwell inserts (Corning) under BEGM for 2 days. After confluence was reached, the basal cell monolayer was fed on the basolateral side only with air-liquid interface media (ALI) medium comprising 50% BEGM and 50% Hi-glucose minimal essential medium with 100 nM retinoic acid. The media was exchanged every 2 to 3 days and the apical surface mucus removed by gentle washing with phosphate-buffered saline (Figure 3.8). When cilia were observed (usually around 2 weeks after ALI culture³⁹¹) on these cells, they were physically removed from the Transwell insert by gentle scraping with a spatula and the ciliated epithelium dissociated by gentle pipetting³⁹². Dissociated ciliated epithelial cells were treated as described below (sections 3.14.4 & 3.14.6) to observe the effect of exposure to neutrophil supernatants.

3.14 Assessment of damage to epithelial cell layers

3.14.1 Poly-L-lysine coating of tissue culture plates

For experiments using A549 and iHBE cells, tissue culture plates (see below) were coated with 0.001% (v/v) poly-L-lysine solution (Sigma) for 5 min. The poly-L-lysine solution was aspirated off the plates and the wells washed twice with sterile PBS and air-dried prior to all experiments.

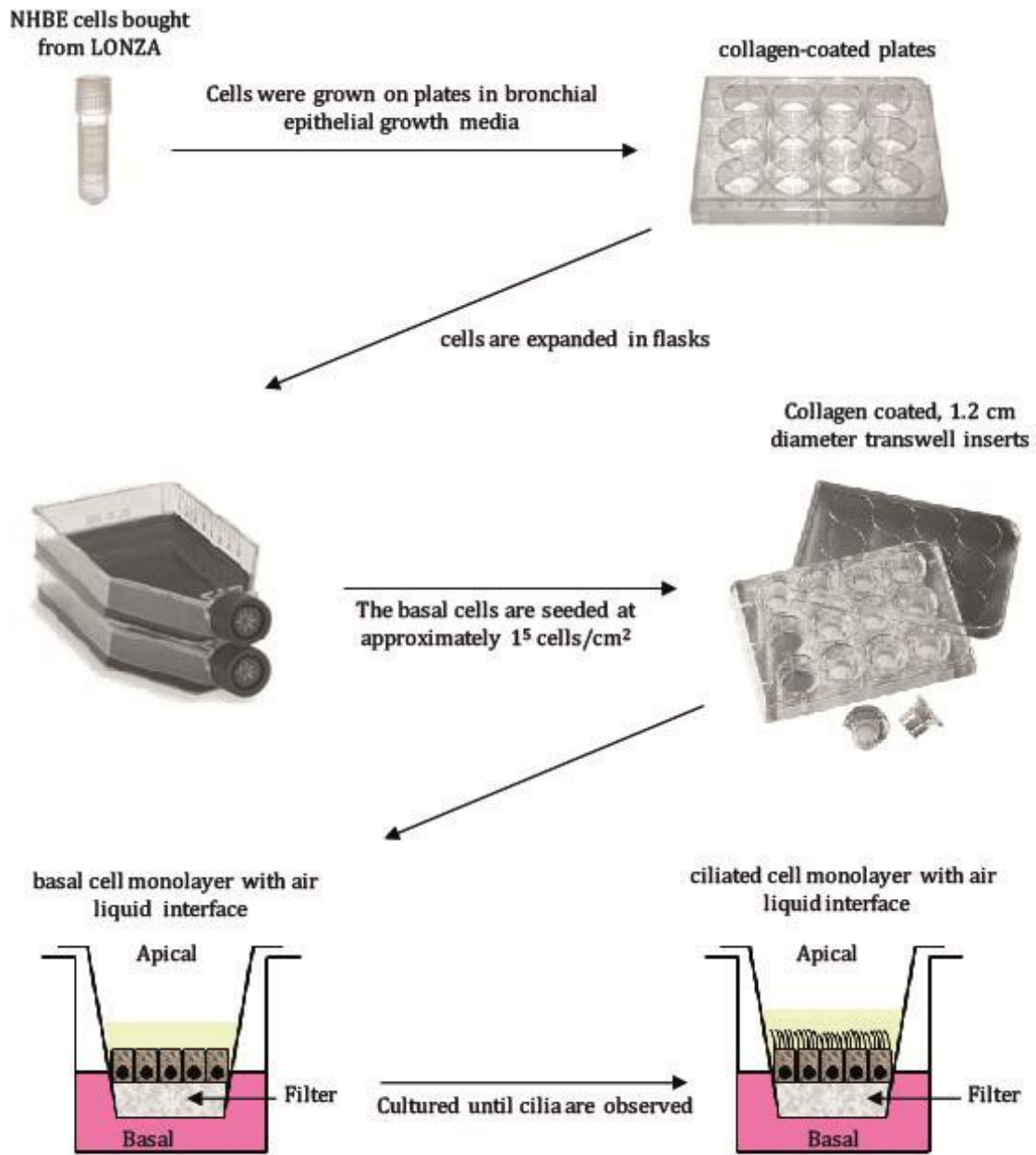


Figure 3.8: NHBE cell culture

NHBE cells (Lonza) were grown on tissue culture trays in BEGM for 2-7 days. The confluent non-ciliated basal cells were expanded into collagen-coated 80 cm² flasks and the BEGM was replaced every 2 to 3 days. The basal cells were then seeded at approximately 10^5 cells/cm² on a collagen-coated 1.2 cm diameter, clear Transwell insert under BEGM for 2 days. After achieving confluence, the basal cell monolayer was fed on the basolateral side only with air-liquid interface. The media was exchanged every 2 to 3 days and the apical surface mucus was removed by gentle washing with phosphate-buffered saline. Ciliation occurred after approximately 2 weeks of ALI-culture and cells were used shortly thereafter.

3.14.2 MTT assay

The MTT assay was used to determine the effect of neutrophil supernatants on A549 cell viability. 3-[4,5-dimethylthiazol-2-yl]-2,5-diphenyl tetrazolium bromide (MTT) is processed in the mitochondria; mitochondrial dehydrogenases of viable cells cleave the tetrazolium ring, yielding purple formazan crystals, which are insoluble in aqueous solution. The crystals are dissolved in isopropanol and the resulting purple solution is measured spectrophotometrically. A549 cells were plated onto 96-well plates (4×10^4 cells/well) and allowed to adhere overnight.

The next day the medium was removed and the neutrophil supernatants (diluted 1 in 2.5) or equivalent volume vehicle controls added. After 72 h incubation at 37°C (based on optimisation experiments using times of 12-120 h), the supernatants were removed and 500 µg/ml of MTT in IMDM added for 2 h at 37°C. After incubation, the MTT solution was removed and the cells dissolved in 100 µl isopropanol. The absorbance of the resulting solution was measured at 540 nm using a plate reader (Biorad). Toxicity of any treatment was expressed as absorbance at 540 nm versus that of medium controls.

3.14.3 Immuno-histochemistry of cell layers

A549/iHBEC cells were plated onto 96-well plates at a density of 8×10^4 cells/well. The cells were incubated at 37°C overnight to adhere and form a confluent monolayer. The next day the medium was removed and the neutrophil supernatants (diluted 1 in 2.5) or diluent controls added. After 48 h at 37°C, the supernatants were removed, and the cell monolayers washed with PBS⁻ and fixed with 3.5% paraformaldehyde (PFA) for 20 min (RT) prior to two final washes with PBS⁻. NHBE cells in ALI culture were exposed to neutrophil supernatants (500 µl, 1:2 dilution) added to the basal side for 6 hours at 37°C. After this exposure the cells were gently scraped off the transwells and fixed in 4% PFA for 30 mins prior to washing twice with PBS. Before staining, cytopins were made of the cell scrapings. All subsequent steps were performed at RT unless otherwise stated. Before staining the cells were permeabilised with 0.5% Triton-X in PBS⁻ for 10 min and washed twice with PBS⁻. Non-specific staining was blocked using PBS-BSA (0.5% BSA, 30 min) and washed 3 times with PBS⁻. The cells were stained with anti-cleaved caspase 3 (goat polyclonal, Santa Cruz, 1:1,000, Cell Signalling) for 1 h, washed twice with PBS⁻ and incubated with secondary antibody (Alexa-Fluor 488 donkey anti-goat IgG, 1:1,000, Invitrogen) for 1 h prior to further washing steps. Rhodamine phalloidin (1:200,

Invitrogen) was then added to the wells to stain for F-actin (30 min), cells washed 3 times with PBS⁻ and finally a DAPI containing mountant (Invitrogen) was added.

Figure 3.9 shows representative images of the A549, iHBE and NHBE cell layers stained in this fashion. The plates were kept on ice and in the dark prior to imaging with a Leica Sp5 confocal microscope. Three representative images were taken in different areas of the well, with care to avoid the edges of the wells. The observer was unblinded to the treatments.

This protocol was developed by Cheng Chen, a Part 2 medical student at the University of Cambridge working under my supervision.

3.14.4 Preparation of NHBE cells for electron microscopy analysis

Cells were cultured as described above. When cilia were observed on the cultures, The wells were fixed by submerging the inserts in Sorensen phosphate-buffered (pH 7.4) glutaraldehyde (4% w/v). Dr Jeremy Skepper (Department of Physiology, Development and Neuroscience, University of Cambridge) completed sample preparation for electron microscopy analysis (as described in section 3.12.1) and took images of the cells using a FEI Verios 460 microscope.

3.14.5 Assessment of cellular leakage by LDH assay

The lactate dehydrogenase (LDH) assay (Sigma) measures membrane integrity by quantifying the release of cytoplasmic LDH into the medium. The assay is based on the reduction of NAD by LDH; reduced NAD (NADH) leads to the stoichiometric conversion of a tetrazolium dye, and the resulting compound is measured colourimetrically at 450 nm a multi-well plate reader (Biorad 680). Media samples (10 μ l) were taken from the basolateral side of a Transwell of NHBE cells exposed to neutrophil supernatants at $t = 0, 1 \text{ h}, 2 \text{ h}, 4 \text{ h}, 8 \text{ h},$ and 24 h . Samples or NADH standard (provided with the kit) were transferred to a 96-well plate and brought to a final volume of 50 μ l with the supplied LDH assay buffer. Next, 50 μ l of the provided reaction master mix was added, and the solution mixed by pipetting up and down 4 times. During subsequent steps the plate was protected from light and incubated at 37°C . After 2 min, the initial measurement was made at 450 nm - $(A450)_{\text{initial}}$. Subsequent measurements were made every 5 min for 1 h using a multi-well plate reader (Fluostar Optima plate reader, BMG Labtech) for 1 h; by this time the most active sample approximated to

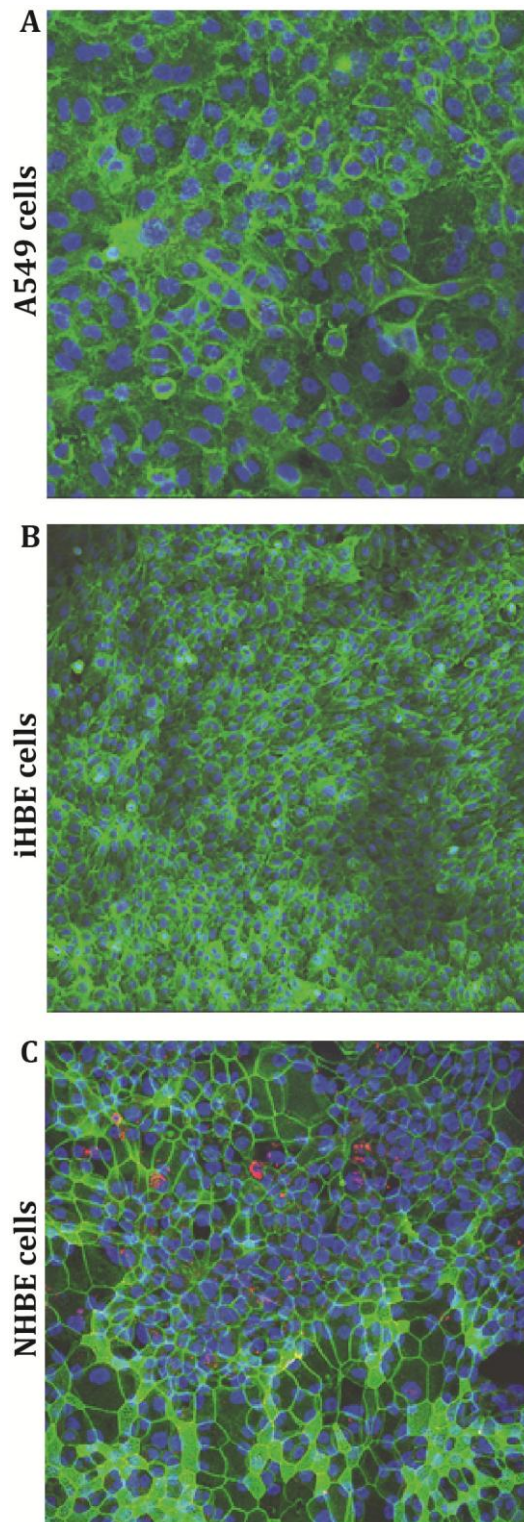


Figure 3.9: Immunocytochemistry of A549, iHBEC and NHBE epithelial cells

Three epithelial cell models were used to look at neutrophil mediated damage. A. A549 cells. B. iHBEC's and C. Primary HBEC's (Lonza) grown to confluence in the recommended tissue culture media and stained with DAPI (nucleus: blue) and rhodamine phalloidin (actin: green), x40 magnification. The iHBEC's and primary cells have a more uniform, cobblestone appearance compared with the A549 cells.

or exceeded the end of the linear range of the standard curve. The measurement $(A450)_{final}$ used for calculating the released enzyme activity is the penultimate reading (when the final measurement of the most active sample falls within the linear range of the standard curve). All measurements were corrected for background. A standard curve was obtained by plotting the absorbance versus the corresponding concentrations of NADH standard.

The change in absorbance was calculated by

$$\Delta A450 = (A450)_{final} - (A450)_{initial}$$

The LDH activity can then be calculated by

$$\text{LDH activity} = (B \times \text{sample dilution factor}) / (\text{reaction time}) \times V$$

B= Amount (nmol) of NADH generated between $T_{initial}$ and T_{final}

Reaction Time = $T_{final} - T_{initial}$ (minutes)

V = sample volume (mL) added to well
LDH activity (mean of duplicates) was expressed as nmol/min/mL

3.14.6 Analysis of ciliary function

3.14.6.1 Assessment of ciliary beat frequency

Ciliated cells were cultured as described above. The ciliated cell layers were gently scraped from the Transwell inserts, suspended in 500 μ l of ALI medium per well and transferred to Eppendorf tubes. The cells were left to settle for 10 min, the medium was removed and the cells exposed to neutrophil supernatants (undiluted). Directly after exposure the cells were transferred onto a chamber-slide (Figure 3.10). Beating ciliated edges were recorded using a digital high-speed video camera (Kodak Ektapro Motion Analyser, Model 1012) at a rate of 500 frames per second (x 63 lens), using a shutter speed of 1 in 2,000. This allows video sequences to be recorded and played back at reduced frame rates or frame by frame. Recordings of 4 different ciliated edges were taken every 30 min up to 2 h. The movies were subsequently analysed for ciliary beat frequency, ciliary dyskinesia and cell damage. For the ciliary beat frequency the movies were processed and cropped to the area of interest (ciliated cells) to eliminate background signal. They were then processed using CiliaFA³⁹³, a program developed by

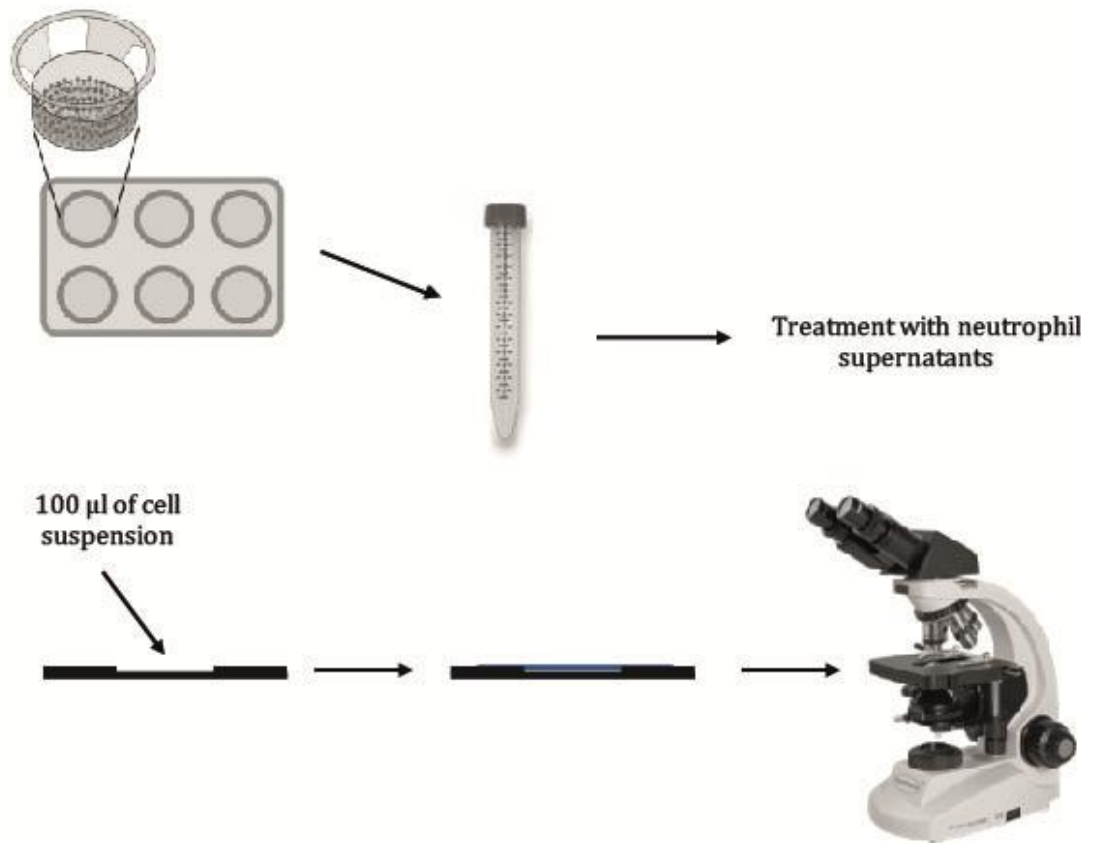


Figure 3.10: Analysis of ciliary function

Ciliated cultures were removed from the Transwell insert by gentle scraping with a spatula and transferred to Eppendorf tubes. The cells were allowed to settle for 10 min after which the media was removed and the cells exposed to neutrophil supernatants. Directly after exposure the cells were transferred to a microscope chamber slide. Beating ciliated edges were recorded using a digital high speed video camera at a rate of 500 frames per second (x63 magnification), using a shutter speed of 1 in 2000. Recordings of 4 different ciliated edges were made every 30 min for 2 h. The movies were subsequently analysed for ciliary beat frequency and ciliary dyskinesia.

Dr Claire M. Smith (Institute of Child Health, University College London). The program is based on Microsoft Excel and ImageJ and uses Fourier transformation to calculate the beat frequency (representative analysis sheet shown in the appendixes, section 8.3).

3.14.6.2 Assessment of ciliary beat pattern

Ciliary dyskinesia was assessed following an adapted version of a Standard Operating Procedure (SOP) for the determination of ciliary dyskinesia used for patient samples in the National Primary Ciliary Dyskinesia (PCD) service, Leicester (see appendix 3.2).

1. Calculation of Immotility Index.

In each movie the total number ciliated cells were counted, with a score of zero attributed to each immotile cilium. This process was repeated for each cell on 4 separate epithelial edges per condition. The Immotility Index is the percentage of zeros scored per edge per condition.

2. Calculation of Dyskinesia Index.

Dyskinetic cilia were defined as those with either no movement, or a slow or abnormal beat pattern. In each movie the total ciliated cells were counted, with dyskinetic cilia given a score of 1. This process was repeated for each cell on 4 separate epithelial edges per condition. The Dyskinesia Index is the percentage of 1's scored per edge per condition.

3.15 Statistical Analysis

Data are reported as mean and SEM or SD from (n) independent experiments and analysed using Prism 5.0 software (GraphPad, San Diego, CA). A p value of 0.05 was considered significant.

Chapter 4

Results: Hypoxia induces a more activated neutrophil phenotype

4. Hypoxia induces a more activated neutrophil phenotype

4.1 Introduction

It is well established that hypoxia modulates neutrophil function; published effects include delayed apoptosis^{354,394} and a reduced respiratory burst, resulting in impaired ROS-dependent killing of *Staphylococcus aureus*³²⁷. Previous work in our laboratory has shown that sustained and stable hypoxia (oxygen tension of the cell culture media ~3kPa) can be obtained using an InVivo400 hypoxic incubator (Ruskin) delivering an atmosphere of 0.8% oxygen within the chamber. This oxygen tension is sufficient to stabilise HIF-1 α in neutrophils incubated in tissue culture medium³⁵⁴ and is physiologically relevant (as shown by Peyssonnaud, C. *et al.*³⁰⁹ and others^{304,325,395,396}). Research undertaken by Peyssonnaud *et al.*³⁰⁹ has confirmed that hypoxic areas are present in normal skin epithelial basal cell layers; this was shown by staining tissues with HypoxyprobeTM-1 reagent (pimonidazole), which binds thiol groups in a redox-dependent fashion, with binding occurring only at oxygen tensions <10mm Hg or 1.3 kPa. Hypoxyprobe reactivity correlated to pronounced immunostaining for HIF-1 α within the epithelial keratinocyte layer. In addition, Iannitti *et al.*³¹⁹ showed that hypoxia is also present in the lungs of mice infected with the pathogenic fungus *Aspergillus fumigatus*, and in both the human and mouse cystic fibrosis (CF) airway.

Since hypoxia is encountered by neutrophils in both the physiological and pathological settings, I wished to expand the preliminary observations made previously in our laboratory by Dr Naomi McGovern that hypoxia augments the release of NE. As well as playing a fundamental role in bacterial killing, degranulation has also been shown to contribute to neutrophil tissue migration³¹ and modulation of the immune response¹³³. Furthermore, the products of neutrophil degranulation have been implicated in tissue destruction, in both a beneficial (promoting granuloma formation to limit the spread of mycobacterial pathogens: Taylor *et al.*³⁹⁷ and a detrimental setting (for example, leading to matrix destruction and generating pro-inflammatory mediators like the neutrophil chemoattractant N-acetyl Pro-Gly-Pro (PGP)^{206,398,399}). Although evidence of intravascular degranulation can be found in extreme clinical settings such as following cardiac arrest and septic shock^{400,401}, degranulation occurs predominantly within tissues, at the site of infection or inflammation, either at the phagosomal membrane in response to pathogen ingestion (killing the engulfed organisms) or extracellularly at the plasma membrane in response to receptor-mediated activation (exposing the extracellular milieu

to potentially damaging proteases). Several groups have found increased levels of NE in conditions that have been associated with hypoxia, for example in COPD sputum samples⁴⁰² and in the circulation of rats after bowel ischemia-reperfusion injury⁴⁰³. Our previous observation³⁷⁹ that hypoxia augments NE release was preliminary made only by means of an ELISA, hence NE activity was not assessed. The distinction between protein detection and NE activity is of physiological relevance as neutrophils also release the protease inhibitor α_1 AT⁴⁰⁴; the ELISA for NE does not distinguish between active NE and NE complexed with α_1 AT.

Furthermore, many granule-derived proteins in addition to NE contribute to both pathogen killing (for example, lactoferrin is directly bactericidal but also inhibits biofilm formation⁴⁰⁵) and tissue injury; for example, an MPO inhibitor halts disease progression in a mouse cigarette smoke exposure model of COPD¹²⁵. To further investigate neutrophil degranulation I have focused on the hallmark proteins of each granule (section 1.3.1-1.3.4): NE and also MPO from the azurophilic granules, lactoferrin from the specific granules, and MMP-9 from the gelatinase granules.

The specific aims of the work presented in this chapter are:

1. To establish whether hypoxia affects the release of any or all of the neutrophil granule sub-populations.
2. To confirm that proteases released under hypoxic conditions display full biological activity.
3. To determine whether cigarette smoke modulates the neutrophil degranulation response under normoxic and hypoxic conditions.
4. To explore the effects of hypoxia on morphological features associated with neutrophil activation and priming.

4.2 Confirmation of the neutrophil hypoxic response

The CO₂ levels in the InVivo400 chamber were titrated to maintain a stable, physiological pH in the culture media during experiments, to prevent acidosis from confounding the results. It should be noted that inflamed hypoxic tissues *in vivo* may also be acidotic with low nutrient availability; however the exploration of these parameters in the context of hypoxia was not thought to fall within the scope of this thesis. Accordingly, the O₂ and

CO₂ levels and pH of the culture media were tested regularly to ensure that stable readings were obtained throughout each experiment and for the entire duration of my experimental work (Normoxia: O₂ = 21.65±0.49 kPa, CO₂ = 4.30±0.28 kPa, pH = 7.40±0.02. Hypoxia: O₂ = 3.35±0.14 kPa, CO₂ = 4.19±0.07 kPa, pH = 7.45±0.01 (section 3.3.2, Figure 3.2). To confirm that I could isolate un-primed, fully responsive neutrophils and could recapitulate the previously published effects of hypoxia on neutrophil function, the ability of neutrophils to mount an oxidative burst was assessed under conditions of normoxia and hypoxia. Primed (GM-CSF, 10 ng/ml) and unprimed (vehicle treated) neutrophils were activated with fMLP (100 nM, G-protein coupled receptor-mediated activation), and the extracellular release of superoxide quantified using the superoxide dismutase-inhibitable reduction of cytochrome C. PMA (200 nM) was used as a maximal, receptor-independent method to achieve NADPH oxidase activation (PMA activates protein kinase C directly). Neutrophils were incubated under normoxic or hypoxic conditions for 1 h in PBS⁺ and stimulated as described above (see also section 2.5). As shown in Figure 4.1A, GM-CSF-priming augmented the fMLP-stimulated respiratory burst substantially (approximately 6-fold up-regulation), whilst (as anticipated) hypoxia significantly impaired the production of superoxide anions. The normoxic primed and activated neutrophils produced 16.90±1.45 nmols O₂⁻/10⁶ cells, while primed hypoxic neutrophils were only able to produce 5.09±1.03 nmols O₂⁻/10⁶ cells on stimulation with fMLP. The inhibitory effect of hypoxia was also apparent upon stimulation with PMA, with the release of superoxide reduced from 22.50±0.95 nmols O₂⁻/10⁶ cells under normoxia to 9.07±0.24 nmols O₂⁻/10⁶ cells under hypoxic conditions.

Another published effect of hypoxia on neutrophils is delayed apoptosis^{354,394}. To recapitulate these data, freshly isolated neutrophils were re-suspended in normoxic or hypoxic media (with 10% serum, 5*10⁶ cells/ml) and incubated under normoxic or hypoxic conditions. After 20 h, cytopins were made and apoptosis assessed by cellular morphology (section 3.7). These data are depicted in Figure 4.1B and confirm that hypoxia promotes neutrophil survival by delaying apoptosis, consistent with the labs previous reports. These results show that the neutrophil isolation process employed yields un-primed and highly responsive cells, and that the hypoxic conditions modulated neutrophil function in a manner consistent with the published literature. Of note, McGovern *et al.*³²⁷ also demonstrated that hypoxia reduced the intracellular oxidative burst generated in response to particle ingestion, which is thought to be of direct relevance to bacterial killing, whilst the extracellular release of ROS has been linked to

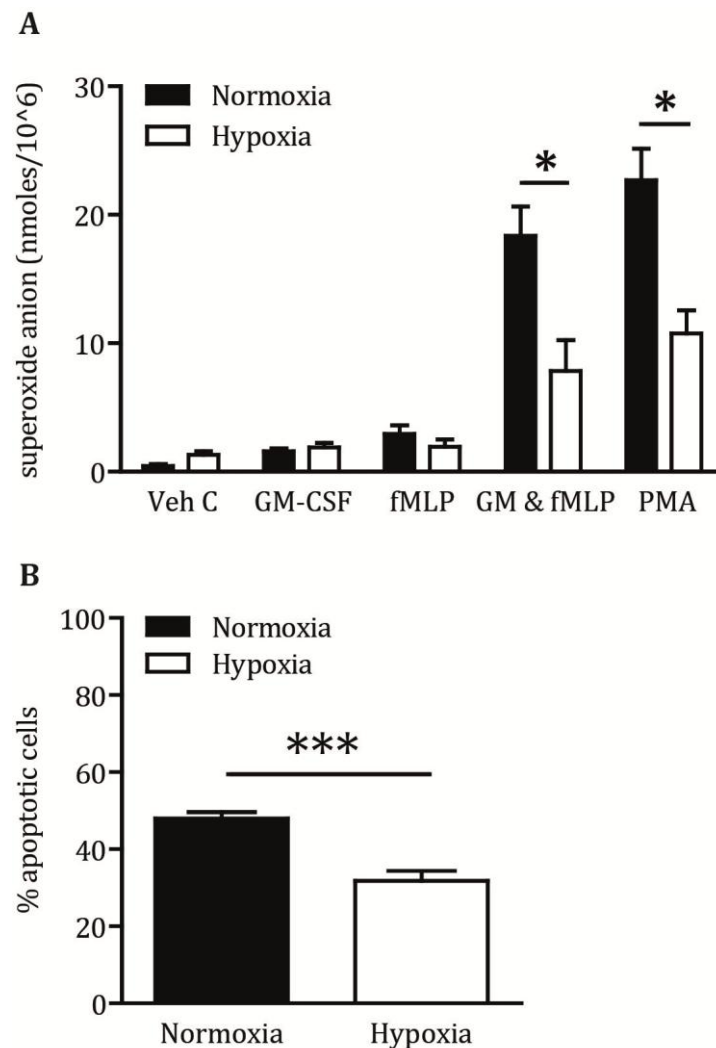


Figure 4.1: Hypoxia alters neutrophil function

A. Neutrophils ($11.1 \times 10^6/\text{ml}$) in PBS^+ were incubated with GM-CSF (10 ng/ml) or vehicle under normoxic (filled bars) or hypoxic (0.8% O_2 and 0.5% CO_2 , open bars) conditions for 1 h at 37°C . The cells were subsequently stimulated with either fMLP (100 nM), PMA (200 nM) or vehicle for 10 min. Extracellular O_2^- release was measured by the superoxide dismutase-inhibitable reduction of cytochrome C as described. Cells were pelleted and the supernatants transferred to fresh tubes before removal from the hypoxic hood prior to measuring the optical density at 550 nm using a scanning spectrophotometer. B. Neutrophils were re-suspended in hypoxic or normoxic IMDM at $11.1 \times 10^6/\text{ml}$. The cells were incubated under normoxia or hypoxia (0.8% O_2 and 5% CO_2) at 37°C for 20 h. Cytospins were prepared and stained with May/Grünwald/Giemsa. Morphology was examined by oil-immersion light microscopy. Results represent mean \pm SEM, A. $n=5$ experiments each performed in triplicate, B. $n=8$, experiments each performed in triplicate. * = $p < 0.05$, *** = $p < 0.001$ (Mann-Whitney test).

neutrophil-mediated tissue injury^{406,407}. The reduced intracellular respiratory burst under hypoxia was associated with impaired killing of *Staph A*, and re-oxygenation restored both ROS generation and killing. However, other mechanisms contribute to bacterial killing, and some bacteria including *Escherichia coli* and *Streptococcus pneumoniae* are killed independently of the NADPH oxidase respiratory burst^{46,408}. Neutrophil granule proteins including serine proteases^{129,409} and lactoferrin⁴¹⁰ contribute to bacterial killing, and NE and MMP-9 have been implicated in tissue injury. Hence I wished to investigate the effect of hypoxia on neutrophil degranulation.

4.3 The effects of hypoxia on neutrophil degranulation

4.3.1 The effects of hypoxia on azurophil granule protein release

Since our preliminary data related to NE, and the considerable body of evidence implicating this protease in tissue injury⁴¹¹⁻⁴¹³, I initially looked at NE activity released by neutrophils (section 3.8.2). Neutrophils were incubated under normoxic or hypoxic conditions at 37°C for 4 h, primed (GM-CSF, 10 ng/ml or Cytochalasin B (Cyt B) 5 µg/ml, 30 min) and activated (fMLP 100 nM, 10 min) prior to measurement of NE activity in the supernatants. As shown in Figure 4.2A, there was little or no detectable NE activity present in the supernatants derived from un-stimulated cells under normal or hypoxic conditions. However, stimulation with the physiological priming agent GM-CSF and activation with fMLP did lead to detectable release of active NE, and importantly, this was significantly increased (almost sixfold) by hypoxia ($10.4 \times 10^3 \pm 7.5 \times 10^3$ Arbitrary units (AU) *versus* $61.2 \times 10^3 \pm 12.4 \times 10^3$ AU.). The combination of Cyt B and fMLP is normally regarded as a maximal (if non-physiological) stimulus for neutrophil degranulation, but even the substantial NE release induced by this combination was further and significantly up-regulated under hypoxic conditions (increasing from $173.4 \times 10^3 \pm 32.5 \times 10^3$ AU. to $324.4 \times 10^3 \pm 24.3 \times 10^3$ AU.).

At the end of the assay, the neutrophils still excluded trypan blue, indicating that the NE release observed was not secondary to loss of membrane integrity or necrosis (data not shown). To determine whether this finding was specific for NE (perhaps reflecting increased expression of NE protein) or resulted from enhanced azurophil granule release, the liberation of a second azurophil granule protein, myeloperoxidase (MPO), was also assessed by means of the H₂O₂-dependent oxidation of o-dianisidine dihydrochloride (section 3.8.5).

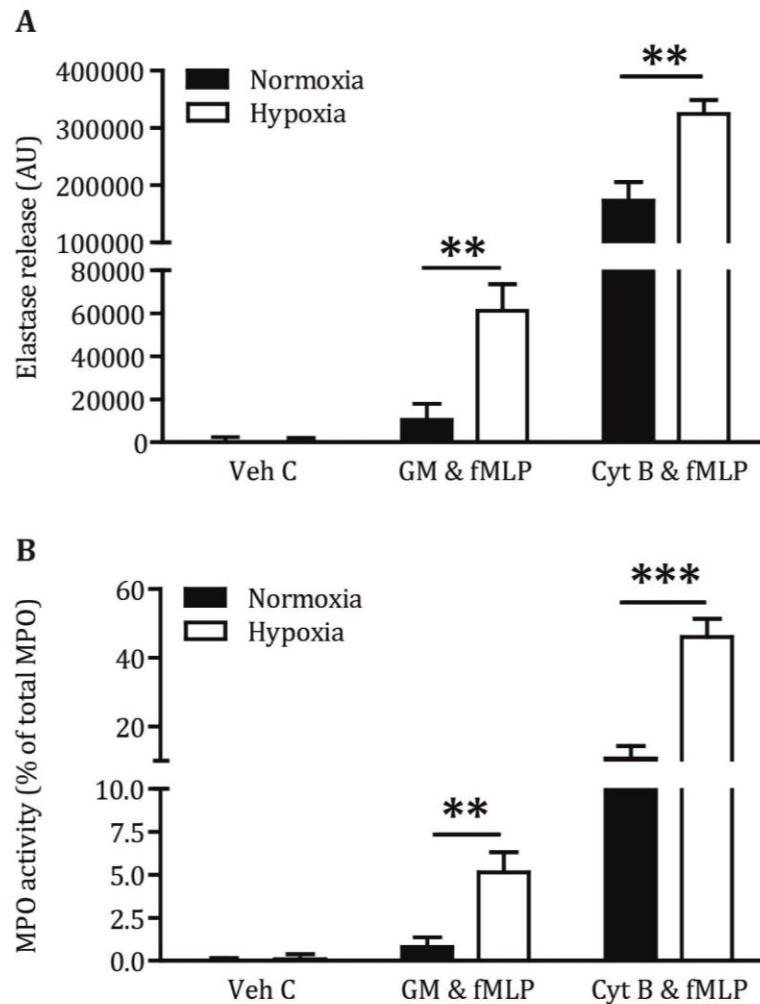


Figure 4.2: Hypoxia augments the exocytosis of azurophil granules

Neutrophils ($11.1 \times 10^6/\text{ml}$) in PBS^+ were incubated under normoxic (filled bars) or hypoxic (0.8% O_2 and 0.5% CO_2 , open bars) conditions for 4 h at 37°C . The cells were primed (or not) with GM-CSF (10 ng/ml, 30 min) or Cyt B (5 $\mu\text{g}/\text{ml}$, 5 min) and activated with fMLP (100 nM, 10 min) or vehicle, and the supernatants assayed for granule protein activity. A. NE activity was measured by the increase in fluorescence caused by the cleavage of DQ-Elastin, $n=10$. B. MPO activity was measured by the H_2O_2 -dependent oxidation of o-dianisidine dihydrochloride (DMB) at 460 nm, $n=8$. The results represent mean \pm SEM; all samples were run in triplicate. ** = $p < 0.01$, *** = $p < 0.001$ (Mann-Whitney test).

Figure 4.2B shows that the release of active MPO closely paralleled that of NE. After stimulation with either GM-CSF plus fMLP or with Cyt B plus fMLP, MPO release was significantly augmented by hypoxia, increasing from $0.8\% \pm 0.56$ of total cellular MPO to $5.1\% \pm 1.18$ with GM-CSF priming and from $10.8\% \pm 3.6$ of total MPO to $46.1\% \pm 5.3$ with Cyt B priming. During these experiments degranulation was measured in neutrophil supernatants only, the total amount of granule proteins in neutrophils after 4 hours of normoxia or hypoxia was not sampled. These results show that the release of both NE and MPO is increased by hypoxia, strongly suggesting that azurophil granule exocytosis is facilitated by these environmental conditions. To explore whether this effect was limited to the azurophilic granules, the effect of hypoxia on the release of gelatinase and specific granules was explored.

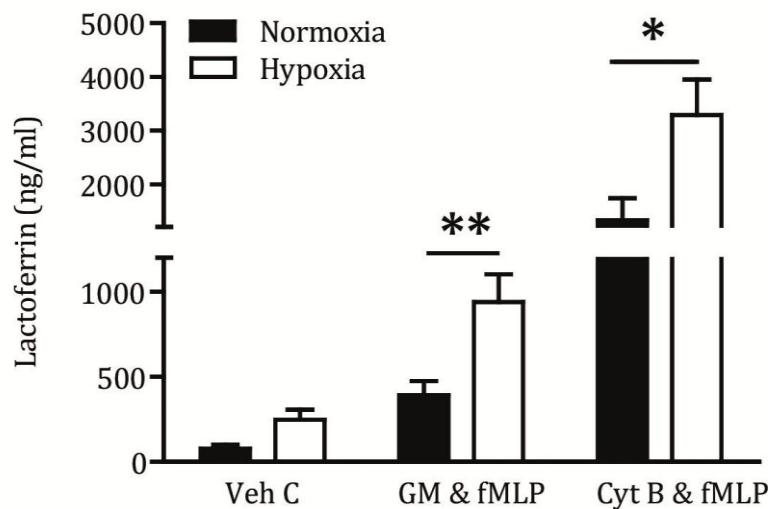
4.3.2 The effects of hypoxia on specific granule protein release

While the proteases present in the azurophil granules are of particular importance to bacterial killing, proteins stored in other granules also contribute to this function and to the potential of the migrating neutrophil to degrade matrix. Since hypoxia can augment the release of azurophil granules, which are considered to be the most resistant to extracellular mobilisation^{68,70}, it was felt plausible that hypoxia might also facilitate the secretion of other neutrophil granule populations.

Lactoferrin is a potent anti-microbial agent, which impairs bacterial growth by the sequestration of iron¹⁰⁹, and is located principally in the specific granules. As shown in Figure 4.3A, the effect of hypoxia on the release of lactoferrin (measured by commercial ELISA as described in section 3.8.6) recapitulated the pattern seen with NE and MPO. Under normoxic conditions, there was minimal release of lactoferrin, but release was increased upon stimulation with GM-CSF and fMLP or Cyt B and fMLP. The release of lactoferrin was further augmented by hypoxia, from 391 ± 82 ng/ml to 1331 ± 407 ng/ml (GM-CSF/fMLP) or from 940 ± 162 to 3286 ± 663 ng/ml (Cyt B/fMLP). Since lactoferrin is not an enzyme, activity assays are not relevant in this context.

4.3.3 The effects of hypoxia on gelatinase granule release

The gelatinase granules are readily exocytosed, reflecting their function as a reservoir of matrix-degrading enzymes and membrane receptors to promote neutrophil extravasation and diapedesis^{104–106}.

**Figure 4.3: Hypoxia up-regulates the exocytosis of specific granules**

Neutrophils ($11.1 \times 10^6/\text{ml}$) in PBS^+ were incubated under normoxic (filled bars) or hypoxic (0.8% O_2 and 0.5% CO_2 , open bars) conditions for 4 h at 37°C . The cells were primed (or not) with GM-CSF (10 ng/ml, 30 min) or Cyt B (5 $\mu\text{g}/\text{ml}$, 5 min) and activated with fMLP (100 nM, 10 min) or vehicle, and the supernatants assayed for granule protein concentration. Lactoferrin release was measured by ELISA (Hycult). Results represent mean \pm SEM from $n=6$ independent experiments; all samples were run in triplicate. * = $p < 0.05$, ** = $p < 0.01$ (Mann-Whitney test).

Hypoxic enhancement of gelatinase granule release could lead to excessive matrix degradation and contribute to disease pathogenesis; for example, Vlahos and colleagues⁶⁷ demonstrated a dramatic up-regulation of MMP-9 in the BAL fluid of patients with COPD and noted a striking correlation with disease severity (21-fold increase in MMP-9 activity in GOLD IV versus GOLD II disease).

To confirm that hypoxia augments neutrophil gelatinase granule release, I assessed the liberation of matrix metalloproteinase-9 (MMP-9, neutrophil gelatinase B), an important component of the gelatinase granules. Total MMP-9 release was quantified by ELISA, and MMP-9 activity was assessed by gelatin zymography. The hypoxia-attributable increase in degranulation was recapitulated for MMP-9, as shown in Figure 4.4A. GM-CSF priming induced a modest release of MMP-9 (37 ng/ml), which was significantly increased by hypoxia (4.4 fold, 165 ng/ml). Of note, under conditions of hypoxia, the fMLP-stimulated release of MMP-9 achieved by GM-CSF priming is almost equivalent to that seen with Cyt B (141 ng/ml versus, 218 ng/ml) consistent with the lower threshold for gelatinase granule release previously reported^{75,233}. However MMP-9 release is only relevant *in vivo* if this protease is active and therefore capable of causing tissue damage, hence neutrophil supernatants were also subjected to gelatin zymography, Figure 4.4B/C. The basis of this assay is that active gelatinase should cleave the gelatin embedded within a polyacrylamide gel. Inclusion of EDTA (0.4 μ M) to inhibit MMP's during the washing and incubation steps resulted in a blank gel, indicating that the bands shown in Figure 4.4C are produced by MMP digestion, not by other enzymes (data not shown). The representative zymogram and quantification of the bands by imageJ of n=3 experiments (Figure 4.4B) illustrates that active MMP-9 is released in a broadly similar pattern to that detected by ELISA. There is an increase in active MMP-9 released in response to GM-CSF/fMLP from 10.5×10^3 arbitrary densitometric units (normoxia) to 22.4×10^3 (hypoxia). There was no apparent difference between normoxia and hypoxia after Cyt B and fMLP stimulation, reflecting the results obtained using the ELISA assay. During these experiments degranulation was measured in neutrophil supernatants only, and the total amount of granule proteins in neutrophils after 4 hours of normoxia or hypoxia was not sampled. However electron microscopy data shown in Figure 4.8 indicates that there is no difference in total number of azurophil granules and data shown in Chapter 6, Figure 6.4 shown that there is no increase in MMP-9 protein after a 4 hour incubation under normoxic or hypoxic conditions.

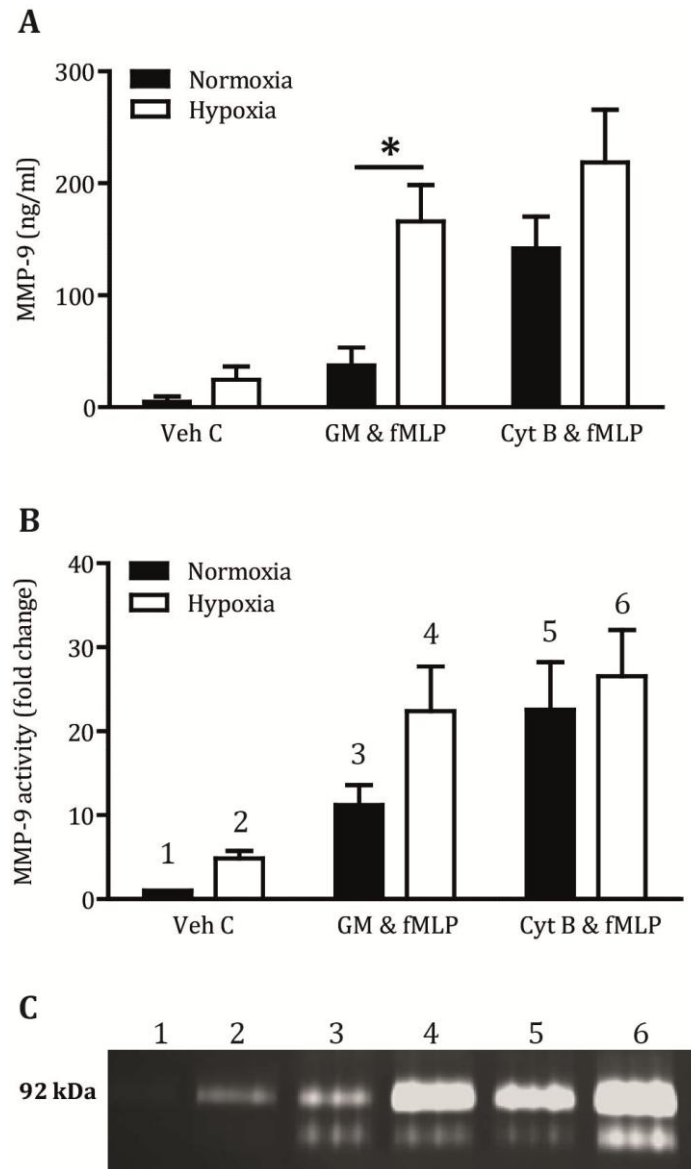


Figure 4.4: Hypoxia up-regulates the exocytosis of gelatinase granules

Neutrophils ($11.1 \times 10^6/\text{ml}$) in PBS^+ were incubated under normoxic (filled bars) or hypoxic ($0.8\% \text{ O}_2$ and $0.5\% \text{ CO}_2$, open bars) conditions for 4 h at 37°C . The cells were primed (or not) with GM-CSF (10 ng/ml , 30 min) or Cyt B ($5 \mu\text{g/ml}$, 5 min) and activated with fMLP (100 nM , 10 min) or vehicle (Vehicle control= Veh C), and the supernatants were assayed for granule protein concentration/activity. A. MMP-9 release was measured by MMP-9 DuoSet ELISA, samples were run in triplicate, $n=5$. B. Quantification of MMP-9 activity by band analysis with ImageJ. Results represent mean \pm SEM from an $n=3$ independent experiments, samples were run in triplicate. * = $p < 0.05$ (Mann-Whitney test) Numbers over bars relate to the lane numbers in C. C. Representative (of $n=3$)

Collectively, these results show that hypoxia augments exocytosis of multiple neutrophil granule populations following stimulation by physiological agonists, conferring the potential for increased tissue injury.

4.4 The effects of cigarette smoke medium (CSM) on NE release

Cigarette smoking is the most important risk factor for the development of COPD, and some papers have reported that cigarette smoke primes/activates neutrophils to induce a destructive phenotype. Mortaz *et al*²⁹⁹. and others have found that CSM induces the release of ROS²⁹⁸, IL-8, NE, MMP-2 and MMP-9 from neutrophils. Zappacosta *et al*.²⁹⁷ also showed an up-regulation of fMLP receptors and CD11B/CD18 integrin expression on the cell surface, consistent with the mobilisation of secretory vesicles. Therefore I wished to investigate whether hypoxia and cigarette smoke have additive or even synergistic effects on neutrophil degranulation, since such an interaction could be highly relevant to the pathogenesis of COPD. Cigarette smoke medium (CSM) was prepared as described above in section 3.4. To confirm that the prepared CSM was capable of eliciting its recognised biological effects, such as induction of oxidative stress, the impact on intracellular neutrophil ROS production was quantified using the reagent DC-FDA, which becomes strongly fluorescent upon interaction with ROS. As shown in Figure 4.5A, CSM induced a concentration-dependent increase in intracellular ROS production. This effect was most pronounced with concentrations of CSM above 25%; the effects of 50% CSM were comparable to those of PMA (a maximal stimulus for the generation of intracellular ROS). Guided by the literature already cited and by the results above, the effect of CSM, alone or in combination with GM-CSF/fMLP, on normoxic and hypoxic neutrophil degranulation was investigated. As shown in Figure 4.5B, rather surprisingly 25% CSM had no direct effect on the release of active NE, under either normoxia or hypoxia, and did not augment the effects of priming and/or stimulation with GM-CSF and fMLP. Even escalating the concentration of CSM to 50% did not augment these responses (figure 3.5B). Incubation of cells with 75% CSM was toxic to the cells and induced substantial mixed apoptosis/necrosis under normoxia (Figure 4.6), whilst hypoxia seemed to ameliorate CSM-induced toxicity somewhat, as judged by light microscopy.

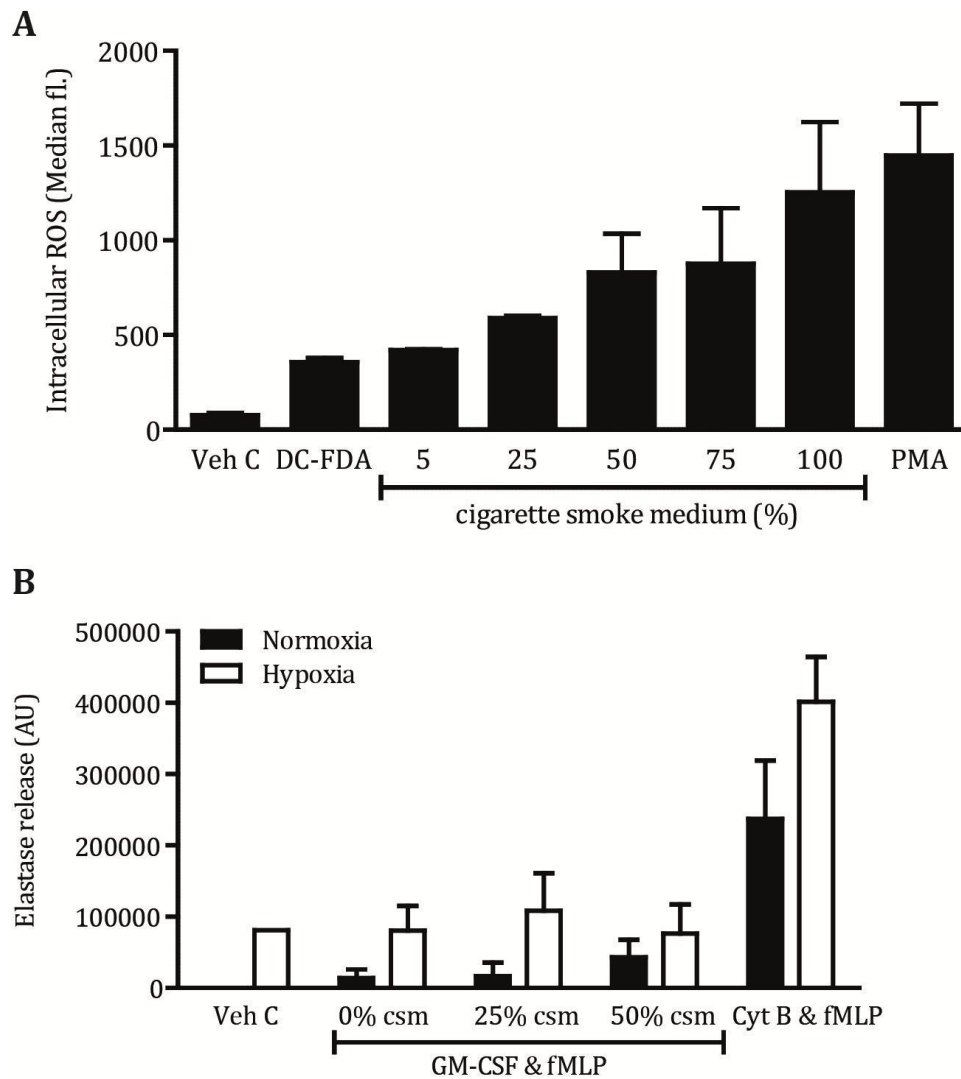


Figure 4.5: CSM induces ROS generation but does not affect NE release

A. Neutrophils (5×10^6 cells/sample) were suspended in HBSS \pm DC-FDA (final concentration $0.1 \mu\text{M}$) and incubated for 10 min prior to re-suspension in HBSS with or without 5, 25, 50, 75, 100% CSM. Following incubation at 37°C for 30 min, $100 \mu\text{l}$ aliquots were transferred to tubes containing optimised Cell FixTM. The cells were then analysed by flow cytometry ($n=2$). B. Neutrophils were re-suspended ($11.1 \times 10^6/\text{ml}$) in normoxic (filled bars) or hypoxic (open bars) IMDM, with or without CSM (0-50 % as indicated), and incubated at 37°C for 4 h. Cells were primed with GM-CSF (10 ng/ml, 30 min) or Cyt B ($5 \mu\text{g}/\text{ml}$, 5 min) and activated with fMLP (100 nM, 10 min). NE activity was measured by the increase in fluorescence caused by the cleavage of DQ-Elastin. Results represent mean \pm SD of $n=2$ independent experiments; all samples were run in triplicate.

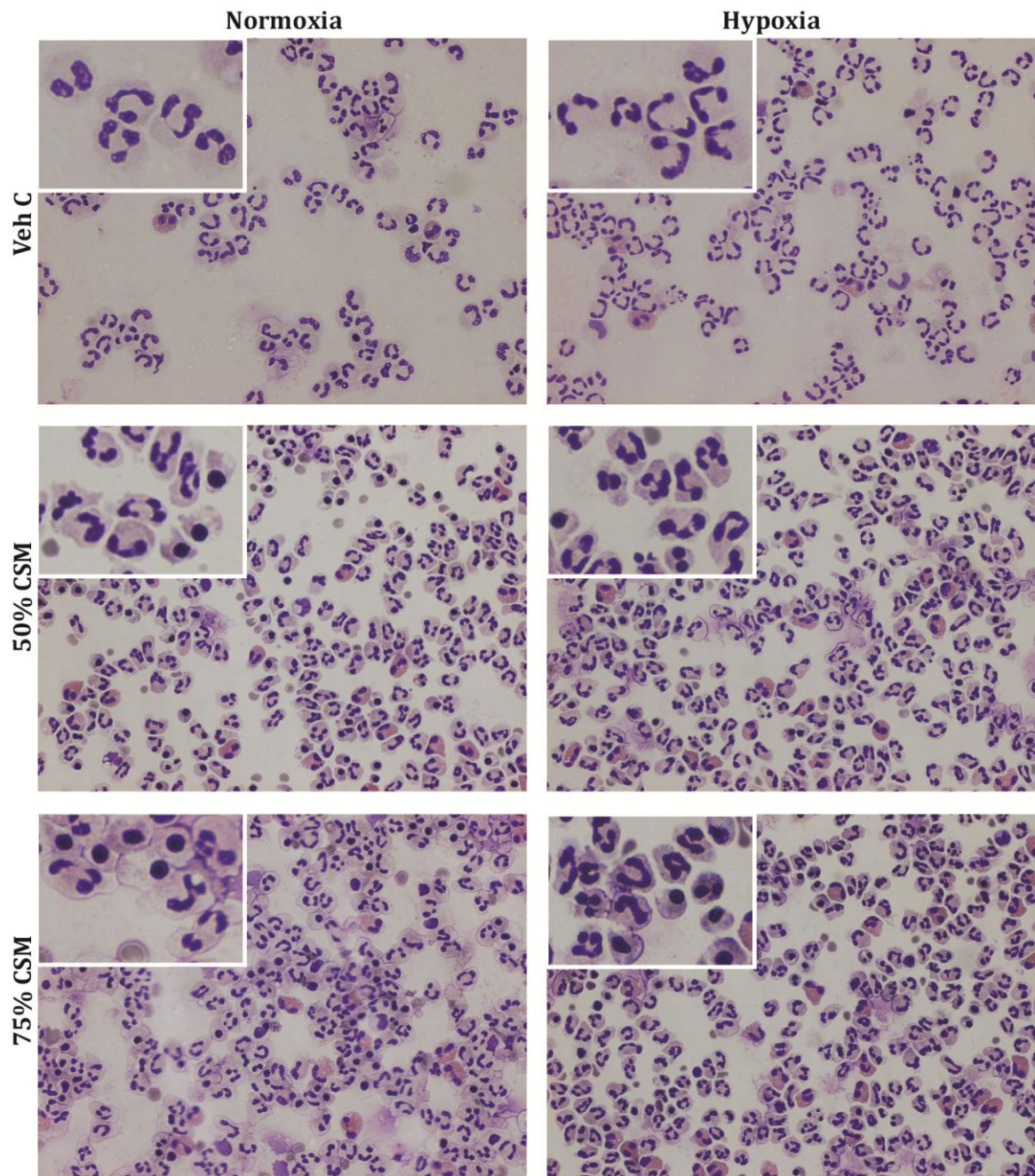


Figure 4.6: High concentrations of CSM are toxic to neutrophils

Neutrophils were re-suspended in hypoxic or normoxic IMDM ($11.1 \times 10^6/\text{ml}$) \pm CSM (5-50 %) incubated under normoxia or hypoxia (0.8% O₂ and 5% CO₂) at 37°C. After 4 hours, aliquots (90 μl) were taken for cytopins and then stained with May/Grünwald/Giemsa. The images are representative photomicrographs of cytopins from 3 independent experiments (x40 magnification).

4.5 The effects of hypoxia on neutrophil morphology

The data for azurophil granule release (Figure 4.2) suggest that even with maximal stimulation there was incomplete neutrophil degranulation; to verify this I studied the morphology of neutrophils pre- and post-degranulation by electron microscopy. The ability for hypoxia to potentiate degranulation suggested that this signal may prime certain aspects of neutrophil function; as a consequence other features that might indicate augmented activation were also determined. Neutrophil shape-change is a feature of neutrophil priming/ activation, requiring changes in actin cytoskeleton conformation to facilitate migration. Furthermore, cytoskeletal remodelling plays an important role in degranulation. Hence Transmission Electron Microscopy (TEM) and confocal microscopy were used to evaluate neutrophil morphology and cytoskeletal organisation in the normoxic and hypoxic setting.

4.5.1 TEM analysis of neutrophils morphology

To study the effects of hypoxia on neutrophil morphology using TEM, the cells were incubated under normal or hypoxic conditions and activated as described above, then fixed (4% glutaraldehyde) and prepared for TEM (section 3.12.1). The images shown (Figure 4.7) were obtained by Dr Jeremy Skepper. Changes in cellular morphology were scored based on published observations made by Mitchell et al.³⁸⁸ and Hoffstein *et al.*⁴¹⁴; the full scoring system is shown in Figure 3.7. Cells were scored (with the observer blinded to the experimental condition) for shape (rounded, irregular or elongated), membrane ruffling (microvilli, small/medium extensions, long extensions), clustering, presence of “empty vacuoles” (none, low or high) and granule density (low, medium or high). The result was an “activity score”, with 6-8 indicating a quiescent cell, 9-12 an activated cell and 13-17 a highly activated cell. As shown in Figure 4.8A, a significant difference in activation status between normoxic and hypoxic cells was obtained in both un-stimulated neutrophils and in neutrophils stimulated with Cyt B/fMLP. Surprisingly, GM-CSF/fMLP-stimulated neutrophils under hypoxic conditions did not differ from comparable normoxic cells when assessed by this method. This may reflect either the cell processing for TEM in some way ‘blunting’ any differences or be an issue related to the scoring system itself. Hence further parameters were assessed using the TEM images. Upon activation the neutrophils surface becomes irregular with formation of microvilli, and the cell adopts a more polarised oval shape.

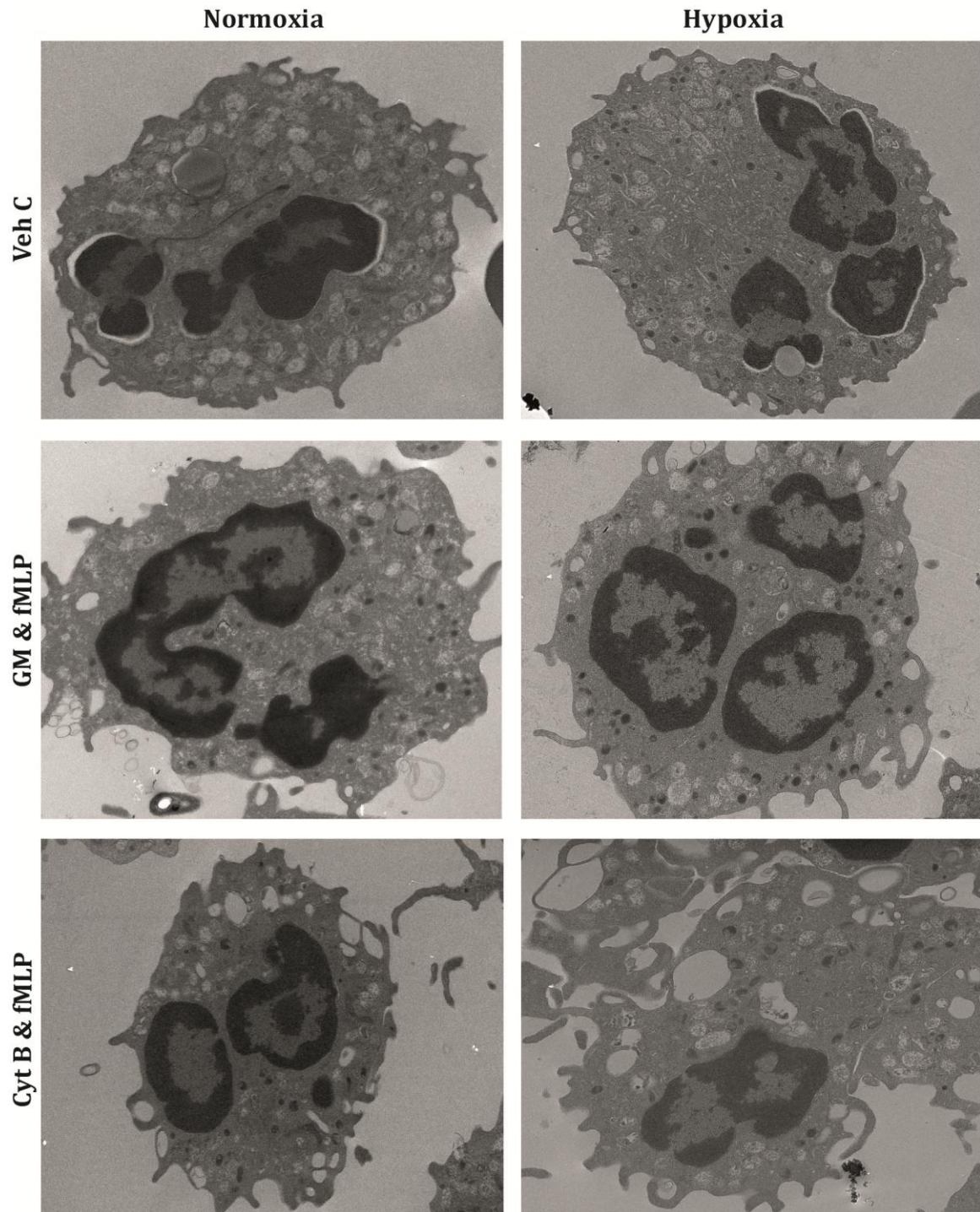


Figure 4.7: Effect of hypoxia on neutrophil morphology: TEM images

Neutrophils were re-suspended in hypoxic (left panels) or normoxic (right panels) IMDM at 11.1×10^6 /ml and incubated under normoxia or hypoxia (0.8% O₂ and 5% CO₂) at 37°C for 4 h. The cells were primed with GM-CSF (10 ng/ml, 30 min) or Cyt B (5 µg/ml, 5 min) and activated with fMLP (100 nM, 10 min). Cells were then fixed with 4% glutaraldehyde and processed for TEM by Dr Jeremy Skepper. Representative images of n=9-15 are shown; magnification = x3500.

The outline of each cell was therefore measured using ImageJ (n=9-10), and was found to increase upon activation; this increase was not greater for Cyt B-primed versus GM-CSF-primed stimulated cells (Figure 4.8B). A statistically difference in circumference between normoxic and hypoxic conditions was seen only when cells were stimulated with CB/fMLP. This methodology may be affected if the cells are not sectioned in the same plane between conditions, although I attempted to compensate for this by choosing cells with the nucleus cut in a similar plane.

Finally the number of azurophilic granules remaining within the cells was counted; these granules are electron dense and hence easy to identify. I predicted an inverse correlation with NE release. However, as shown (Figure 4.8C), only treatment with Cyt B/fMLP noticeable decreased the number of intracellular azurophilic granules remaining, versus unstimulated control cells. This may reflect the fact that GM-CSF/fMLP treatment, even under conditions of hypoxia, results in the release of less than 10% of the total azurophil granule content (Figure 4.2B), and suggests that this methodology may not be sensitive enough to detect such minor changes in intracellular granule content.

Although these data are not definitive, they do suggest that hypoxia promotes changes in neutrophil morphology. Since the actin cytoskeleton plays such a key role in shape change and in neutrophil degranulation, I chose to investigate more directly whether hypoxia might induce actin cytoskeletal remodelling.

4.5.2 Cytoskeletal changes under hypoxic conditions

Upon activation the neutrophil acquires a polarised morphology with an actin-rich lamellipodium (leading edge) and an elongated tail-like uropod at the rear end. This shape change facilitates rapid directional movement along a chemokine gradient (chemotaxis). Besides migration, actin re-organisation is also essential for the uptake of bacteria and the release of granule proteins^{276,415}.

Neutrophils were incubated under normal or hypoxic conditions for 4 h and stimulated with fMLP (100 nM) for 5 minutes prior to fixing and staining as described above (section 3.12.2). Under normoxic conditions, un-stimulated neutrophils displayed diffuse green F-actin staining, with slight polarisation apparent under hypoxia in the absence of other stimulation. Upon activation with fMLP (100 nM) polarised actin staining, with the formation of actin ‘caps’ was detected. This fMLP-induced morphological change was substantially increased and apparent in a far higher proportion of cells under hypoxic

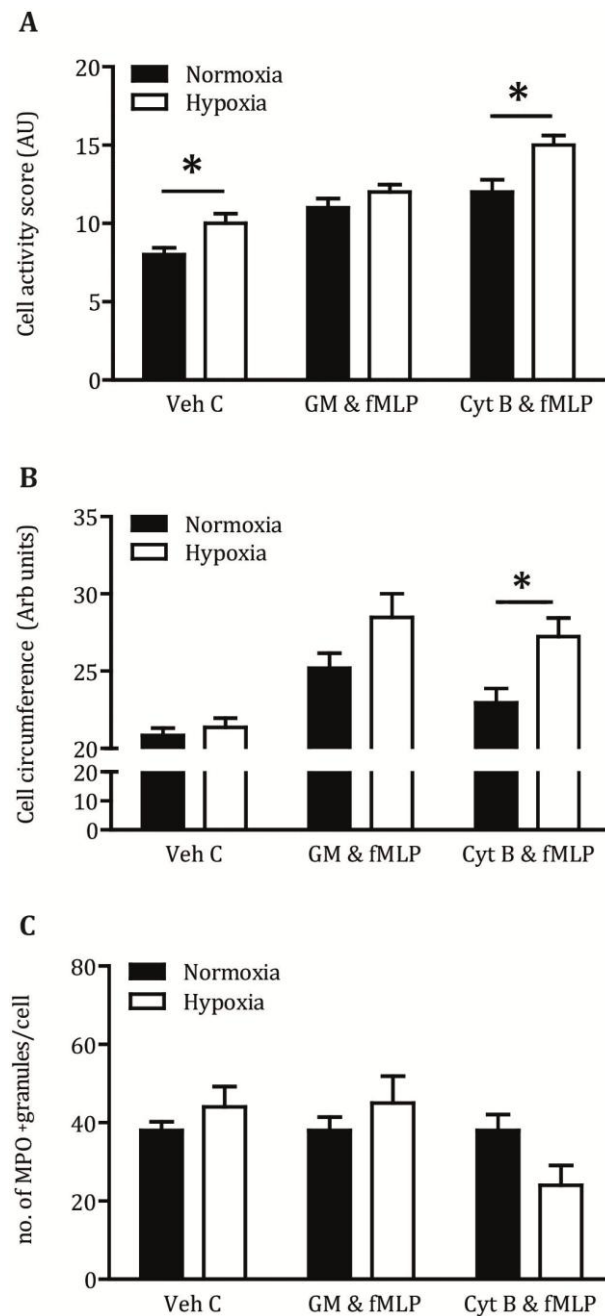


Figure 4.8: Effect of hypoxia neutrophil morphology: TEM quantification

Neutrophils incubated under normoxia or hypoxia (0.8% O₂ and 5% CO₂) at 37°C for 4 h were primed (GM-CSF 10 ng/ml, 30 min or Cyt B 5 µg/ml, 5 min) and then activated with fMLP (100 nM, 10 min). Cells were fixed with 4% glutaraldehyde and processed for TEM. Representative EM images (from n=9-15) are shown in Figure 3.7 above. A. Cells were scored for morphology, clustering, granule density, membrane ruffling and vacuole formation to give a ‘cell activity’ score in arbitrary units (AU). B. Cell circumference was measured by drawing around each cell margin and quantification with ImageJ. C. MPO⁺ granule quantification by counting. For A-C, values are mean ± SEM, with 9 images analysed per condition. * = p < 0.05 (Mann-Whitney test).

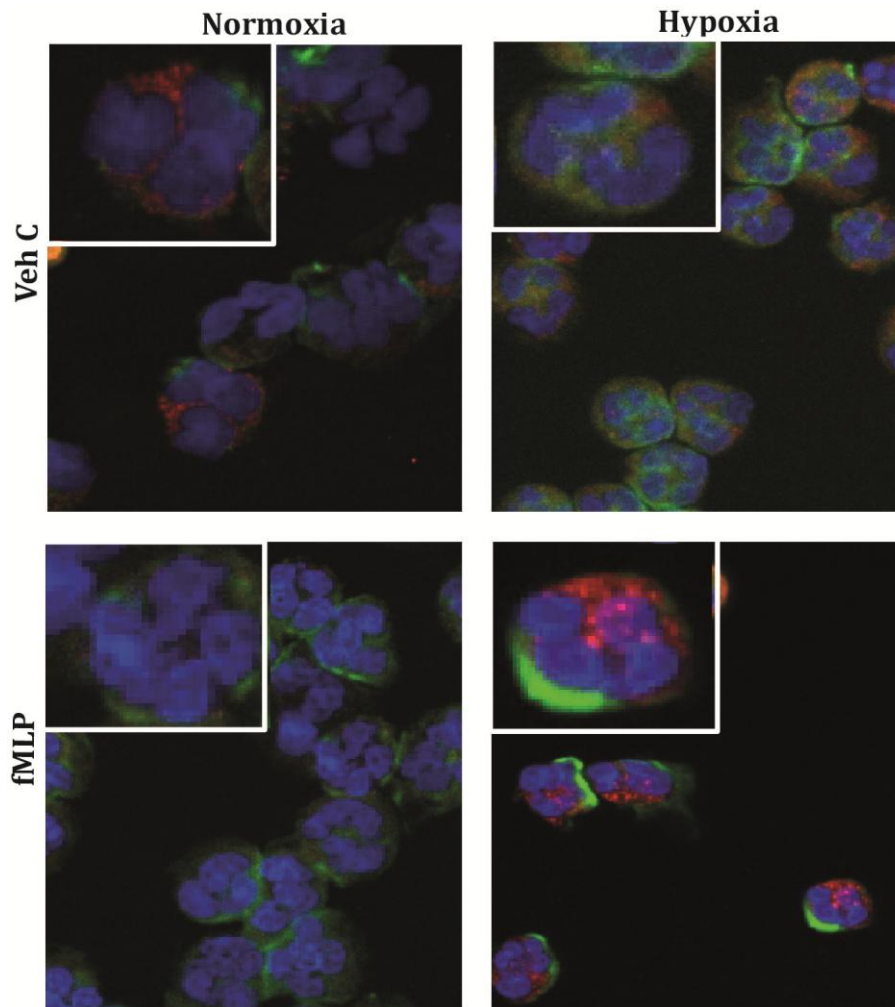


Figure 4.9: Activation and hypoxia induce actin cytoskeletal remodelling

Neutrophils were re-suspended in hypoxic or normoxic IMDM at $11.1 \times 10^6/\text{ml}$ and incubated under normoxia or hypoxia (0.8% O_2 and 5% CO_2) at 37°C for 4 h. The cells were stimulated with fMLP (100 nM) for 5 min, prior to fixing and permeabilisation. The cells were stained for the cell nucleus (DAPI, Blue), NE (goat IgG and Alexa Fluor 488–donkey anti-goat IgG, red) and F-actin (rhodamine-phalloidin, green), magnification =x60. Representative images shown of n=3 independent experiments.

conditions as shown in Figure 4.9 (representative images from n=3 experiments)

Cheng Chen, a 3rd year Medical Student undertaking a 12-week project in the laboratory, performed these experiments under my direct supervision and with my assistance.

4.6 Discussion

Neutrophilic inflammation predominates in the COPD airway wall^{63,64,416}, and an extensive body of evidence (from cell culture to murine models and finally to the susceptibility of human patients with α_1 AT deficiency to develop COPD) implicates NE as a key mediator of tissue damage and the relentless decline in lung function that occurs in this disease. It is known that hypoxia can influence neutrophil function profoundly^{327,354}. My results confirm and extend these observations; using a range of different techniques I have shown that hypoxia induces an altered neutrophil phenotype with an activated morphology, actin remodelling and - most importantly - increased degranulation. The increased degranulation response includes all the neutrophil granule types and leads to the enhanced release of NE, MPO, MMP-9 and lactoferrin; by implication the release of other histotoxic granule products such as cathepsins and proteinase-3 is highly likely to be also augmented by hypoxia. I have also shown that these liberated products are biologically active, and hence have the potential to cause significant tissue damage both in vitro and in vivo. There is no direct histological evidence of increased neutrophil degranulation present in areas of cellular damage in hypoxic tissue in the literature; however a substantial body of evidence links elevated levels of neutrophil granule proteins with the presence of tissue hypoxia. The tumour microenvironment, for example, is profoundly hypoxic, as rapidly growing tumours outgrow their vascular supply. Neutrophil granule proteins have been found to play a role in cancer; in particular NE has been implicated in tumour proliferation and metastasis. NE directly induced tumour cell proliferation in both human and mouse lung adenocarcinomas in part by gaining access to an endosomal compartment within tumour cells, where it degraded insulin receptor substrate-1 (IRS-1) and led to PI3K activation⁴¹⁷. A NE inhibitor was found to prevent hepatic and lung metastasis in a mouse model involving intrasplenic injection of Lewis lung adenocarcinoma cells, partly by inhibition of neutrophil NET formation⁴¹⁸. In COPD, the airway wall may experience significant hypoxia, as evidenced by the presence of HIF in bronchial epithelial cells in biopsies from COPD patients but not in the biopsies of the healthy controls^{419,420}; however it must be acknowledged that inflammation as well as hypoxia can lead to stabilisation of

HIF^{363,421}. Polosukhin⁴¹⁹ and colleagues also showed that HIF-1 α expression was associated with areas of goblet cell hyperplasia (93.2 \pm 3.9% of goblet cells were HIF-1 α positive) whereas nuclear HIF-1 α was not detected in individuals without COPD. This, combined with data from Stockley et al.⁶⁶ and others including Vlahos et al.⁶⁷ show that circulating NE and MMP-9 levels increase during exacerbations and that NE is related to disease severity in COPD supporting the hypothesis that hypoxia contributes to the enhanced neutrophil degranulation that is felt to be pathogenic in this condition.

Although there has been no previous published study of the effects of hypoxia on neutrophil degranulation, some researchers have studied this phenomenon in other cell types. There is evidence that hypoxia can induce mast cell granule release^{382,383}, although others have suggested that this is an indirect effect mediated by the release of MCP-1 by hypoxic alveolar macrophages³⁸⁴. Additionally, Pinsky et al.³⁸⁵ and others³⁸⁶ showed that hypoxia induces the exocytosis of endothelial cell Weibel-Palade bodies (WP-bodies), releasing von Willebrand factor (vWF) as well as increasing expression of the WP-body-derived PMN adhesion molecule, P-selectin. Pinsky et al.³⁸⁵ postulated that endothelial WP-body exocytosis occurs during hypothermic cardiac preservation, priming the vasculature to recruit PMNs during reperfusion. The two groups differed in their assessment of the length of hypoxic exposure required to induce WP body release; Pinsky et al.³⁸⁵ saw only a small increase in degranulation around 1 hour, with a more significant increase at 4 hours, whilst Goerge et al.³⁸⁶ found a very rapid degranulation response with a substantial difference between normoxic and hypoxic conditions as early as 5 minutes, maintained at 1 hour. Both groups use the same cell type and quantification method so the reason for this difference in the rate of degranulation is unclear. Of note, the kinetic pattern of degranulation reported by Pinsky et al.³⁸⁵ resembles previous data on hypoxic NE release from our laboratory³⁷⁹.

Given the important role of cigarette smoke in the pathogenesis of COPD, and the fact that NE and other neutrophil-derived proteases may be important in mediating this effect, I explored the potential for cigarette smoke to synergise with hypoxia in augmenting neutrophil degranulation. No previous literature exploring the effect of CSM under hypoxic conditions was found, but a substantial amount of data exist reporting the effects of CSM on neutrophils under normoxia. However, the results presented by different authors vary significantly. Different laboratories use different methods to prepare CSM, and some laboratories have used commercially available cigarettes rather than

standardised research cigarettes. The quantification of the CSM and the concentration used by different laboratories is also substantially different, ranging from 1 cigarette per 5 mls of medium to 1 cigarette per 20 mls of medium. Since commercial preparations of cigarette smoke extract and condensate have also been reported to vary considerably, I prepared my own CSM using research grade cigarettes, and verified the activity of the CSM by demonstrating that it induced intracellular oxidative stress as predicted and in a concentration-dependent fashion. I also demonstrated that high (>50%) concentrations of CSM were directly toxic to neutrophils and induced necrosis/apoptosis. Although (interestingly) hypoxia largely prevented CSM-induced cell death, concentrations of CSM that were able to induce detectable intracellular oxidase activity had no effect on neutrophil viability/survival at 4 hours and hence were used to study degranulation. No effect on basal or stimulated NE secretion, either in ambient oxygen or hypoxic conditions was found. These data contrast with those reported by Koethe *et al.*²⁹⁶, who showed a priming effect of CSM on neutrophils, leading to increased NE release following stimulation with fMLP, whilst Mortaz *et al.*²⁹⁹ and Overbeek *et al.*³⁰⁰ found that CSM induced the production of reactive oxygen species, IL-8, NE, MMP-2 and MMP-9 directly. However, both of these groups used a much longer incubation time (9 h) and a higher concentration of CSM than employed herein (smoke from 1 cigarette bubbled through medium in comparison to smoke from 3 cigarettes in 25 ml medium). For the experiments involving hypoxia, the 4 h incubation period was deliberately selected as sufficient to induce maximal up-regulation of degranulation, but not sufficient to effect neutrophil survival (which might confound the results). As I could detect no effect of CSM on neutrophil degranulation in the time-frame relevant to my studies, I did not study this interaction further).

To ensure that the enhanced release of granule proteins did not reflect a loss of cellular integrity, and to explore the effects of hypoxia on cellular features characteristic of priming and activation, I performed a detailed morphological analysis. Using TEM I have shown that the treatments I have used leave the cells fully intact, but that hypoxia induces a number of morphological changes, over and above those induced by activation alone. The scoring system I used was based on the observations of Mitchell *et al.*³⁸⁸, who show that activated neutrophils have a more elongated profile, and also observed more empty vacuoles; these are similar to the morphological changes I saw and which are depicted in Figure 4.7. In an attempt to obtain quantitative data on cellular morphology I analysed neutrophil circumference from the TEM images, using nuclear morphology to try to

ensure the selected cells had been cut in a similar plane (although this is still a potential source of error). In agreement with Mitchell et al.³⁸⁸, activation increased cellular circumference, perhaps by increasing the number of cellular protrusions; hypoxia alone had no significant effect on this index but did enhance the effect of Cyt B. A significant reduction in the number of intracellular electron-dense granules was detected only when neutrophils had been treated with Cyt B/fMLP under conditions of hypoxia; as shown in Figure 4.2, this is the only condition where >10% of total MPO was released from the cell, suggesting that the TEM quantification is not sufficiently sensitive to detect these smaller changes. I did not observe the peripheral granule redistribution reported by Rittner et al.⁴²² in response to fMLP, perhaps reflecting the very high agonist concentrations used by this group (fMLP, 5 μ M). However, this set of experiments did confirm that the detection of increased extracellular granule proteins in response to hypoxic stimulation depicted in Figure 4.2-Figure 4.4 reflects the liberation of intact granules rather than non-specific cellular damage.

The neutrophil cytoskeletal changes in response to hypoxia described in this thesis have not been, to my knowledge previously reported. Hypoxia has been shown to affect the actin cytoskeleton and induce shape change in neuronal cells⁴²³ and proximal renal tubular cells⁴²⁴ in culture, but the mechanism and consequences of these effects were not explored. Working in our laboratory, Dr Naomi MCGovern did not detect hypoxia-induced neutrophil shape change when using a FACS-based method, however by immunofluorescence microscopy I have shown a clear effect of hypoxia on the distribution of polymerised F-actin to cap-like structures. Since cytoskeletal rearrangements have been linked to degranulation^{276,425}, this observation may provide a mechanistic insight into the hypoxic up-regulation of neutrophil degranulation. The mechanism of neutrophil degranulation under hypoxia and the possibility of enhanced degranulation leading to more epithelial cell damage are the focus of my subsequent chapters.

Chapter 5

Results: The effect of neutrophil-induced damage to lung epithelial cells

5. The effect of hypoxia on neutrophil-induced damage to lung epithelial cells

5.1 Introduction

There is abundant evidence that neutrophil proteases can cause substantial tissue damage as exemplified by research into COPD. Factors contributing to the occurrence and progression of emphysema include chronic neutrophilic inflammation with protease/anti-protease imbalance and oxidative stress in the alveolar environment, and lung epithelial cell apoptosis⁴²⁶; neutrophil-derived proteases can contribute to all of these processes⁴²⁷. Neutrophil elastase (NE) in particular has been shown to play an important role in the development of emphysema^{127,133}; direct installation of purified NE (porcine pancreatic elastase or NE) into the lungs of mice is used as an animal model of emphysema¹³³, and mice deficient in NE are protected from cigarette smoke-induced emphysema¹³⁶. NE has also been shown to cause mucous gland hyperplasia²¹⁰ and enhance the secretion of mucus^{180,428}, and incubation with elastase-positive but not elastase-negative respiratory secretions led to a decrease in ciliary beat frequency of primary nasal epithelial cells⁴²⁹.

Beside NE, both MPO^{193,196} and MMP-9 have been shown to promote inflammation and cause tissue injury^{200,201}. Together, MMP-9 and NE are capable of degrading almost every extracellular matrix component including collagen, fibronectin, proteoglycans, heparin, and cross-linked fibrin¹⁷¹. MMP-9 has further been related to parenchymal destruction and lung function decline in subclinical and established emphysema^{200,201}. Other studies have shown MMP-9 to be elevated in the sputum of patients with COPD in comparison to healthy control subjects, and MMP-9 levels were found to correlate with increased neutrophilia and decreased lung function^{94,202,203}. MPO can cause oxidative stress in inflammatory settings and serum MPO levels have been shown to correlate with a decline in lung function¹⁹².

Furthermore, neutrophil proteases can compromise local pulmonary immune responses; NE has been shown to cleave critical protein components of the bronchial defenses, such as the C3Bi opsonophagocytic receptor CR1¹⁷⁹, immunoglobulin¹⁸⁰ and SPLUNC1 (short palate, lung, and nasal epithelial clone 1¹⁸¹), which is thought to exert anti-microbial activity in the context of pulmonary pseudomonas infection⁴³⁰. MPO has been shown to up-regulate the inflammatory response directly; MPO internalised by endothelial cells leads to IL-6, IL-8 and ROS release with the potential for the perpetuation of inflammation and injury^{195,196}.

These data suggests an important role for neutrophil proteases in a range of lung diseases. In the light of the evidence summarised above, I wished to investigate the potential pathophysiological relevance of my finding that hypoxia substantially upregulates neutrophil degranulation. In order to do this, I explored the effects of supernatants collected from neutrophils cultured under normoxic or hypoxic conditions on lung epithelial cells in culture.

These supernatants were generated by priming neutrophils (3×10^6 cells per sample) with GM-CSF (10 ng/ml) and activating the cells with fMLP (100 nM) under normoxic or hypoxic conditions (0.8 % O₂, 5% CO₂, section 3.8.1). The amount of active NE in each neutrophil supernatant was quantified to counter any batch to batch variability and samples were stored for no longer then 6 weeks to ensure there was no time dependent loss of protease activity. Initial experiments were performed using the A549 lung adenocarcinoma cell line; I then progressed my findings to explore the effects on immortalised Normal Human Bronchial Epithelial Cells (iHBECs) and ultimately primary human bronchial epithelial cells grown in air-liquid interface (ALI) cultures.

The specific aims of the work presented in this chapter are:

1. To establish whether the hypoxic enhancement of neutrophil degranulation has the potential to damage A549 epithelial cell monolayers.
2. To investigate the nature of the damage-inducing components of the neutrophil supernatants.
3. To extend any relevant findings in A549 cells to cells which more closely resemble human bronchial epithelial cells in vivo.
4. To explore the effects of normoxic and hypoxic neutrophil supernatants on ciliary function.

5.2 The effect of hypoxia on neutrophil-induced damage to A549 cells

For my initial experiments I used the A549 lung epithelial cell line. These cells are alveolar basal epithelial cells derived from a human lung adenocarcinoma; they are often used as a lung epithelial cell model^{431,432}, having the advantages of being well-characterised, readily available and easy to grow in the cell culture environment. The cells were used only at early passage number (up to 6 passages after defrosting) and were visually checked for signs of infection on a daily basis.

5.2.1 The effects of hypoxia on neutrophil induced toxicity to A549 cells

To investigate the ability of neutrophil supernatants to cause damage to lung epithelial cell layers, A549 cells were plated onto poly-L-lysine coated plates (96-well plates, 40,000 cells per well) and cultured overnight at 37 °C (5% CO₂) in F-12K medium with antibiotic/antimycotic solution and 10% FCS overnight to obtain a fully confluent monolayer. The next day the cell layers were exposed to neutrophil supernatants (150 µl, 1:2.5 dilution, 37°C) for 72 h (earlier time-points did not show significant cell damage visually, data not shown). To visualise cellular damage and delineate cell monolayer integrity, the A549 cell layers which had been exposed to neutrophil supernatants for 72 h were stained with the fluorescent dye 4',6-diamidino-2-phenylindole (DAPI) (which binds to chromatin) and 5-(and 6)-Carboxyfluorescein diacetate succinimidyl ester (CFSE), which is able to cross cell membranes and hence highlights the cytoplasm. As shown by the photomicrographs in Figure 5.1A, there was a striking difference in A549 monolayer integrity induced by supernatants derived from neutrophils activated (with GM-CSF/fMLP) under normoxia *versus* those activated under hypoxia. Exposure to hypoxic activated neutrophil supernatants resulted in only a minimal remaining intact cell layer, whilst in the wells exposed to supernatants from normoxic neutrophils, a relatively intact cell layer is still present (Figure 5.1A, representative image from n=11 experiments). Since the supernatants from hypoxic neutrophils led to substantial disruption of monolayer integrity on visual inspection, the direct toxicity of the neutrophil supernatants was quantified more precisely by 3-(4,5-dimethylthiazol-2-yl)-2,5-diphenyltetrazolium bromide MTT assay. Experimental conditions were precisely as described above. After 72 h, the supernatants were aspirated from the epithelial monolayers and the cells were incubated with MTT (100 µl, 500 µg/ml final concentration) in IMDM for 2 h at 37°C. The resultant purple formazan crystals, formed by the mitochondria of viable cells, were dissolved in isopropanol after a 2 h incubation and the absorbance measured at 540 nm. The absorbance of cells exposed to control media (IMDM) is used as 100% living cells (presence of an intact, fully confluent cell layer was confirmed by microscopy). The exposure of the cell layers to neutrophil supernatants led to reduced absorbance at 540 nm, presented as percentage (%) of living cells. Figure 5.1B shows that the supernatants from normoxic neutrophils, even those activated by GM-CSF/fMLP, caused minimal (<10%) cell death. In contrast, even the supernatants from hypoxic unstimulated neutrophils induced substantial (39%) cell death, and this increased to 60% A549 cell

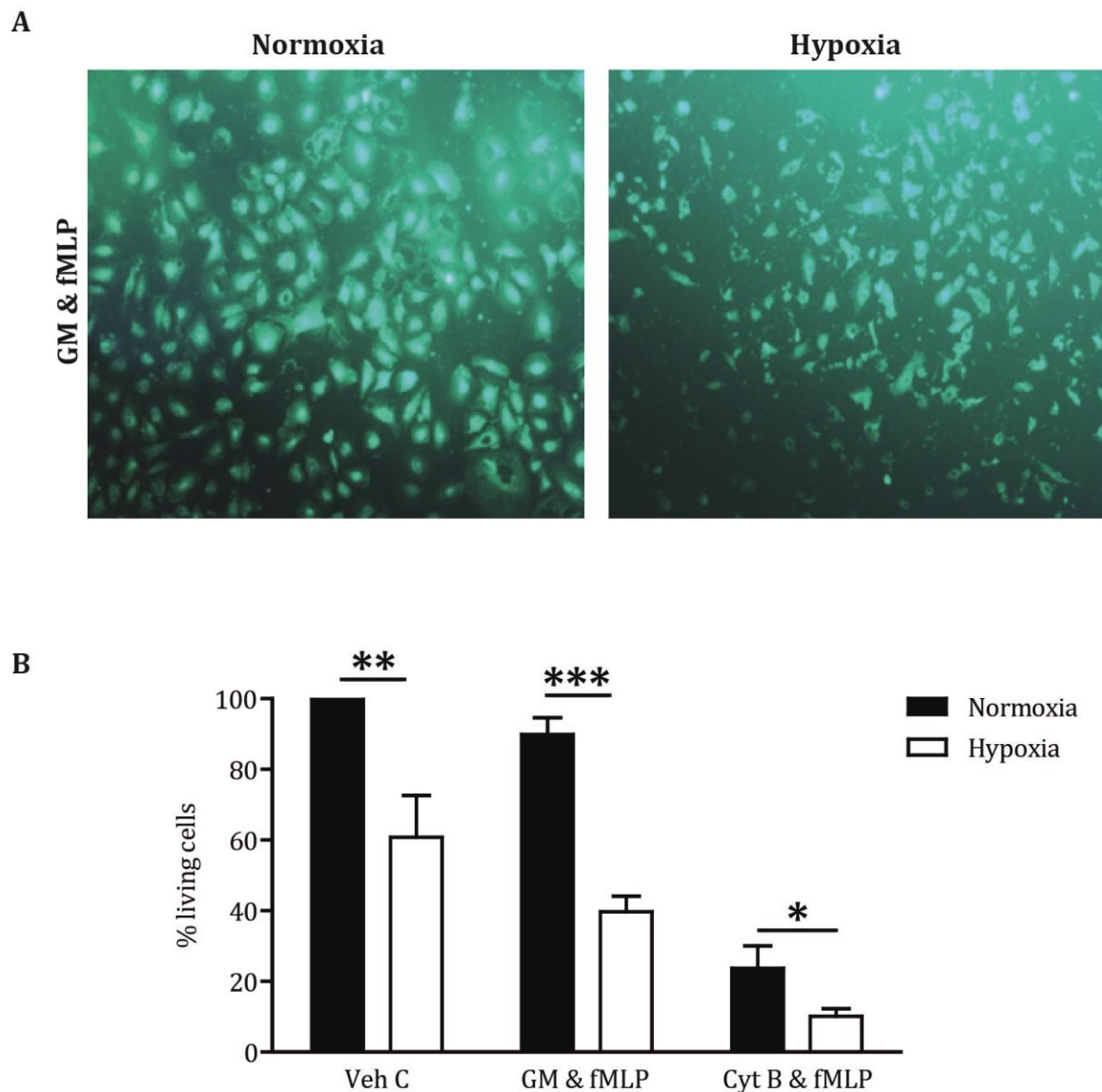


Figure 5.1: Hypoxic neutrophil supernatants compromise A549 cells survival

A549 cells were cultured in Poly-L-Lysine coated 96-well plates (80,000 cells per well) to obtain a fully confluent cell layer, and were exposed to IMDM (Veh C) or supernatants (1:2.5 dilution) from neutrophils cultured and activated (GM-CSF/fMLP) under normoxic (filled bars) or hypoxic (open bars) conditions. After 72 h the cells were stained with cytoplasmic (CFSE) and nuclear (DAPI) dyes (A) or assessed for viability by MTT assay (B). A. Immunocytochemistry microscopy images from a single representative experiment (of n=11) magnification = x20, B. MTT toxicity assay, n=11, each performed in triplicate. Values are mean \pm SEM, *= p <0.05, **= p <0.01, ***= p <0.001.

death upon exposure to the supernatants from neutrophils activated by GM-CSF/fMLP under hypoxia. Toxicity was even more marked when supernatants from Cyt B/fMLP-treated neutrophils were used, and again the effects were significantly enhanced by hypoxic versus normoxic neutrophil incubation.

These preliminary experiments show that supernatants produced by hypoxic neutrophils can exert a highly damaging effect on A549 lung adenocarcinoma-derived epithelial cells. The following experiments were designed to explore this phenomenon in more detail.

5.2.2 The effect of hypoxia on neutrophil-induced detachment of A549 cells

Immunocytochemistry was used to interrogate the damage caused by the neutrophil supernatants in more detail and to explore the mechanism of A549 cell death. The A549 cells were plated onto poly-L-lysine coated plates (96 well optical plates (Ibidi), 80,000 cells per well) and incubated at 37°C overnight to obtain a fully confluent monolayer, before exposure to supernatants from normoxic and hypoxic neutrophils stimulated (or not) with GM-CSF/fMLP as above (150 µl, 1:2.5 dilution) for 48 h. After the incubation the supernatants were removed, the cell layers fixed with 3.5% PFA (20 min, 22°C) and stained for cleaved caspase 3 (anti-cleaved caspase 3 goat IgG antibody (1:1000 1 h, 22°C) and Alexa Fluor 488–donkey anti-goat IgG, red (1:1000, 1 h, 22°C), F-actin (rhodamine-phalloidin, green, 1:200, 30 min, 22°C), nucleus (DAPI containing mountant, blue 22°C). Caspase 3 is activated via extrinsic (death ligand) and intrinsic (mitochondrial) pathways; cleavage and activation of caspase 3 irreversibly commits a cell to apoptosis and is therefore often used as a marker for early apoptosis^{433,434}.

For analysis three representative images were taken in different areas of the well, with care to avoid the edges of the wells. Exposure to hypoxic activated supernatants (Figure 5.2A. panel hypoxia, GM/fMLP) led to a substantial increase in cleaved caspase 3 staining, which was not seen upon exposure to normoxic supernatants (full set of images for all conditions are shown in the appendixes, section 8.3).

Figure 5.2A (representative images from n=6 experiments) also shows that exposure to the hypoxic, but not the normoxic supernatants caused extensive cellular detachment from the tissue culture surface, in keeping with the data presented in Figure 5.1. The cell layer detachment seen on confocal images was quantified by measuring the "empty" areas using imageJ, and the data are represented as detached area as a percentage of total area.

This quantification is shown in Figure 5.2B. No cellular detachment was induced by

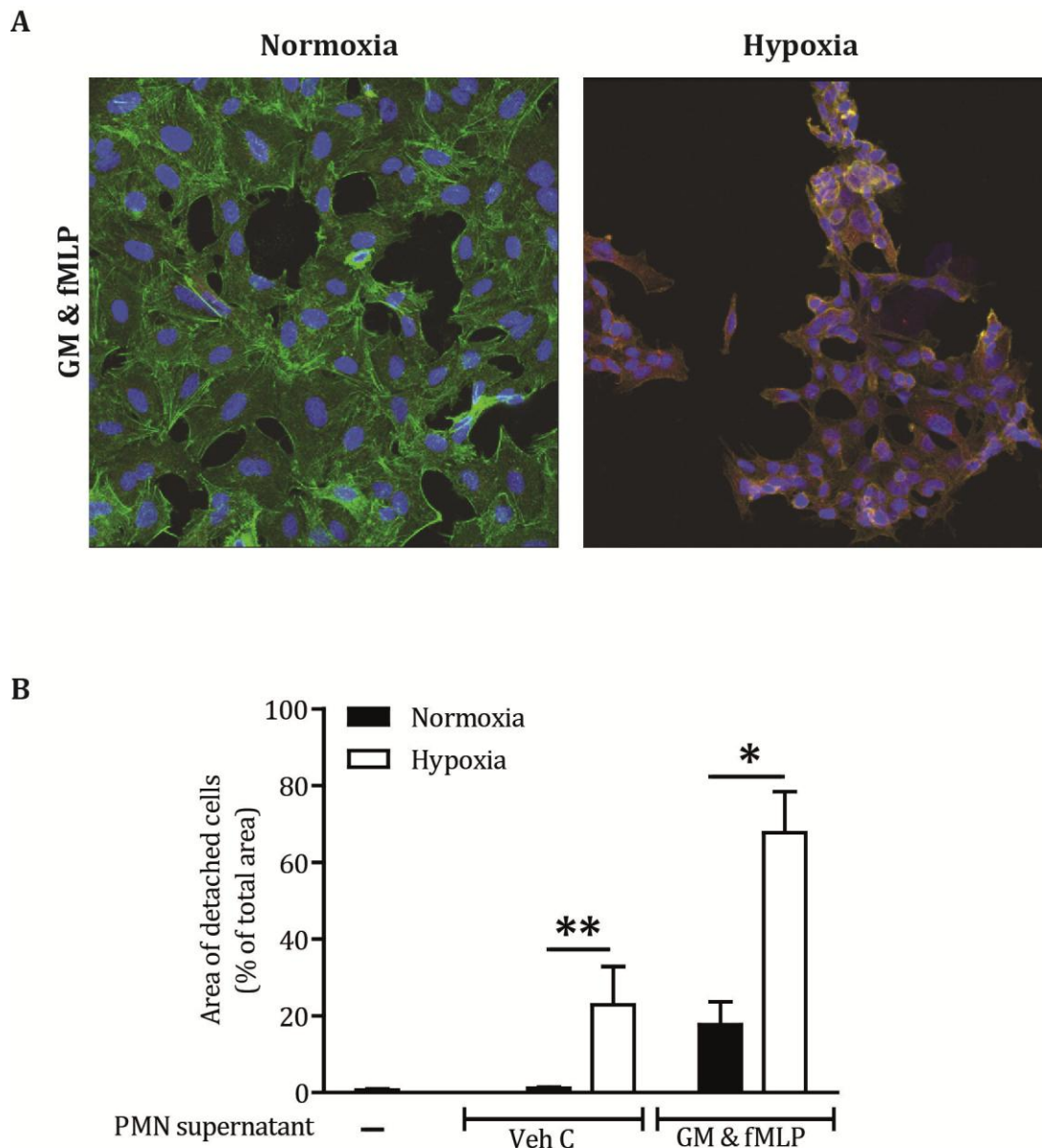


Figure 5.2: Hypoxic neutrophil supernatants induce A549 cell detachment and apoptosis

A549 cells were cultured in Poly-L-Lysine coated, 96 well plates to obtain a fully confluent cell layer. The cells were exposed to neutrophil supernatants (1:2.5 dilution) from neutrophils cultured and activated (GM-CSF/fMLP) under normoxic (filled bars) or hypoxic (open bars) conditions for 48 h before the cell layers were fixed with 3.5% PFA and stained for F-actin (rhodamine-phalloidin, green), nucleus (DAPI, blue) and cleaved caspase 3 (goat IgG anti-cleaved caspase 3 antibody and Alexa Fluor 488–donkey anti-goat IgG, red). A. Representative images from n=6 experiments, x40. Full set of images is shown in appendix 8.3 B. Quantification of cell layer detachment measured by imageJ, shown as percentage of detachment of total area per field of view. n=6, each performed in triplicate, values are mean \pm SEM, *= $p < 0.05$, **= $p < 0.01$.

supernatants from resting normoxic neutrophils, whilst supernatants from resting hypoxic neutrophils induced detachment of 15.5% of the total area. Damage to the epithelial cells layers increased upon exposure to supernatants from activated neutrophils; detachment of 17.8% of the total area was observed with the application of supernatants generated by activation under normoxia, increasing to 67.7% detachment in response to analogous hypoxic supernatants.

Together with the data from the MTT toxicity assay, these results show that neutrophil supernatants generated under hypoxic conditions can cause substantial damage to A549 lung epithelial cell layers. However, it does not tell us whether the damage is protease- or even protein-dependent, or whether there is a contribution from other factors present in the neutrophil supernatants. This was further investigated as outlined below.

5.2.3 Nature of the damaging agent in hypoxic neutrophil supernatants

It has been shown that neutrophil proteases, especially NE, can cause cell damage and even cell death. For example NE applied to A549 cells induced concentration- and time-dependent apoptosis; Nakajoh et al.⁴³⁵ showed that exposure to NE concentrations of 0.1 U/ml or greater for 24 h significantly compromised A549 cell viability, supporting the hypothesis that neutrophil proteases in the lung have the capacity to cause epithelial cell damage locally. Importantly, this effect was inhibited by the addition of the serine protease inhibitor α_1 AT.

To recapitulate this observation, A549 cell monolayers were exposed to increasing concentrations of porcine pancreatic elastase (PPE) and stained with a nucleic (DAPI) and a cytoplasmic (CFSE) dye exactly as described above. This resulted in epithelial cell layer damage (Figure 5.3A) visually indistinguishable from the damage induced by neutrophil supernatants and shown in Figure 5.1A. The MTT toxicity also showed a concentration-dependent toxicity of PPE on the A549 cells (Figure 5.3B), with the concentration of 0.1 U/ml PPE being the equivalent of the amount of NE present in the hypoxic, Cyt B/fMLP activated supernatants as measured by the NE activity assay.

Thus hypoxic neutrophil supernatants in particular can damage lung epithelial cell layers, and this effect can be re-capitulated using purified PPE. However, these experiments do not prove that neutrophil-derived proteases, or even proteins, are responsible for this cellular toxicity. To investigate whether the damage is protein-dependent, the supernatants were boiled (10 min, 99^oC) to denature any proteins present. A549 cell

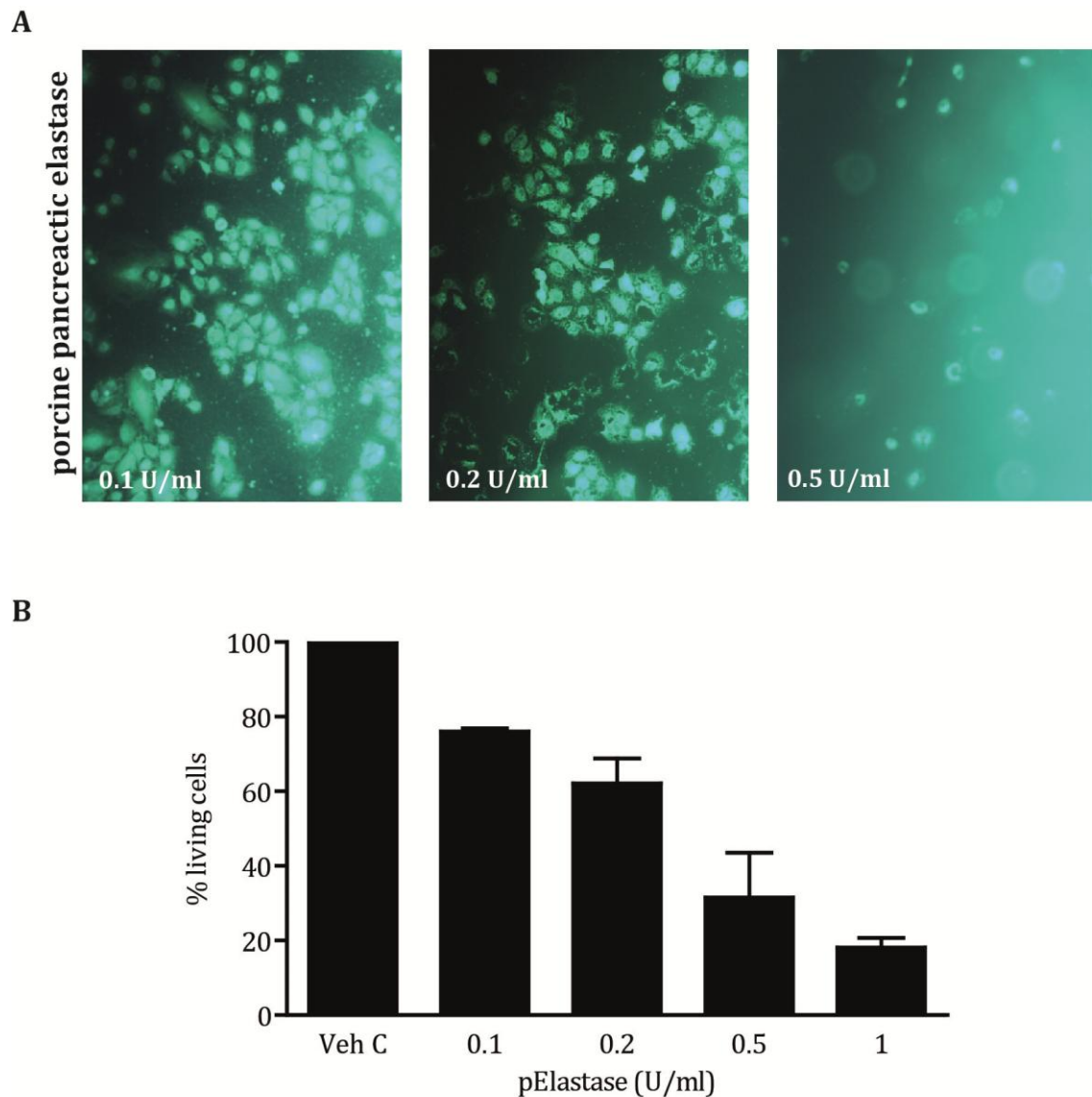


Figure 5.3: Porcine pancreatic elastase recapitulates the damage caused by neutrophil supernatants

A549 cells were cultured in Poly-L-Lysine coated 96-well plates to confluence. The cells were exposed to IMDM (Veh C) or porcine pancreatic elastase at the indicated concentrations for 72 h before staining of the cell layer (A) with a cytoplasmic dye (CFSE) and nucleic dye (DAPI) or determining the percentage of live cells by MTT assay (B). A. Representative images from n=1 experiment with triplicate wells, magnification = x20. B. MTT-assay data, n=1, each assay performed in triplicate. Values are mean \pm SEM.

layers were cultured as before and exposed to the boiled and intact neutrophil supernatants (1:2.5 dilution) for 48 h. Boiling the supernatants abolished the damaging effects as illustrated in Figure 5.4A, confirming protein-dependence. The quantification of cell layer detachment is shown in Figure 5.4B and confirms complete protection is provided by protein denaturation. To assess whether the cell injury was protease-dependent, the physiological serine protease inhibitor α_1 -anti-trypsin (α_1 AT) was used. α_1 AT does not only inhibit NE but also a range of other proteases present in the neutrophil granules including cathepsin G and proteinase 3⁴³⁶.

Neutrophil supernatants were pre-incubated with α_1 AT (10 min. 4.6-46 μ g/ml) and the cell layers treated as described above. These concentrations were chosen based on the ability of α_1 AT to inhibit pure NE in a 2:1 ratio⁴³⁷. From data from McGovern et al.³⁷⁹ and chapter 4, figure 4.3 it can be calculated that neutrophils primed stimulated with GM/fMLP released approximately 2 μ g/ml of NE (from 1×10^6 cells). As α_1 AT inhibits a range of proteases I used the inhibitor at a 2:1 ratio and higher. As shown in Figure 5.5A and B, α_1 AT decreased cell layer detachment in a concentration-dependent fashion. The highest concentration of α_1 AT reduced the damage induced by H-GM-CSF/fMLP from 70.5% to 6.9 %, which is close to the baseline seen with vehicle alone. The fact that α_1 AT concentrations of greater than 4.6 μ g/ml were required to achieve significant protection may suggest that proteases other than NE may be involved in the cell damage/detachment caused by hypoxic supernatants.

Data from the experiments shown in figures 4.3, 4.4 and 4.5 were performed with my assistance and under my direct supervision by Ms Cheng Chen, a third year Medical Student undertaking a 12-week project in the laboratory.

5.3 The effect of hypoxia on neutrophil induced damage to immortalized primary bronchial epithelial cells.

Using A549 cells I have shown that neutrophil supernatants, particularly those generated in a hypoxic environment can cause substantial damage. Although commonly cited as a model for lung epithelial cells in the literature, the A549 cell line is still a cancer cell line and may therefore have undergone substantial alterations in biochemical and functional properties. When compared to primary cells A549 cell morphology is very irregular in comparison to the more consistent cobblestone appearance of primary cells (Figure 3.9).

To use cells which more closely resemble the endogenous lung epithelium, and to

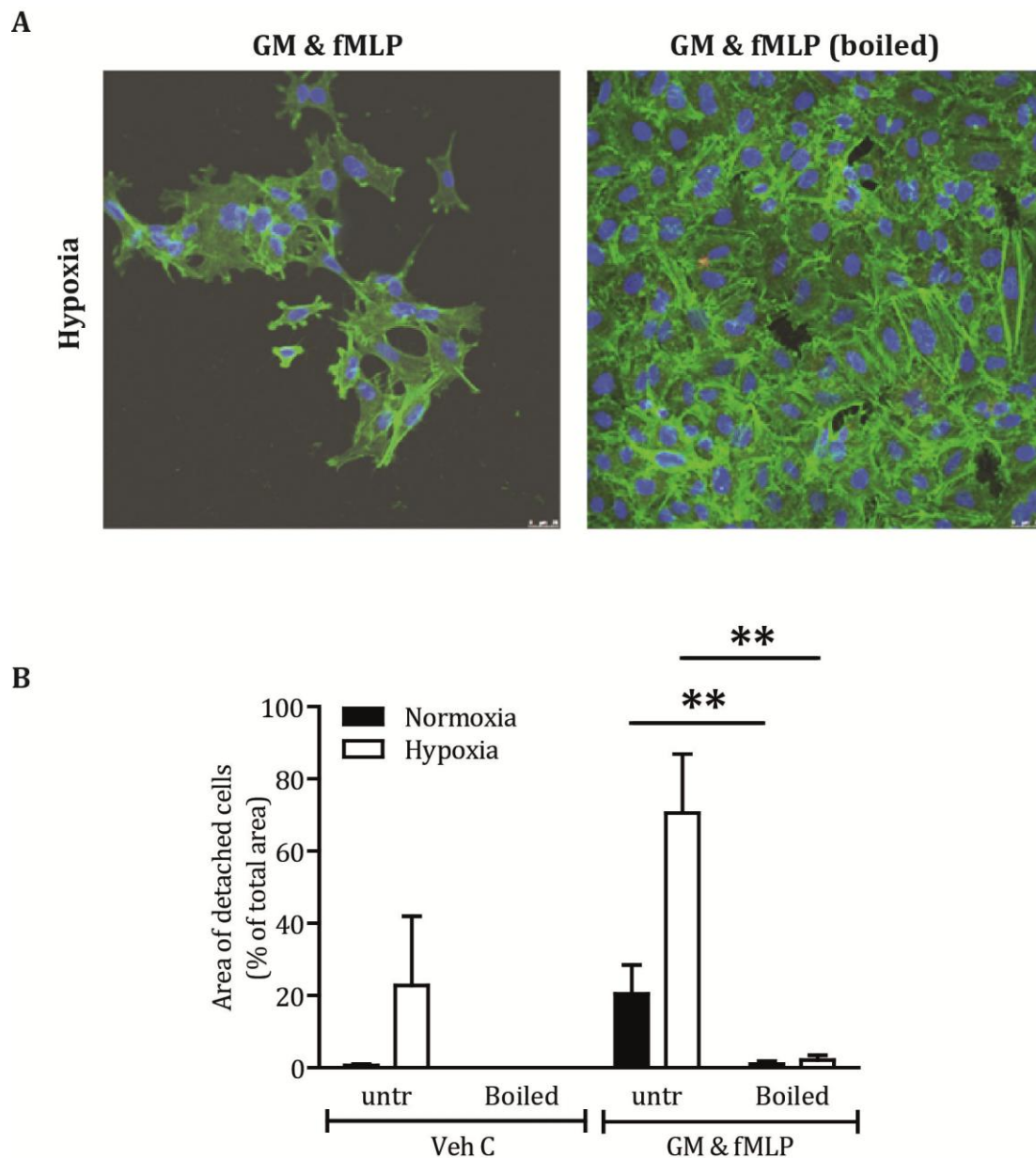


Figure 5.4: A549 cell damage caused by neutrophil supernatants is protein-dependent

Confluent A549 cells monolayers in Poly-L-Lysine coated 96-well plates were exposed to IMDM (Veh C), (boiled, 5 min 99°C) or intact supernatants (1:2.5 dilution) from neutrophils cultured and activated (GMSCF/fMLP) as indicated under normoxic (filled bars) or hypoxic (open bars) conditions for 48 h. The cell layers were then fixed with 3.5% PFA and stained for F-actin (rhodamine-phalloidin, green) and nucleus (DAPI, blue). A. Representative images of n=4, each performed in triplicate, magnification = x40. Full set of images is shown in appendix 8.3. B. Quantification of cell layer detachment measured by imageJ, shown as percentage of detachment of total area per field of view. n=4, each performed in triplicate values are mean \pm SEM, **= $p < 0.01$.

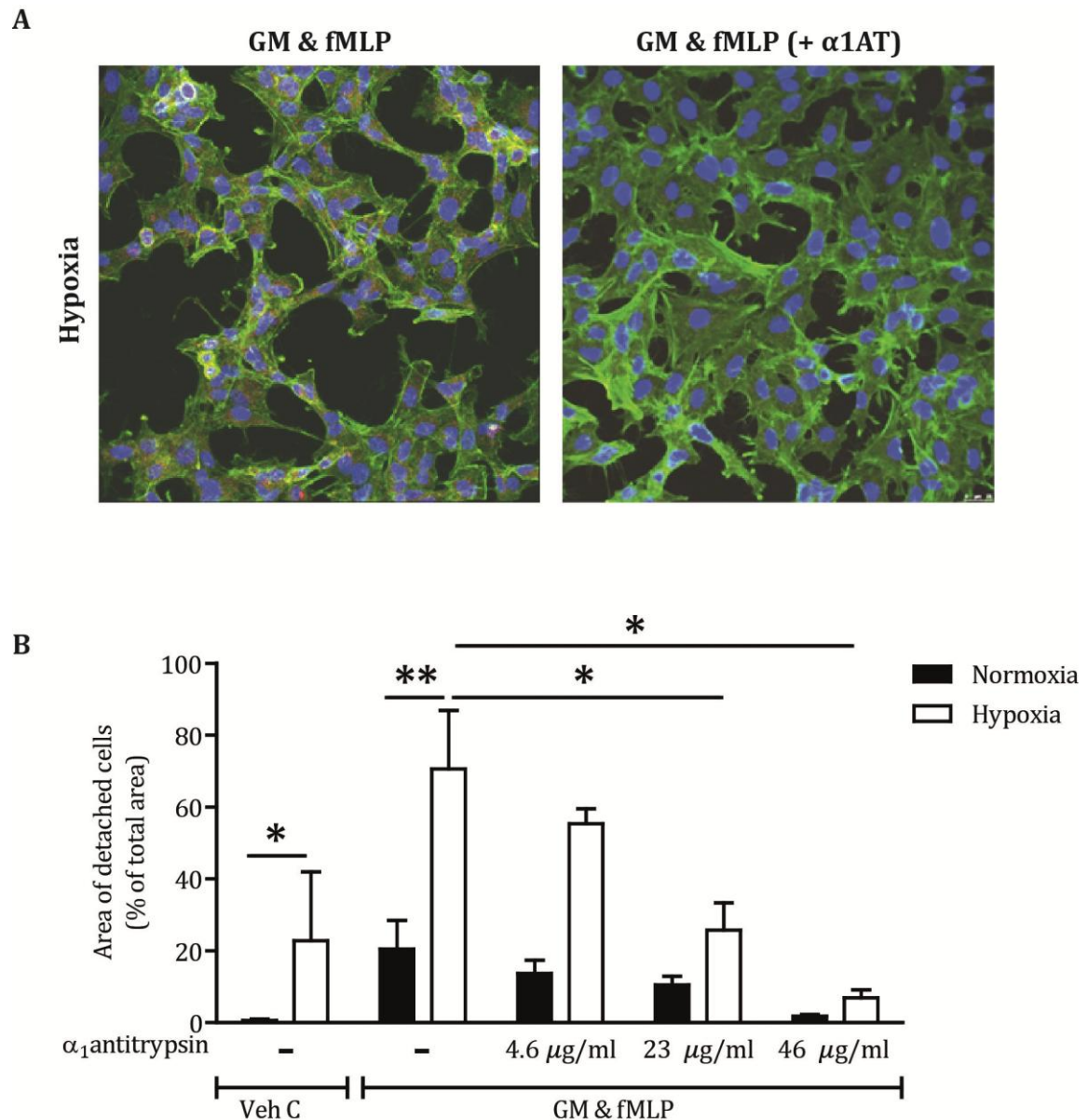


Figure 5.5: A549 cell damage caused by neutrophil supernatants is protease-dependent

A549 cells were cultured in Poly-L-Lysine coated, 96 well plates to confluence. The neutrophil supernatants from cells cultured and activated (GM-CSF/fMLP) under normoxic (black bars) or hypoxic (open bars) were pre-incubated with α_1 AT (0, 4.6, 23 or 46 μ g/ml as indicated) for 10 min prior to application to the A549 cell layers. Following a 48 h exposure, the cell layers were fixed with 3.5% PFA and stained for F-actin (rhodamine-phalloidin, green) and nucleus (DAPI, blue). A. Representative images from 1 of n=4 experiments, each performed in triplicate, magnification = x40, 46 μ g/ml. Full set of images is shown in appendix 8.3. B. Quantification of cell layer detachment measured by imageJ, shown as percentage of detachment of total area per field of view. n=3-8, values are mean \pm SEM, *= p <0.05, **= p <0.01.

confirm that the damage to A549 cells caused by neutrophil supernatant is not due to a specific cell line-specific susceptibility, the immunocytochemistry experiment performed with the A549 cells were repeated using immortalised human bronchial epithelial cells (iHBECs). These cells were originally derived in the laboratory of Professor Jerry Shay, and with his permission were gifted to us by Professor Gisli Jenkins (Nottingham Respiratory Research Unit, Nottingham City Hospital).

They are normal primary epithelial cells immortalized by transfection with cyclin-dependent kinase (Cdk) 4 and hTERT³⁸⁹. These cells do not have a cancer cell phenotype; they do not form colonies on agar plates and have an intact p53 checkpoint pathway.

To assess the capacity of neutrophil supernatants to cause damage to the iHBEC's cell layers, the cells were cultured as described above (section 5.2.1) and exposed to neutrophil supernatants (1:2.5 dilution) for 48 h. After the exposure the cell layers were stained exactly as described above for F-actin (rhodamine-phalloidin, , 1:200, green) and nucleus (DAPI, blue) and detachment was quantified by measuring the "empty" areas with ImageJ (Figure 5.6). The results obtained from these experiments align closely with those seen with A549 cells; as shown in Figure 5.2 the supernatants from normoxic stimulated neutrophils induced some cell layer detachment, but this was approximately three-fold less than that seen with supernatants derived under hypoxic conditions (11.5% versus 29.3 % detachment).

Together with the A549 cell data these results show that hypoxic neutrophils stimulated under hypoxic conditions display an augmented potential to cause significant damage to lung epithelial cells. To further place these results in a physiological context I wished to investigate the effect of neutrophil-derived supernatants on cells grown in air-liquid interface (ALI) cultures.

5.4 The effect of hypoxia on neutrophil induced damage on ALI-cultures.

Besides the structural damage found in the lungs of COPD patients, there is also an susceptibility to respiratory infections^{438,439}, and a proportion of patients with COPD are colonised with potentially pathogenic organisms such as *Haemophilus spp.*⁴³⁹ and *Moraxella catarrhalis*⁴⁴⁰. The respiratory tract is lined with ciliated epithelial cells, which function as a 'muco-ciliary escalator' to move mucus and entrapped particles/organisms upwards and expel them from the lungs via the cough reflex. A delay of muco-ciliary clearance has been observed in chronic bronchitis due to a loss

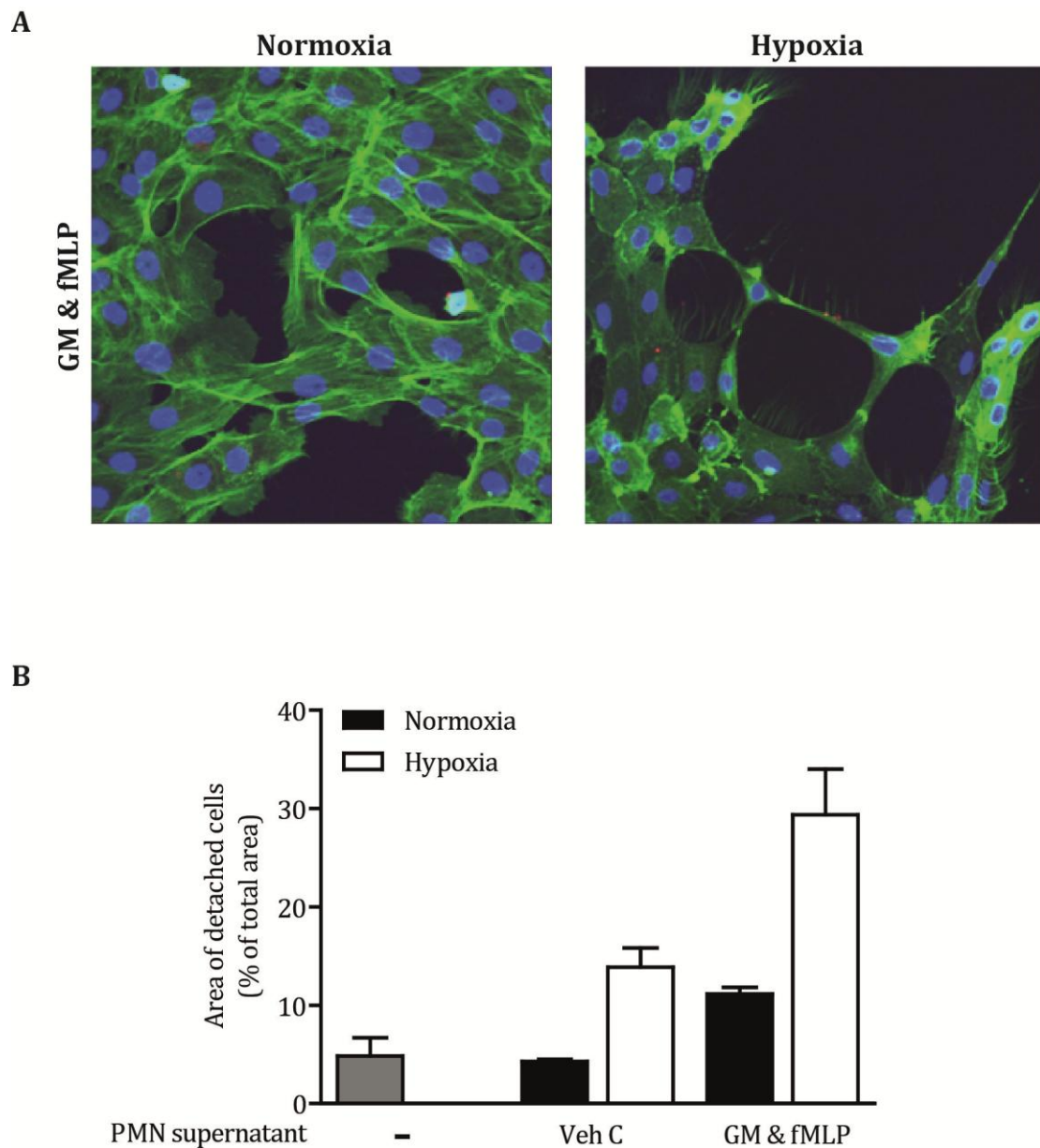


Figure 5.6: Hypoxic neutrophil supernatants damage iHBE cells layers

iHBE cells were cultured in Poly-L-Lysine coated 96-well plates to obtain a fully confluent cell layer. The cells were exposed to exposed to IMDM (grey bar) or neutrophil supernatants (1:2.5 dilution) from neutrophils cultured/activated under normoxic (black bars) or hypoxic (open bars) conditions for 48 h. The cell layers were then fixed with 3.5% PFA and stained for F-actin (rhodamine-phalloidin, green) and nucleus (DAPI, blue). A. Representative images from n=3 experiments, each performed in triplicate, x40 magnification. B. Quantification of cell layer detachment measured by imageJ, shown as percentage of detachment of total area per field of view. n=3, each performed in triplicate. Values are mean \pm SEM.

of ciliated cells that have been replaced by goblet cells⁴⁴¹, also leading to mucus hyper-secretion. The impaired mucus clearance may play a role in the first step of mucosal colonisation, and mucus hyper-secretion is associated with increased mortality related to infection⁴⁴². Ciliary dysfunction has also been associated with an increased susceptibility to infection in other diseases like Primary Cilia Dyskinesia (PCD)⁴⁴³ and pulmonary nontuberculous mycobacterial disease⁴⁴⁴.

Therefore I was interested to investigate whether exposure to neutrophil supernatants, and in particular those derived from hypoxic neutrophils, would affect ciliary function, in addition to exploring the effects of neutrophil supernatants on cells growing in conditions that more closely resemble the human airway environment than monolayer tissue cultures. Professor Chris O'Callaghan (Portex Unit, Great Ormond Street Hospital and University of Leicester) runs a national diagnostic service for PCD, using a 3-dimensional culture system of primary ciliated bronchial epithelial cell layers. These cultures allow differentiation into goblet cells, basal cells and ciliated epithelial cells (Figure 5.7); this team have accrued extensive expertise in the assessment of ciliary function and structure using high-speed digital video microscopy. Furthermore, the use of an air-liquid interface (ALI) culture system more closely mimics the *in vivo* environment of alveolar epithelial cells which are exposed to inhaled air at their apical aspect, but are in contact with tissue fluid/pulmonary circulation basally^{392,445}. To undertake the following experiments I worked in the PCD Centre, Department of Infection, Immunity and Inflammation at the University of Leicester, under the supervision of Dr Robert A. Hirst.

5.4.1 The effect of hypoxia on neutrophil induced cell damage in ALI cultures.

Primary HBECs were purchased from Lonza and cultured and differentiated into a polarised system incorporating basal, goblet and ciliated cells over a period of approximately 2 months as described in section 3.13.3. Cultures that failed to ciliate or which became infected were discarded. To confirm that the ALI-cultures (grown on Transwell[®] inserts) did indeed incorporate ciliated epithelial cells, scanning electron microscopy (SEM) images were prepared from the cell layers. The ALI-cultures were exactly as described (section 3.14.4). Images were obtained by Dr Jeremy Skepper (Cambridge Advanced Imaging Centre, Department of Physiology, Development and Neuroscience, University of Cambridge).

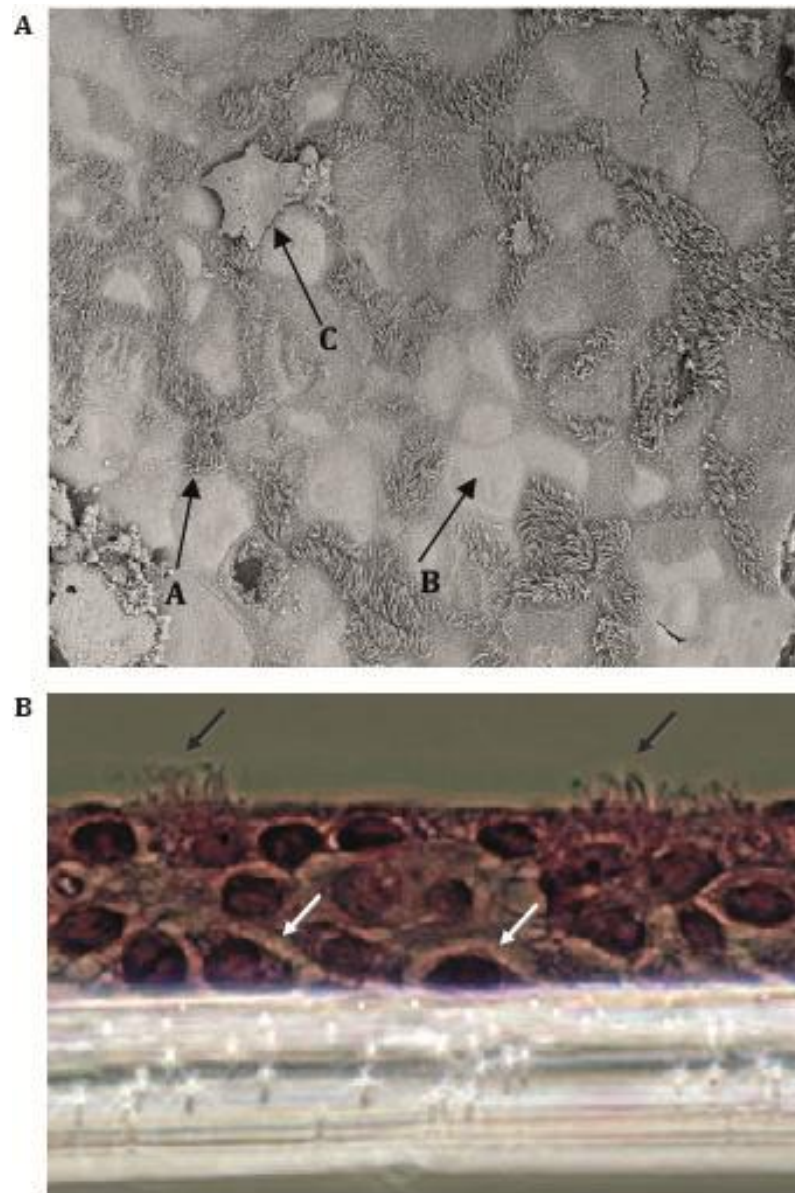


Figure 5.7: Scanning electron microscopy of primary HBECs grown in ALI culture

A. Representative scanning electron microscope image (of $n=2$) showing (black arrows) ciliated cells (A), basal cells (B), and mucus (C). The HBECs were grown on collagen-coated 1.2 cm diameter Transwell[®] inserts and transferred into ALI-cultures. Mature cultures with ciliated cells were fixed in the well with Sorensen phosphate-buffered (pH 7.4) glutaraldehyde (4% v/w). Dr. Jeremy Skepper (Cambridge Advanced Imaging Centre) completed sample preparation for electronmicroscopy and took the images using a FEI Verios 460 microscope. B. Photomicrograph of section through HBECs growing in ALI culture. Black arrow indicate ciliated cells, white arrows indicate basal cells image imported from <http://www.lonza.com/>).

Figure 5.7 shows a representative SEM image of one of the ALI-culture NHBE cell layers (Figure 5.7B), demonstrating the presence of ciliated cells (A), basal cells (B) and mucus (C) and a photomicrograph of a section through HBECs growing ALI culture (Figure 5.7B, taken from Lonza website).

The length of the culture period required, and the difficulties of obtaining full ciliation were a limiting factor in the number of experiments that could be undertaken in this section of work; to maximise the experimental outputs I used the same supernatant-exposed cultures in a range of assays, which restricted the time-points I was able to analyse. Since ciliation is unique to this culture system, I prioritised experiments to study ciliary beat frequency (CBF) and co-ordination, hence other assays were restricted in number and scope. To map onto the data obtained for A549 and iHBEC submerged monolayer culture cells and investigate the effect of neutrophil supernatants on the integrity of these cells layers I employed immunocytochemistry and LDH assay (to assess cell damage by means of cellular leakage).

Immunocytochemistry was used to look at cell damage and the induction of apoptosis, as previously undertaken using A549 cells and iHBEC's. The ALI cultures were exposed to neutrophil supernatants (500µl, 1:2 dilution) added to the basal side for 6 h at 37°C; this relatively short time period of exposure was dictated by the need to study ciliary motion. After exposure the cells were gently scraped of the transwells and fixed in 4% PFA for 30 mins prior to washing twice with PBS. Before staining, cytopins were made of the cell scrapings. They were then stained for F-actin (rhodamine-phalloidin, 1:200 green), nuclei (DAPI, blue) and cleaved caspase 3 (anti-cleaved caspase 3 goat IgG antibody, 1:1000 and Alexa Fluor 488 donkey anti-goat IgG, 1:1000, red). Representative images (of n=3 stained edges imaged per condition, n=1 experiment) are shown in Figure 5.8. There is an increase in cleaved caspase 3 detection, even following this brief exposure to hypoxic activated supernatants relative to the normoxic equivalents. This is entirely consistent with the previous data obtained using A549 and iHBEC submerged monolayer cultures. No other significant signs of damage could be seen in the cell layer structure after this brief exposure. Although the immunocytochemistry data from ALI-culture primary cells align with my previous experiments, this data is only qualitative/semi-quantitative. In an attempt to obtain quantitative data to measure toxicity to ALI cultures induced by neutrophil supernatants, I used a commercial LDH assay, which can be undertaken on a small sample volume. Unfortunately, insufficient cells were available to undertake this

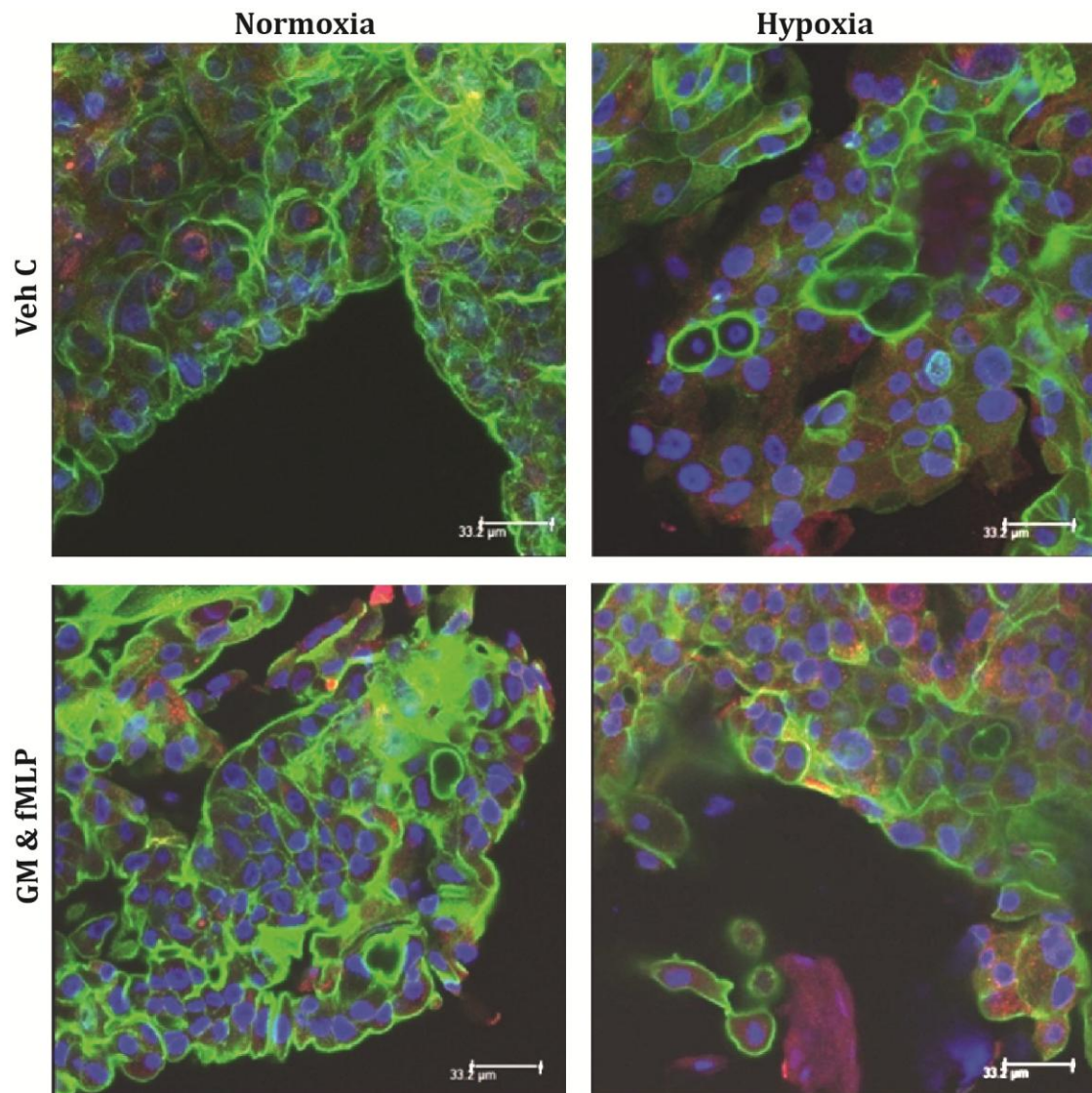


Figure 5.8: Hypoxic neutrophil supernatants induce apoptosis in ALI cultures

ALI-cultures were cultured and matured as described above. The cells were exposed to neutrophil supernatants (1:2 dilution) generated from neutrophils cultured and activated (GM-CSF/fMLP) under normoxic or hypoxic conditions for 6 h before the cell layers were fixed with 3.5% paraformaldehyde (4 h) and stained for F-actin (rhodamine-phalloidin, green), nucleus (DAPI, blue) and cleaved caspase 3 (anti-cleaved caspase 3 goat IgG antibody and Alexa Fluor 488 – donkey anti-goat IgG, red) as a marker of apoptosis. Representative images of n=1 experiment performed in triplicate, magnification = x63.

assay on only one occasion, due to the difficulties inherent in maintaining and differentiating the primary HBECs in ALI culture conditions. ALI-cultures were exposed to neutrophil supernatants (1:2.5. dilution) on the basal side for 24 h at 37°C. 10 µl samples of the tissue culture media bathing the cells were removed at times t=0, 4, 8 and 24 h and analysed for LDH activity (Figure 5.9). Consistent with my previous data sets, a time-dependent increase in LDH release (indicative of cellular damage) was seen upon exposure to the supernatants, especially those derived from the hypoxic, activated neutrophils; in these culture conditions, the released LDH activity more than tripled (from 16.9 to 50.2 nmol/min/ml). Statistical analysis could not be undertaken on these data since insufficient cells were available from subsequent ALI cultures to repeat this experiment.

5.4.2 The effect of hypoxia on neutrophil induced ciliary dysfunction

Ciliary dysfunction has been linked to increased susceptibility to infection; hence the effects of neutrophil supernatants on ciliary function (CBF and ciliary beat pattern) were assessed. The ALI cultures were gently scraped from the Transwell[®] inserts, suspended in 500 µl of ALI medium per well, and the cell suspension was divided into 2 Eppendorff tubes. Cells were left to settle for 10 min before the medium was removed and the cells were exposed to undiluted neutrophil supernatants. Directly after exposure the cells were transferred onto a chamber-slide (Figure 3.10). Beating ciliated edges were recorded using a digital high-speed video camera (Kodak Ektapro Motion Analyser, Model 1012) at a rate of 500 frames per second (x 63 lens). Figure 5.10A shows single still images captured from representative movies (of n=3) of ciliated edges exposed to neutrophil supernatants for 2 h; the movies are included on a CD supplied with the thesis. They show that epithelial cell cilia are profoundly affected by the neutrophil supernatants, application of which resulted in a reduction of the number of normally beating cilia and cell swelling. These effects were most apparent when the ciliated edge was exposed to the hypoxic activated supernatants (not significant). The quantification of the ciliary beat frequency was done by ImageJ and ciliaFA (programme developed by Dr. Claire Smith, university Collge London, Institute of Child Health, *Smith et al.*³⁹³). Fresh human respiratory tract cilia beat in a coordinated fashion at a frequency of approximately 10 to 14 Hz⁴⁴⁶, and my readings were in agreement with this. Figure 5.10 shows that even exposure to supernatants from “resting” neutrophils cultured under normoxia reduced

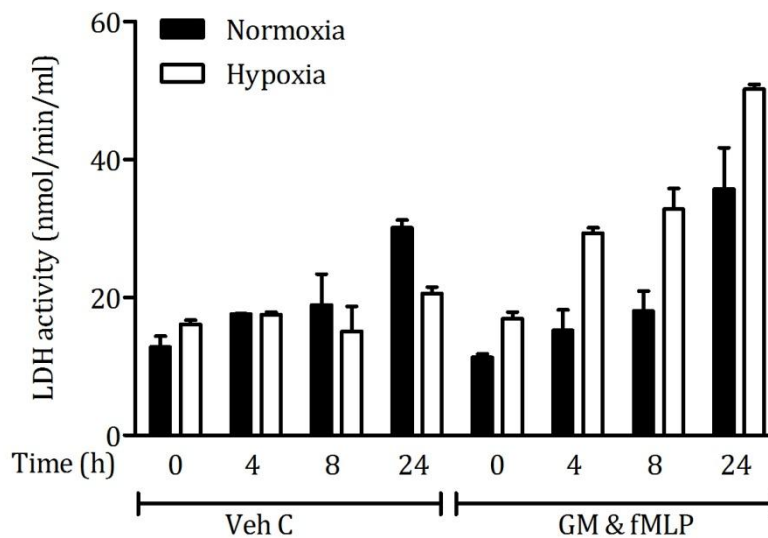


Figure 5.9: Hypoxic neutrophil supernatants induce LDH release from ALI cultures

ALI cultures of primary HBECs were maintained and matured exactly as described. The cells were exposed to supernatants (1:2.5 dilution) derived from neutrophils activated as indicated under normoxic (filled bars) or hypoxic (open bars) conditions, applied to the basal side (500 μ l). 10 μ l samples were aspirated from the basal side at 0, 4, 8, and 24 h and analysed by commercial LDH assay according to the manufacturer's instructions. Results represent a single experimental procedure with all samples run in duplicate. Values represent mean \pm SEM.

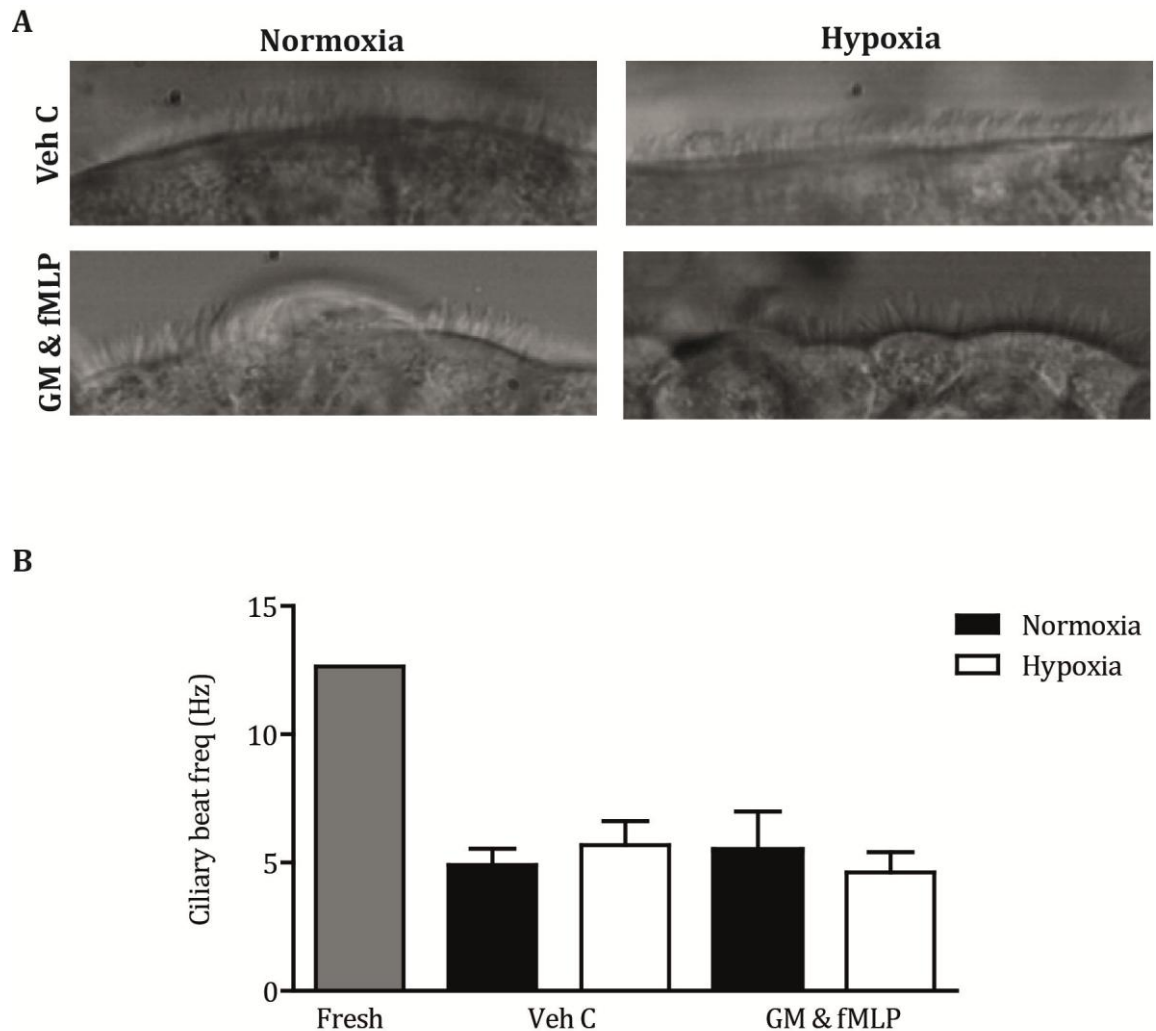


Figure 5.10: Neutrophil supernatants do not affect ciliary beat frequency

Primary HBECs grown in ALI culture were scraped from the Transwell[®] inserts, transferred to a chamber slide and exposed to undiluted neutrophil supernatants for 2 h. Recordings were made at 0 and 2 h with a high-speed camera (500 fps). A. Representative still images from n=3 movies, magnification = x100. B. Ciliary beat frequency determined by analysis of n=3 movies with CiliaFA at t=2 h; fresh cells t=0 hours.

CBF to 4.9Hz, and this effect was not more pronounced when supernatants from activated or hypoxic neutrophils were applied (ie the decrease in CBF did not correlate precisely with the enhanced degranulation products present in the hypoxic and activate cells). These results may suggest that either alternative (non granule-derived) components of the neutrophil supernatants are responsible for depressing CBF, or that maximal impairment of this function is seen even with the level of granule components release by resting normoxic neutrophils. Alternatively, the lack of a quantifiable effect of increasing protease content in the applied supernatants might be due to the fact that static cilia are not included in this calculation of beat frequency.

To investigate the latter possibility, ciliary beat pattern per cell was scored, based on established clinical protocols used to diagnose patients with PCD. Dyskinetic cilia were scored (includes static cilia, score of 1) and the resultant Dyskinesia Index is the percentage of '1's' scored per edge per condition. The cells were also scored for static cilia (score of 0) and the Motility Index is the percentage of '0's' scored per edge per condition.

As shown in Figure 5.11A-D, incorporating data from n=3 experiments using different batches of primary HBECs, there was a dramatic decrease in healthy cilia and a marked increase in static cilia on exposure to the neutrophil supernatants after just 1 h, the percentage of immotile cilia increased even further after 2 h. Although a trend towards a more pronounced effect with the hypoxic supernatants was observed, with no healthy cilia at all remaining after just a 1 h incubation, the differences between hypoxic versus normoxic supernatants did not reach statistical significance. This can in part be explained by the variability between different ALI cultures, but mostly reflects the considerable detrimental effect of the normoxic resting neutrophil supernatants alone, narrowing the window for a further effect of hypoxia to be observed.

5.5 Discussion

Neutrophil proteases have been implicated in mediating cell and tissue damage using a range of experimental methodologies; these range from cell culture systems to mouse models, and finally to the detection of increased proteases in the BALF derived from patients lung diseases such as COPD and ARDS^{193,196,200}.

As sites of inflammation are profoundly hypoxic³¹⁴ and hypoxia alters neutrophil function^{327,354}, the impact of hypoxia on neutrophil function may have direct relevance to

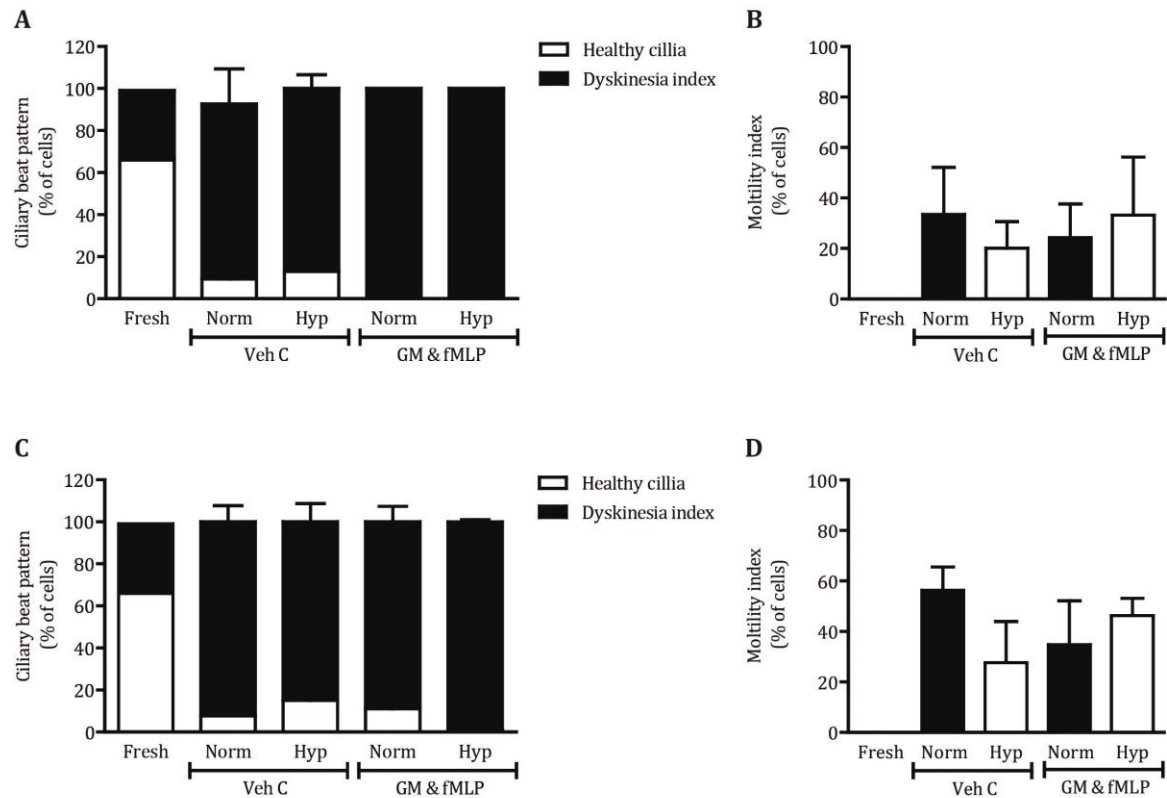


Figure 5.11: Neutrophil supernatants induce ciliary dysfunction in ALI cultures

Primary HBECs grown in ALI culture were scraped from the Transwell[®] inserts, transferred to a chamber slide and exposed to undiluted neutrophil supernatants for 2 h. Recordings were made at $t=1$ h and 2 h with a high-speed camera (500 fps). A&B. Ciliary beat pattern at $t=1$ h. C&D. Ciliary beat pattern at $t=2$ h. Values represent mean \pm SEM. 4 ciliated edges were examined per condition from $n=3$ experiments.

diseases of the lung and other organ systems. My discovery that hypoxia has a marked up-regulatory effect on neutrophil degranulation (as detailed in Chapter 4) suggests that hypoxia may promote neutrophil-mediated tissue injury. I therefore felt it was important to explore the effects of hypoxia on the ability of neutrophil-derived supernatants generated under conditions of normoxia and hypoxia to damage relevant target tissue. I chose to study lung epithelial cells as these are thought to be important targets in human neutrophil-mediated lung diseases.

My results show that increased release of proteases in the context of hypoxia can cause substantial damage to lung epithelial cell monolayers grown in submerged or ALI conditions. The damage to A549 cells caused by supernatants from neutrophils activated under hypoxic conditions resembles data reported by Nakajoh et al.⁴³⁵ that elastase (extracted from purulent human sputum samples) induced a concentration dependent decrease in the viability of lung epithelial cell lines (both A549 cells and BEAS-2b cells), and also of primary human tracheal cells; they further noted a time-dependent increase in the detection of cleaved caspase 3, again re-capitulating my findings. Additionally, Venaille et al.⁴⁴⁷ demonstrated that neutrophil-derived proteases present in CF sputum samples (most likely NE and cathepsin G) led to epithelial cell damage and detachment (although these authors used amniotic rather than respiratory epithelial cells).

Most published studies have focused on the damage caused by a single isolated protease such as NE; however this does not represent the physiological situation where a wide range of granule proteins and proteases are released in conjunction, and which can influence each other's functions. For example; it has been shown that co-culture of MMP's and NE results in the conversion of latent to active MMPs, thereby increasing the potential for tissue injury⁴⁴⁸. In agreement with the extensive range neutrophil degranulation products, and the likely damaging contribution of multiple rather than single factors present in neutrophil supernatants the damage to A549 cells could be mostly ameliorated by incubation with the more serine protease inhibitor α_1 AT.

The primary HBEC cultures comprise a far more complex system, with polarised layers of basal, secretory and ciliated cells cultured on Transwell[®] inserts, in the setting of an air-liquid interface, to more closely resemble the situation in the environment of the human lung. These ALI-cultures are challenging to undertake, with a requirement for approximately 6-8 weeks of culture in an air-liquid interface to obtain optimal ciliary growth and development (defined as visible cilia over > 10% of the surface area of the culture). The cells were purchased from Lonza, and the initial batch of cells grew far

better than subsequent batches; one attempt at ALI culture did not yield ciliated cells and a further batch of cells became infected; these cells had to be discarded. Further, higher passage number cells grew less vigorously in culture and did not yield sufficient cell numbers to repeat all of my initial experiments. Because of the limiting cell numbers, the time taken to culture to ciliation, and also the expense of this system, I was not able to refine my experimental conditions and had insufficient cells to repeat some of my initial assays in subsequent experimental runs. Ideally I would have wished to go on to dilute my neutrophil supernatants, to see whether I could delineate a greater effect of the hypoxic samples; with the conditions initially selected, the damage to the sensitive cilia was too great with the resting supernatants to see a differential effect with hypoxia. Further, it has been shown that CBF and ciliary beat pattern may be affected environmental factors such as pH and temperature^{449,450} to prevent temperature influencing the results the chamber-slides were kept in an incubator at 37°C (5% CO₂) between time points and on a heated microscope stage during analysis. However we were not able to control for changes in pH; as the cells are on a chamber-slide in a small volume for 2 h, this could have affected basal CBF and ciliary beat pattern.

The technique used for the above experiments required me to gently scrape the cells of the Transwell[®] to obtain a suspension of cell “strips” that are used to analyse ciliary beat frequency and beat pattern. Thomas et al.⁴⁵¹ determined with high speed digital video microscopy that the cilia on disrupted epithelial edges showed significantly reduced beat frequency and significantly increased dyskinesia compared with those on intact, undisrupted ciliated epithelial edges (13.4 for intact edges to 9.2 Hz for strips with isolated ciliated cells). With the first set of ALI-cultures analysed, mostly intact, undisrupted ciliated epithelial edges were obtained; unfortunately, subsequent sets of ALI-cultures were not as heavily ciliated and edges with a fewer and more isolated ciliated cells had to be used. Additionally exposure to the neutrophil supernatants induced visible cell damage, leading to smaller, damaged cell strips and making ciliary analysis increasingly challenging. The varying quality of the ALI cultures thus resulted in variability in the ciliary beat pattern analysis between experiments (Figure 5.10).

Despite these experimental challenges, the results shown above are in broad agreement with published studies investigating the effects of neutrophil proteases on CBF and epithelial cell damage. Amitani et al.²⁰⁹, demonstrate that NE reduced CBF and disrupted the ultrastructure of human nasal ciliated respiratory epithelium, leading to cell detachment, cytoplasmic blebbing and mitochondrial damage, although the cilia

themselves remained intact. These studies suggest that NE and other neutrophil-derived granule products may contribute to the delayed mucociliary clearance and epithelial damage observed in patients with chronic bronchial infections in the setting of COPD and bronchiectasis. Furthermore, a single installation of elastase into rabbit lung led to goblet cell metaplasia and the formation atypical cilia. Although most data in the literature relates to NE, application of MMP-9 has also been shown to lead to detachment and detachment-induced cell death of airway epithelial cells by damaging components of the tight junction and the adherent junctions⁴⁵². By targeting cell-cell junctions MMP-9 may disrupt the barrier function of the lung epithelium, allowing pathogens to gain access to the epithelial basolateral surface increasing infection efficiency. I have studied the effects of secreted neutrophil products by exposing the epithelial cell layers to neutrophil supernatants in an isolated cell culture system. It would be of interest to look at a more complex, interactive system or an *in vivo* model, as there is data showing that NE induced a 4.4 fold increase in neutrophil chemo attractant IL-8 release from A549 cells⁴⁵³. Both hypoxia and neutrophil granule products^{133,195,196} can induce an inflammatory phenotype in lung epithelial cells^{320,321,323,324} creating a complex feedback system potentially leading to more neutrophil recruitment and activation. This makes further investigation of the epithelial cell phenotype under conditions of normoxia/hypoxia and in the presence or absence of neutrophils an interesting progression of this research.

In summary, I have demonstrated that enhanced neutrophil degranulation promoted by hypoxia imparts a greater capacity for these cells to damage delicate respiratory epithelial monolayers. This was seen in the A549 cancer cell line, in iHBECs and in primary HBECs grown in ALI culture conditions. Since inflammatory sites are characterised by hypoxia, preventing this hypoxic up-regulation of extracellular degranulation may limit neutrophil-mediated tissue damage in inflammatory diseases. To achieve this, a better insight into the mechanism of enhanced degranulation is required, and the signalling mechanisms that might underpin this effect are the focus of the experimental work presented in the next chapter.

Chapter 6

Results: The mechanism of augmented degranulation under hypoxia

6. The mechanism of augmented neutrophil degranulation under hypoxic conditions

6.1 Introduction

Neutrophils are exposed to a wide range of oxygen tensions even in health, from 13 kPa in the alveolar capillaries, through 5 kPa in mixed venous blood to oxygen levels as low as 0.5 kPa in the lymphoid organs³⁰⁷; this hypoxic exposure may be exacerbated and prolonged when neutrophils are recruited to sites of inflammation. Like other cells, neutrophils adapt to these changes in oxygen tension by stabilisation of HIF-1 α , the near-ubiquitous orchestrator of cellular hypoxic responses. HIF-1 α migrates to the nucleus to form a heterodimer with HIF-1 β , recruits the coactivators p300/CBP, and induces expression of its transcriptional targets via binding to upstream hypoxia-responsive elements (HREs). HREs are composite regulatory elements, comprising a conserved HIF-binding sequence together with a highly variable (and poorly characterised) flanking sequence that modulates the transcriptional response.

Changes in oxygen tension and HIF-1 α stabilisation have profound effects on neutrophil function as described above (section 1.8.4 and section 4.3). However, the mechanism by which hypoxia modulates the degranulation response is currently unknown. Since HIF-1 α is the master regulator of hypoxic responses, it is plausible that it also modifies the degranulation response. Peyssonnaud *et al.*³⁵⁰ suggested a role for HIF-1 α in the production of neutrophil granule proteases; HIF-1 α -null mouse neutrophils showed decreased enzymatic activity of NE and cathepsin G in comparison to WT neutrophils, while vHL-null neutrophils exhibited increased protease activity. However, mature circulating neutrophils have been shown to be transcriptionally inert with regard to granule proteins; no mRNA transcripts of neutrophil granule proteins could be found after neutrophil maturation^{78,380}.

As neutrophil granules are formed during maturation in the bone marrow, which is a hypoxic environment⁴⁵⁴, HIF-1 α may well play a significant role in the transcriptional regulation of granule content proteins in early stages of neutrophil development. However, this mechanism may be less relevant in the context of mature peripheral blood neutrophils experiencing a relatively brief (4 h) hypoxic exposure.

In addition to a direct effect of hypoxia on granule protein content, hypoxia could modulate the signal transduction pathways that control degranulation (section 1.8.5). The

short duration of hypoxic incubation required to entrain the enhanced degranulation response makes it unlikely (although not impossible) that increased expression of key signalling components such as PI3 kinase or PLC underpins this effect. There is little published data to suggest how hypoxia might modulate such signalling pathways in neutrophils or other relevant cell types, either via HIF1- α or by other means. Hence I wished to elucidate the mechanism of the augmented degranulation seen under hypoxic conditions. My initial focus was on HIF-1 α ; I then progressed to explore the role of the key regulators of neutrophil degranulation.

The specific aims of the work presented in this chapter are as follows:

1. To explore the role of HIF in the hypoxic enhancement of neutrophil degranulation by the use of hypoxia-mimetics and other compounds.
2. To explore whether enhanced degranulation is dependent on *de novo* protein synthesis (of granule proteins or of other proteins).
3. To investigate whether the hypoxic up-regulation of degranulation is dependent on tyrosine kinase, PLC/Ca²⁺ or PI3 kinase signalling pathways.

6.1.1 Hypoxia and HIF-1 α stabilizers delay neutrophil apoptosis

It has been shown previously that hypoxia induces stabilisation of neutrophil HIF-1 α at 20 h³⁵⁴, that this is required to establish the increased lifespan of hypoxic neutrophils, and that HIF-1 α stabilizers replicate this effect. Our laboratory previously has shown that hypoxia can induce stabilisation of HIF-1 α and HIF-2 α at earlier time points (including 4 h, personal communication and published thesis Dr. L. Porter⁴⁵⁵). I was unable to replicate this data due experimental challenges with HIF-1 α antibodies and the high number of cells needed. Since this is published data I did not spend significant amounts of time trying to replicate these findings. To confirm that I could recapitulate the established effects of HIF stabilizers, I measured the effect of dimethyloxallylglycine (DMOG), deferoxamine mesylate (DFO) and cobalt chloride (CoCl₂) on neutrophil apoptosis. All three compounds work by slightly different mechanisms (section 1.8.3.1), but all result in the stabilisation of HIF (both HIF-1 α and HIF-2 α). DMOG is a 2-oxoglutarate analogue that acts as a competitive inhibitor of PHDs and FIH. DFO is an iron chelator, and chelation of Fe²⁺ bound to the active site of PHDs inhibits its enzymatic activity. CoCl₂ also works as an iron chelator, but has also been reported to bind to the PAS domain,

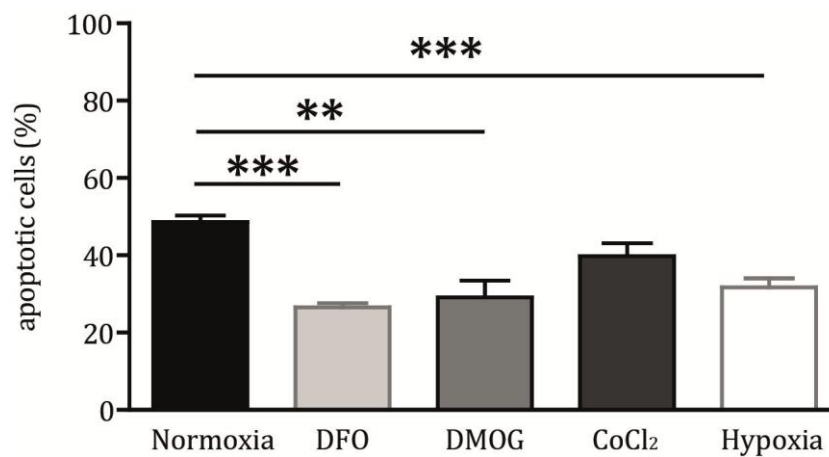


Figure 6.1: Hypoxia and HIF stabilizers delay neutrophil apoptosis

Neutrophils were re-suspended in hypoxic or normoxic IMDM at 11.1×10^6 /ml with or without DMOG (1 μ M), DFO (1 μ M), or CoCl₂ (100 nM). The cells were incubated under normoxia or hypoxia (0.8% O₂ and 5% CO₂) at 37°C for 20 h. Cytospins were prepared and stained with May/Grünwald/Giemsa. Morphology was examined by oil-immersion light microscopy. $N \geq 5$, results represent mean \pm SEM, samples were analysed in triplicate. ** = $p < 0.01$ *** = $p < 0.001$ (Mann-Whitney test).

blocking HIF-1 α -pVHL binding and thereby increasing HIF-1 α stability. Neutrophils were cultured in 96 well plates (5×10^6 /ml in IMDM with 10% serum) under normoxic conditions with or without DMOG (1 μ M), DFO (1 μ M) or CoCl₂ (100 nM), or under standard hypoxic conditions, for 20 h at 37°C. After these incubations, cytopins were prepared and the slides were stained with May/Grünwald/Giemsa. The percentage of apoptotic cells was determined based on the nuclear and cytoplasmic morphology, with the observer blinded to the incubation conditions. HIF-1 α stabilizers DMOG and DFO could fully (and significantly) mimic the inhibition of neutrophil apoptosis observed at low oxygen tensions; however the effect of CoCl₂ did not attain statistical significance (Figure 6.1). These results are in agreement with data reported Mecklenburg *et al.*³⁷⁷. Neutrophil apoptosis was reduced from 48.6% at 20 h under normoxia to 31.7% after 20 h of hypoxic exposure and the mimetics recapitulated the effect of true hypoxia; apoptosis was reduced to 26.8% (DFO) and 29.1% (DMOG) after incubation with the hypoxia-mimetics DMOG and DFO.

6.1.2 The effects of HIF-1 α stabilizers on neutrophil degranulation

As HIF-1 α stabilizers can recapitulate the effects of hypoxia by stabilising HIF-1 α , their ability to reproduce the effect of hypoxia on neutrophil degranulation was assessed. For this experiment neutrophils were re-suspended in normoxic (\pm DMOG (1 μ M), DFO (1 μ M) or CoCl₂ (100 nM)) or hypoxic IMDM (11.1×10^6 /ml), incubated under normoxic or hypoxic conditions for 4 h at 37°C and activated as described before. Neutrophil degranulation was assessed by active NE release, measured by activity assay. Unlike true hypoxia, none of the HIF-1 α stabilizers induced any increase in NE release, either in either resting or activated neutrophils (Figure 6.2). These results suggest that either the enhanced degranulation is not dependent on HIF-1 α stabilisation, or that the hypoxia mimetics are less able to stabilise HIF-1 α in the short 4 h timeframe than true hypoxic incubation. To further investigate the possible role of the transcription factor HIF-1 α in the increased degranulation response I wished to determine whether there was increased abundance of granule constituent mRNA or expression of neutrophil granule proteins following a hypoxic incubation.

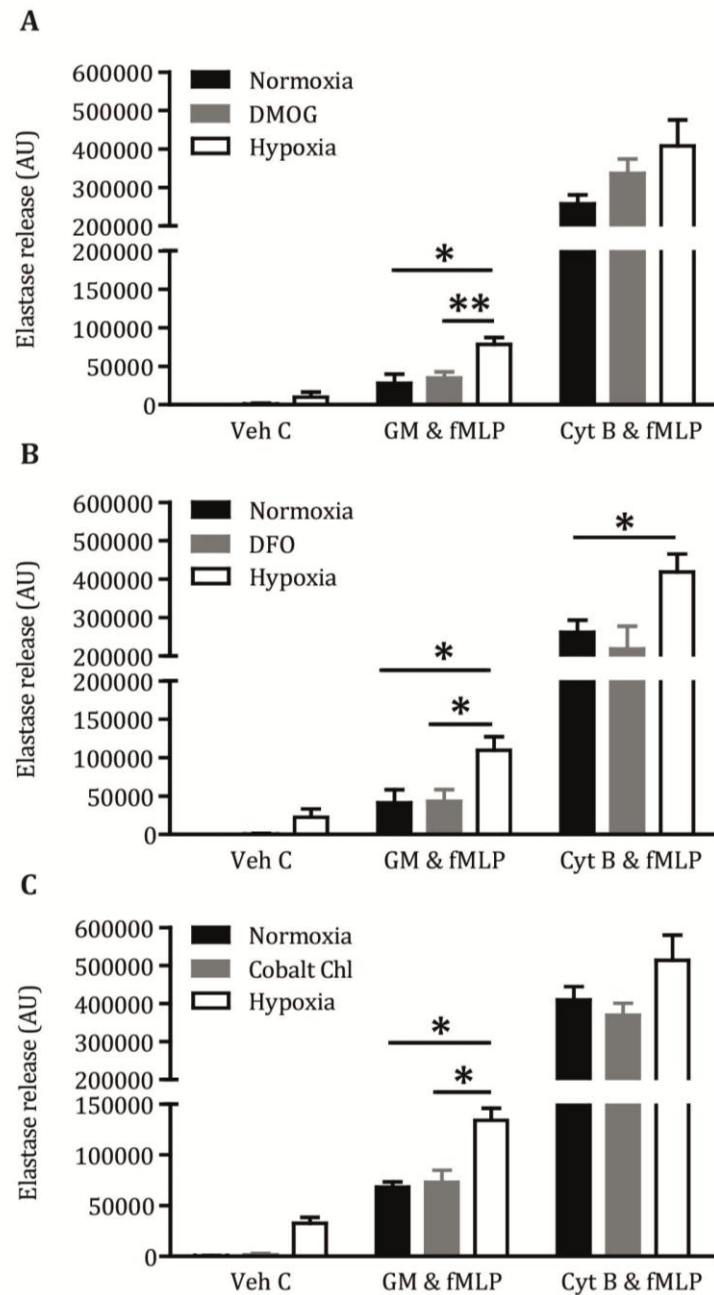


Figure 6.2: HIF-1 α stabilizers do not recapitulate the hypoxic upregulation of NE release

Neutrophils were re-suspended in hypoxic (open bars) or normoxic (filled bars) IMDM at 11.1×10^6 /ml with or without 1 μ M DMOG (A) or DFO (B) or 100 nM CoCl₂ (C) (hypoxia mimetics depicted by grey bars). The cells were incubated under normoxia (including the cells with hypoxia-mimetics) or hypoxia (0.8% O₂ and 5% CO₂) for 4 h at 37°C. The cells were then primed and activated (GM-CSF/fMLP). NE activity was measured in the supernatants by the increase in fluorescence caused by cleavage of DQ-Elastin. A. Effect DMOG on NE release, n=5. B. Effect of DFO on NE release, n=6. C Effect of CoCl₂ on NE release, n=5. Samples were run in duplicate. Results represent mean \pm SEM. * = p < 0.05, ** = p < 0.01 (Mann-Whitney test).

6.1.3 The effects of hypoxia on de-novo granule protein production

6.1.3.1 The effects of hypoxia on granule protein transcription

HIF exerts its functions mainly by inducing the transcription of a range of target proteins. As discussed (section 1.8.3.1 and Figure 1.10), under hypoxic conditions stabilised HIF-1 α translocates to the nucleus and binds to hypoxic response elements (HRE's) to influence gene transcription. To further investigate the role of HIF in neutrophil degranulation, Dr S. Farrow (GlaxoSmithKlein, Stevenage, Hertfordshire) performed a bioinformatics screen for hypoxic response elements (HRE's, which comprise a conserved HIF binding site A/GCGTG, plus highly variable and poorly understood flanking sequences⁴⁵⁶) in the upstream regulatory elements of key granule protein genes. Potential HRE's were identified in the promoter sequence of NE, MPO and MMP-9, but not in the promoter region of lactoferrin (see the appendixes, section 8.5). Although circulating peripheral blood neutrophils (as used in all of my experiments) are terminally differentiated, and no granule protein mRNA transcripts could be identified in a previous report^{78,380}, this study did not encompass hypoxia, hence it is still possible that HIF-1 α induces *de novo* transcription of these genes in mature cells. Hypoxia up-regulates lactoferrin release as well as that of NE, MPO and MMP-9, but our understanding of HREs is incomplete, hence our failure to identify an HRE for lactoferrin does not preclude this mechanism. Hence qPCR was performed on RNA isolated from freshly isolated neutrophils and from neutrophils incubated under normal or hypoxic conditions (4 h, 37°C) identical to those used for the degranulation assays.

As a positive control, 2 well-established HIF-1 α targets were used to investigate whether hypoxia induced stabilisation of HIF-1 α under the conditions documented; BCL2 and adenovirus E1B 19 kDa interacting protein (BNIP) is part of subfamily of BCL2 family proteins and plays a role in autophagy and apoptosis, and GLUT-1 is a glucose transporter^{342,457}. As shown in Figure 6.3A, BNIP transcription was substantially induced by exposure of neutrophils to hypoxia for 4 h, but GLUT-1 transcription was not. This difference is likely to reflect the fact that BNIP is an early-hypoxic response gene whilst GLUT-1 is a late-hypoxic response gene. Using commercial primers (See the appendixes, section 8.6), mRNA transcripts for NE, MPO and MMP-9 were quantified (Figure 6.3A). No increase in mRNA abundance was detected for any of the granule proteins, indicating that hypoxia does not induce granule protein transcription in neutrophils.

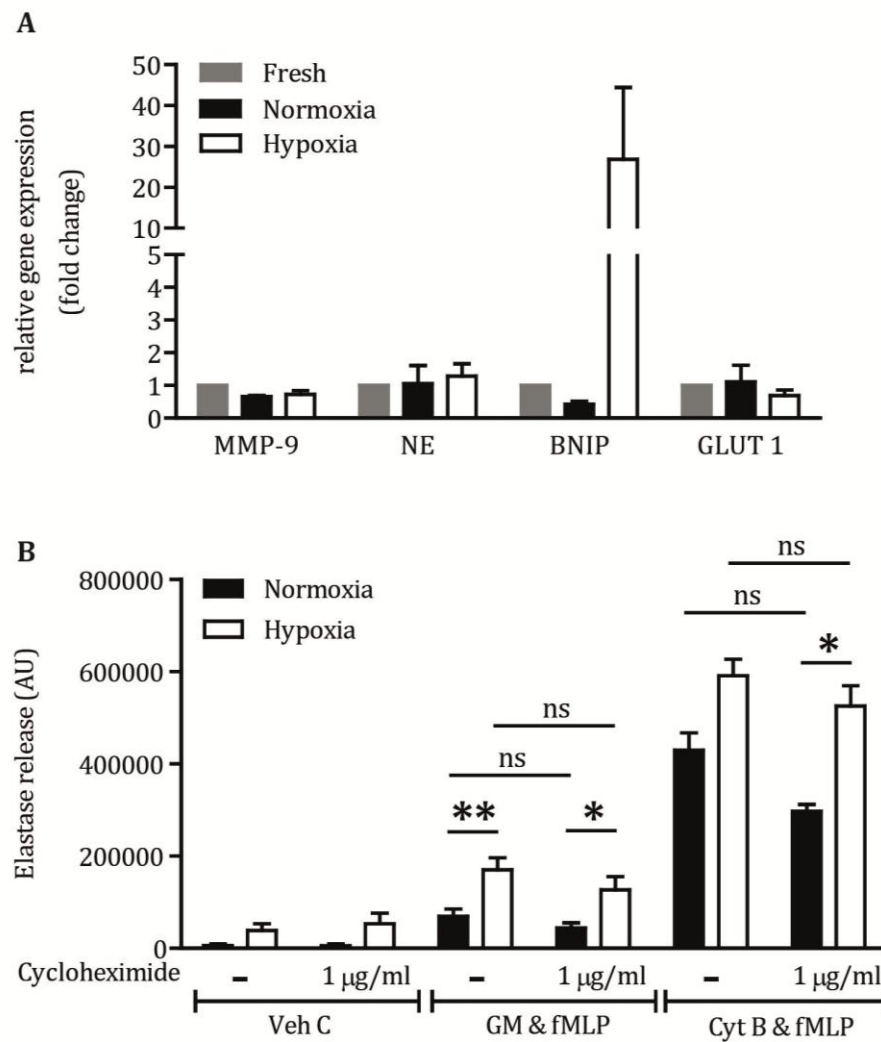


Figure 6.3: Hypoxia does not increase transcription or translation of granule proteins

A. Freshly isolated neutrophils were re-suspended in hypoxic or normoxic IMDM at 11.1×10^6 /ml and incubated at 37°C for 4 h under normoxic (black bars) or hypoxic (0.8% O_2 , 5% CO_2 , open bars) conditions. RNA was extracted from freshly isolated neutrophils (grey bars) or neutrophils incubated under normoxic or hypoxic conditions and qPCR performed. Expression was normalised to β -actin. $n=3$ independent experiments, all samples run in duplicate. B. Neutrophils were re-suspended in normoxic (black bars) or hypoxic (open bars) IMDM at 11.1×10^6 /ml with or without cycloheximide (1 $\mu\text{g}/\text{ml}$). The cells were then primed and activated with GMCSF/fMLP as previously. NE activity in the supernatants was measured by the increase in fluorescence caused by the cleavage of DQ-Elastin. Values represent mean \pm SEM, samples were run in duplicate, $n=5$. * = $p < 0.05$, ** = $p < 0.01$ (Mann-Whitney test).

6.1.3.2 The effects hypoxia granule protein translation

To investigate whether hypoxic incubation of neutrophils might to an increase in granule protein through increased translation, cycloheximide was used. Cycloheximide inhibits translation through inhibition of the elongation phase through binding to the E-site of the 60S ribosomal unit and interfering with deacetylated tRNA. For this experiment freshly isolated neutrophils were re-suspended in normoxic or hypoxic IMDM ($11.1 \times 10^6/\text{ml}$) \pm cycloheximide (1 $\mu\text{g}/\text{ml}$; a concentration previously established in our laboratory to inhibit translation in neutrophils without detectable toxicity), incubated under normoxic or hypoxic conditions (4 h, 37°C) and activated as described before. Figure 6.3B shows that incubation with cycloheximide had no significant effect on NE release from unstimulated or primed/stimulated cells under normoxic or hypoxic conditions.

As a final confirmation that the enhanced release of granule proteins seen following hypoxic incubation is due to enhanced degranulation rather than to increased granule protein expression, the level of an exemplar granule protein (MMP-9) was assessed by Western blotting. Freshly isolated neutrophils were re-suspended in normoxic or hypoxic IMDM ($5 \times 10^6/\text{ml}$) and incubated under normoxic or hypoxic conditions for 4 h at 37°C. After incubation the cells were gently scraped off the plates, pelleted and lysed (200 μl ice-cold hypotonic lysis buffer with protease inhibitors (section 3.9.1). Lysates were prepared for Western Blot analysis exactly as described (section 3.9.1). Polyacrylamide gels were transferred to PVDF membranes, which were probed for MMP-9; β -actin staining was used to confirm equal protein loading. Incubation of neutrophils under for 4 h led to a marked decrease in the detection of MMP-9 in comparison to protein levels seen in freshly isolated neutrophils (Figure 6.4); this reduction was more marked under hypoxic conditions, perhaps reflecting the increased basal release of MMP-9 under in this setting (Figure 6.4). An possible alternative explanation is that hypoxia leads to autophagic destruction of neutrophil granules. These results suggest that increased availability of granule proteins does not underlie their increased release following hypoxic incubation.

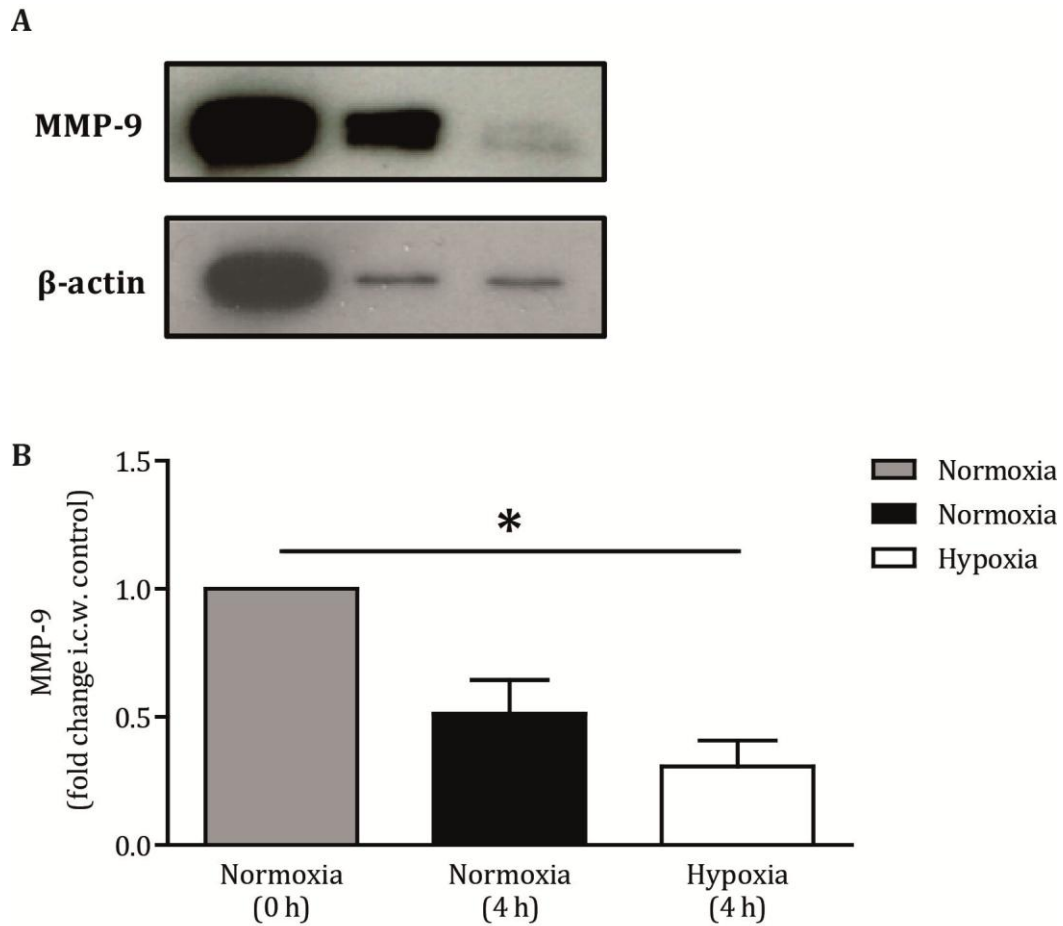


Figure 6.4: Granule MMP-9 protein content decreases under hypoxic conditions

Neutrophils were analysed immediately (grey bars) or re-suspended in normoxic (filled bars) or hypoxic (open bars) IMDM at $11.1 \times 10^6/\text{ml}$ and incubated under normoxia or hypoxia (0.8% O_2 and 5% CO_2) at 37°C for 4 h. Cells were gently scraped off the plate, pelleted and laced on ice immediately upon leaving the hypoxic hood. Lysates were prepared and corrected for protein content. Polyacrylamide gels were run and proteins transferred to PVDF membranes as described. The membranes were probed for MMP-9 (rabbit polyclonal), and β -actin (rabbit polyclonal). A. Representative Western blot. B. Fold change of MMP-9, corrected for protein loading, densitometry analysis by ImageJ. $n=3$, values are mean \pm SEM. * = $p < 0.05$ (paired T-test).

6.1.4 The effects of re-oxygenation on the hypoxic up-regulation of neutrophil degranulation

Previous studies from our laboratory have shown that the hypoxic impairment of the neutrophil respiratory burst and bacterial killing is due to depletion of molecular oxygen (a substrate for the NADPH oxidase), since a brief period of re-oxygenation (15 min) restored these functions³²⁷. To see whether re-oxygenation would affect degranulation, neutrophils were subjected to normoxia or hypoxia as described before, and a set of samples was removed from the hypoxic hood after 4 h and re-oxygenated for 15 min before priming with GM-CSF (10 ng/ml) and activation with fMLP (100 nM). Figure 6.5 shows that this re-oxygenation had no significant impact on the hypoxic up-regulation of NE release, suggesting that a lack of molecular oxygen does not underlie this effect, either directly or indirectly (via the effect on the NADPH oxidase). Taken together these experiments indicate that hypoxia does not induce the *de novo* synthesis of neutrophil granule protein by either transcription or translation, and that the hypoxic up-regulation of degranulation is not mediated by the canonical transcription factor HIF or by an NADPH oxidase-dependent mechanism. In view of this unexpected finding (HIF-mediated signalling underpins the vast majority of hypoxic responses) I decided to investigate the effects of hypoxia on both established and novel pathways with potential links to hypoxia that are implicated in the control of degranulation/secretory responses.

6.2 The effects of hypoxia on degranulation signalling pathways

The signalling pathways that regulated neutrophil degranulation are complex, and although some key players have been identified there are still gaps in our knowledge (section 1.6). As fMLP has been used as the stimulus to activate neutrophils in most of the experiments I have undertaken, I focused on GPCR-activated signalling pathways. Activation of GPCRs leads to the downstream phosphorylation and activation of a large range of proteins. To identify potential hypoxic targets an unbiased phospho-kinase array was performed. Additionally, key players in the GPCR-dependent degranulation pathway, including PI3K, PLC, and calcium flux, were assessed for their role in the augmented degranulation response seen under hypoxia. However, firstly I investigated a possible role for a novel oxygen-sensing pathway based on peptidoglycine monooxygenase (PAM).

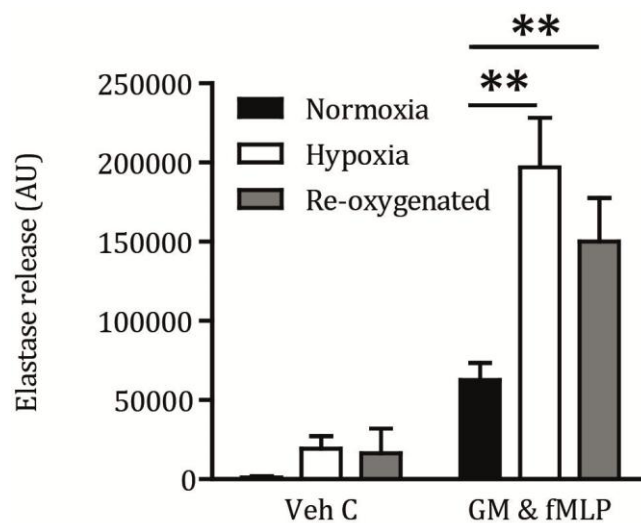


Figure 6.5: Re-oxygenation does not affect the augmented degranulation response seen under hypoxia

Neutrophils were re-suspended in hypoxic (open bars) or normoxic (black bars) IMDM at 11.1×10^6 /ml. The cells were incubated under normoxia or hypoxia (0.8% O₂ and 5% CO₂) for 4 h at 37°C. After 4 h a set of samples were taken out of the hypoxic hood and re-oxygenated (room air, normoxia) for 15 min (grey bars). The cells were then primed and activated with GM-CSF/fMLP as previously described. NE activity was measured by the increase in fluorescence caused by the cleavage of DQ-Elastin. n=4, all conditions analysed in duplicate. Results represent mean \pm SEM, ** = p<0.01 (Mann-Whitney test).

6.2.1 The effects of peptidylglycine-monoxygenase on neutrophil degranulation

I investigated a potential role for peptidylglycine-monoxygenase (PAM) in the hypoxic upregulation of neutrophil degranulation at the suggestion of Professor Peter Ratcliffe (University of Oxford), in the light of unpublished data generated by Dr Norma Masson. Using a bronchial carcinoid-derived cell line (H727) that exhibits rapid secretion of bio-active peptides in response to hypoxia, Dr Masson has identified a novel HIF-independent secretory pathway. Peptidoglycine monoxygenase (PAM) was identified as a possible oxygen sensor in this setting, and PAM inhibition or knockdown by siRNA led to increased secretion of chromogranin A from the secretory granules of H727 cells (personal communication, Dr Norma Masson). Chromogranin A⁴⁵⁸ and PAM can be found in neutrophils, therefore the effect of the PAM inhibitor 4-phenyl 3 butenoic acid (4p3-butenoic acid) on neutrophil degranulation was investigated. Freshly isolated neutrophils were re-suspended in normoxic or hypoxic medium ($11.1 \times 10^6/\text{ml}$) \pm 4p3-butenoic acid (1, 10, 100, 250 and 500 μM) for 4 h at 37 °C and activated as previously. Toxicity of 4p3-butenoic acid to neutrophils was assessed by trypan blue staining and by assessment of cell morphology with cytopins. 4p3-butenoic acid had no significant effect on degranulation under normoxic or hypoxic conditions at any of the concentrations tested (Figure 6.6). Cells were 99% trypan blue negative even at the highest concentration of 4p3-butenoic acid, but inhibitor concentrations of 1mM or more resulted in a vacuolated morphology (data not shown). This experiment suggests that PAM is unlikely to underlie enhanced neutrophil degranulation seen in the hypoxic environment.

6.2.2 The effects of hypoxia on kinase signalling

To perform an unbiased screen for kinases/phosphoproteins that might be involved in degranulation under normal and hypoxic conditions, a human phospho-kinase antibody array (R&D Systems) was used. It detects the relative site-specific phosphorylation of 43 kinases including MAP kinase, PI3K and Src family kinases (a full range of targets is given in Table 3.3). Each capture antibody is spotted in duplicate onto a nitrocellulose membrane, and levels of the phosphorylated proteins are assessed using phospho-specific antibodies and chemiluminescence detection.

Freshly isolated neutrophils were re-suspended in normoxic or hypoxic medium (11.1×10^6 cells/ml), incubated under normal or hypoxic conditions for 4 h (37°C) and primed with GM-CSF (10 ng/ml, 30 min) and activated with fMLP (100 nM, 10 min).

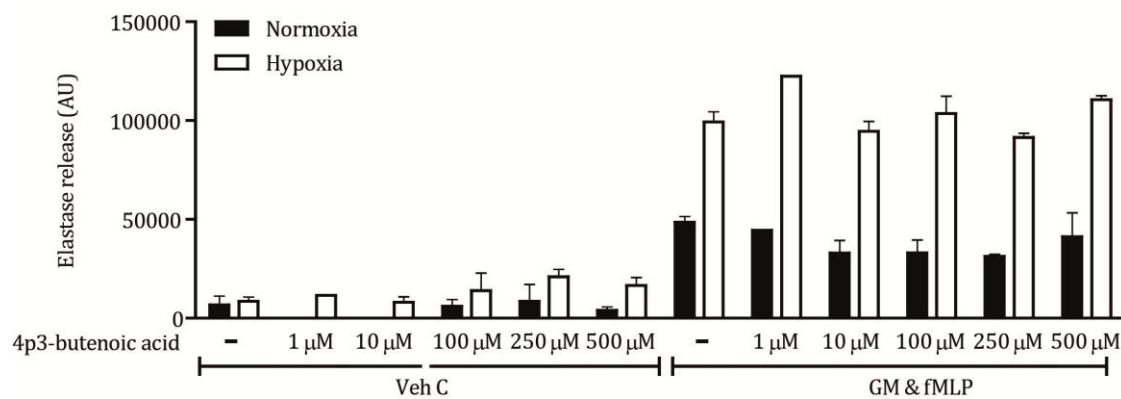


Figure 6.6: PAM does not influence neutrophil degranulation

Neutrophils were re-suspended in hypoxic (open bars) or normoxic (black bars) IMDM at $11.1 \times 10^6/\text{ml}$ with or without the PAM inhibitor 4p3-butenoic acid at the indicated concentrations (1, 10, 100, 250, 500 μM). The cells were incubated under normoxia or hypoxia (0.8% O_2 and 5% CO_2) for 4 h at 37°C . The cells were then primed and activated with GMCSF/fMLP as previously described. NE activity was measured by the increase in fluorescence caused by the cleavage of DQ-Elastin. $n=2$ experiments, all samples analysed in duplicate. Results represent mean \pm StDev.

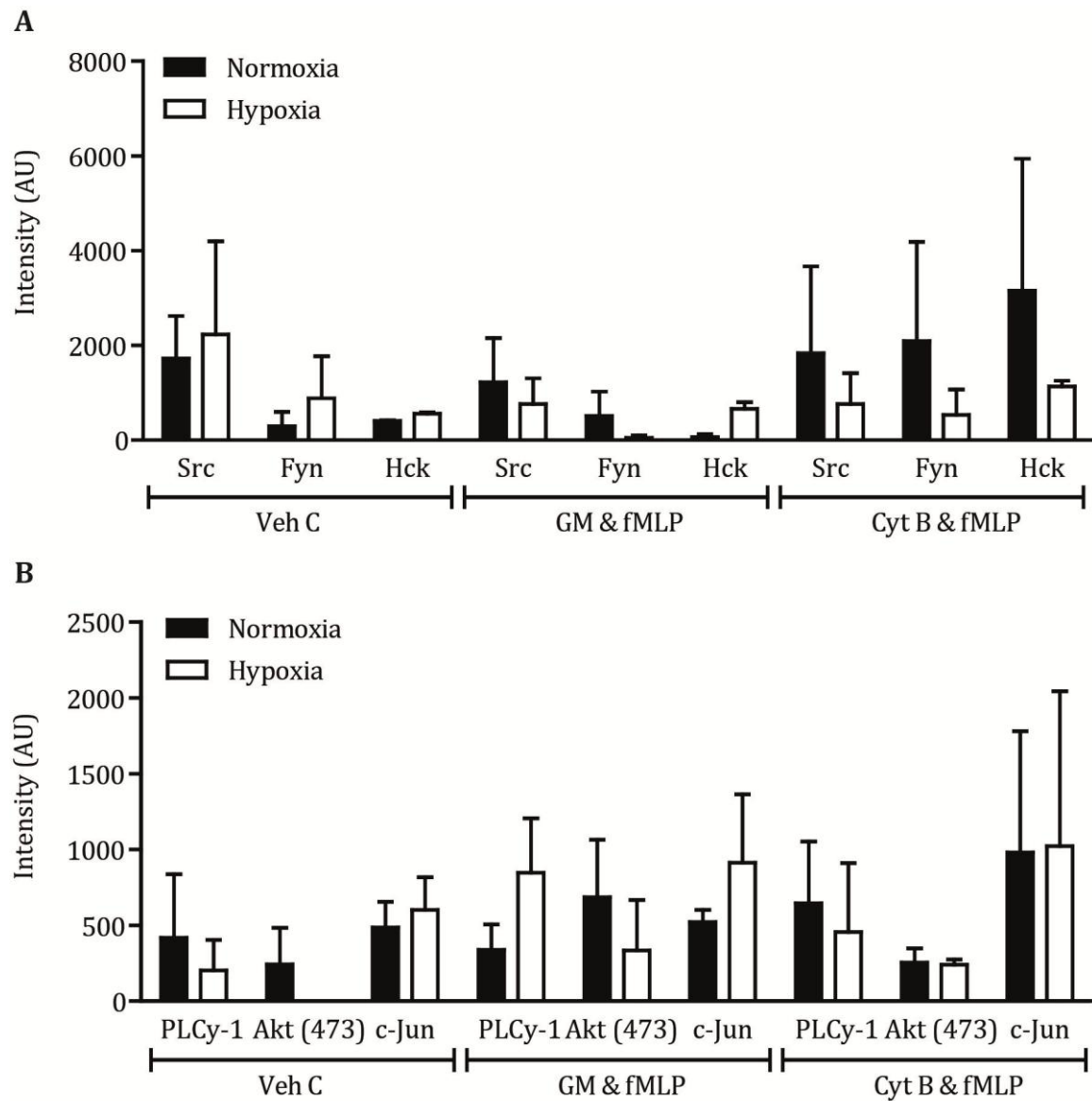


Figure 6.7: Phospho-kinase array performed under normoxia and hypoxia

Neutrophils were re-suspended in hypoxic (open bars) or normoxic (black bars) IMDM at $11.1 \times 10^6/\text{ml}$ and incubated under normoxia or hypoxia (0.8% O_2 and 5% CO_2) for 4 h at 37°C . The cells were then primed and activated as described (section 2.8). Neutrophils were pelleted and lysed. Lysates were adjusted for protein concentration and the phospho-kinase array was run according to the manufacturer's instruction. Samples were run in singlicate, $n=2$. Results represent mean \pm StDev.

After activation, the cells were gently scraped off the plates, placed on ice and lysed immediately using the lysis buffer provided. The resulting samples were adjusted for protein content (BCA protein assay) and the kinase array was undertaken according to the manufacturer's instructions (as detailed in section 3.11). The resulting dot-blot were quantified using ImageJ.

Figure 6.7 and Appendix 8.7 show the proteins demonstrating differential phosphorylation levels in different conditions, grouped by pathway. Figure 6.7A shows the Src family kinases, which have been shown to play a role in degranulation. There was a trend towards increased phosphorylation of Src, Hck and Fyn in unstimulated cells after hypoxic exposure, but upon priming this difference disappeared; after subsequent activation with fMLP, phosphorylation of these tyrosine kinases was in fact reduced under conditions of hypoxia, although none of the detected changes attained statistical significance. Figure 6.7B shows the results obtained for kinases involved in the PI3K/PLC/AKT pathway. At the single time point studied, there were no significant differences in the phosphorylation of PLC γ , Akt or cJun between normoxic- and hypoxic-incubated cells. Likewise, a wide range of other proteins/kinases in the array (not known to be relevant to the degranulation response) did not show significant differences or even consistent trends towards increased or decreased phosphorylation following hypoxic incubation (appendix 8.7).

Thus the results of the unbiased phospho-kinase array did not identify novel signalling pathways that might be relevant to the hypoxic uplift of neutrophil degranulation. Therefore, in subsequent experiments, I undertook a more detailed analysis of the known key signalling elements that influence degranulation downstream of GPCRs. G $\beta\gamma$ subunits released upon GPCR ligation in neutrophils directly trigger two key signal transduction cascades in parallel, namely the activation of PLC β with resultant calcium flux, and the stimulation of PI3-kinases (PI3Ks) γ and δ , leading to PIP $_3$ accumulation, Akt phosphorylation and activation of small GTPases (section 1.6).

6.2.3 The effects of phospholipase C (PLC) inhibition on the hypoxic uplift of neutrophil degranulation

GPCR ligation induces the activation of PLC β , which mediates the hydrolysis of PIP $_2$ to generate inositol 1,4,5-trisphosphate (IP $_3$), in turn leading to the release of intracellular Ca $^{2+}$ from the endoplasmic reticulum. PIP $_2$ hydrolysis also yields diacylglycerol and

results in the activation conventional protein kinase C (PKC) isoforms. Ca^{2+} flux in particular has been strongly linked to degranulation²³³. U-73122 is a phospholipase C and A_2 inhibitor, which prevents the PLC-dependent hydrolysis of PIP_2 to IP_3 and DAG. To enable me to dissect out the known immediate effects of fMLP (rapid but transient activation of PLC) from any PLC-dependent signal that was generated earlier during the hypoxic incubation period, U-73122 (2 μM) was added either at the start of the 4 h incubation or just 10 minutes prior to activation with fMLP. The concentration used was determined via a dose response curve (data not shown) to be the optimal concentration without inducing cell toxicity and aligns with concentrations used in the literature.^{459,460} The incubation and stimulation conditions were exactly as described previously, and degranulation was assessed by the detection NE (activity assay) and of MMP-9 (DUO-set ELISA) into the supernatants. As shown in Figure 6.8A, addition of the PLC inhibitor just prior to fMLP activation had an inhibitory effect on the release of both NE and MMP-9. Elastase release decreased from $52.1.2 \times 10^3$ arbitrary units (AU) to 1.7×10^3 AU under normoxia and from 114.2×10^3 AU to 30.5×10^3 AU under hypoxic conditions; however, this data also shows that the significant hypoxic uplift of NE release (from 1.7×10^3 AU to 30.5×10^3 AU) remains when fMLP-dependent PLC activation is prevented, despite the much lower baseline value (Figure 6.8A). The effect on MMP-9 release was similar in this setting, decreasing from 64.0 ng/ml to 10.7 ng/ml under normoxia and from 221.2 ng/ml to 90.5 ng/ml under hypoxic conditions (Figure 6.8A); thus again, a significant hypoxic uplift was preserved. Of note, PLC inhibition from the start of the hypoxic/normoxic incubation had a more marked suppressive effect on degranulation (Figure 6.8B), and in this setting there was no longer a significant difference between the normoxic and hypoxic cells, although a trend towards increased hypoxic degranulation was still present (2.8×10^3 AU under normoxic conditions in comparison to 15.5×10^3 AU under hypoxic conditions). These results suggested that PLC activation may comprise part of the hypoxia-mediated signal to augment degranulation responses, and prompted me to explore the role of Ca^{2+} flux in this setting.

6.2.4 The effects of modulating intracellular Ca^{2+} transients on the hypoxic uplift of neutrophil degranulation

Due to the limitations of working within the hypoxic hood, it was not possible to perform direct measurements of intracellular Ca^{2+} flux in real time in hypoxic neutrophils, and

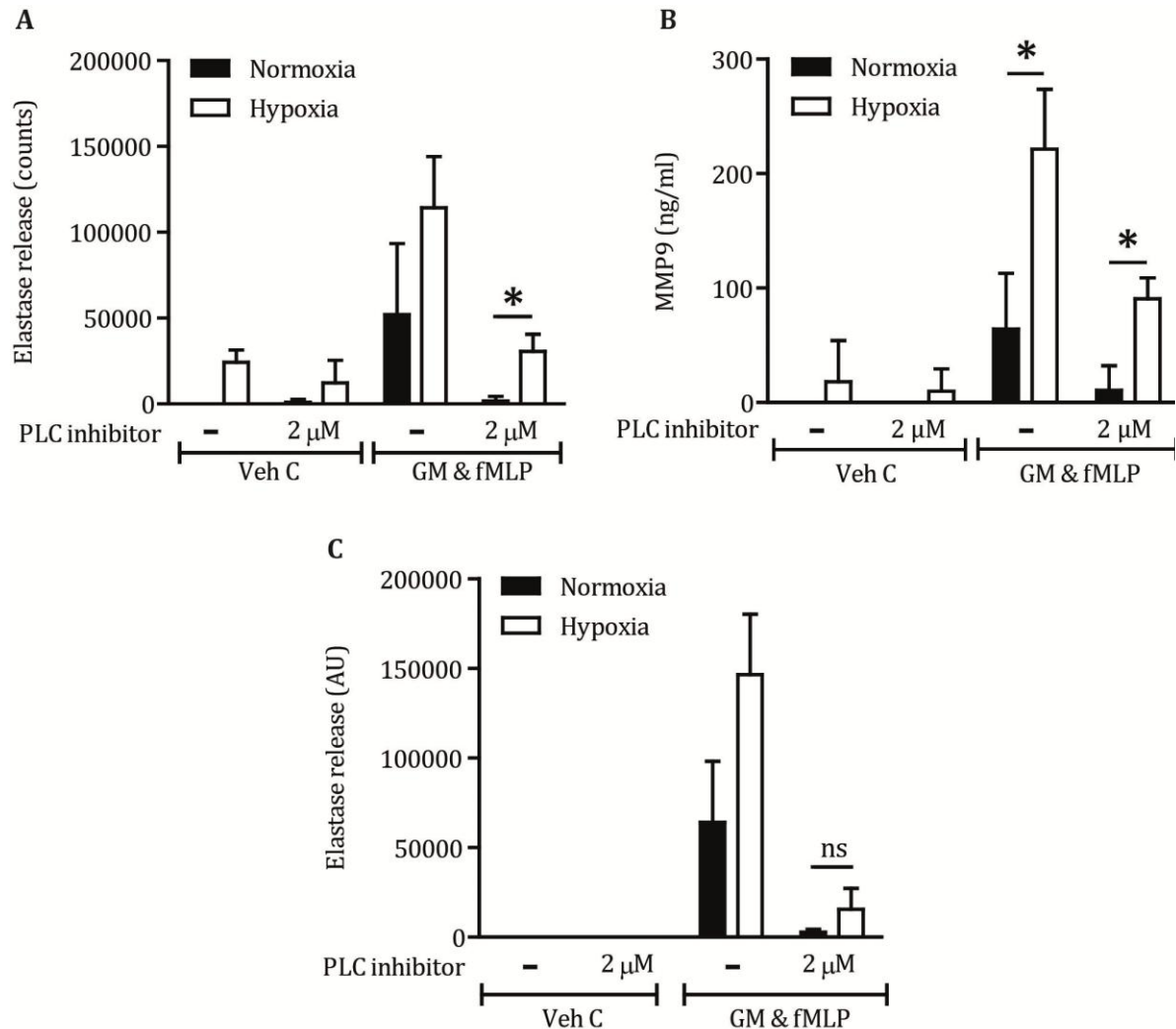


Figure 6.8: Role of phospholipase C activation in the hypoxic augmentation of degranulation

Neutrophils were re-suspended in hypoxic (open bars) or normoxic (black bars) IMDM at $11.1 \times 10^6/\text{ml}$. The cells were incubated under normoxia or hypoxia (0.8% O_2 and 5% CO_2) at 37°C for 4 h. The cells were then primed with GM-CSF (10 ng/ml) for 30 min and stimulated with fMLP 100nM. The PLC inhibitor (U-73122 2 μM) was added either 10 min prior to activation with fMLP (A and B) or from the outset of the incubation (C). Cells were pelleted and the supernatants were assessed for NE activity by the cleavage of DQ-Elastin (A and C) or for MMP-9 release by ELISA (C). A: $n=4$, B: $n=4$ C: $n=3$. Values represent mean \pm SEM, samples were run in triplicate, * = $p < 0.05$ (Mann-Whitney test).

because of concerns regarding the confounding effects of re-oxygenation, these studies were not undertaken on cells made hypoxic and then removed from the hypoxic incubator. Activation of GPCRs is known to lead to a biphasic increase in intracellular calcium; the first phase is due to Ca^{2+} release from IP_3 -sensitive, intracellular stores such as the endoplasmic reticulum (ER), whilst the second phase is secondary to Ca^{2+} influx from the extracellular fluid/media²³⁵. To assess the role of calcium flux via both routes under hypoxic as well as normoxic conditions, EGTA and thapsigargin were used. EGTA chelates divalent cations, and when compared to EDTA it is more selective for calcium rather than magnesium. EGTA chelates calcium in a 1:1 ratio, and since there is 1.5 mM Ca^{2+} present in IMDM, EGTA was added at a concentration of 2 mM. Freshly isolated neutrophils were re-suspended in normoxic or hypoxic IMDM (11.1×10^6 cells/ml) \pm EGTA (2 mM), incubated under normoxic or hypoxic conditions for 4 h (37°C) and stimulated as described before. Degranulation was quantified by the detection of NE (activity assay) and MMP-9 (DUO-set ELISA) in the supernatants. Depletion of extracellular calcium with EGTA had no effect on the (minor) release of granule proteins from unstimulated neutrophils under normoxia or hypoxia (Figure 5.9). However, extracellular calcium depletion significantly reduced the release of NE (Figure 6.9A) and MMP-9 (Figure 6.9B) under both normoxic and hypoxic conditions (from 64.4×10^3 AU to 16.8×10^3 AU under normoxic condition and from 124.3×10^3 to 60.6×10^3 AU under hypoxic conditions). NE release was affected irrespective of oxygenation conditions, and a significant increase (3.6 fold) in NE release was still seen with hypoxic incubation in the presence of EGTA (from 16.8×10^3 AU under normoxic condition to 60.6×10^3 under hypoxic conditions) For MMP-9, the results were less reproducible, but the trend was similar. Inclusion of EGTA reduced the detection of MMP-9 in the cellular supernatant whether normoxic or hypoxic incubation was employed, but the variation in release between experiments meant that EGTA-dependent differences did not reach statistical significance. Since these results suggested that modulation of the extracellular influx of calcium does not fully explain the effects of hypoxia on neutrophil degranulation, I proceeded to explore the effects of thapsigargin. Thapsigargin releases calcium from intracellular stores to induce an intracellular calcium spike. Freshly isolated neutrophils were re-suspended in normoxic or hypoxic IMDM (11.1×10^6 cells/ml), incubated under normoxic or hypoxic conditions for 4 h (37°C) and primed with GM-CSF (10 ng/ml) before incubation with thapsigargin (10, 50 or 100 nM) and immediate addition of fMLP (100 nM).

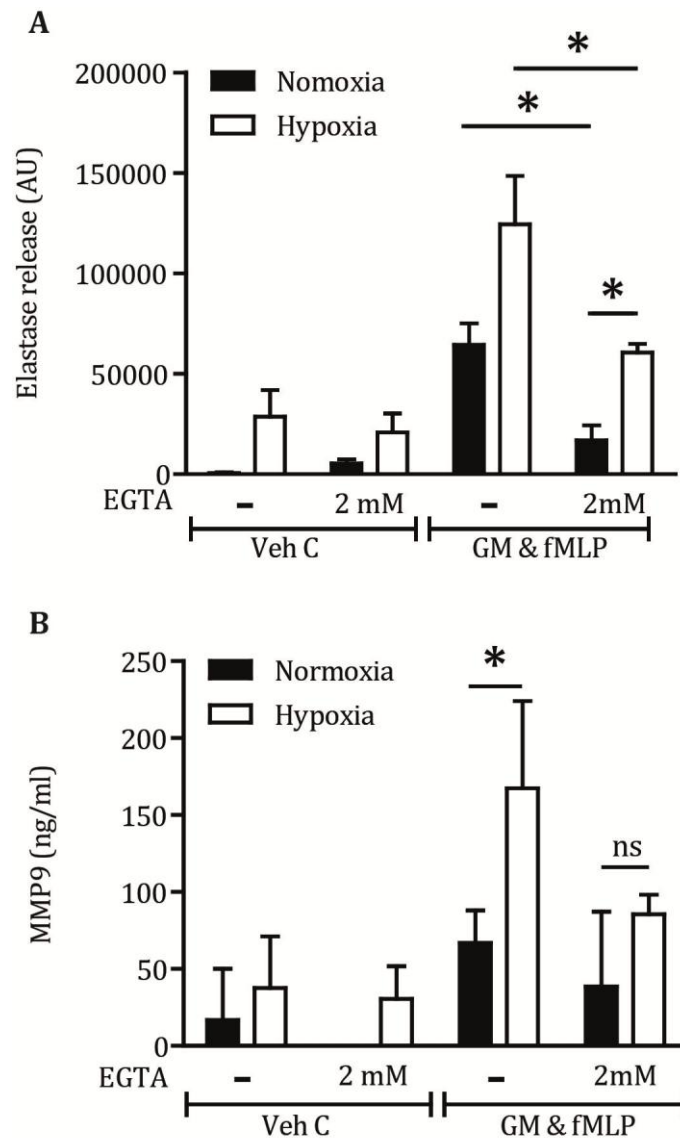


Figure 6.9: Role of calcium influx in the hypoxic augmentation of neutrophil degranulation

EGTA (2mM) was added to the media used in these experiments 10 min before re-suspension. Neutrophils were re-suspended in hypoxic (open bars) or normoxic (black bars) IMDM \pm EGTA at 11.1×10^6 /ml. The cells were incubated under normoxia or hypoxia (0.8% O₂ and 5% CO₂) at 37°C for 4 h. The cells were then primed and activated with GMCSF and fMLP as described. Cells were pelleted and the supernatant transferred to fresh tubes before removal from hypoxic hood for further analysis. A. NE activity was measured by the increase in fluorescence caused by the cleavage of DQ-Elastin. B. MMP-9 release was measured by MMP-9 ELISA. Values represent mean \pm SEM, samples were run in triplicate, n=4. * = p< 0.05 (Mann-Whitney test).

After 10 min supernatants were collected and assessed for NE and MMP-9. Both MMP-9 and NE release was significantly increased (Figure 6.10). Thapsigargin did not augment or diminish the hypoxic upregulation of GMCS/fMLP-stimulated NE release, which remained constant (approximately twofold) at all thapsigargin concentrations examined (normoxia versus hypoxia, no thapsigargin: 10.8×10^3 AU increasing to 20.0×10^3 AU; normoxia versus hypoxia, 100 nM thapsigargin: 17.1×10^3 AU increasing to 36.9×10^3 AU; see Figure 6.10A). In the absence of thapsigargin, MMP-9 release was upregulated 2.8 fold under hypoxic conditions (from 100.6 ng/ml to 275.4 ng/ml). In unstimulated cells, thapsigargin had little effect on NE release, but induced marked MMP-9 release (figure 5.10B), an effect more marked when neutrophils were hypoxic. Thapsigargin increased MMP-9 release from primed and stimulated cells, but again had a more pronounced effect when the incubation was normoxic rather than hypoxic; in the presence of 100 nM thapsigargin, there was no significant hypoxic uplift in MMP-9 release (figure 6.10B). This difference between NE and MMP-9 in response to thapsigargin may reflect the known differential sensitivity of the 2 granule populations (azurophilic and gelatinase) to Ca^{2+} -induced release.

Thus modulation of Ca^{2+} -flux appeared to have little impact on the hypoxic up-regulation of NE release, although a probable contributory role was detected for the liberation of MMP-9. In view of this, I went on to explore the role of PI3K in the hypoxic up-regulation of azurophilic granule release.

6.2.5 The effects of PI3K inhibition on the hypoxic uplift of neutrophil degranulation

The PI3K pathway (see section 1.5.2) plays a key role in GPCR signalling and is one of the earliest kinases to be activated upon receptor ligation. PI3K activation induces the production of phosphatidylinositol (4,5)-bisphosphate (PIP_3) from phosphatidylinositol (4,5)-bisphosphate (PIP_2)²²¹. PIP_3 is an important messenger and plays a role in a range of cell processes including neutrophil polarisation and degranulation. $\text{PI3K}\gamma$ and $\text{PI3K}\delta$ are expressed predominantly in leukocytes and are key to a number of neutrophil functions such as the oxidative burst⁴⁶¹ and chemotaxis⁴⁶². $\text{PI3K}\gamma$ is the principal isoform activated on ligation of GPCRs and has been implicated in the control of neutrophil degranulation⁴⁶³. To investigate the role of PI3K signalling in degranulation under hypoxic conditions, 3 different inhibitors were used; LY294002 (10 μM), which is a pan-PI3K inhibitor, AS605240 (3 μM), a selective $\text{PI3K}\gamma$ -isoform inhibitor and

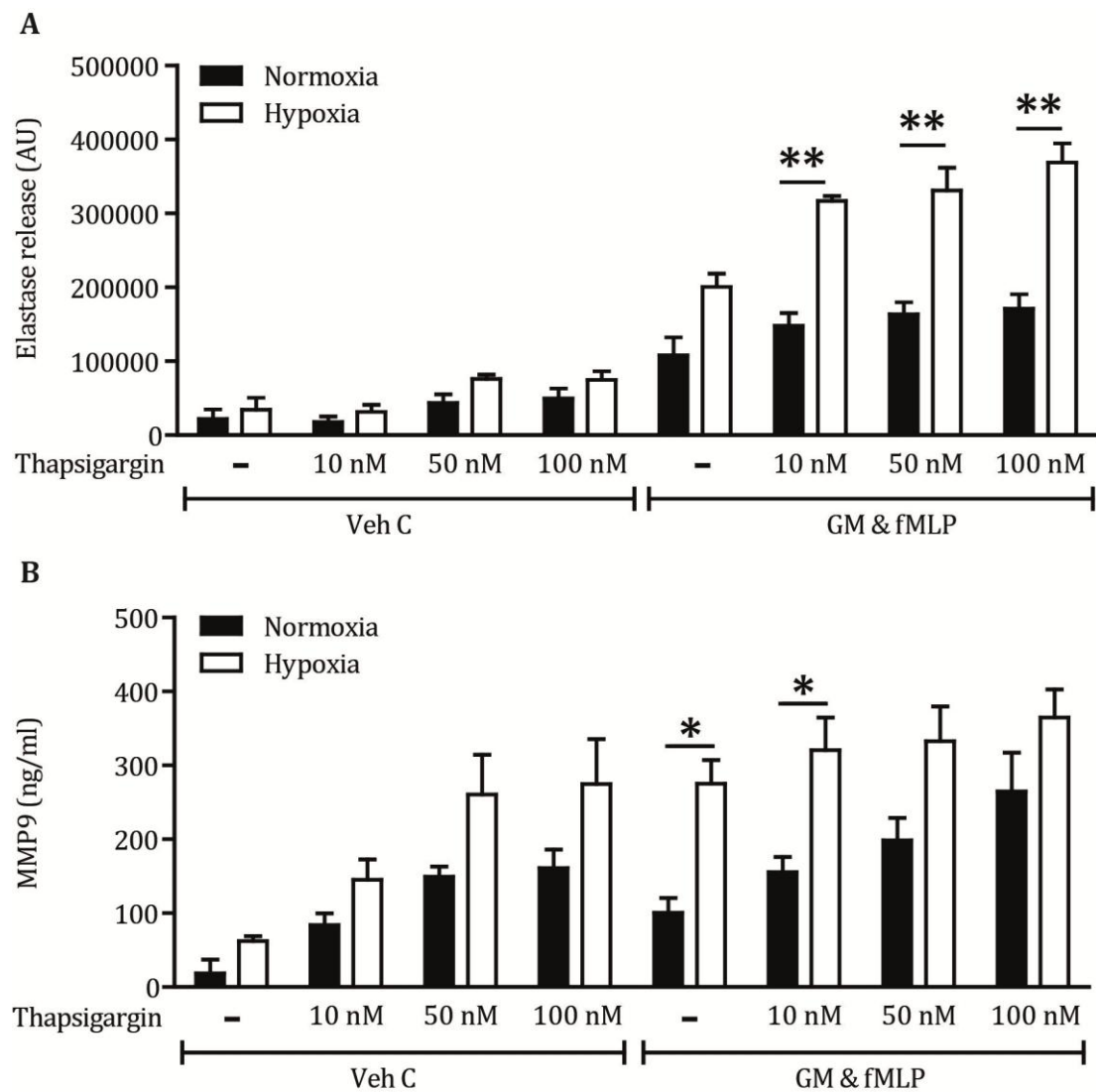


Figure 6.10: Role of calcium release from intracellular stores in the hypoxic augmentation of neutrophil degranulation

Neutrophils were re-suspended in hypoxic (open bars) or normoxic (black bars) IMDM at 11.1×10^6 /ml. The cells were incubated under normoxia or hypoxia (0.8 % O₂ and 5% CO₂) at 37°C for 4 h. The cells were primed with GM-CSF (10 ng/ml) for 30 min. Thapsigargin (10, 50 or 100 nM) was then added before the cells were activated with fMLP (100 nM) for 10 min. Cells were pelleted and the supernatant transferred to fresh tubes before removal from hypoxic hood for further analysis. A. NE activity was measured by the increase in fluorescence caused by the cleavage of DQ-Elastin. Values represent mean \pm SEM, samples were run in triplicate, n=5. B. MMP-9 release was measured by MMP-9 ELISA. Values represent mean \pm SEM, samples were run in triplicate, n=4. * = p<0.05, ** = p<0.01 (Mann-Whitney test).

IC87114 (3 μM), a selective PI3K δ -isoform inhibitor. These PI3K inhibitors are frequently used in our lab and have been shown to be active at the used concentrations^{464,465} for example by inhibiting neutrophil apoptosis and inhibition of AKT phosphorylation. The inhibitors were added either at the start of the 4 h incubation or 10 minutes prior to fMLP; this was to enable me to dissect out the known effects of fMLP (rapid but transient accumulation of PIP₃) from any PI3K-dependent signal that was generated earlier during the hypoxic incubation period. The incubation and stimulation conditions were exactly as described previously, and degranulation was assessed by supernatant NE activity. In the unprimed/unstimulated cells, neither the pan- nor the isoform-selective inhibitors modulated degranulation in a significant fashion, whether the cells were maintained under conditions of normoxia or hypoxia (Figure 6.11). In the setting of normoxic culture, addition of LY294002 just prior to GPCR ligation by fMLP (figure 5.12A) had a significant impact on degranulation: NE release was reduced from 61.3×10^3 AU to 11.9×10^3 AU; the PI3K γ inhibitor has a very similar effect (reduction to 19.6×10^3 AU), whilst the PI3K δ inhibitor had little effect (reduction only to 51.7×10^3 AU). Under hypoxic conditions the same pattern was seen; both LY294002 and AS605240 decreased NE release (from 128.9×10^3 AU to 52.1×10^3 AU with LY294002 and to 52.2×10^3 AU with AS605240). Interestingly, the hypoxic uplift remained approximately the same; 2.3 fold without inhibitors and approximately 2.5 fold with inhibitors. Importantly, when the pan-PI3K inhibitor and the PI3K γ inhibitor were added at the beginning of the normoxic or hypoxic incubation they suppressed NE release to baseline, and completely eliminated the augmented NE release induced by hypoxia (from 87.8×10^3 AU to 3.9×10^3 AU with the pan-PI3K inhibitor and to 3.2×10^3 AU with the PI3K γ inhibitor under normoxic condition and from 193.5×10^3 AU to 9.0×10^3 AU with the pan-PI3K inhibitor and 4.5×10^3 AU with the PI3K γ inhibitor under hypoxic conditions). In contrast, the isoform-selective PI3K δ inhibitor had a less marked effect on degranulation and did not eliminate the hypoxic uplift of NE release (NE release was reduced from 87.8×10^3 AU to 32.5×10^3 AU under normoxic condition and from 193.5×10^3 AU to 108.0×10^3 AU under hypoxic conditions). Together the data presented in this chapter show that the augmented degranulation seen under hypoxic conditions is not HIF- or protein synthesis-dependent. Investigation of key molecules of degranulation signalling pathways indicated a key role for PI3K γ in the enhanced release of NE seen with hypoxic incubation; a probable role was also identified for PLC-dependent Ca²⁺ flux, contributing in particular to the hypoxia-mediated release of MMP-9.

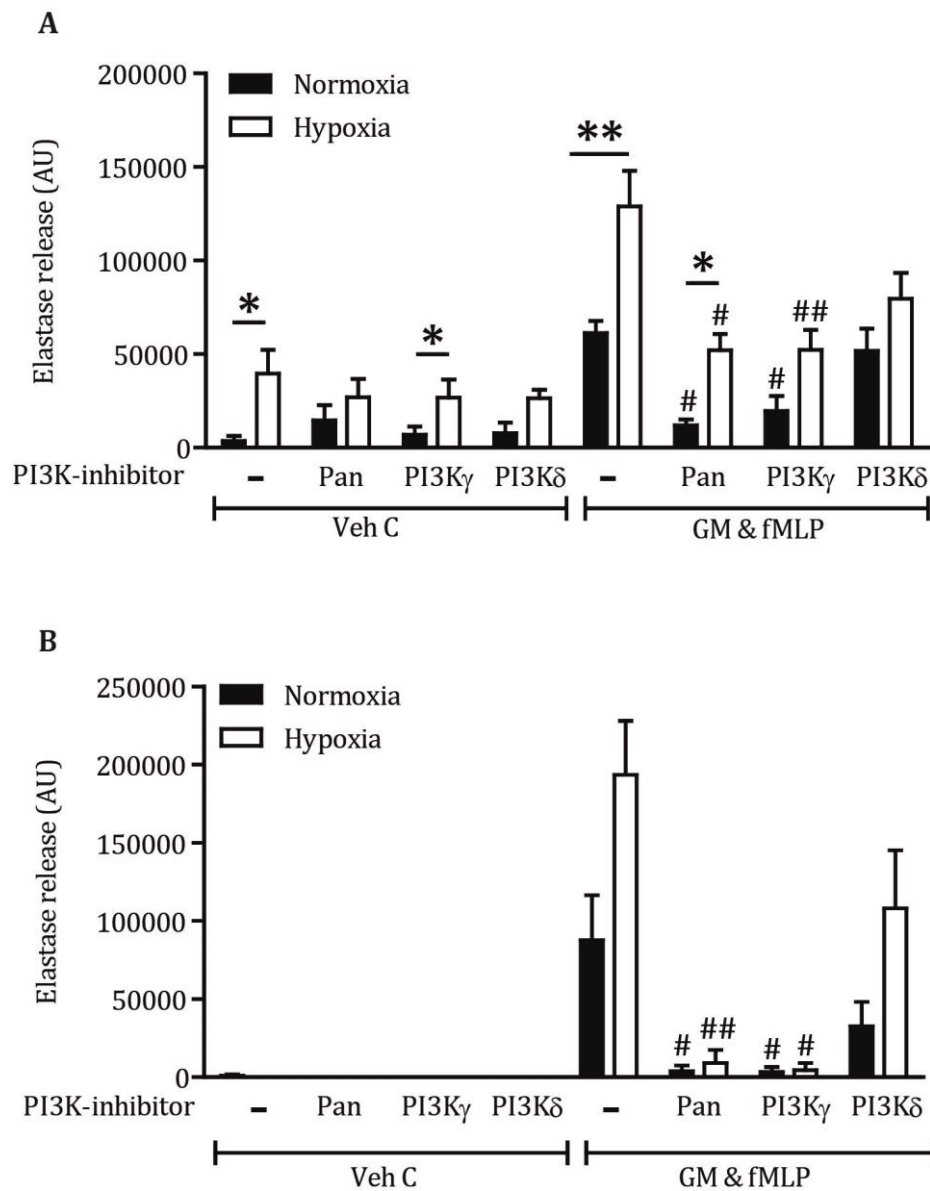


Figure 6.11: Role of PI3K signalling in the hypoxic augmentation of NE release

Neutrophils were re-suspended in hypoxic (open bars) or normoxic (black bars) IMDM at 11.1×10^6 /ml. Inhibitors (pan-PI3K inhibitor Ly294002 10 μ M, PI3K γ inhibitor AS605240, 3 μ M or PI3K δ inhibitor IC87114, 3 μ M) were added just prior to fMLP stimulation (A) or from the outset of the incubation (B). The cells were incubated under normoxia or hypoxia (0.8% O₂ and 5% CO₂) at 37°C for 4 h, then primed (GM-CSF, 10 ng/ml, 30 min) and activated (fMLP, 100 nM, 10 min). Neutrophils were pelleted and the supernatants transferred to fresh tubes before removal from the hypoxic hood. NE activity was measured by the increase in fluorescence caused by the cleavage of DQ-Elastin. Values represent mean \pm SEM, samples were prepared in duplicate, n=3-5. # is the significant decrease in NE release after inhibitor treatment in comparison with the activated normoxic or hypoxic neutrophils. * or # = p < 0.05, ** or ## = p < 0.01 (Mann-Whitney test).

6.3 Discussion

Since neutrophil degranulation products have been implicated in the pathogenesis of many diseases, and hypoxic augmentation of degranulation in the inflammatory environment is biologically plausible, identification of the signalling mechanism by which this effect is established may be of therapeutic relevance. HIF-1 α can modulate protein transcription of a large range of target proteins; there is some evidence that it modulates neutrophil granule protein production, at least during development in the hypoxic environment of the bone marrow.

We therefore hypothesised that hypoxic stabilisation of HIF-1 α induces *de novo* granule protein synthesis, leading to enhanced release of granule proteins on stimulation following such hypoxic exposure. My initial experimental focus was therefore directed to investigate this hypothesis. Consistent with the hypothesis, putative HRE's were identified in the promoter regions of MMP-9, MPO and NE. The timeframe of hypoxic incubation (4 h) is very brief to induce an effect via protein synthesis, but of note, transcription of BNIP was markedly up-regulated (almost 30-fold) at this time point. However, to our surprise, HIF-stabilisation by HIF stabilizers did not lead to increased degranulation. Since it was possible that HIF stabilizers might stabilise HIF-1 α to a lesser extent or with different kinetics to hypoxia, I also quantified the effects of hypoxia on mRNA and protein levels of selected granule proteins. Hypoxia did not increase transcript or protein levels (in fact, neutrophil MMP-9 protein was diminished by hypoxia).

To exclude a role for HIF-1 α in modulating the levels of other relevant signalling proteins, I explored the effect of cycloheximide, and found that this compound did not diminish the hypoxic up-regulation of NE release. Together these data suggest that the effect of hypoxia on degranulation is not mediated by HIF-1 α , at least via its role as a transcription factor. Ideally I would have liked to study the stabilisation of HIF-1 α in neutrophil lysates directly by Western blotting, and compared the effects of true hypoxia with those of the hypoxia-mimetics. However, detection of HIF-1 α in neutrophils is technically challenging and requires large numbers of cells³⁵⁴; attempts to undertake these experiments, even with the assistance of Dr Andrew Cowburn (who works in the laboratory of Professor Randall Johnson, Department of Physiology, University of Cambridge) did not consistently detect HIF-1 α in hypoxic neutrophil lysates. It would be of interest to pursue these experiments in the future, particularly if better detection reagents became available.

The signalling pathways regulating neutrophil degranulation are surprisingly poorly understood, considering the importance of degranulation to innate immunity and to disease pathogenesis. Rather than simply focusing on the pathways previously identified to be relevant in degranulation response, I wished to perform an unbiased screening assay, to ensure I did not miss novel signalling pathways engaged by the combination of hypoxia, priming and stimulation. Since protein phosphorylation events are critical in a range of neutrophil functions, a phospho-kinase array was used as an initial screen for hypoxic targets. However, it is important to note that this methodology has significant limitations. Firstly, although a large number of target proteins can be studied, only a single time-point can be examined for each experimental run; since phosphorylation events are transient, this may limit the sensitivity of detection. Secondly, the reproducibility of the findings was found to be low (Figure 6.7), and the arrays are costly, making it difficult to identify statistically significant results. Thirdly, many proteins are phosphorylated on multiple sites, and studying a single phosphorylation target may not be an ideal readout of activation status. As discussed in more detail below, I did not find significant results using this assay even with targets known to be involved in signalling degranulation, and did not identify pathways subsequently shown to be relevant in the hypoxic up-regulation of degranulation.

Src family kinases are known to play an important role in neutrophil degranulation, especially in integrin-dependent signalling^{231,232}. Src-dependent pathways can activate Rac2 in parallel with PI3-kinase, and hence could impact on cytoskeletal re-arrangements in degranulation⁴⁶⁶; of note, I found that hypoxia induced neutrophil cytoskeletal remodelling (section 4.5.2). Furthermore, Src-pathways and PI3K have been shown to be activated in the context of hypoxia/reperfusion⁴⁶⁷⁻⁴⁶⁹. Unfortunately, I did not find any detectable increase in the phosphorylation of Src-family kinases in response to priming/stimulation with GM-CSF/fMLP, and even CytB/fMLP had only a marginal effect (Figure 6.7A). This suggests that the phospho-kinase array did not adequately interrogate this pathway under the conditions studied; hence the apparent reduction in Src-family kinase phosphorylation seen on stimulation in the context of hypoxia (Figure 6.7A) likely reflects the limitations of this assay alluded to above. A slight increase in AKT phosphorylation was seen in response to treatment with GM-CSF/fMLP, as would be expected; this response appeared to be diminished in the setting of hypoxia (figure 5.7B). However, in the light of the finding that activation of the PI3K pathway seems to be highly relevant to the hypoxic augmentation of NE release (section 6.2.5), this finding of

reduced AKT phosphorylation does not seem biologically plausible, and again suggests that the phospho-kinase assay is not sufficiently sensitive to pick up known or unknown relevant pathways under the selected experimental conditions. This assay was hence not pursued any further.

There has been no previous published study specifically exploring the effects of hypoxia on neutrophil degranulation, although some data sets have been published in other contexts that suggest hypoxia can modulate signalling pathways that regulate degranulation in other cell types. In certain settings, hypoxia has been shown to activate p42/44 MAPK (e.g in PC12 cells³⁵⁸), p38MAPK (human neutrophils³⁵⁶) and also PI3K (in mouse microglial cells⁴⁷⁰) and in ras-transformed NIH3T3 cells⁴⁷¹, PKC and Src family kinases (in rat cardiac myocytes³⁵⁹). A key finding reported in this chapter is that inhibition of PI3K, and specifically of PI3K γ , could prevent degranulation under both normoxic and hypoxic conditions. It is important to note that the full effect of PI3K inhibition on the hypoxic up-regulation of degranulation occurred only when the inhibitors were present from the outset of the hypoxic incubation, and not when they were added prior to the addition of fMLP. This suggests that their effect on degranulation is not simply due to the inhibition of the established fMLP-induced activation of PI3K γ and PI3K δ isoforms⁴⁶¹, but instead implies that a PI3K-dependent signal is entrained prior to the addition of fMLP during the preceding hypoxic incubation period. At present the nature and timing of this signal are unclear and future studies will focus on delineating these responses in more detail. It would also be of considerable interest to explore the mechanism by which hypoxia modulates PI3K activation.

The literature detailing the effects of hypoxia on PI3K activation is surprisingly limited, and is mainly derived from cancer cell lines such as HeLa cells. Alvarez-Tejado et al.^{472,473} found activation of the PI3-kinase/Akt signalling pathway after 4 h of hypoxic incubation in rat pheochromocytoma PC12 cells, which could be prevented by cycloheximide or actinomycin D, suggesting *de novo* protein synthesis was required to mediate this effect. A later paper by the same group showed that activation of PI3-kinase/Akt was downstream of HIF-1 α . Clearly, this does not align with my findings in neutrophils. Perhaps more in keeping with my results, Mottet et al.⁴⁷⁴ saw a biphasic response to hypoxia in HepG2 cells with an initial PI3K dependent HIF-1 α stabilisation at 5 h; by 16 h hypoxic exposure PI3K activation was no longer detectable and GSK3 β activation led to depletion of HIF. Kilic-Eren et al.⁴⁷⁵ also found that PI3K acted upstream of HIF-1 α , since LY294002 reduced the detection and DNA binding activity of this

transcription factor. Finally, Kim et al.⁴⁶⁹ showed that hypoxia and CoCl_2 induced IL-8 mRNA and protein expression via activation of the PI3K/Akt and p38 MAPK signalling pathways. Since my data suggest that the hypoxic up-regulation is independent of HIF-mediated transcriptional activity, these published studies do not shed a light on the mechanism of this effect and further underscore the need for future studies.

Similarly, a limited amount of data exists to support a role for hypoxia in modulating PLC activity, IP_3 accumulation and intracellular calcium concentrations. Yadav et al.⁴⁷⁶ reported that acute hypoxia significantly enhanced PLC activity in mouse pulmonary arteries smooth muscle cells (PASMCs), by increasing mitochondrial complex III Rieske iron-sulfur protein (RISP)-dependent mitochondrial ROS production in complex III. The resultant IP_3 production and Ca^{2+} release were found to play an important role in hypoxic contractile responses in PASMCs. As for PI3K signalling, inhibition of PLC from the outset of the hypoxic incubation period had a greater suppressive effect than addition of the inhibitors prior to stimulation with fMLP. Given the fact that both PLC and PI3K signalling seem to be up-regulated by hypoxia in this context, it would be of considerable interest to measure the effects of hypoxia on membrane phospholipid content, and in particular on the levels of PIP_2 , which is the substrate for both of these enzymes.

It would also be of interest to explore whether the formation of DAG and the activation of PKC isoforms was modified in the setting of hypoxia. A further line of enquiry is to explore the downstream effectors of PI3K/PLC signalling and how they interface with the degranulation machinery. Downstream effectors of PI3K include a range of kinases like Akt, but also adaptor proteins and regulators of small GTPases including Rac and Rho. Recently, Shuang Ma et al.³⁷⁸ found that hypoxia increased cell polarisation in response to fMLP in HL-60 cells (a neutrophil like cell line), which concurs with my data (section 4.5.2, Figure 4.9) that hypoxia induces the formation of an F-actin leading edge. It could be speculated that hypoxia modulates degranulation via a PI3-kinase/PLC-dependent effect on small GTPases to modulate F-actin distribution, or the fusion and docking stage of degranulation (discussed in more detail in section 1.6.5). The GTPase Rac plays an important role in F-actin polarisation^{261,477} and the release of azurophil granules^{83,264}. Furthermore, research by Dooley et al.⁴⁷⁸ indicated an additional role for Rac2 in the release of MMP-2/-9 from macrophages and neutrophils.

Other Rho-family GTPases may also be involved in aspects of neutrophil degranulation, since different granule populations have partially distinctive regulatory pathways. Rac1 and Rac2 have been shown to play distinct role in antigen stimulated mast cell exocytosis;

Rac1-mediates membrane ruffling and Rac2-mediates calcium influx in this setting²⁶⁵. Additionally, Rab family GTPases have been implicated in vesicle transport and docking^{277,278}, Rab3, Rab4 and Rab5 co-localise with neutrophil granules²⁸⁰. Hypoxia has been shown to modulate a range of Rab family GTPases, it can activate Rab11⁴⁷⁹, increase Rab20 expression⁴⁸⁰ and increases Rab4 dependent trafficking in cancer cells⁴⁸¹. This makes hypoxic modulation of degranulation through Rab GTPases a possibility. Thus although I have identified a role for PI3K and PLC in mediating the hypoxic uplift of neutrophil degranulation, several important questions remain. Firstly, how might hypoxias affect these signalling molecules, and is this a cell-specific or a more ubiquitous phenomenon? Secondly, what are the kinetics of this response? Thirdly, what are the downstream effectors and how do they interface with the degranulation machinery in the neutrophil? Exploring these questions will form the basis of a further exciting research project.

Chapter 7

Discussion

7. Discussion

7.1 Overview

Neutrophils are the ‘rapid response’ frontline troops of the innate immune system. Circulating neutrophils sense tissue injury and/or invading microbial pathogens by means of membrane receptors that recognise products of tissue injury, chemoattractants, and microbial compounds, which ‘flag’ the affected tissue or organ as requiring their attention. Neutrophils arrive early (within minutes) during acute inflammatory responses, and represent the most abundant immune cells in the inflamed tissues for many hours. In their capacity as first responders, the primary role of these professional phagocytes is to kill invading pathogens. To kill ingested microbes they can deploy the phagocyte NADPH oxidase and an array of proteolytic enzymes and antimicrobial peptides contained in membrane-encapsulated granules; the products of both systems are discharged into the phagosome³⁶. This potent anti-microbial armamentarium is what makes the neutrophil an effective frontline defensive cell. Paradoxically, these same antimicrobial responses can, under pathological circumstances, lead to considerable host tissue injury in a form of unintended “collateral damage”. In such circumstances, neutrophil-derived antimicrobial compounds may be released into the extracellular space in excess quantities, resulting in inflammatory tissue injury. Although neutrophils can emigrate from the vasculature without causing injury, there is abundant evidence *in vitro* and *in vivo* experimental models that an intense influx of neutrophils may incite pathological inflammation in a range of organs and may contribute to the pathogenesis of conditions such as acute lung injury¹⁴⁹, inflammatory bowel disease⁴⁸², nephritis¹¹⁷, arthritis⁵⁶, ischemia-reperfusion injury⁹³, myocardial infarction⁴⁸³, and stroke⁴⁸³.

To understand this transition toward a maladaptive inflammatory state, it is essential to consider the physiological properties of the environment in which the recruited neutrophils must operate, and to recapitulate those conditions when studying neutrophil function in the laboratory. As previously discussed, inflammatory sites are often profoundly hypoxic, yet most studies of neutrophil function are undertaken in ambient oxygen tensions that do not reflect the pathological setting in which these cells routinely operate. Tissue damage is a feature of infection and although it can be beneficial on a small scale, larger scale damage is detrimental and contributes to the pathogenesis of a wide range of inflammatory diseases. Neutrophil proteases can cleave almost any extracellular matrix component and have been closely linked to tissue damage in, for

example, COPD. The effect of hypoxia on neutrophil function is highly relevant to this disease, as the neutrophil the most abundant inflammatory cell present in the bronchial wall and lumen of patients with COPD^{63,64,416,484}, the COPD lung is a hypoxic environment^{485,486}, and HIF-1 α immunostaining has been detected specifically in COPD airways. Whilst HIF-1 α can be stabilized by inflammatory stimuli as well as hypoxia, our laboratory has recently found direct evidence that the inflamed airways are hypoxic by means of demonstrating HypoxyprobeTM staining in the IL-13 transgenic mouse, which displays spontaneous airway inflammation (Dr Andrew Cowburn, personal communication).

It is known that hypoxia can influence neutrophil function profoundly, with delayed neutrophil apoptosis and reduced killing of pathogenic bacteria such as *Staphylococcus aureus*^{327,379}. My results confirm and extend these observations, and suggest that the phenotype of a neutrophil in a hypoxic environment may be highly destructive, with not only impaired capacity to kill pathogens but also enhanced potential to damage the surrounding tissues.

7.2 Experimental challenges

Inconsistency of data between different studies of neutrophil function has arisen in some cases from the different isolation methods used. Neutrophil priming can alter neutrophil function and has been shown to be a consequence of exposure to temperature changes and certain chemicals used during the isolation process^{487,488}. The PercollTM-gradient method used to generate the results reported in this thesis is very gentle and induces minimal priming⁴⁸⁷, as exemplified by near-undetectable levels of basal shape-change and of fMLP-induced superoxide release. Any neutrophil preparation that yielded basally primed cells was discarded. All of my experiments were performed on primary human neutrophils freshly isolated from the peripheral blood of healthy, un-medicated human volunteers. I used a short hypoxic exposure (4 h) as these cells are terminally differentiated and have a short life span; importantly, hypoxia dramatically increases neutrophil longevity, and the survival curves for normoxic and hypoxic neutrophils start to diverge after 6 h³⁷⁷, hence the selection of a 4h incubation period rather than a longer hypoxic exposure.

Hypoxia alters neutrophil function, but re-oxygenation also has profound effects⁴⁸⁹⁻⁴⁹¹. Some groups may have investigated the effect of hypoxia on neutrophil function after

inadvertent re-oxygenation or have simply taken cells out of hypoxic chambers to undertake functional assays, which can profoundly affect the results obtained. Therefore the oxygen levels in the hypoxic hood were carefully monitored, and the oxygen tension of tissue culture medium was also monitored using a blood gas analyser. Great care was taken to avoid re-oxygenation during the experiments performed; any reactions were fully stopped, prior to removal of samples and all experiments were performed under normoxic conditions outside of the hood in parallel. The InVivo₄₀₀ hypoxic hood used throughout the thesis was over 5 years old at the beginning of my studies, and unfortunately developed faults on several occasions, which were detected by the means described above; again, all such experiments were discarded.

To determine the capacity of hypoxic neutrophils to induce tissue injury I studied the effect of neutrophil supernatants on cultured respiratory epithelia. Although I initially used A549 cells, I was concerned that this lung cancer-derived cell line would not necessarily reflect the characteristics of true bronchial epithelial cells. I extended my observations using iHBEC cells, and the results I obtained with these cells were reassuringly very similar. My experiments with primary HBECs were limited by the difficulty and expense of growing these cells to a ciliated morphology in ALI culture systems, but the data I obtained by microscopy studies and LDH release supported an increased toxicity secondary to exposure to hypoxic neutrophil supernatants. I geared these experiments to gather data on the impact on ciliary function, but unfortunately, all of the supernatants used (including those from unstimulated neutrophils) had a profound impact on CBF and ciliary co-ordination. It is possible that some component of the neutrophil medium (DMEM) was toxic to the ciliated cells, but this was felt to be unlikely by Dr Rob Hirst (University of Leicester, personal communication); there is very little protein in control medium (1, lane A). It seems more likely that ciliary function is more sensitive to disturbance than the other indicators of damage I have studied (loss of membrane integrity, activation of caspase 3, cell death and detachment) and that future studies should use more diluted supernatants.

7.3 Discussion of results

In the work presented in this thesis I have shown that hypoxia markedly increases the liberation of (active) neutrophil granule proteins including elastase and MPO from the azurophilic granules, lactoferrin from the specific granules and MMP-9 from the

gelatinase granules. These are exemplar granule contents and the liberation of the whole spectrum of granule proteins will, by implication, also be released in parallel.

Intriguingly, in collaboration with Dr Wei Li, a structural biologist working in the Department of Medicine, I have also shown that certain cytoplasmic proteins (including the S100 family) are liberated in particular from hypoxic primed and stimulated neutrophils (Figure 7.1). Since these cells treated in this fashion show a marked increase in longevity the release of cytoplasmic proteins does not reflect impaired membrane integrity, and the mechanism and consequences of this phenomenon are currently unclear but warrant further investigation.

In keeping with my finding that hypoxic neutrophil supernatants contain increased active degranulation products, these supernatants caused substantially more damage to lung epithelial cell layers than did supernatants from neutrophils cultured under normoxic conditions; this damage was protein- and protease-dependent. Preliminary inhibitor studies suggest that the damage to epithelial cells was not secondary to a single protease or protein but reflected a combinatorial effect of the ‘toxic soup’ of released products. Again of interest, preliminary data obtained in collaboration with Dr Wei Li has suggested that hypoxic but not normoxic neutrophil supernatants can cleave the endogenous circulating vascular protective factor BMP-9, and that this effect is mediated specifically by NE (Figure 7.2). Thus while certain aspects of tissue injury may reflect the action of multiple neutrophil products and hence necessitate inhibition of degranulation to suppress the resulting damage, other damaging consequences of enhanced degranulation may be more amenable to specific inhibitors such as those for NE. This may have relevance to the endothelial dysfunction (both pulmonary and systemic) associated with COPD, and this observation is the basis for an MRC Research Training Fellowship awarded to Dr Katharine Lodge.

I have shown that the increased granule protease release by neutrophils under hypoxic conditions can damage to lung epithelial cells in a tissue culture setting, even when the supernatants are diluted. Whilst it is difficult to equate the addition of neutrophil supernatants to the *in vivo* pathological setting, the fact that neutrophil products have been shown to contribute to injury in disease makes this hypoxic uplift a biologically plausible mechanism for promoting such damage. I have progressed my findings from submerged cultures of a cancer-cell line to ALI cultures of primary HBECS, with similar results. In the future it would be of value to explore the effects of direct neutrophil-epithelial

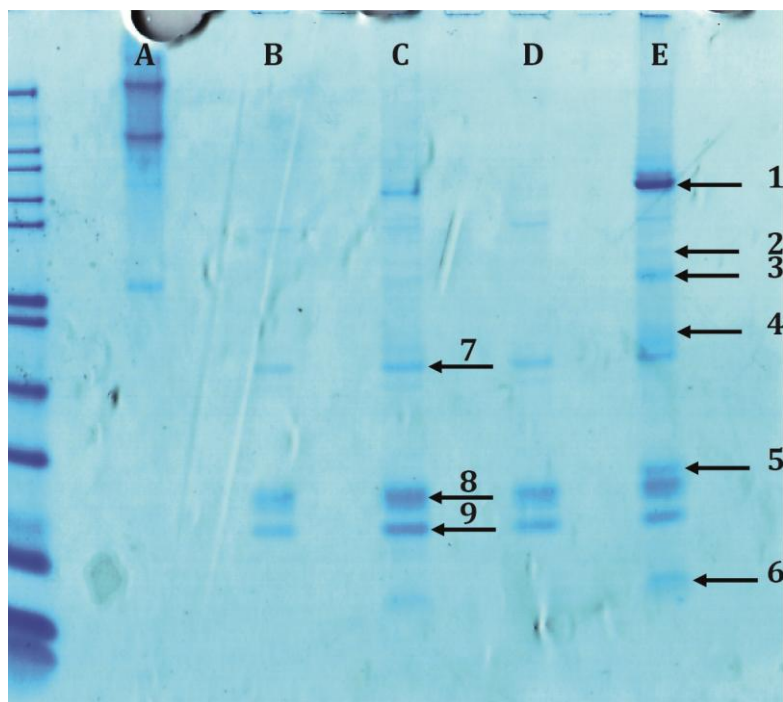


Figure 7.1: Supernatants from normoxic and hypoxic neutrophils contain cytoplasmic proteins

Neutrophil supernatants were run on a polyacrylamide gel, stained with Coomassie stain, and bands identified by mass spectrometry by Dr Wei Li. Lanes: A. Control medium (no neutrophils) B. Normoxic unstimulated neutrophils C. Hypoxic unstimulated neutrophils. 3. Normoxic neutrophils stimulated with GMCSF/fMLP. 4. Hypoxic neutrophils stimulated with GMCSF/fMLP. Proteins: 1. Lactoferrin 2. Neutrophil lipocalin 3. Myeloperoxidase 4. Chain A, Human Cathepsin G 5. Lysozyme 6. Keratin 7. Calprotectin 8. Protein S100-A9. 9. Protein S100-A8.

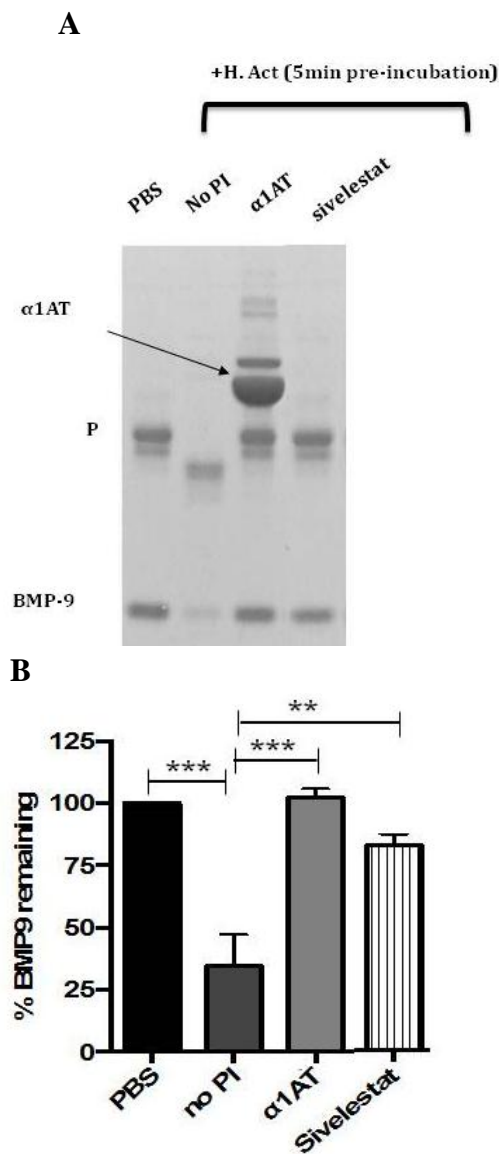


Figure 7.2: BMP-9 is cleaved following exposure to hypoxic neutrophil supernatants BMP-9 was incubated with PBS or supernatants activated under hypoxic conditions in the absence or presence of protease inhibitors. Exposure to hypoxic supernatants induced cleavage of recombinant BMP-9 that was inhibited by α ₁AT or the elastase inhibitor sivelestat. A. Representative example (of n=3) SDS-PAGE. Lanes: PBS only (no supernatant); hypoxic activated supernatants in the presence of no protease inhibitor (no PI), α ₁AT and sivelestat. B. Quantification of n=3 experiments using ImageJ. SDS-PAGE was undertaken by Dr Wei Li.

interactions under conditions of hypoxia, to establish the number of neutrophils and the degree of hypoxia required to lead to significant cellular injury and death.

Surprisingly, the mechanism of hypoxia-augmented degranulation was found to be independent of the transcription factor HIF-1 α (the ‘master-regulator’ of hypoxic responses); thus, hypoxia did not increase mRNA transcript or protein abundance of the major granule components, and HIF stabilizers/hypoxia mimetics failed to recapitulate the degranulation phenotype. If HIF signalling does not underpin the enhanced secretory phenotype demonstrated by hypoxic neutrophils, what might be the alternative mechanisms? It is possible that hypoxia somehow works as a priming agent, amplifying signals or increasing the cells sensitivity to priming agents. The classical manifestation of neutrophil priming (enhanced ROS generation) cannot be seen using my experimental conditions; indeed the oxidative burst is suppressed due to the lack of substrate (molecular oxygen). Priming is known to augment degranulation²²⁷, however the effect of hypoxia is additive with that of GM-CSF at full priming doses, suggesting an alternative mechanism may be operative. Although I see alterations in the neutrophil cytoskeleton under hypoxic conditions (see below), previous work in our laboratory has not identified a major change in the cell surface markers CD11b and CD62L, nor an enhancement in IL-8 secretion³²⁷, both features that would be expected in the setting of neutrophil priming. These features suggest that hypoxia does not simply ‘prime’ neutrophils in the conventional manner of cytokine priming.

Since I demonstrated a global hyper-secretory effect rather than an effect on individual proteins, I then examined the signalling pathways regulating neutrophil degranulation. An unbiased phospho-kinase screen did not reveal any novel targets, but for the reasons discussed (section 6.3) this methodology was not felt to be optimal, and it would be pertinent to pursue the effects of hypoxia on neutrophils using newly emerging techniques such as RNAseq or more extended phospho-proteomics studies. Since such studies were outside the remit of my PhD thesis, I instead focussed on the effects of hypoxia on signalling pathways already known to regulate neutrophil secretory function. Since inhibition of either PI3K or PLC is known to limit degranulation responses^{224,225,229}, I needed to demonstrate that the inhibitors had an additional effect that was specific to the hypoxic up-regulation rather than simply preventing all fMLP-mediated stimulation; I did this by comparing the impact of inhibitor addition at the beginning of the hypoxic incubation with that of delayed addition of inhibitors immediately prior to stimulation

with fMLP. Delayed inhibitor addition reduced degranulation under normoxia and hypoxia equally, such that the fold up-regulation of NE release entrained by hypoxia was preserved; however this uplift was largely abolished when the inhibitors were added prior to the hypoxic incubation. This implies that hypoxia activates PI3K/PLC signalling pathways and that the signals so generated mediate the subsequent augmented release of neutrophil granule contents stimulated by further priming/activation events. The mechanism by which hypoxia might influence PI3K/PLC signalling is unknown at present; the fact that cycloheximide is without impact suggests that increased enzyme/lipid kinase levels are unlikely to be responsible, although it is possible that hypoxia could stabilise these proteins independent of protein synthesis. Another possibility is that hypoxia might alter the lipid content of plasma membranes and increase the availability or accessibility of PIP₂, the substrate of both PLC and PI3K.

Although the inhibition of PLC markedly attenuated degranulation under both normoxic and hypoxic conditions, manipulation of calcium signalling did not precisely recapitulate the impact of PLC inhibition on NE release, suggesting that other downstream effectors such as PKC activation may be relevant. Manipulation of calcium flux had a greater impact on MMP-9 release, in keeping with the known calcium-sensitivity of this response. Since PI3K activation leads to the downstream activation of a large range of signalling molecules via PIP₃ it is possible that hypoxia modulates multiple degranulation pathways in parallel to Ca²⁺ signalling.

Hypoxia has been shown to affect the actin cytoskeleton and induce shape change in neuronal cells⁴²³ and proximal renal tubular cells⁴²⁴ in culture. In our laboratory, Dr Linsey Porter has demonstrated that hypoxia induced more shape-change in fMLP activated neutrophils (Dr Linsey Porter, personal communication) and I have shown a clear effect of hypoxia on the distribution of polymerised F-actin to cap-like structures. Since cytoskeletal re-arrangements have been linked to degranulation^{276,425} this observation may provide a mechanistic insight into the hypoxic up-regulation of neutrophil degranulation. Downstream signalling molecules that play a role in cytoskeletal re-organisation include the small GTPases Rac and Rho, and importantly Rac2 has been shown to play a role in the release of azurophil granules^{83,264,478}. Furthermore, Rac2 has been shown to be a downstream effector of PI3K in human neutrophils^{492,493}, and Rac1-dependent cytoskeletal re-organisation has been reported to occur in hypoxic endothelial cells⁴⁹⁴; thus activation of Rac could plausibly link the

hypoxic regulation of PI3K activity with actin re-distribution and degranulation. To pursue this possible link, I undertook some preliminary experiments to study the activation of Rac in the setting of hypoxia using a G-LISA method. These experiments were technically challenging, in part because peak activation of Rac in fMLP-stimulated neutrophils occurs at only 10s⁴⁹⁵; however, the G-LISA methodology was not sufficiently sensitive to detect Rac activation in fMLP-stimulated neutrophils even at this early time point. The alternative methodology to detect Rac activation is a complex ‘pull-down’ assay that was not felt to be achievable within the confines of the hypoxic hood without considerable work to adapt the method to this environment. Additionally, Rab family GTPases have been implicated in vesicle transport and docking^{277,278}, Rab3, Rab4 and Rab5 co-localise with neutrophil granules²⁸⁰ and hypoxia has been shown to modulate a range of Rab family GTPases⁴⁷⁹⁻⁴⁸¹. Hence exploring Rab localisation during normoxic and hypoxic incubation by immunofluorescence analysis, with co-staining of the relevant granule populations, would also be of interest in future studies.

What might be the translational potential of this work? New light on the destructive potential of the neutrophil at inflammatory sites may inform therapeutic strategies in neutrophil-mediated disease. My work suggests that either anti-protease strategies or perhaps inhibitors of PI3K γ may be worth exploring in diseases where neutrophilic inflammation occurs in a hypoxic environment. An example of the application of anti-protease therapy can already be found in a small subset of patients with COPD. Current therapy for ‘usual’ smoking-related COPD is largely symptomatic⁴⁹⁶, with only long term oxygen therapy shown to increase life expectancy⁴⁹⁷. In contrast, in the setting of COPD associate with deficiency of the protease inhibitor α 1AT, augmentation therapy with α 1AT has been shown to both ameliorate lung function decline^{498,499} and reduce the frequency and severity of pulmonary exacerbations^{500,501}. However, this treatment requires weekly intravenous infusions of human plasma-derived α 1AT, is licensed only for the small proportion (~2%) of patients who have α 1AT deficiency, and is not available in all countries. Whilst α 1AT augmentation therapy in usual COPD (without α 1AT deficiency) inhibits NE and prevents elastin degradation⁵⁰² both systemically and in the lung, early (short duration) trials of AZD9668, an orally available NE inhibitor, had no impact on respiratory symptomatology or lung function in patients with COPD^{503,504}. Sivelestat, another neutrophil inhibitor, has been used in clinical situations, the benefits of such interventions have been somewhat disappointing; sivelestat did have a beneficial

effect on the pulmonary function of ARDS patients with systemic inflammatory response syndrome (SIRS)⁵⁰⁵ but was not associated with decreased mortality¹³⁷. These latter studies are wholly in keeping with my observations that hypoxic neutrophils release a broader range of granule proteases aside from NE. These trials, together with my experimental results, underscore the potential utility of combating/preventing the release of the whole spectrum of neutrophil-derived proteases, and emphasise the need for orally active or inhaled compounds that can prevent local neutrophil degranulation.

My finding that PI3K γ is instrumental in signalling the hypoxic uplift of degranulation is particularly exciting, since small molecule inhibitors of this lipid kinase (and of PI3K γ) are entering the clinical domain. Inhibition of the signalling event that results in degranulation is an attractive prospect as it would prevent the release of all granule contents rather than just neutralise a subset of proteases. Studies using PI3K γ knockout mice have suggested that inhibition of this isoform may be advantageous in a range of inflammatory conditions including acute pancreatitis⁵⁰⁶, acute lung injury⁵⁰⁷, inflammatory bowel disease⁵⁰⁸ and ischaemia-reperfusion injury^{509,510}. However, any advantage would need to be weighed against the risk of impaired innate immune function, as PI3K γ is important in mediating neutrophil recruitment and the oxidative burst^{461,269}, particularly in the setting of treatment for a chronic disease. In respiratory diseases such as COPD, topical application of such medications might ameliorate such potential risks.

7.4 Future research avenues

I have shown that hypoxia induces a destructive neutrophil phenotype, with increased release of multiple histotoxic proteases. This may contribute to tissue injury and disease pathogenesis in a range of clinically important conditions. Hypoxia induces a global hyper-secretory state; hence targeting individual proteases such as NE alone is unlikely to be sufficient when hypoxia and inflammation co-exist. It therefore seems relevant to further characterise the extent of this phenomenon and to uncover more about the mechanisms leading to the establishment of the destructive neutrophil phenotype engendered by hypoxia, in the hope that such information might identify additional pathways/mechanisms as targets.

7.4.1 Elucidating the mechanism of augmented degranulation under hypoxia

To target the capacity of hypoxia to up-regulate agonist-stimulated neutrophil degranulation in a therapeutic setting, we need to identify the biochemical signals(s) and mechanisms that underpin it. I would like to extend our observations to encompass a broader range of oxygen tensions/agonists, quantitate the phosphorylation of AKT under conditions of hypoxic stimulation, explore the role of the PIP₃ and other signalling molecules downstream of PI3K activation, and perform an unbiased screen of the neutrophil transcriptome and lipidome under conditions of normoxia and hypoxia, with the aim of identifying novel effectors and potential therapeutic targets. I would also wish to explore the capacity of hypoxia to modulate degranulation neutrophils obtained from PI3K γ , PI3K δ and PLC knockout mice. Clearly, this work is not within the remit of my thesis and will be further explored by other laboratory members in future projects.

To put the increased degranulation under hypoxic condition into a broader, physiological window, it would be valuable to study the effects of a wider set of mediators relevant to COPD and other inflammatory diseases. For the experiments in this thesis the neutrophil were primed/activated with GM-CSF and fMLP; it would be of value to extend the observations by studying the effects of inflammatory cytokines and chemokines such as LPS, TNF, IL-1 β , leukotriene B₄, IL-6 and IL-8 on neutrophil degranulation in the context of hypoxic incubation. It would also be relevant to explore the effect of lesser (and greater) degrees of hypoxia, and in particular such levels as may be present in the systemic setting of lung diseases such as COPD.

To reach the plasma membrane or the membrane of the phagolysosome, a granule must negotiate the sub-cortical actin filament network; Cytochalasin B inhibits actin polymerisation and the formation of actin filament networks, and is a potent stimulus for neutrophil degranulation. Hypoxia augments neutrophil shape change and induces dramatic redistribution of the sub-cortical actin network to a focal 'cap' (Figure 4.9), which I predict will allow unrestricted granule mobilisation to the 'non-capped' areas of the neutrophil surface. In view of these results, it would be useful to study whether hypoxia alters granule distribution in "resting" and activated cells. Mitchell et al. (2008) have already shown the formation of an actin cap and granule re-distribution in neutrophil activated with fMLP, and I anticipate that hypoxia will augment this effect.

Additionally, elucidating the role of agents that modulate cytoskeletal function including the small GTPase families Rac, CDC42, and Rho in the augmented degranulation under

hypoxia would be informative. The final step of exocytosis involves the mutual recognition of secretory granules and target membranes, which is postulated to involve a set of intracellular receptors that guide the docking and fusion of granules. SNAP-SNARE proteins, which play a role in the docking and fusion stage of degranulation, are candidates for hypoxic modulation. Syntaxin 4, SNAP-23, VAMP-1, VAMP-2 and VAMP-7⁸⁴ have all been shown to associate with granules and hypoxia has been shown to modulate SNAP/SNARE function^{511,512}.

7.4.2 The effects of hypoxia on neutrophil function in an epithelial cell system

The impaired ciliary function induced by neutrophil supernatants warrants further research. Primary ciliated epithelial cells are expensive and are challenging to culture. The Condliffe/Chilvers laboratory has recently obtained iHBEC's, and these can ciliate when grown at air-liquid interface; this may provide a more accessible alternative system to take these observations forwards; alternative sources of material include mouse tracheal cells and even human nasal scrapings or bronchial biopsies. The experiments undertaken in this thesis were performed on ALI-cultures scraped off the Transwell[®] to enable us to use multiple conditions per well. Looking at intact ALI-cultures would provide us with a way to analyse ciliary function without the added stress of disrupting the cell layers or the time spend on the chamber-slide. Additionally it would be beneficial to look at neutrophil function under hypoxia in a more complex system, perhaps with intact neutrophils rather than supernatants. This would allow us look at the interplay between the epithelial cell layers and neutrophils. As hypoxia has been shown to induce an inflammatory phenotype in endothelial cells it is possible that neutrophil-epithelial cell interactions induces a more activated neutrophil phenotype and augment degranulation, and that augmented secretion from damaged epithelial cells might signal further neutrophil recruitment.

7.4.3 Translational studies

It would be very valuable to determine the relevance of the *in vitro* data presented in this thesis to the effects of systemic and tissue hypoxia on neutrophil function *in vivo*. The Condliffe/Chilvers laboratory has demonstrated previously that peripheral blood neutrophils obtained from patients experiencing an acute exacerbation of COPD display delayed apoptosis relative to healthy controls, and that this phenomenon is transient and

normalizes on recovery⁴⁶⁴, consistent with a previous report that COPD neutrophils isolated during exacerbation are basally primed and display abnormal chemotactic responses⁵¹³. Furthermore, we have obtained preliminary data that the supernatants from hypoxic neutrophils cleave the vascular quiescence factor bone morphogenetic protein-9 (BMP-9) in a NE-dependent fashion, which resonates with the known increase in circulating NE activity during COPD exacerbations⁵¹⁴ and the endothelial dysfunction observed in stable COPD⁵¹⁵.

We hope to further explore the role of BMP-9 cleavage in the endothelial dysfunction in both the pulmonary and systemic circulation in patients with COPD by a number of approaches:

1. By correlating circulating NE levels, BMP-9 levels, and estimated pulmonary artery pressures in patients with stable and exacerbating COPD.
2. By challenging healthy volunteers with nebulised LPS (to mimic a COPD exacerbation) with or without co-incident hypoxia (achieved by reducing inspired O₂ levels).
3. By hypoxic challenge of COPD patients.

The effects of such challenges on circulating and lung neutrophil degranulation could be measured in addition to the effects on circulating NE and BMP in both healthy volunteers and COPD patients.

7.5 Final summary and conclusions

To develop new therapies for the treatment of persistent infection and prolonged inflammation a better understanding of how neutrophils function in physiologically relevant oxygen levels is required. In this thesis I have extended our knowledge of neutrophil function under hypoxic conditions and shown that hypoxia profoundly augments the release of (active) granule proteins from all granule populations. My results suggest that the phenotype of a neutrophil in a hypoxic environment may be highly destructive, with not only impaired capacity to kill pathogens³²⁷ but also enhanced potential to damage the surrounding tissues. I have demonstrated that hypoxic neutrophil supernatants have the capacity to damage respiratory epithelial cells reflecting the effects of not just one but of multiple proteases. In a disease setting such as COPD (Figure 7.3) I propose that cigarette smoke and pathogens can induce

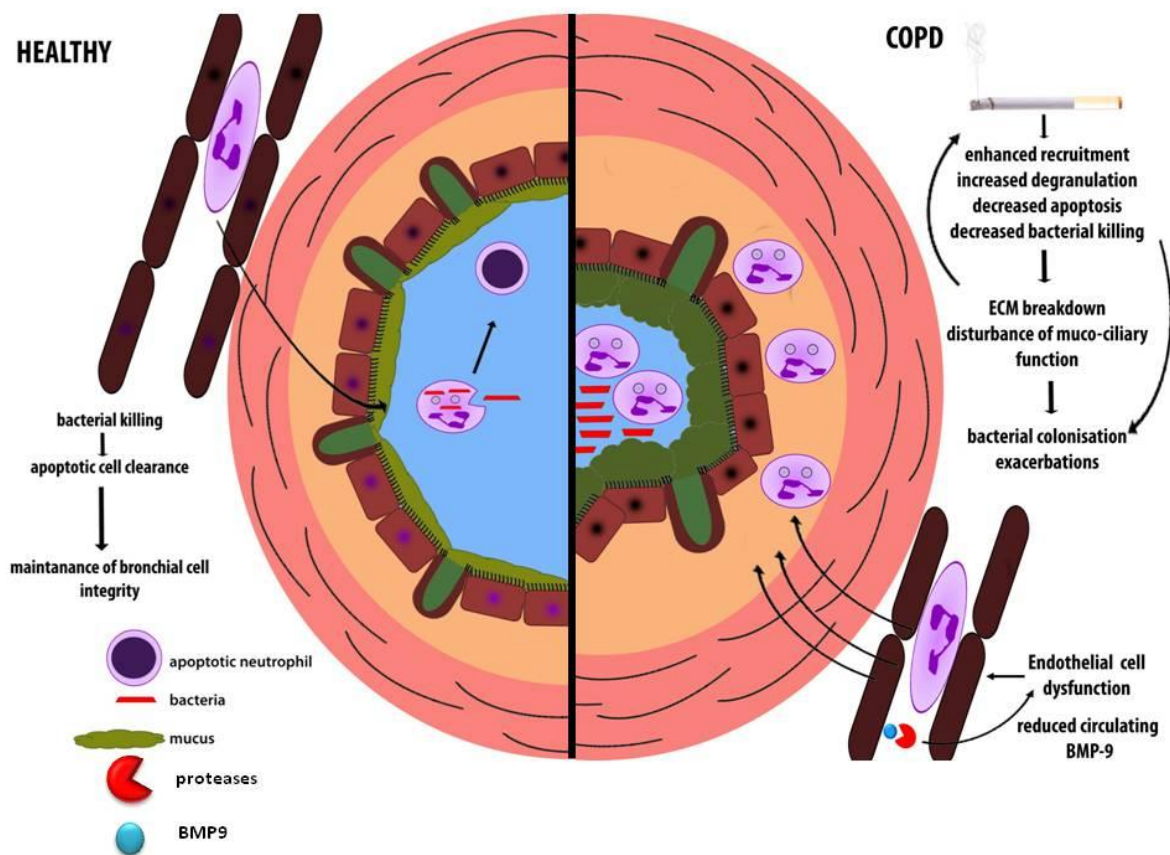


Figure 7.3: Neutrophil function in healthy and chronic obstructive pulmonary disease (COPD) airways

Healthy airways are protected from infection by the innate immune system; bacteria are cleared by the mucociliary escalator, by the action of antibacterial peptides, and by resident phagocytes. Pathogens that evade these first-line defenses are ingested and killed by recruited neutrophils, which then undergo apoptosis and efferocytosis, controlling infection and limiting inflammation. In the COPD airway, cigarette smoke exposure may damage local defenses, with impairment of the mucociliary system and the phagocytic capacity of alveolar macrophages. Cigarette smoke and pathogens trigger the release of chemoattractants, promoting the recruitment of neutrophils and other inflammatory cells. Although there is increased neutrophil infiltration, local or systemic hypoxia impairs bacterial killing and increases the release of proteases, resulting in further mucociliary dysfunction and cellular and tissue injury. The proinflammatory state is perpetuated by increased neutrophil lifespan secondary to hypoxia and inflammatory cytokines. The increased release of NE further results in increased cleavage of BMP-9 which in health is an endogenous vascular quiescence factor. ECM = extracellular matrix, BMP-9 = bone morphogenetic protein. (Adapted from Hoenderdos & Condliffe.⁵¹⁶).

neutrophil inflammation resulting in inflammation and local hypoxia. Cytokines and hypoxia synergize to alter neutrophil function as demonstrated, with impaired bacterial killing (impaired oxidative burst), increased lifespan (HIF-1 α and NF- κ B) and the enhanced release of multiple proteases (PI3K γ /PLC). These proteases have the capacity to degrade ECM, generating further recruitment signals, and to promote airway epithelial cell apoptosis and mucociliary dysfunction.

Thus a vicious cycle of injury, further further inflammation and hypoxia may be perpetuated. Finally, in the light of the data obtained in collaboration with Dr. Li Wei, I speculate that systemic neutrophil priming, coupled with hypoxia, may induce endothelial cell dysfunction due to an increased cleavage of BMP-9 by NE (Figure 7.3). Whilst this hypothesis is 'personalised' to COPD, the inflammation and hypoxia co-exist at most inflammatory sites and the same paradigm may apply to other diseases in the lung and elsewhere.

Although HIF modulates many neutrophil functions under hypoxic conditions, I have shown that the augmented granules release is largely independent of transcriptional regulation, implying that it is predominantly HIF-independent. Instead, hypoxia influences the PLC/PI3K pathway (Figure 7.4, green). Inhibition of either of these signaling molecules profoundly suppresses degranulation, and abolishes the hypoxic uplift. Although inhibition of Ca²⁺ flux (Figure 7.4, red) did not prevent the augmented release of NE found under hypoxic conditions, it is possible that hypoxia modulates pathways in parallel to Ca²⁺ signaling through PI3K and PIP₃. Possible targets (Figure 7.4, blue) include PKC and also Rac2.

I hope that the data I have generated and presented in this thesis will lead to further work to elucidate the mechanism of hypoxia-augmented neutrophil degranulation, and ultimately that greater understanding of this process may lead to improved treatments for a range of inflammatory disease.

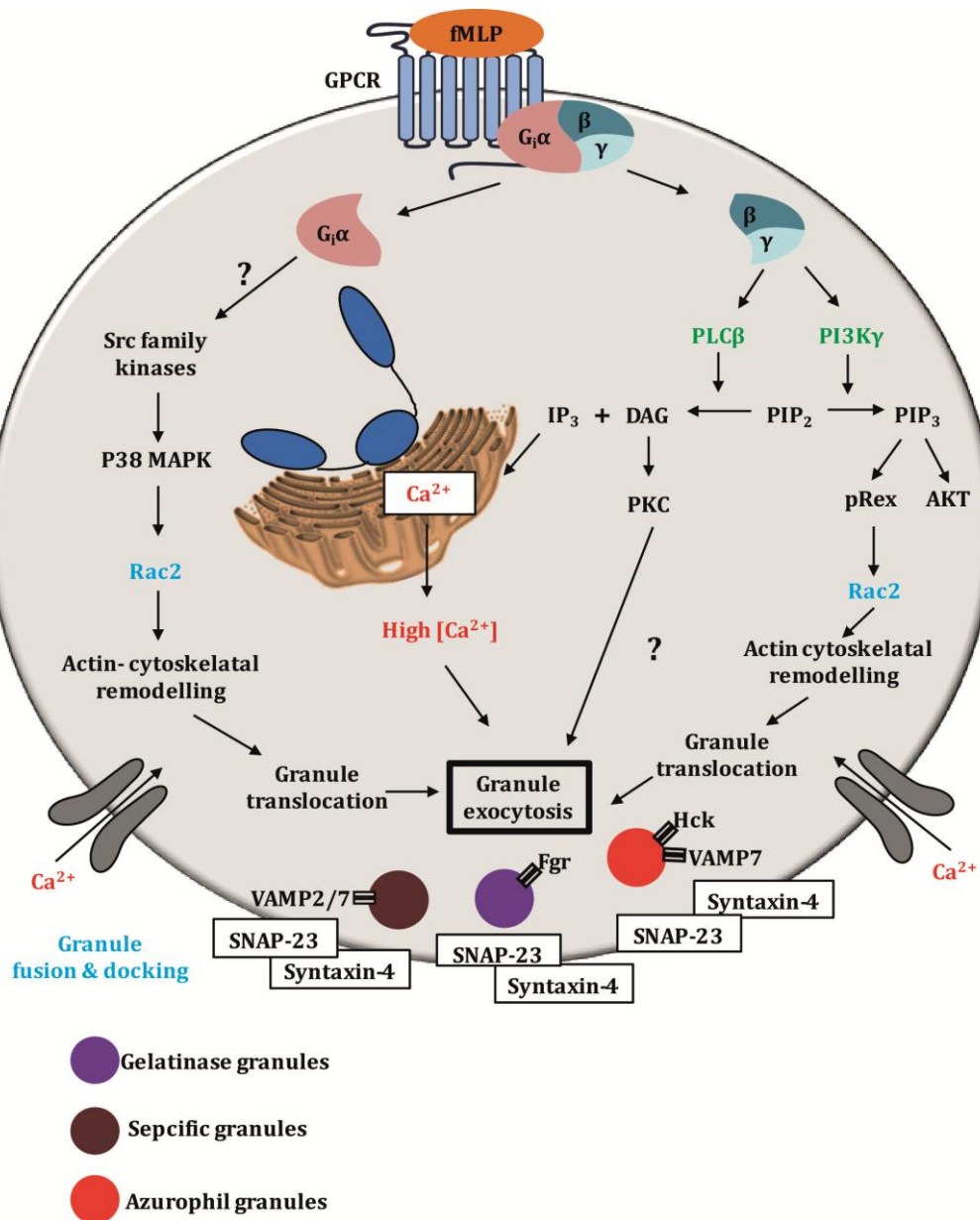


Figure 7.4: Neutrophil signalling pathways involved in the augmented degranulation under hypoxic conditions

Hypoxia influences both the PI3K and the PLC signalling pathway (green text) to promote the release of neutrophil granules. Activation of PLC β leads to Ca $^{2+}$ influx and intracellular Ca $^{2+}$ release from the endoplasmic reticulum, which did not play a role in the hypoxia-augmented release of azurophilic granules (red text) but did promote gelatinase granule release. Activation of PI3K γ induces the production of PIP $_3$ by phosphorylation of PIP $_2$. Through PIP $_3$ signalling, hypoxia can modulate a range of targets, include Rac2 (which modulates cytoskeletal pathways) and RAB family GTPases, which play a role in granule fusion and docking. **Green:** modified by hypoxia, **Red:** not modified by hypoxia, **Blue:** possibly modified by hypoxia.

8. Appendixes

8.1: Elastase targets

Cytokines/chemokines		Receptors	
Target	Biological function	Target	Biological function
Chemerin, IL-8 (CXCL8)	Modulation of cytokine half-life time, activation of chemotaxis	TLR4	Modulation of cytokine half-life time, , activation of chemotaxis
IL-6, TNF-a, IL-2 EGF	Modulation of cytokine half-life time	PAR-1, 2 and 3	Inactivation, modulation of response, apoptosis
SDF1 (CXCL12) MIP1 (CCL3)	Modulation of cytokine half-life time, inhibition of chemotaxis	IL-2R, TNF-RII	Inhibiting cellular response and prolongation of cytokine half-life time
G-CSF	Growth inhibition	CD88 (C5aR)	Inhibition of chemotaxis, feedback mechanism
Integrins/others		CD35 (C3b/C4b R)	Inhibition of complement signaling
Target	Biological function	CD87(urokinase R)	Modulation of cell migration
ICAM-1, Vascular endothelium cadherin	Modulation of adhesion	GCSF-R	Growth inhibition
Proepithelin	Wound healing	CD43, CD16	Modulation of adhesion
TGF-B binding protein	Enhanced growth factor availability	CD14	Inhibition of LPS-mediated cell activation
IGF binding protein	Enhanced growth factor availability	CD2,4 and 8	Impairment of T lymphocytes

8.2: HIF targets

HIF targets	
Energy metabolism	Vaso-motor regulation
<ul style="list-style-type: none"> • Glucose transporter-1 • Hexokinase-2 • 6-Phosphofructo-1-kinase L • Glyceraldehyde-3-phosphate dehydrogenase • Aldolase A • Enolase 1 • Phosphoglycerate kinase-1 • Lactate dehydrogenase A • 6-phosphofructo-2-kinase • Carbonic anhydrase-9 • PFKB3 	<ul style="list-style-type: none"> • Endothelin-1 • Adrenomedullin • Tyrosine hydroxylase • A_{1β}-adrenergic receptor • Inducible nitric-oxide synthase • Endothelial nitric-oxide synthase • Haem oxygenase • Atrial natriuretic peptide
Oxygen transport	Matrix and barrier function
<ul style="list-style-type: none"> • Erythropoietin • Transferrin • Transferrin receptor • Ceruloplasmi 	<ul style="list-style-type: none"> • Procollagen prolyl hydroxylase-α_1 • Interstitial trefoil factor • Ecto-5'-nucleotidase
Angiogenic Signalling	Cell migration
<ul style="list-style-type: none"> • Vascular endothelial growth factor A • Endothelial-gland-derived vascular endothelial growth factor • vascularendothelial growth factor receptor-1 • Plasminogen activator inhibitor -1 	<ul style="list-style-type: none"> • Chemokine receptor CXCR4 • C-Met
Growth and apoptosis	Transcriptional regulation
<ul style="list-style-type: none"> • Insulin-like growth factor binding protein-1 • NIP3 • Endoglin • Wilms' tumor suppressor α-Fetoprotein • Calcitonin receptor like receptor 	<ul style="list-style-type: none"> • DEC1 and DEC2 • ETS1 • P35srj
Virus related	Others
<ul style="list-style-type: none"> • Retrotransposon VL30 	<ul style="list-style-type: none"> • Multidrug-resistance P-glycoprotein • Leptin

8.3 Hypoxic neutrophil supernatants induce A549 cell detachment and apoptosis

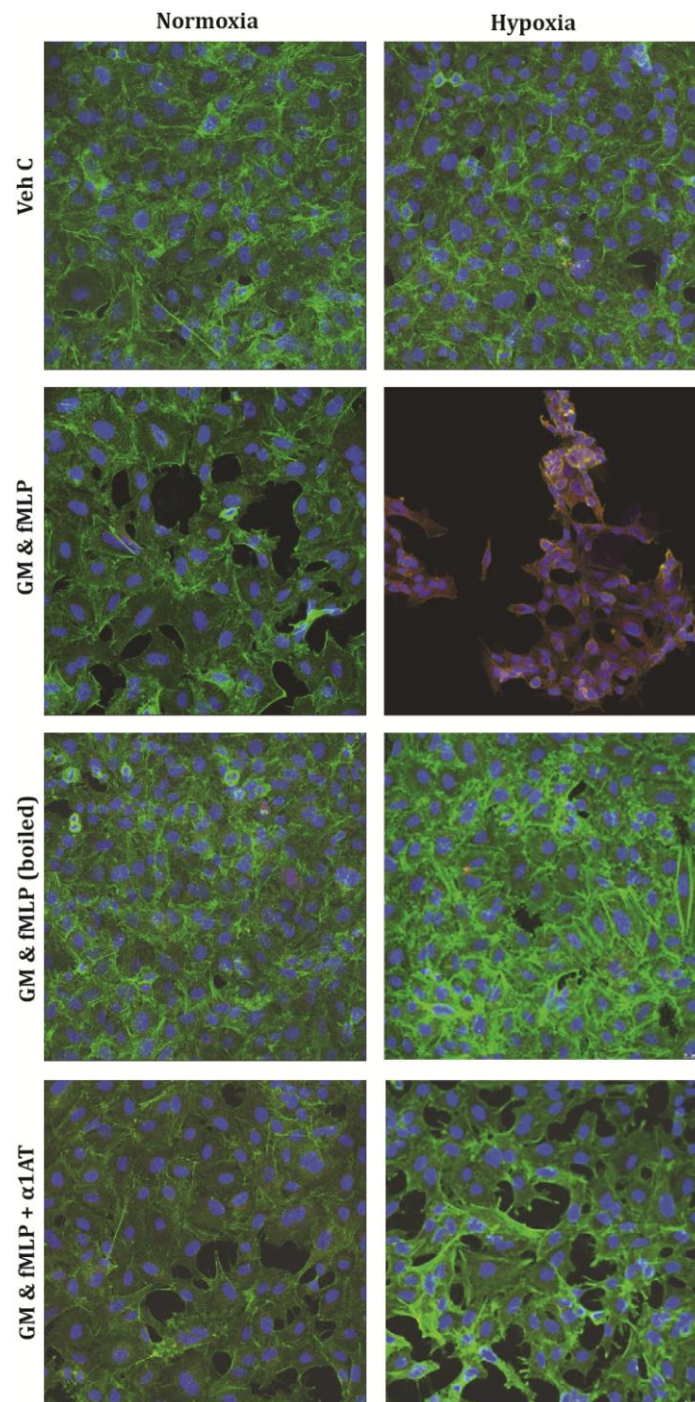
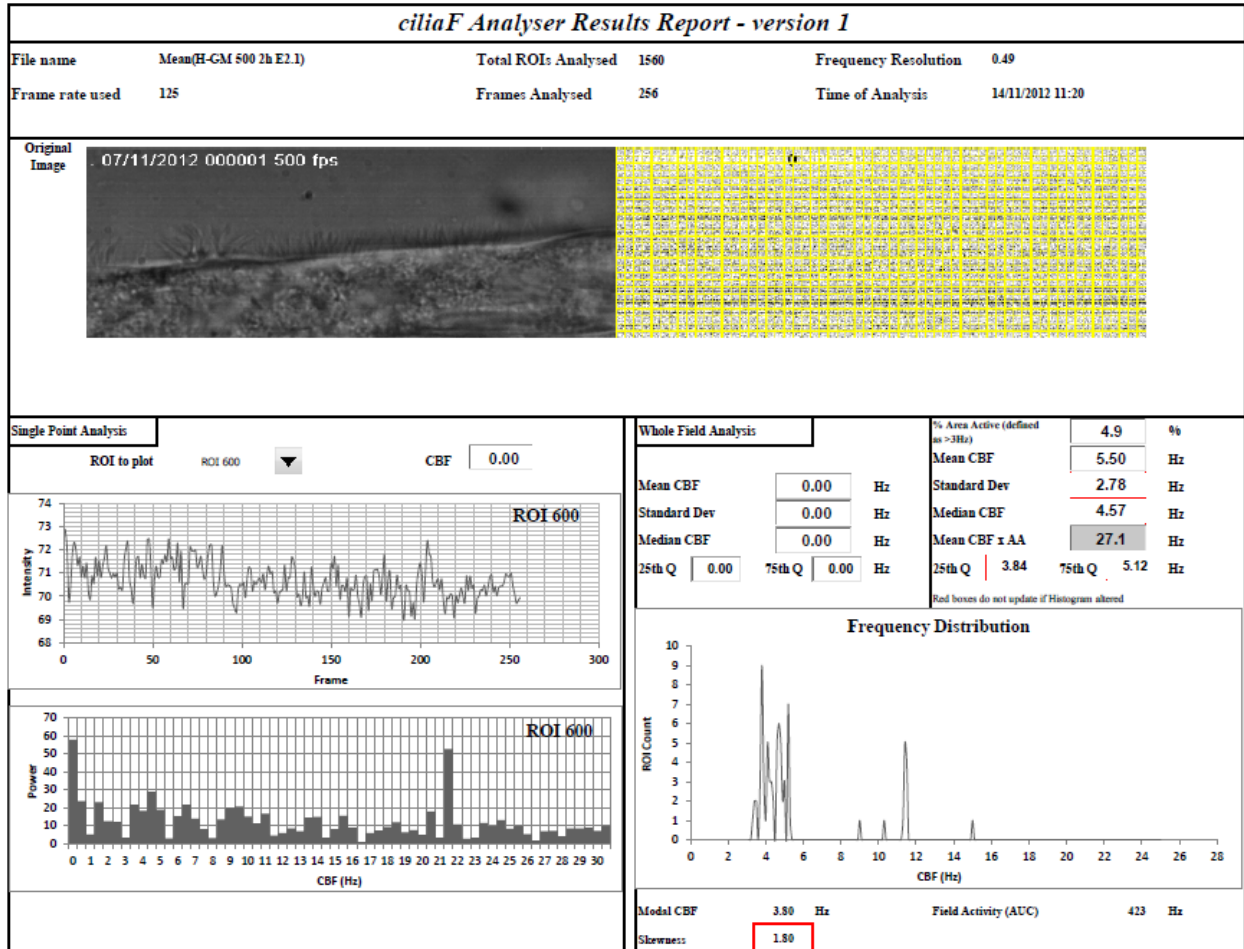


Figure 8.3: Hypoxic supernatants induce A549 cell detachment and apoptosis

A549 cells were cultured in Poly-L-Lysine coated, 96 well plates to obtain a fully confluent cell layer. The cells were exposed to neutrophil supernatants (1:2.5 dilution) from neutrophils cultured/activated under normoxic or hypoxic conditions for 48 hours before the cell layers were fixed with 3.5% PFA and stained for F-actin (rhodamine-phalloidin, green), nucleus (DAPI, blue) and cleaved caspase 3 (goat IgG anti-cleaved caspase 3 antibody and Alexa Fluor 488 – donkey anti-goat IgG, red). A. Representative images from n=3-6 experiments, x40.:

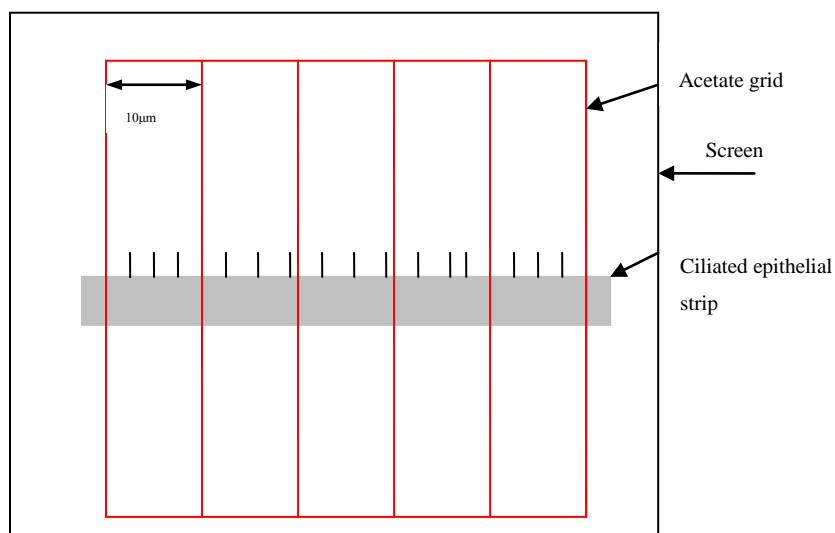
8.4 Ciliary function

8.4.1 Ciliary beat frequency



8.4.2 Standard Operating Procedure for the determination of ciliary dyskinesia

Using the 100x oil immersion lens find a minimum 50 μ m length of continuous ciliated epithelium. Align the epithelial strip horizontally in the middle of the screen. Place the acetate grid over the screen so that cilia are present in each of the 10 μ m sectors. See below:



1. Calculation of Immotility Index.

In each grid 2 ciliary beat frequency readings are measured. When there is no movement a zero is scored which is an immotile cilia. This is repeated for each 10 μ m section on 10 separate epithelial strips per patient. The Immotility Index is the percentage of zeros scored per 10 ciliated strips per patient. Number of zeros per 100 readings (total number of readings per patient) \approx percent).

2. Calculation of Dyskinesia Index.

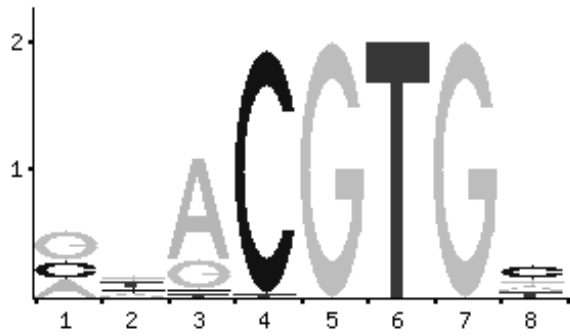
10 individual edges per patient are visualised in the grid and a percentage of each edge where there is dyskinetic cilia is determined. The overall Dyskinesia Index is the average \pm standard deviation of each percentage of 10 measurements.

e.g.

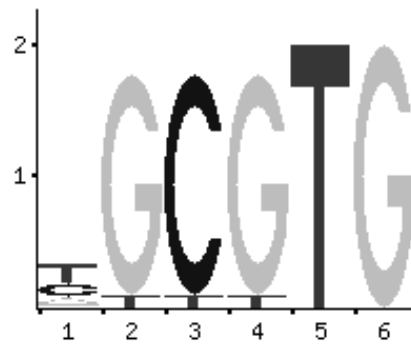
strip 1	10%	strip 6	50%	
strip 2	15%	strip 7	10%	
strip 3	10%	strip 8	15%	
strip 4	12%	strip 9	30%	
strip 5	60%	strip 10	20%	23.2 \pm 17.1

8.5 HRE's in the promoter regions of neutrophil granule proteins

HIF1A:ARNT (Human, Mouse, Rat)



ARNT (Mouse) ARNT:AHR (Mouse)



NM_001972 elastase, neutrophil expressed (ELANE),

```
>19 dna:chromosome chromosome:GRCh37:19:850271:852391:1
CTGGAGGCCAAGCCCCTTCCAAAGATACGGCGTCCCCCACCCTGAAATCCCCCACC
CGACTTGAAACAGGGCTGTGTAGACAGTAGGCGCTTACTAAGTGCACTGTGGTGATGTTA
AGGCAGCAAGGTGGGAACCCTGCCAAAAGGGGAGGGGAGAAGGCAGGGTAGTGTGTGTCT
GATTAAGCTGAGGACAGGGCAGACATGGACTGAGCGCTGCTGTGTGCCAGGCTCTGGGA
GGGCAGGGCCATTGTCTCCCTAACCCGAGAGCCATGGGGGTCCACTTGCCCTGTGGTCAG
TCAGGACTCCAGCCTGGCCAGGCTCTGCGTGTCCCCGGGTGCCCTCGCCCCGCCTATTC
CTGGAGACAGGCCCGTTGGTTCCCTTCCCCTCCCCTTGTCTGGAGCCAGGAGGACGTTG
GTTCTTGCACAGCCTTGGCCCGGCCGTTGCAGCTGGAACATCGTGGGGGAGATGGGAAG
AGGAACGGGGCCCGGAGCCCGGGGCTGGGTCTGGGAATCCCTTTCCCGCAGCTGGGACT
CCAGCTCCCCTGCCAGTTCCTCCAGGCGGAAGCCCTCAGGCTTGGTCCTCACTCCAGCCT
CCCGGCCTGGACAGGAATTCTCTCTCCAGCAGCCCTGCCAGATGCCCCGCCAGCCCCTGC
CTCAGGCGGGGAGGGCTTCAGGGAAAGCTCACCAAGGCAGAAGGGCGGGAGAGATTGTCAG
AGCCCCAGCTGGTGTCCAGGGACTGACCGTGAGCCTGGGTGAAAGTGAGTTCCCCGTTGG
AGGCAACAGACGAGGAGAGGATGGAAGGCCTGGCCCCCAAGAATGAGCCCTGAGGTTTCAG
GGAGCGGCTGGAGTGAGCCGGCCCCAGATCTCCGTCCAGCTGCGGGTCCCAGAGGCCTGG
GTTACACTCGCAGCTCCTGGGGGAGGCCCTTGACGTGCCTCAGTTCCTCAAACAGGAACC
TGGGAAGGACCAGAGAAGTGCCTATTGCGCAGTGAGTGCCCGACACAGCTGCATGTGGCC
GGTATCACAGGGCCCTGGGTAAACTGAGGCAGGCGACACAGCTGCATGTGGCCGGTATCA
CAGGGCCCTGGGTAAACTGAGGCAGGCGACACAGCTGCATGTGGCCGGTATCACAGGGCC
CTGGGTAAACTGAGGCAGGCGACACAGCTGCATGTGGCCGTATCACAGGGCCCTGGGTAA
ACTGAGGCAGGTGACACAGCTGCATGTGGCCGGTATCACGGGGCCCTGGATAAACAGAGG
CAGGCGACACAGCTGCATGTGGCCGGTATCACGGGGCCCTGGGTAAACTGAGGCAGGCGA
GGCCACCCCATCAAGTCCCTCAGGTCTAGGTTTGGCAGGTTTGGCAAAAACACAGCAAC
GCTCGGTTAAATCTGAATTCGGGTAAAGTATATCCTGGGCCTCATTTGGAAGAGACTTAG
ATTAATAAAAAAAAAACGTCGAGACCAGCCCGGCCAACACGGTGAAACCCCGTCTCTACTAAA
AATACAAAAAATTAGCCAGGCGCAGTGGCTCACGCCTGTGATCCCAGCACTCTGGGAGGC
TGAGGCAGGCGGATCACCCGAGGTCAGATGTTCAAGACCAGCCTGGCCGACAGGGCGAAA
CACTGTCTCTACTACAAATACAAAAATTAGCCGGGAGTGGTGGCAGGTGCCTGTAATCTC
AGCTATTCAGGAGGCTGAGGCAGGAGAATCACTTGAACCTGGGAGGCGGAGGTTGCCGTG
AGCCGGGATCACGCCACCGCACTCCAGCCTGGGCGATAGAGCAAGACTCTGTCTCCAAAA
AAATAAATTAATAAACCCACATTGATTATCTGACATTTGAATGCGATTGTGCATCCTGAA
TTTTGTCTGGAGGCCCCACCCGAGCCAATCCAGCGTCTTGTCCCCTTCTCCCCTTTTC
ATCAACGCCCTGTGCCAGGGGAGAGGAAGTGGAGGGCGCTGGCCGGCCGTGGGGCAATGC
AACGGCCTCCCAGCACAGGGCTATAAGAGGAGCCGGGCGGGCACGGAGGGGCAGAGACC
CGGAGCCCCAGCCCCACCATGACCCTCGGCCGCGACTCGCGTGTCTTTTCTCGCCTGT
GTCCTGCCGGCCTTGCTGCTG
```

NM_000250 myeloperoxidase (MPO)

>17 dna:chromosome chromosome:GRCh37:17:56358196:56361032:-1
CCAGAGGCTACTGGGTAAAGAGCACTGGTTTGGAAAGTCAGGAGACTGGGCATGGAGATTA
TTCTGAACTGTGTACACTGCTGACCTTGGTCAAGTCGTTTCCTTCCCTGGGCTCCTTCT
TTCTCAGCTCTACAATAAGGGGCTTGCAATAAATATCTCTCCCCTGTTGAGCCTTGACAA
TTCCCTTAAAAGAGCGAAAGGACACTCAAGCATACTCAAGGTTGACAAGGGTGACAGGGG
ACAGGTGCTCTCATGCATGGCTGATGGGAGGATGAGGTAAAATCTTCAGCAGGCCATTTG
ACTATCAATATTAATAAGCCCTAAAACACGCATACCCAAATACGCAGGAATTTTACTTCT
TGCCTAAGGAAATAATTGACGATGTGGCGAGAGATTTAACTCCATGGATGCTTATCCTAG
TACTACTTATAATAATGAAAATCAGAAACAACCTCTAAGTATCTAATGAGATAGAATTAGT
TAATAAATCATATAAAATAGTTATATGAAAATATTATACAGACATAAAAATGAAGTAAACC
TGTATTTATTGACACAGGGAGATGCTCAGACTAAAATTGTTAAGTACCAGAAAGTAGATGG
TAAAACAATATTTAAAGTTCTTCTTATCAATATTTAAAAATATATATTATGTTTACATAT
AGGATATCAAATTTCTAAATGAGGTATTGGTGAAGTGGTGGGATTATGGGCAATTATTTTC
CTTCTATTGTTTATTATGTGAAGACAATGATAAACCTTGAAAGAAAAAAGTACCACA
ATCTCACTTGATGATGAGTAATTTTGATTTATTTTTATTTTTGCATACTCGTGTCTCAA
ACTTTTCATCAGTGAAAATTATATTACTTAAAGGATTGAAAAATCATTTCAAAAGCCTC
TAAAATTCTAGAGCTTGATTACAAAAGAGCCACTCGACCAACTTCACACACAGCAAGTCA
CTGGCAGGGCAAAGCTTGGTTCCTTCTCAGCAGGGACAGAATCCCTGGACACACTG
GGAAGATATTCTGGGTGTTGCTGTCCCTTGTCCCTTGGCCAAGAGGTGGTCTGGGCATAG
AAGACAAGAGTGGGCCGGGCGGTGGCTCACGCCTGTAATCCCAACAGTGGGTGGATCA
GGAGGAGGTCAGGAGTTTGAGACCAGCCTGGCCAACATGTTGAAACCCCATCTCTACTAA
AAATACAAAATATTAGCCGGGCATGGTGGCGGGCGCCTGTAATCCCAGCTACTTGGGAGG
CTGAGGCAGGAGAATTGCTTGAACCCAGGAGGCAGAGGTTGCAGTGAGCCGAGATTGCAC
CACTGTACTCCAGCTCCGCCAACAGTGAGAGACCTGTCTCAAAAAAAAAAAAAAAAAAAAA
AAGAGTGGGTGGCGGGAAGGTGGCTGAAGGTAGGAGGGGGAACCTAAATGGGACATGGGA
GGCATGGTTGGCAGGAGCTCAGCCTGACCAGGGCCAGAGAGGTAGACTGATTCAAGTCAA
AAGTCGTAGTACTTTTCTGCTGAGATTGGTGGCCCTTTTGTGGGCTTTCTCAAGCAAG
AAATATCCTCTTCTGTTTTCAGAATTATTCTGAATCATTAACCCAAGTCTCCCAACTGCA
CTGATCCTGTCCAGAGAGGCCCTGGGCTGCATCACCTAACTGATCACTAACCACAACCA
GTTCTGCTCTCTCTGGTTCTGAAATCCAGGAGCAGATGGTGGTGGGAGGAGGAGTTT
GGAGACAGCCCTCTACCAGAAGCCAAGAAGAAAGGGAGTGAGGAGGGATAGAGGAAGTT
ATCTTGGTCCTGCGCCACAGTCCCAGGGTCTCCTTCTGTGAAGCCCAACGGTCTCC
AGCCAGATTTCTGTCCCCTTAGCCCCACCAAGAACCAGAGGCTGCCATTGGGTGGCTG
TTGGATGCAGGTTACTGTTGGAGTGGGGATGGCCACCTGAGGCCAATTGGGTCACTTT
ACTCCAGGTCTCCCTTTCATCCTCCTGTCTTCCCTGGGGGCACTCTATTCCCTGCAATTC
CTTGGGCTACCAGTTCCCTGACTTTTGTTCCTTTCAAAGGAACCCTGGATAACCAGTGTA
CCAGAATTTAGAGGGGTTAGTTGTGTGTATCCCTGGGGACAAGCACTGGTATAGGCAC
ACAATGGTGAGCTGAGAAATCTTGGGCTGGTAGTGCTAAATTCAAAGGCTGGGGACAGGC
TGGGGCCAGTGGCTCATGCCTGTAATCCCAGCACTTTGGGAGGCTGAGGCGGGTGGATCA
CTTGGAGGTCAGGAGTTCAAGACCAGCCTGGCCAACATGGTGAACCCCTGTATCTACTAAA
AATACAAAATTAGCTTCTTGCCTAAGGAAAAATACAAAATTACTTCTTGCCTAAGGAA
ATAATTGATGATGTGGCTAGAGGCTAGGGCGTGGTGGCGGGCACCTGTAATCCCAGCTAC
TCGGGAGGCTGAGGCAGAAGAATCGCTTGAACCATTGCACATCAGCCTGGGCAACAGAGC
AAGATAACGTCTCAAAAAAAAAAAAAAAAAAAGGCTGGGGACAATGCTGGCCCTCCTTTC
CTGCCCCCTCCCCCATTTTCAGGGGCCCTCTGTGTGTACCTTCCAACCCAGTGGGGGA
GGAGAAAGAGTTTCACTCAGGATCAGACCTTCTCTACCTCACCCACCCCAAGCTTA
GAGGACATAAAAGCGCAGATTGAGCTAAGAGGAGCT**GACAATATCAGGTGAGCTGTGGAG**
GTGGGGTCCTTGGAAGCTGGATGACAGCAGCTGGCAAGGGGATAAGAGAGCAGTGAGCCC
CTCCCTCAAGGAGGTCT

NM_002343 lactotransferrin (LTF), transcript variant 1, mRNA

Note that human LTF is encoded by two transcript variants with divergent first exons and there is a 'cluster' of promoter features immediately upstream of the observed transcriptional start sites, spanning ~2.5kb of genomic sequence. This associated genomic nucleotide sequence was as input for prediction of HIFA Res

.>3 dna:chromosome chromosome:GRCh37:3:46506498:46509101:-1

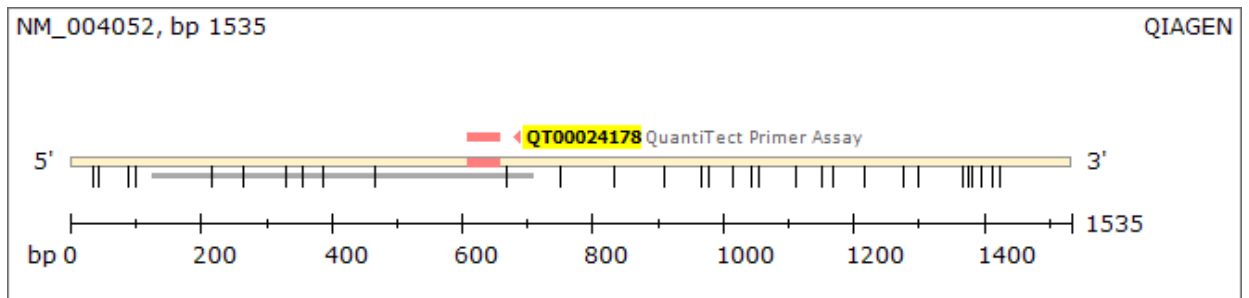
```

CCAGAAAGCCAGAGGGAACTTTTGTGTGCCCTAGTGCTCAGGTAATTGGTCACTGGGTTTC
ATGCTCCCAAGCCTTTACTTGTGGTTGTTTACTTTACAGAAATGCTCTACCTGTAGAAA
TCCCACCCTTCCCTTCAGGTACCCAGGCTAAATCTTCCCTGGAGTTCTTCTGGAGCCCTCAT
GATGGGTGCTGGTCATTCCTCCTCTGGGCCCTCACACTCACTTGCTTTATGCTGCTGGC
CTCTTCTTAGGGAGCCTCTGTGATAGAAGTGCATTCTGTGACTGTCCCTCCCCCATAGT
GCTGTGAGCTCCTGAGGGCAAGGACAGACCCCTCTTCTCTCATGGCATCTACCA
GTTCTGGCATGAATGAATGAATGAATGAATGAATGAATGCTGTTAATAGATCAGTGAAAC
TTCATTGTTTTTTGGGCGAGACTCATCCCCTACATCAGCCTCCTCTGCAAATGGCCTTGA
GGGGCTGCTCTGCCTGTGTCCAGATGCTCACATCCCTGCCCTGGGGCTGGGCTGTTCCAA
CAGGCACAGCAGGAAAACAGTCTGCCCTGTTGCCTACCCATGCTGCCTTCAGGGCACTCC
TTAAGCTGAGCCTCTTGGTAGTGGCCCCAGGTTCTCTGTGTTCTTGCCAACACTGTAACA
TACTTAAGAGGGCCAGGGCCCTCTGACCTCCCAGTCATCCTTTTTTAAAATTTGGACTC
AGAAAAGAGACACGGGTTATGATGTTTCTTAATTCTTTTATAATGATGAAAAGGCAAAG
TCTTGTGCAATTTAGGTACAAAGATGCTTCAGCACTCCTGGGAATTAGTCAATTTTGT
ATTTCTTCAGTATTTTTGAAAGAACTTATTGCAATTATTGATGATGGCAACTTTAAATGG
TGCAATATCATGTTTCCAAACAATGAGAGACCTTGGATCTGTCACCCCAAAACCCAGCTG
GTGATTCTAGCACCAAATCTCAGACCCAGTCTCATGGCAGGCAAGCATGATCCCTGATT
AGCCTCCACCCTGTGCCTTGGCAGGATCATGCCAGAAATGGAGGGGCTCCCCAGCCTCC
TTAATGGCCTCTCCACCTTGGGCTGAGCCTGCTTCTCCATGGCTAGGTGCCCACTGCATG
CTCACTCTTGGCAGAGCTGGCTCCCTGGGGCATTGCCTATCTGCTCCAGGAAATGCTTTT
TAGTACCAAGTAGTCTAAGCAGAGTCAAGACCAGCTTTTCAGAATAAGCAGATTTTCAGAG
TCACATATTGGTCAGACTCACCTGCCAAGAAAGGTGTTTCAGGTGACCTATTATTTCCCTC
ACTGTTAGTACCTTTTTTCTTCACTTAGTTACCCTTTTTTTTTTTGGTGGGGGTTACAGA
GTCTTACTCTATTGCCAGGCTGCAGTGCAGTGACATGATCATGGCTCACTGCCACCTTC
ATCTCCCAGGCTCAAATGGTCCCTCCCACTTTAGCCTCCCAAGTAGCTGGGACCATAGGCA
TACACCACCATGCTGGGCTAATTTTTGTATTTTTGTAGAGATGGGGGTTTCCCTATGTT
GCCAGGCTAGTCTTGAACCTCCTGGGCTCAAGCGATCCTCCCATCTTGGCCTCCCAAAGT
GCTGGGATTACAGGCATGAGCCACTGTGCCCTGCCTAGTTACTCTTGGGCTAAGTTCACA
TCCATACACACAGGATATTCTTCTGAGGCCCCCAATGTGTCCACAGGCACCATGCTGT
ATGTGACACTCCCCTAGAGATGGATGTTTAGTTTGCTTCCAACCTGATTAATGGCATGCAG
TGGTGCCTGGAAACATTTGTACCTGGGGTGTGTGTGTCATGGGAATGTATTTACGAGAT
GTATTCTTAGAAGCAGTATTCTAGCTTTTGAATTTTAAAATCTGACATTTATGGCGATTG
TTAAAATGAGGTTACCATTTCCCTACTGAATACTATCAACACCAAAAAGAAGAAGGAGGA
GATGGAGAAAAAAGACAAAAAAGTGGTAGGGCATCTTAGCCATAGGGCAT
CTTTCTCATTGGCAAATAAGAACATGGAACCAGCCTTGGGTGGTGGCCATTCCCCTCTGA
GGTCCCTGTCTGTTTTCTGGGAGCTGTATTGTGGGTCTCAGCAGGGCAGGGAGATACCCC
ATGGGCAGCTTGCTGAGACTCTGGGCAGCCTCTCTTTTCTCTGTGCTGCTGCTCAGCTGCTCCCTAGGC
TGCTGCTGGGGGTGGTCCGGTCACTTTTTCAACTCTCAGCTCACTGCTGAGCCAAGGTGA
AAGCAAATCCACCTGCCCTAAGTGGCTCCTAGGCACCTTCAAGGTCACTGCTGGAAGAAG
ATAGCAGTCTCACAGGTCAAGGCGATCTTCAAGTAAAGACCCTCTGCTCTGTGTCTGCTGCC
CTCTAGAAGGCACTGAGACCAGAGCTGGGACAGGGCTCAGGGGGCTGCGACTCCTAGGGG
CTTGCAGACTAGTGGGAGAGAAAGAACATCGCAGCAGCCAGGCAGAACCAGGACAGGTGA
GGTGCAGGCTGGCTTTCTCTCGCAGCGCGGTGTGGAGTCTCTGCTGCCTCAGGGCTTT
TCGGAGCCTGGATCCTCAAGGAAC

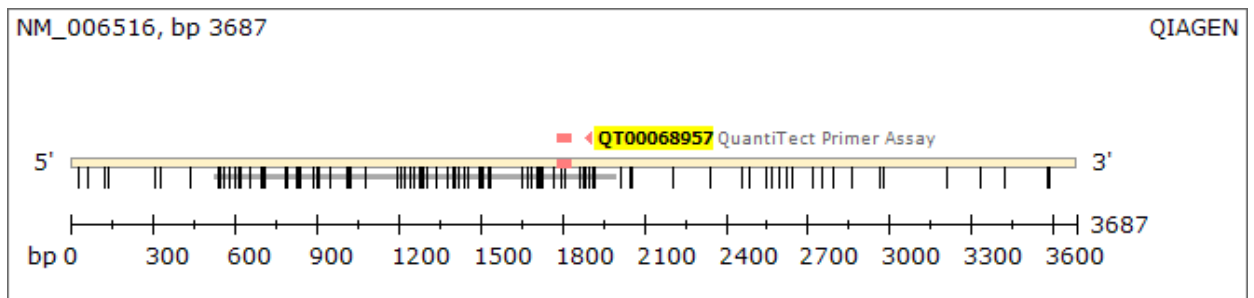
```


8.6 Primer sequences of primers used in section 5.1.3.1

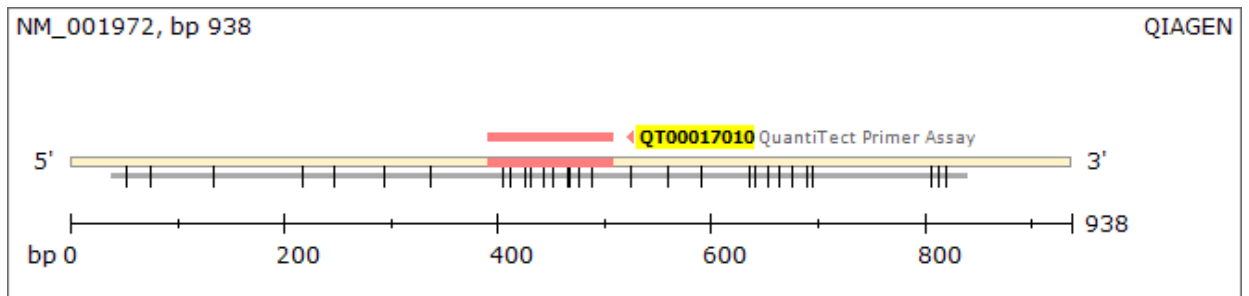
BNIP



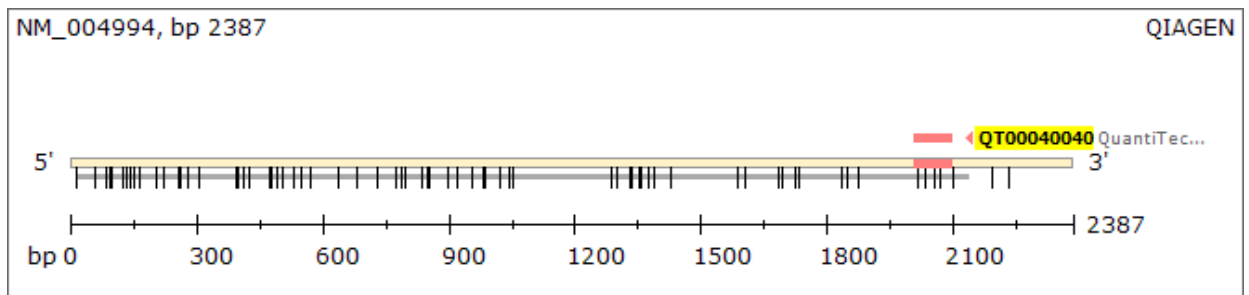
GLUT1



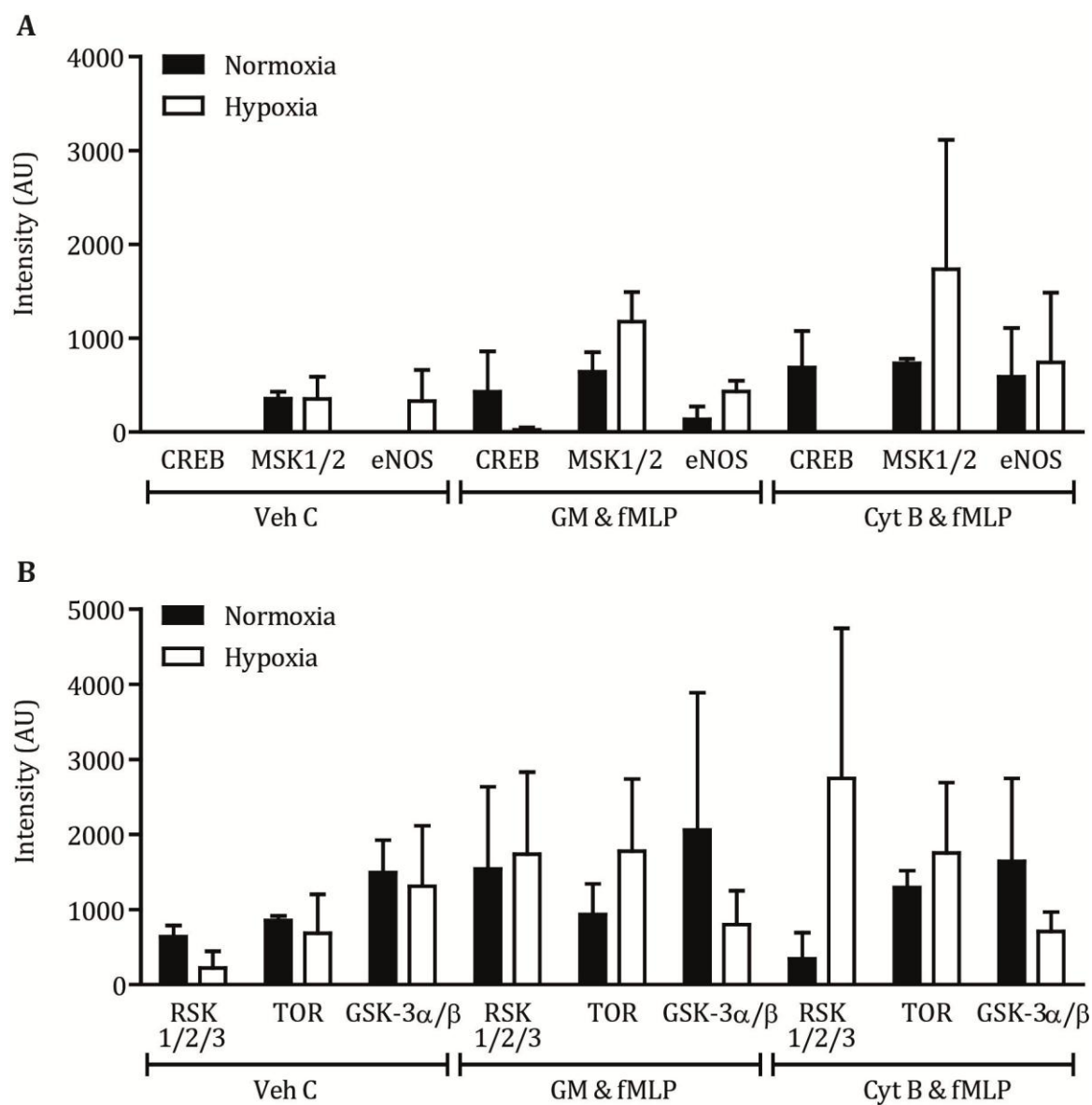
Elastase



MMP-9



8.7 Phospho-kinase array

**Figure 8. 7: Phospho-kinase array performed under normoxia and hypoxia**

Neutrophils were re-suspended in hypoxic (open bars) or normoxic (black bars) IMDM at $11.1 \times 10^6/\text{ml}$ and incubated under normoxia or hypoxia (0.8% O_2 and 5% CO_2) for 4 h at 37°C . The cells were then primed and activated as described (section 2.8). Neutrophils were pelleted and lysed. Lysates were adjusted for protein concentration and the phospho-kinase array was run according to the manufacturer's instruction. Samples were run in singlicate, $n=2$. Results represent mean \pm StDev.

8.8 Publications arising from this thesis

8.8.1 Papers

The Neutrophil in Chronic Obstructive Pulmonary Disease. Too Little, Too Late or Too Much, Too Soon? K. Hoenderdos, A.M. Condliffe, *Am J. Respir. Cell. Mol. Biol.* Vol. 48, Iss. 5, pp 531–539, May 2013

The Effect of Hypoxia on neutrophil degranulation, K. Hoenderdos, C Cheng, R.A. Hirst*, C. O’Callaghan**, ER. Chilvers, A.M. Condliffe, Department of Medicine, University of Cambridge Addenbrooke’s Hospital, Cambridge, UK, *Department of Infection, Immunity and Inflammation, University of Leicester, Leicester, UK, **University College London, Institute of Child Health, London, UK. *manuscript in prep.*

Neutrophil- and redox-dependent proteolysis of BMP9 and the potential role in the pathogenesis of pulmonary arterial hypertension, W. Li^a, Z. Wei^a, K. Hoenderdos^a, R. T. Zamanian^b, I. Nikolic^c, R. M. Salmon^a, P. D. Upton^a, P. B. Yu^c, M. Rabinovitch^b, A. M. Condliffe^a, E. R. Chilvers^a, N. W. Morrell^a, ^aDepartment of Medicine, University of Cambridge, UK, ^bStanford University School of Medicine, USA, ^cDepartment of Medicine, Harvard Medical School, Boston, Massachusetts, USA, *manuscript in prep.*

8.8.2 Abstracts

The Effects of Hypoxia on Neutrophil Elastase Release, poster presentation, Keystone meeting, February 2012, Advances in Hypoxic Signalling: From Bench to Bedside, Banff, Alberta Canada

The Effects of Hypoxia on Neutrophil degranulation, poster presentation, Department of Medicine Research day, 2012, Cambridge, UK

The Effects of Hypoxia on Neutrophil Degranulation, poster presentation, British Thoracic Society winter meeting, December 2012, London, UK

The Effects of Hypoxia on Neutrophil Degranulation, poster presentation, European Society for Clinical Immunology meeting, April 2013, Albufeira, Portugal.

The effects of Hypoxia on Neutrophil Mediated Tissue Damage, oral presentation, Cambridge Immunology PhD and Postdoc Day, Cambridge, UK

The Effects of Hypoxia on Neutrophil Degranulation, poster presentation, School of Clinical Medicine Research Day, Cambridge, UK.

The effects of Hypoxia on Neutrophil Mediated Tissue Damage in the Lung, oral presentation Department of Medicine Research day, November 2013, London, UK

The effects of Hypoxia on Neutrophil Mediated Tissue Damage in the Lung, oral presentation British Thoracic Society winter meeting, December 2013, London, UK

The Effects of Hypoxia on Neutrophil Degranulation, poster presentation, European Society for Clinical Immunology meeting, April 2014, Utrecht, The Netherlands.

The Effects of Hypoxia on Neutrophil Degranulation, poster presentation, The Neutrophil Conference, May 2014, Montreal, Canada.

9. References

1. Peter Parham. *The Immune system*. (Garland Science, 2009).
2. Mollinedo. Human neutrophil granules and exocytosis molecular control. *Immunologia* **22**, 340–358 (2003).
3. Borregaard, N. Development of Neutrophil Granule Diversity. *Ann. N. Y. Acad. Sci.* **832**, 62–68 (1997).
4. Rankin, S. M. The Bone Marrow: A Site of Neutrophil Clearance. *J. Leukoc. Biol.* **88**, 241–251 (2010).
5. Cascão, R., Rosário, H. S. & Fonseca, J. E. Neutrophils: warriors and commanders in immune mediated inflammatory diseases. *Acta Reumatol. Port.* **34**, 313–326 (2009).
6. Stossel, T. P. The E. Donnall Thomas Lecture, 1993. The machinery of blood cell movements. *Blood* **84**, 367–379 (1994).
7. Futosi, K., Fodor, S. & Mócsai, A. Neutrophil cell surface receptors and their intracellular signal transduction pathways. *Int. Immunopharmacol.*
doi:10.1016/j.intimp.2013.06.034
8. Forehand, J. R., Pabst, M. J., Phillips, W. A. & Johnston, R. B. Lipopolysaccharide priming of human neutrophils for an enhanced respiratory burst. Role of intracellular free calcium. *J. Clin. Invest.* **83**, 74–83 (1989).
9. Berkow, R. L., Wang, D., Larrick, J. W., Dodson, R. W. & Howard, T. H. Enhancement of neutrophil superoxide production by preincubation with recombinant human tumor necrosis factor. *J. Immunol. Baltim. Md 1950* **139**, 3783–3791 (1987).
10. Fleischmann, J., Golde, D. W., Weisbart, R. H. & Gasson, J. C. Granulocyte-macrophage colony-stimulating factor enhances phagocytosis of bacteria by human neutrophils. *Blood* **68**, 708–711 (1986).
11. Vercellotti, G. M., Yin, H. Q., Gustafson, K. S., Nelson, R. D. & Jacob, H. S. Platelet-activating factor primes neutrophil responses to agonists: role in promoting neutrophil-mediated endothelial damage. *Blood* **71**, 1100–1107 (1988).
12. Guthrie, L. A., McPhail, L. C., Henson, P. M. & Johnston, R. B. Priming of neutrophils for enhanced release of oxygen metabolites by bacterial lipopolysaccharide.

- Evidence for increased activity of the superoxide-producing enzyme. *J. Exp. Med.* **160**, 1656–1671 (1984).
13. Kitchen, E., Rossi, A., Condliffe, A., Haslett, C. & Chilvers, E. Demonstration of reversible priming of human neutrophils using platelet-activating factor. *Blood* **88**, 4330–4337 (1996).
 14. Condliffe, A. M., Chilvers, E. R., Haslett, C. & Dransfield, I. Priming differentially regulates neutrophil adhesion molecule expression/function. *Immunology* **89**, 105–111 (1996).
 15. Fittschen, C., Sandhaus, R. A., Worthen, G. S. & Henson, P. M. Bacterial lipopolysaccharide enhances chemoattractant-induced elastase secretion by human neutrophils. *J. Leukoc. Biol.* **43**, 547–556 (1988).
 16. Doerfler, M. E., Danner, R. L., Shelhamer, J. H. & Parrillo, J. E. Bacterial lipopolysaccharides prime human neutrophils for enhanced production of leukotriene B₄. *J. Clin. Invest.* **83**, 970–977 (1989).
 17. Doerfler, M. E., Weiss, J., Clark, J. D. & Elsbach, P. Bacterial lipopolysaccharide primes human neutrophils for enhanced release of arachidonic acid and causes phosphorylation of an 85-kD cytosolic phospholipase A₂. *J. Clin. Invest.* **93**, 1583–1591 (1994).
 18. Koenderman, L. *et al.* Monitoring of neutrophil priming in whole blood by antibodies isolated from a synthetic phage antibody library. *J. Leukoc. Biol.* **68**, 58–64 (2000).
 19. Borregaard, N. Neutrophils, from marrow to microbes. *Immunity* **33**, 657–670 (2010).
 20. Summers, C. *et al.* Neutrophil kinetics in health and disease. *Trends Immunol.* **31**, 318–324 (2010).
 21. Burg, N. D. & Pillinger, M. H. The neutrophil: function and regulation in innate and humoral immunity. *Clin. Immunol. Orlando Fla* **99**, 7–17 (2001).
 22. Moore, K. L. *et al.* P-selectin glycoprotein ligand-1 mediates rolling of human neutrophils on P-selectin. *J. Cell Biol.* **128**, 661–671 (1995).

23. Patel, K. D., Nollert, M. U. & McEver, R. P. P-selectin must extend a sufficient length from the plasma membrane to mediate rolling of neutrophils. *J. Cell Biol.* **131**, 1893–1902 (1995).
24. Zarbock, A., Lowell, C. A. & Ley, K. Syk signaling is necessary for E-selectin-induced LFA-1-ICAM-1 association and rolling but not arrest. *Immunity* **26**, 773–783 (2007).
25. Patterson, A. M. *et al.* Differential binding of chemokines to macrophages and neutrophils in the human inflamed synovium. *Arthritis Res.* **4**, 209–214 (2002).
26. Zarbock, A. & Ley, K. Neutrophil adhesion and activation under flow. *Microcirc. N. Y. N 1994* **16**, 31–42 (2009).
27. Xu, J., Wang, F., Van Keymeulen, A., Rentel, M. & Bourne, H. R. Neutrophil microtubules suppress polarity and enhance directional migration. *Proc. Natl. Acad. Sci. U. S. A.* **102**, 6884–6889 (2005).
28. Van Keymeulen, A. *et al.* To stabilize neutrophil polarity, PIP3 and Cdc42 augment RhoA activity at the back as well as signals at the front. *J. Cell Biol.* **174**, 437–445 (2006).
29. Pick, R., Brechtefeld, D. & Walzog, B. Intraluminal crawling versus interstitial neutrophil migration during inflammation. *Mol. Immunol.* **55**, 70–75 (2013).
30. Kang, T. *et al.* Subcellular distribution and cytokine- and chemokine-regulated secretion of leukolysin/MT6-MMP/MMP-25 in neutrophils. *J. Biol. Chem.* **276**, 21960–21968 (2001).
31. Delclaux, C. *et al.* Role of gelatinase B and elastase in human polymorphonuclear neutrophil migration across basement membrane. *Am. J. Respir. Cell Mol. Biol.* **14**, 288–295 (1996).
32. Llewellyn-Jones, C. G., Lomas, D. A. & Stockley, R. A. Potential role of recombinant secretory leucoprotease inhibitor in the prevention of neutrophil mediated matrix degradation. *Thorax* **49**, 567–572 (1994).
33. Owen, C. A., Campbell, M. A., Sannes, P. L., Boukedes, S. S. & Campbell, E. J. Cell surface-bound elastase and cathepsin G on human neutrophils: a novel, non-

oxidative mechanism by which neutrophils focus and preserve catalytic activity of serine proteinases. *J. Cell Biol.* **131**, 775–789 (1995).

34. Campbell, E. J., Campbell, M. A., Boukedes, S. S. & Owen, C. A. Quantum proteolysis by neutrophils: implications for pulmonary emphysema in alpha 1-antitrypsin deficiency. *J. Clin. Invest.* **104**, 337–344 (1999).

35. Takeyama, K. *et al.* Neutrophil-dependent goblet cell degranulation: role of membrane-bound elastase and adhesion molecules. *Am. J. Physiol.* **275**, L294–302 (1998).

36. Segal, A. W. How neutrophils kill microbes. *Annu. Rev. Immunol.* **23**, 197–223 (2005).

37. Weiss, S. J. Tissue Destruction by Neutrophils. *N. Engl. J. Med.* **320**, 365–376 (1989).

38. Heinecke, J. W., Li, W., Mueller, D. M., Bohrer, A. & Turk, J. Cholesterol chlorohydrin synthesis by the myeloperoxidase-hydrogen peroxide-chloride system: potential markers for lipoproteins oxidatively damaged by phagocytes. *Biochemistry (Mosc.)* **33**, 10127–10136 (1994).

39. Heinecke, J. W. Tyrosyl radical production by myeloperoxidase: a phagocyte pathway for lipid peroxidation and dityrosine cross-linking of proteins. *Toxicology* **177**, 11–22 (2002).

40. Song, E. *et al.* Chronic granulomatous disease: a review of the infectious and inflammatory complications. *Clin. Mol. Allergy CMA* **9**, 10 (2011).

41. Brinkmann, V. *et al.* Neutrophil Extracellular Traps Kill Bacteria. *Science* **303**, 1532–1535 (2004).

42. Steinberg, B. E. & Grinstein, S. Unconventional roles of the NADPH oxidase: signaling, ion homeostasis, and cell death. *Sci. STKE Signal Transduct. Knowl. Environ.* **2007**, pe11 (2007).

43. Urban, C. F. *et al.* Neutrophil extracellular traps contain calprotectin, a cytosolic protein complex involved in host defense against *Candida albicans*. *PLoS Pathog.* **5**, e1000639 (2009).

44. Wartha, F. *et al.* Capsule and d-alanylated lipoteichoic acids protect *Streptococcus pneumoniae* against neutrophil extracellular traps. *Cell. Microbiol.* **9**, 1162–1171 (2007).
45. Li, P. *et al.* PAD4 is essential for antibacterial innate immunity mediated by neutrophil extracellular traps. *J. Exp. Med.* **207**, 1853–1862 (2010).
46. Kaplan, M. J. Role of neutrophils in systemic autoimmune diseases. *Arthritis Res. Ther.* **15**, 219 (2013).
47. Villanueva, E. *et al.* Netting Neutrophils Induce Endothelial Damage, Infiltrate Tissues, and Expose Immunostimulatory Molecules in Systemic Lupus Erythematosus. *J. Immunol.* **187**, 538–552 (2011).
48. Manzenreiter, R. *et al.* Ultrastructural characterization of cystic fibrosis sputum using atomic force and scanning electron microscopy. *J. Cyst. Fibros. Off. J. Eur. Cyst. Fibros. Soc.* **11**, 84–92 (2012).
49. Biggar, W. D., Buron, S. & Holmes, B. Chronic granulomatous disease in an adult male: A proposed X-linked defect. *J. Pediatr.* **88**, 63–70 (1976).
50. Klastersky, J. Empirical treatment of sepsis in neutropenic patients. *Int. J. Antimicrob. Agents* **16**, 131–133 (2000).
51. Nathan, C. F. Neutrophil activation on biological surfaces. Massive secretion of hydrogen peroxide in response to products of macrophages and lymphocytes. *J. Clin. Invest.* **80**, 1550–1560 (1987).
52. Nathan, C. Neutrophils and immunity: challenges and opportunities. *Nat Rev Immunol* **6**, 173–182 (2006).
53. Henson, P. M. & Johnston, R. B. Tissue injury in inflammation. Oxidants, proteinases, and cationic proteins. *J. Clin. Invest.* **79**, 669–674 (1987).
54. Lekstrom-Himes, J. A. & Gallin, J. I. Immunodeficiency Diseases Caused by Defects in Phagocytes. *N. Engl. J. Med.* **343**, 1703–1714 (2000).
55. Roos, D. & Law, S. K. Hematologically important mutations: leukocyte adhesion deficiency. *Blood Cells. Mol. Dis.* **27**, 1000–1004 (2001).
56. Wipke, B. T. & Allen, P. M. Essential role of neutrophils in the initiation and progression of a murine model of rheumatoid arthritis. *J. Immunol. Baltim. Md 1950* **167**, 1601–1608 (2001).

57. Cascão, R. *et al.* Identification of a cytokine network sustaining neutrophil and Th17 activation in untreated early rheumatoid arthritis. *Arthritis Res. Ther.* **12**, R196 (2010).
58. Strell, C., Lang, K., Niggemann, B., Zaenker, K. S. & Entschladen, F. Neutrophil granulocytes promote the migratory activity of MDA-MB-468 human breast carcinoma cells via ICAM-1. *Exp. Cell Res.* **316**, 138–148 (2010).
59. Fridlender, Z. G. *et al.* Polarization of Tumor-Associated Neutrophil Phenotype by TGF- β : ‘N1’ versus ‘N2’ TAN. *Cancer Cell* **16**, 183–194 (2009).
60. Mishalian, I. *et al.* Tumor-associated neutrophils (TAN) develop pro-tumorigenic properties during tumor progression. *Cancer Immunol. Immunother. CII* **62**, 1745–1756 (2013).
61. Dumitru, C. A. *et al.* Neutrophils Activate Tumoral CORTACTIN to Enhance Progression of Oropharynx Carcinoma. *Front. Immunol.* **4**, (2013).
62. Shamamian, P. *et al.* Activation of progelatinase A (MMP-2) by neutrophil elastase, cathepsin G, and proteinase-3: a role for inflammatory cells in tumor invasion and angiogenesis. *J. Cell. Physiol.* **189**, 197–206 (2001).
63. Ludwig, P. W., Schwartz, B. A., Hoidal, J. R. & Niewoehner, D. E. Cigarette smoking causes accumulation of polymorphonuclear leukocytes in alveolar septum. *Am. Rev. Respir. Dis.* **131**, 828–830 (1985).
64. Pesci, A. *et al.* Neutrophils infiltrating bronchial epithelium in chronic obstructive pulmonary disease. *Respir. Med.* **92**, 863–870 (1998).
65. Stănescu, D. *et al.* Airways obstruction, chronic expectoration, and rapid decline of FEV1 in smokers are associated with increased levels of sputum neutrophils. *Thorax* **51**, 267–271 (1996).
66. Stockley, R. A., Mistry, M., Bradwell, A. R. & Burnett, D. A study of plasma proteins in the sol phase of sputum from patients with chronic bronchitis. *Thorax* **34**, 777–782 (1979).
67. Vlahos, R., Wark, P. A. B., Anderson, G. P. & Bozinovski, S. Glucocorticosteroids Differentially Regulate MMP-9 and Neutrophil Elastase in COPD. *PLoS ONE* **7**, (2012).

68. Faurschou, M., Sørensen, O. E., Johnsen, A. H., Askaa, J. & Borregaard, N. Defensin-rich granules of human neutrophils: characterization of secretory properties. *Biochim. Biophys. Acta* **1591**, 29–35 (2002).
69. Andreasson, E., Onnheim, K. & Forsman, H. The Subcellular Localization of the Receptor for Platelet-Activating Factor in Neutrophils Affects Signaling and Activation Characteristics. *Clin. Dev. Immunol.* **2013**, (2013).
70. Kjeldsen, L., Bjerrum, O. W., Askaa, J. & Borregaard, N. Subcellular localization and release of human neutrophil gelatinase, confirming the existence of separate gelatinase-containing granules. *Biochem. J.* **287** (Pt 2), 603–610 (1992).
71. Fletcher, M. P. & Seligmann, B. E. Monitoring human neutrophil granule secretion by flow cytometry: secretion and membrane potential changes assessed by light scatter and a fluorescent probe of membrane potential. *J. Leukoc. Biol.* **37**, 431–447 (1985).
72. Faurschou, M. & Borregaard, N. Neutrophil granules and secretory vesicles in inflammation. *Microbes Infect.* **5**, 1317–1327 (2003).
73. Bainton, D. F. & Farquhar, M. G. Origin of granules in polymorphonuclear leukocytes. Two types derived from opposite faces of the Golgi complex in developing granulocytes. *J. Cell Biol.* **28**, 277–301 (1966).
74. Bainton, D. F., Ulliyot, J. L. & Farquhar, M. G. The development of neutrophilic polymorphonuclear leukocytes in human bone marrow. *J. Exp. Med.* **134**, 907–934 (1971).
75. Borregaard, N., Kjeldsen, L., Lollike, K. & Sengeløv, H. Granules and secretory vesicles of the human neutrophil. *Clin. Exp. Immunol.* **101 Suppl 1**, 6–9 (1995).
76. Sørensen, O., Arnljots, K., Cowland, J. B., Bainton, D. F. & Borregaard, N. The human antibacterial cathelicidin, hCAP-18, is synthesized in myelocytes and metamyelocytes and localized to specific granules in neutrophils. *Blood* **90**, 2796–2803 (1997).
77. Arnljots, K., Sørensen, O., Lollike, K. & Borregaard, N. Timing, targeting and sorting of azurophil granule proteins in human myeloid cells. *Leukemia* **12**, 1789–1795 (1998).

78. Bjerregaard, M. D., Jurlander, J., Klausen, P., Borregaard, N. & Cowland, J. B. The in vivo profile of transcription factors during neutrophil differentiation in human bone marrow. *Blood* **101**, 4322–4332 (2003).
79. Spicer, S. S. & Hardin, J. H. Ultrastructure, cytochemistry, and function of neutrophil leukocyte granules. A review. *Lab. Investig. J. Tech. Methods Pathol.* **20**, 488–497 (1969).
80. Cowland, J. B. & Borregaard, N. The individual regulation of granule protein mRNA levels during neutrophil maturation explains the heterogeneity of neutrophil granules. *J. Leukoc. Biol.* **66**, 989–995 (1999).
81. Sengeløv, H., Kjeldsen, L. & Borregaard, N. Control of exocytosis in early neutrophil activation. *J. Immunol. Baltim. Md 1950* **150**, 1535–1543 (1993).
82. Tapper, H., Furuya, W. & Grinstein, S. Localized exocytosis of primary (lysosomal) granules during phagocytosis: role of Ca²⁺-dependent tyrosine phosphorylation and microtubules. *J. Immunol. Baltim. Md 1950* **168**, 5287–5296 (2002).
83. Abdel-Latif, D. *et al.* Rac2 is critical for neutrophil primary granule exocytosis. *Blood* **104**, 832–839 (2004).
84. Mollinedo, F. *et al.* Combinatorial SNARE complexes modulate the secretion of cytoplasmic granules in human neutrophils. *J. Immunol. Baltim. Md 1950* **177**, 2831–2841 (2006).
85. Borregaard, N., Miller, L. J. & Springer, T. A. Chemoattractant-regulated mobilization of a novel intracellular compartment in human neutrophils. *Science* **237**, 1204–1206 (1987).
86. Smith, G. P., Sharp, G. & Peters, T. J. Isolation and characterization of alkaline phosphatase-containing granules (phosphasomes) from human polymorphonuclear leucocytes. *J. Cell Sci.* **76**, 167–178 (1985).
87. Borregaard, N. *et al.* Human neutrophil granules and secretory vesicles. *Eur. J. Haematol.* **51**, 187–198 (1993).
88. Bakowski, B. & Tschesche, H. Migration of polymorphonuclear leukocytes through human amnion membrane--a scanning electron microscopic study. *Biol. Chem. Hoppe. Seyler* **373**, 529–546 (1992).

89. Borregaard, N. & Cowland, J. B. Granules of the Human Neutrophilic Polymorphonuclear Leukocyte. *Blood* **89**, 3503–3521 (1997).
90. Owen, C. A. & Campbell, E. J. The cell biology of leukocyte-mediated proteolysis. *J. Leukoc. Biol.* **65**, 137–150 (1999).
91. O’Kane, C. M. *et al.* Salbutamol up-regulates matrix metalloproteinase-9 in the alveolar space in the acute respiratory distress syndrome. *Crit. Care Med.* **37**, 2242–2249 (2009).
92. Schmalfeldt, B. *et al.* Increased Expression of Matrix Metalloproteinases (MMP)-2, MMP-9, and the Urokinase-Type Plasminogen Activator Is Associated with Progression from Benign to Advanced Ovarian Cancer. *Clin. Cancer Res.* **7**, 2396–2404 (2001).
93. Kato, H. *et al.* MMP-9 Deficiency Shelters Endothelial Pecam-1 Expression and Enhances Regeneration of Steatotic Livers After Ischemia and Reperfusion Injury. *J. Hepatol.* doi:10.1016/j.jhep.2013.12.022
94. Mercer, P. *et al.* MMP-9, TIMP-1 and inflammatory cells in sputum from COPD patients during exacerbation. *Respir. Res.* **6**, 151 (2005).
95. Lanchou, J. *et al.* Imbalance between matrix metalloproteinases (MMP-9 and MMP-2) and tissue inhibitors of metalloproteinases (TIMP-1 and TIMP-2) in acute respiratory distress syndrome patients. *Crit. Care Med.* **31**, 536–542 (2003).
96. Shyamsundar, M. *et al.* Simvastatin decreases lipopolysaccharide-induced pulmonary inflammation in healthy volunteers. *Am. J. Respir. Crit. Care Med.* **179**, 1107–1114 (2009).
97. Cederqvist, K. *et al.* Matrix metalloproteinases-2, -8, and -9 and TIMP-2 in tracheal aspirates from preterm infants with respiratory distress. *Pediatrics* **108**, 686–692 (2001).
98. Mollinedo, F., Gajate, C. & Schneider, D. L. Cytochrome b co-fractionates with gelatinase-containing granules in human neutrophils. *Mol. Cell. Biochem.* **105**, 49–60 (1991).

99. Mollinedo, F., Manara, F. S. & Schneider, D. L. Acidification activity of human neutrophils. Tertiary granules as a site of ATP-dependent acidification. *J. Biol. Chem.* **261**, 1077–1082 (1986).
100. Jabado, N. *et al.* Natural resistance to intracellular infections: natural resistance-associated macrophage protein 1 (Nramp1) functions as a pH-dependent manganese transporter at the phagosomal membrane. *J. Exp. Med.* **192**, 1237–1248 (2000).
101. Gallin, J. I. Neutrophil specific granule deficiency. *Annu. Rev. Med.* **36**, 263–274 (1985).
102. Gombart, A. F. & Koeffler, H. P. Neutrophil specific granule deficiency and mutations in the gene encoding transcription factor C/EBP(epsilon). *Curr. Opin. Hematol.* **9**, 36–42 (2002).
103. McIlwaine, L., Parker, A., Sandilands, G., Gallipoli, P. & Leach, M. Neutrophil-specific granule deficiency. *Br. J. Haematol.* **160**, 735 (2013).
104. Jesaitis, A. J. *et al.* Ultrastructural localization of cytochrome b in the membranes of resting and phagocytosing human granulocytes. *J. Clin. Invest.* **85**, 821–835 (1990).
105. Mollinedo, F. *et al.* Major co-localization of the extracellular-matrix degradative enzymes heparanase and gelatinase in tertiary granules of human neutrophils. *Biochem. J.* **327** (Pt 3), 917–923 (1997).
106. Joiner, K. A., Ganz, T., Albert, J. & Rotrosen, D. The opsonizing ligand on *Salmonella typhimurium* influences incorporation of specific, but not azurophil, granule constituents into neutrophil phagosomes. *J. Cell Biol.* **109**, 2771–2782 (1989).
107. Cramer, E., Pryzwansky, K. B., Villeval, J. L., Testa, U. & Breton-Gorius, J. Ultrastructural localization of lactoferrin and myeloperoxidase in human neutrophils by immunogold. *Blood* **65**, 423–432 (1985).
108. Masson, P. L., Heremans, J. F. & Schonhe, E. Lactoferrin, an iron-binding protein in neutrophilic leukocytes. *J. Exp. Med.* **130**, 643–658 (1969).
109. Oram, J. D. & Reiter, B. Inhibition of bacteria by lactoferrin and other iron-chelating agents. *Biochim. Biophys. Acta* **170**, 351–365 (1968).
110. Chapple, D. S. *et al.* A helical region on human lactoferrin. Its role in antibacterial pathogenesis. *Adv. Exp. Med. Biol.* **443**, 215–220 (1998).

111. Shoki, A. H., Mayer-Hamblett, N., Wilcox, P. G., Sin, D. D. & Quon, B. S. Systematic review of blood biomarkers in cystic fibrosis pulmonary exacerbations. *Chest* **144**, 1659–1670 (2013).
112. Triebel, S., Bläser, J., Reinke, H. & Tschesche, H. A 25 kDa alpha 2-microglobulin-related protein is a component of the 125 kDa form of human gelatinase. *FEBS Lett.* **314**, 386–388 (1992).
113. Goetz, D. H. *et al.* The neutrophil lipocalin NGAL is a bacteriostatic agent that interferes with siderophore-mediated iron acquisition. *Mol. Cell* **10**, 1033–1043 (2002).
114. Friedl, A., Stoesz, S. P., Buckley, P. & Gould, M. N. Neutrophil gelatinase-associated lipocalin in normal and neoplastic human tissues. Cell type-specific pattern of expression. *Histochem. J.* **31**, 433–441 (1999).
115. Nielsen, B. S. *et al.* Induction of NGAL synthesis in epithelial cells of human colorectal neoplasia and inflammatory bowel diseases. *Gut* **38**, 414–420 (1996).
116. Mishra, J. *et al.* Neutrophil gelatinase-associated lipocalin (NGAL) as a biomarker for acute renal injury after cardiac surgery. *Lancet* **365**, 1231–1238 (2005).
117. Ding, H. *et al.* Urinary neutrophil gelatinase-associated lipocalin (NGAL) is an early biomarker for renal tubulointerstitial injury in IgA nephropathy. *Clin. Immunol. Orlando Fla* **123**, 227–234 (2007).
118. Chakraborty, S., Kaur, S., Guha, S. & Batra, S. K. The multifaceted roles of neutrophil gelatinase associated lipocalin (NGAL) in inflammation and cancer. *Biochim. Biophys. Acta* **1826**, 129–169 (2012).
119. Klebanoff, S. J. Myeloperoxidase. *Proc. Assoc. Am. Physicians* **111**, 383–389 (1999).
120. El Kebir, D., József, L., Pan, W. & Filep, J. G. Myeloperoxidase delays neutrophil apoptosis through CD11b/CD18 integrins and prolongs inflammation. *Circ. Res.* **103**, 352–359 (2008).
121. Jerke, U. *et al.* β 2 integrin-mediated cell-cell contact transfers active myeloperoxidase from neutrophils to endothelial cells. *J. Biol. Chem.* **288**, 12910–12919 (2013).

122. Teismann, P. [Myeloperoxidase in the neurodegenerative process of Parkinson's disease]. *Dtsch. Med. Wochenschr.* 1946 **139**, 99–102 (2014).
123. Gorudko, I. V. *et al.* Functional activity of neutrophils in diabetes mellitus and coronary heart disease: role of myeloperoxidase in the development of oxidative stress. *Bull. Exp. Biol. Med.* **154**, 23–26 (2012).
124. Barczyk, A. Decreased Levels of Myeloperoxidase in Induced Sputum of Patients With COPD After Treatment With Oral Glucocorticoids. *Chest* **126**, 389–393 (2004).
125. Churg, A. *et al.* Late intervention with a myeloperoxidase inhibitor stops progression of experimental chronic obstructive pulmonary disease. *Am. J. Respir. Crit. Care Med.* **185**, 34–43 (2012).
126. Odobasic, D. *et al.* Neutrophil myeloperoxidase regulates T-cell-driven tissue inflammation in mice by inhibiting dendritic cell function. *Blood* **121**, 4195–4204 (2013).
127. Korkmaz, B., Horwitz, M. S., Jenne, D. E. & Gauthier, F. Neutrophil elastase, proteinase 3, and cathepsin G as therapeutic targets in human diseases. *Pharmacol. Rev.* **62**, 726–759 (2010).
128. Belaouaj, A., Kim, K. S. & Shapiro, S. D. Degradation of outer membrane protein A in *Escherichia coli* killing by neutrophil elastase. *Science* **289**, 1185–1188 (2000).
129. Hahn, I. *et al.* Cathepsin G and neutrophil elastase play critical and nonredundant roles in lung-protective immunity against *Streptococcus pneumoniae* in mice. *Infect. Immun.* **79**, 4893–4901 (2011).
130. Tkalcevic, J. *et al.* Impaired immunity and enhanced resistance to endotoxin in the absence of neutrophil elastase and cathepsin G. *Immunity* **12**, 201–210 (2000).
131. Reece, S. T. *et al.* Serine protease activity contributes to control of *Mycobacterium tuberculosis* in hypoxic lung granulomas in mice. *J. Clin. Invest.* **120**, 3365–3376 (2010).
132. Borregaard, N. Severe congenital neutropenia: new lane for ELANE. *Blood* **123**, 462–463 (2014).

133. Lungarella, G., Cavarra, E., Lucattelli, M. & Martorana, P. A. The dual role of neutrophil elastase in lung destruction and repair. *Int. J. Biochem. Cell Biol.* **40**, 1287–1296 (2008).
134. Mihara, K., Ramachandran, R., Renaux, B., Saifeddine, M. & Hollenberg, M. D. Neutrophil elastase and proteinase-3 trigger G protein-biased signaling through proteinase-activated receptor-1 (PAR1). *J. Biol. Chem.* **288**, 32979–32990 (2013).
135. Benabid, R. *et al.* Neutrophil elastase modulates cytokine expression: contribution to host defense against *Pseudomonas aeruginosa*-induced pneumonia. *J. Biol. Chem.* **287**, 34883–34894 (2012).
136. Shapiro, S. D. *et al.* Neutrophil Elastase Contributes to Cigarette Smoke-Induced Emphysema in Mice. *Am. J. Pathol.* **163**, 2329–2335 (2003).
137. Iwata, K. *et al.* Effect of neutrophil elastase inhibitor (sivelestat sodium) in the treatment of acute lung injury (ALI) and acute respiratory distress syndrome (ARDS): a systematic review and meta-analysis. *Intern. Med. Tokyo Jpn.* **49**, 2423–2432 (2010).
138. Griese, M., Kappler, M., Gaggar, A. & Hartl, D. Inhibition of airway proteases in cystic fibrosis lung disease. *Eur. Respir. J. Off. J. Eur. Soc. Clin. Respir. Physiol.* **32**, 783–795 (2008).
139. Rees, D. D., Brain, J. D., Wohl, M. E., Humes, J. L. & Mumford, R. A. Inhibition of Neutrophil Elastase in CF Sputum by L-658,758. *J. Pharmacol. Exp. Ther.* **283**, 1201 – 1206 (1997).
140. Kelly, E., Greene, C. M. & McElvaney, N. G. Targeting neutrophil elastase in cystic fibrosis. *Expert Opin. Ther. Targets* **12**, 145–157 (2008).
141. Kushner, Mackiewicz A. in 3–19 (CRC Press, 1993).
142. Fregonese, L., Stolk, J., Frants, R. R. & Veldhuisen, B. Alpha-1 antitrypsin Null mutations and severity of emphysema. *Respir. Med.* **102**, 876–884 (2008).
143. Sallenave, J. M. Antimicrobial activity of antiproteinases. *Biochem. Soc. Trans.* **30**, 111–115 (2002).
144. Rice, W. G. & Weiss, S. J. Regulation of proteolysis at the neutrophil-substrate interface by secretory leukoprotease inhibitor. *Science* **249**, 178–181 (1990).

145. Ganz, T. *et al.* Defensins. Natural peptide antibiotics of human neutrophils. *J. Clin. Invest.* **76**, 1427–1435 (1985).
146. Daher, K. A., Selsted, M. E. & Lehrer, R. I. Direct inactivation of viruses by human granulocyte defensins. *J. Virol.* **60**, 1068–1074 (1986).
147. Wimley, W. C., Selsted, M. E. & White, S. H. Interactions between human defensins and lipid bilayers: evidence for formation of multimeric pores. *Protein Sci. Publ. Protein Soc.* **3**, 1362–1373 (1994).
148. Chertov, O. *et al.* Identification of human neutrophil-derived cathepsin G and azurocidin/CAP37 as chemoattractants for mononuclear cells and neutrophils. *J. Exp. Med.* **186**, 739–747 (1997).
149. Soehnlein, O. *et al.* Neutrophil degranulation mediates severe lung damage triggered by streptococcal M1 protein. *Eur. Respir. J.* **32**, 405–412 (2008).
150. J.C.E. Underwood. *General and Systematic Pathology*. (Churchill Livingstone, 2004).
151. Ornitz, D. M. & Yin, Y. Signaling Networks Regulating Development of the Lower Respiratory Tract. *Cold Spring Harb. Perspect. Biol.* **4**, a008318 (2012).
152. Dobbs, L. G. & Johnson, M. D. Alveolar epithelial transport in the adult lung. *Respir. Physiol. Neurobiol.* **159**, 283–300 (2007).
153. Katzenstein, A.-L. A. Smoking-related interstitial fibrosis (SRIF), pathogenesis and treatment of usual interstitial pneumonia (UIP), and transbronchial biopsy in UIP. *Mod. Pathol. Off. J. U. S. Can. Acad. Pathol. Inc* **25 Suppl 1**, S68–78 (2012).
154. Behr, J. & Costabel, U. [Interstitial lung diseases - historical development, current status, future prospects]. *Pneumol. Stuttg. Ger.* **64**, 573–576 (2010).
155. Hogg, J. C. Pathophysiology of airflow limitation in chronic obstructive pulmonary disease. *Lancet* **364**, 709–721 (2004).
156. Spina, D. Epithelium smooth muscle regulation and interactions. *Am. J. Respir. Crit. Care Med.* **158**, S141–145 (1998).
157. Boers, J. E., Ambergen, A. W. & Thunnissen, F. B. Number and proliferation of basal and parabasal cells in normal human airway epithelium. *Am. J. Respir. Crit. Care Med.* **157**, 2000–2006 (1998).

158. Jeffery, P. K. Morphologic features of airway surface epithelial cells and glands. *Am. Rev. Respir. Dis.* **128**, S14–20 (1983).
159. Jeffery, P. K. Morphology of the airway wall in asthma and in chronic obstructive pulmonary disease. *Am. Rev. Respir. Dis.* **143**, 1152–1158; discussion 1161 (1991).
160. Lumsden, A. B., McLean, A. & Lamb, D. Goblet and Clara cells of human distal airways: evidence for smoking induced changes in their numbers. *Thorax* **39**, 844–849 (1984).
161. Knight, D. A. & Holgate, S. T. The airway epithelium: structural and functional properties in health and disease. *Respirol. Carlton Vic* **8**, 432–446 (2003).
162. De Water, R. *et al.* Ultrastructural localization of bronchial antileukoprotease in central and peripheral human airways by a gold-labeling technique using monoclonal antibodies. *Am. Rev. Respir. Dis.* **133**, 882–890 (1986).
163. Tam, A., Wadsworth, S., Dorscheid, D., Man, S. F. P. & Sin, D. D. The airway epithelium: more than just a structural barrier. *Thor. Adv. Respir. Dis.* **5**, 255–273 (2011).
164. Voynow, J. A. & Rubin, B. K. Mucins, mucus, and sputum. *Chest* **135**, 505–512 (2009).
165. Thornton, D. J., Rousseau, K. & McGuckin, M. A. Structure and function of the polymeric mucins in airways mucus. *Annu. Rev. Physiol.* **70**, 459–486 (2008).
166. Nicholas, B. *et al.* Shotgun proteomic analysis of human-induced sputum. *Proteomics* **6**, 4390–4401 (2006).
167. Hasenberg, M., Stegemann-Koniszewski, S. & Gunzer, M. Cellular immune reactions in the lung. *Immunol. Rev.* **251**, 189–214 (2013).
168. Voynow, J. A. *et al.* Neutrophil elastase induces mucus cell metaplasia in mouse lung. *Am. J. Physiol. Lung Cell. Mol. Physiol.* **287**, L1293–1302 (2004).
169. Voynow, J. A. *et al.* Neutrophil elastase increases MUC5AC mRNA and protein expression in respiratory epithelial cells. *Am. J. Physiol.* **276**, L835–843 (1999).
170. Fischer, B. M., Pavlisko, E. & Voynow, J. A. Pathogenic triad in COPD: oxidative stress, protease-antiprotease imbalance, and inflammation. *Int. J. Chron. Obstruct. Pulmon. Dis.* **6**, 413–421 (2011).

171. Travis, J. Structure, function, and control of neutrophil proteinases. *Am. J. Med.* **84**, 37–42 (1988).
172. Stockley, R. A. Neutrophils and protease/antiprotease imbalance. *Am. J. Respir. Crit. Care Med.* **160**, S49–52 (1999).
173. Pham, C. T. N. Neutrophil serine proteases: specific regulators of inflammation. *Nat Rev Immunol* **6**, 541–550 (2006).
174. Senior, R. M. *et al.* The induction of pulmonary emphysema with human leukocyte elastase. *Am. Rev. Respir. Dis.* **116**, 469–475 (1977).
175. Andersen, M. P., Parham, A. R., Waldrep, J. C., McKenzie, W. N. & Dhand, R. Alveolar fractal box dimension inversely correlates with mean linear intercept in mice with elastase-induced emphysema. *Int. J. Chron. Obstruct. Pulmon. Dis.* **7**, 235–243 (2012).
176. Laurell, C. & Eriksson, S. Electrophoretic Alpha1-Globulin Pattern of Serum in Alpha1-Antitrypsin Deficiency. *Scand. J. Clin. Lab. Invest.* **15**, 132–& (1963).
177. Gross, P., Pfitzer, E. A., Tolker, E., Babyak, M. A. & Kaschak, M. EXPERIMENTAL EMPHYSEMA: ITS PRODUCTION WITH PAPAINE IN NORMAL AND SILICOTIC RATS. *Arch. Environ. Health* **11**, 50–58 (1965).
178. Lieberman, J., Winter, B. & Sastre, A. Alpha 1-antitrypsin Pi-types in 965 COPD patients. *Chest* **89**, 370–373 (1986).
179. Sommerhoff, C. P., Nadel, J. A., Basbaum, C. B. & Caughey, G. H. Neutrophil elastase and cathepsin G stimulate secretion from cultured bovine airway gland serous cells. *J. Clin. Invest.* **85**, 682–689 (1990).
180. Tosi, M. F., Zakem, H. & Berger, M. Neutrophil elastase cleaves C3bi on opsonized pseudomonas as well as CR1 on neutrophils to create a functionally important opsonin receptor mismatch. *J. Clin. Invest.* **86**, 300–308 (1990).
181. Jiang, D. *et al.* Human Neutrophil Elastase Degrades SPLUNC1 and Impairs Airway Epithelial Defense against Bacteria. *PLoS One* **8**, e64689 (2013).
182. Carden, D. L. & Korthuis, R. J. Protease inhibition attenuates microvascular dysfunction in postischemic skeletal muscle. *Am. J. Physiol.* **271**, H1947–1952 (1996).

183. Kawabata, K. *et al.* Delayed neutrophil elastase inhibition prevents subsequent progression of acute lung injury induced by endotoxin inhalation in hamsters. *Am. J. Respir. Crit. Care Med.* **161**, 2013–2018 (2000).
184. Kaynar, A. M., Houghton, A. M., Lum, E. H., Pitt, B. R. & Shapiro, S. D. Neutrophil elastase is needed for neutrophil emigration into lungs in ventilator-induced lung injury. *Am. J. Respir. Cell Mol. Biol.* **39**, 53–60 (2008).
185. Gehrig, S. *et al.* Lack of neutrophil elastase reduces inflammation, mucus hypersecretion, and emphysema, but not mucus obstruction, in mice with cystic fibrosis-like lung disease. *Am. J. Respir. Crit. Care Med.* **189**, 1082–1092 (2014).
186. Houghton, A. M. *et al.* Neutrophil Elastase-Mediated Degradation of IRS-1 Accelerates Lung Tumor Growth. *Nat. Med.* **16**, 219 (2010).
187. Ho, A.-S. *et al.* Neutrophil elastase as a diagnostic marker and therapeutic target in colorectal cancers. *Oncotarget* **5**, 473–480 (2014).
188. Stockley, R. *et al.* Phase II study of a neutrophil elastase inhibitor (AZD9668) in patients with bronchiectasis. *Respir. Med.* **107**, 524–533 (2013).
189. Zhang, R. *et al.* Association between myeloperoxidase levels and risk of coronary artery disease. *JAMA J. Am. Med. Assoc.* **286**, 2136–2142 (2001).
190. Lee, S. S., Adu, D. & Thompson, R. A. Anti-myeloperoxidase antibodies in systemic vasculitis. *Clin. Exp. Immunol.* **79**, 41–46 (1990).
191. Yoo, D. *et al.* Release of cystic fibrosis airway inflammatory markers from *Pseudomonas aeruginosa*-stimulated human neutrophils involves NADPH oxidase-dependent extracellular DNA trap formation. *J. Immunol. Baltim. Md 1950* **192**, 4728–4738 (2014).
192. Park, H. Y. *et al.* The Relation of Serum Myeloperoxidase to Disease Progression and Mortality in Patients with Chronic Obstructive Pulmonary Disease (COPD). *PLoS ONE* **8**, e61315 (2013).
193. O'Donnell, C. *et al.* 3-Chlorotyrosine in sputum of COPD patients: relationship with airway inflammation. *COPD* **7**, 411–417 (2010).

194. Churg, A., Sin, D. D. & Wright, J. L. Everything prevents emphysema: are animal models of cigarette smoke-induced chronic obstructive pulmonary disease any use? *Am. J. Respir. Cell Mol. Biol.* **45**, 1111–1115 (2011).
195. Lefkowitz, D. L. *et al.* The endothelium and cytokine secretion: the role of peroxidases as immunoregulators. *Cell. Immunol.* **202**, 23–30 (2000).
196. Yang, J. J. *et al.* Internalization of Proteinase 3 Is Concomitant with Endothelial Cell Apoptosis and Internalization of Myeloperoxidase with Generation of Intracellular Oxidants. *Am. J. Pathol.* **158**, 581–592 (2001).
197. Haegens, A., Vernooij, J. H. J., Heeringa, P., Mossman, B. T. & Wouters, E. F. M. Myeloperoxidase modulates lung epithelial responses to pro-inflammatory agents. *Eur. Respir. J.* **31**, 252–260 (2008).
198. Nakayama, T., Church, D. F. & Pryor, W. A. Quantitative analysis of the hydrogen peroxide formed in aqueous cigarette tar extracts. *Free Radic. Biol. Med.* **7**, 9–15 (1989).
199. Bridges, R. B., Fu, M. C. & Rehm, S. R. Increased neutrophil myeloperoxidase activity associated with cigarette smoking. *Eur. J. Respir. Dis.* **67**, 84–93 (1985).
200. Betsuyaku, T. *et al.* Neutrophil granule proteins in bronchoalveolar lavage fluid from subjects with subclinical emphysema. *Am. J. Respir. Crit. Care Med.* **159**, 1985–1991 (1999).
201. Finlay, G. A. *et al.* Elevated levels of matrix metalloproteinases in bronchoalveolar lavage fluid of emphysematous patients. *Thorax* **52**, 502–506 (1997).
202. Vignola, A. M. *et al.* Sputum metalloproteinase-9/tissue inhibitor of metalloproteinase-1 ratio correlates with airflow obstruction in asthma and chronic bronchitis. *Am. J. Respir. Crit. Care Med.* **158**, 1945–1950 (1998).
203. Vernooij, J. H. J., Lindeman, J. H. N., Jacobs, J. A., Hanemaaijer, R. & Wouters, E. F. M. Increased activity of matrix metalloproteinase-8 and matrix metalloproteinase-9 in induced sputum from patients with COPD. *Chest* **126**, 1802–1810 (2004).
204. Masure, S., Proost, P., Van Damme, J. & Opdenakker, G. Purification and identification of 91-kDa neutrophil gelatinase. Release by the activating peptide interleukin-8. *Eur. J. Biochem. FEBS* **198**, 391–398 (1991).

205. Itoh, Y. & Nagase, H. Preferential inactivation of tissue inhibitor of metalloproteinases-1 that is bound to the precursor of matrix metalloproteinase 9 (progelatinase B) by human neutrophil elastase. *J. Biol. Chem.* **270**, 16518–16521 (1995).
206. Weathington, N. M. *et al.* A novel peptide CXCR ligand derived from extracellular matrix degradation during airway inflammation. *Nat. Med.* **12**, 317–323 (2006).
207. Keatings, V. M. & Barnes, P. J. Granulocyte activation markers in induced sputum: comparison between chronic obstructive pulmonary disease, asthma, and normal subjects. *Am. J. Respir. Crit. Care Med.* **155**, 449–453 (1997).
208. Eagan, T. M. *et al.* Neutrophil gelatinase-associated lipocalin: a biomarker in COPD. *Chest* **138**, 888–895 (2010).
209. Amitani, R. *et al.* Effects of human neutrophil elastase and *Pseudomonas aeruginosa* proteinases on human respiratory epithelium. *Am. J. Respir. Cell Mol. Biol.* **4**, 26–32 (1991).
210. Lucey, E. C. *et al.* Effect of combined human neutrophil cathepsin G and elastase on induction of secretory cell metaplasia and emphysema in hamsters, with in vitro observations on elastolysis by these enzymes. *Am. Rev. Respir. Dis.* **132**, 362–366 (1985).
211. Burgoyne, R. D. & Morgan, A. Secretory granule exocytosis. *Physiol. Rev.* **83**, 581–632 (2003).
212. Lacy, P. & Eitzen, G. Control of granule exocytosis in neutrophils. *Front. Biosci. J. Virtual Libr.* **13**, 5559–5570 (2008).
213. Jog, N. R. *et al.* The actin cytoskeleton regulates exocytosis of all neutrophil granule subsets. *Am. J. Physiol. - Cell Physiol.* **292**, C1690–C1700 (2007).
214. Bengtsson, T., Dahlgren, C., Stendahl, O. & Andersson, T. Actin Assembly and Regulation of Neutrophil Function: Effects of Cytochalasin B and Tetracaine on Chemotactic Peptide-Induced O₂- Production and Degranulation. *J. Leukoc. Biol.* **49**, 236–244 (1991).
215. Naucler, C., Grinstein, S., Sundler, R. & Tapper, H. Signaling to Localized Degranulation in Neutrophils Adherent to Immune Complexes. *J. Leukoc. Biol.* **71**, 701–710 (2002).

216. Berton, G. & Lowell, C. A. Integrin signalling in neutrophils and macrophages. *Cell. Signal.* **11**, 621–635 (1999).
217. Huizinga, T. W. *et al.* Phosphatidylinositol-linked FcRIII mediates exocytosis of neutrophil granule proteins, but does not mediate initiation of the respiratory burst. *J. Immunol. Baltim. Md 1950* **144**, 1432–1437 (1990).
218. Richter, J., Ng-Sikorski, J., Olsson, I. & Andersson, T. Tumor necrosis factor-induced degranulation in adherent human neutrophils is dependent on CD11b/CD18-integrin-triggered oscillations of cytosolic free Ca²⁺. *Proc. Natl. Acad. Sci. U. S. A.* **87**, 9472–9476 (1990).
219. Suchard, S. J. & Boxer, L. A. Exocytosis of a subpopulation of specific granules coincides with H₂O₂ production in adherent human neutrophils. *J. Immunol. Baltim. Md 1950* **152**, 290–300 (1994).
220. Neptune, E. R., Iiri, T. & Bourne, H. R. Gα₁₂ is not required for chemotaxis mediated by Gi-coupled receptors. *J. Biol. Chem.* **274**, 2824–2828 (1999).
221. Lehmann, D. M., Seneviratne, A. M. P. B. & Smrcka, A. V. Small molecule disruption of G protein beta gamma subunit signaling inhibits neutrophil chemotaxis and inflammation. *Mol. Pharmacol.* **73**, 410–418 (2008).
222. Stephens, L. *et al.* A novel phosphoinositide 3 kinase activity in myeloid-derived cells is activated by G protein beta gamma subunits. *Cell* **77**, 83–93 (1994).
223. Li, Z. *et al.* Roles of PLC-β2 and -β3 and PI3Kγ in chemoattractant-mediated signal transduction. *Science* **287**, 1046–1049 (2000).
224. Kämpe, M. *et al.* PI3-kinase regulates eosinophil and neutrophil degranulation in patients with allergic rhinitis and allergic asthma irrespective of allergen challenge model. *Inflammation* **35**, 230–239 (2012).
225. Fensome, A. *et al.* ARF and PIP3 restore GTP γS-stimulated protein secretion from cytosol-depleted HL60 cells by promoting PIP2 synthesis. *Curr. Biol. CB* **6**, 730–738 (1996).
226. Bohnacker, T. *et al.* PI3Kγ adaptor subunits define coupling to degranulation and cell motility by distinct PtdIns(3,4,5)P₃ pools in mast cells. *Sci. Signal.* **2**, ra27 (2009).

227. Cadwallader, K. A. *et al.* Effect of priming on activation and localization of phospholipase D-1 in human neutrophils. *Eur. J. Biochem. FEBS* **271**, 2755–2764 (2004).
228. Sato, T., Hongu, T., Sakamoto, M., Funakoshi, Y. & Kanaho, Y. Molecular Mechanisms of N-Formyl-Methionyl-Leucyl-Phenylalanine-Induced Superoxide Generation and Degranulation in Mouse Neutrophils: Phospholipase D Is Dispensable. *Mol. Cell. Biol.* **33**, 136–145 (2013).
229. Niggli, V. Signaling to migration in neutrophils: importance of localized pathways. *Int. J. Biochem. Cell Biol.* **35**, 1619–1638 (2003).
230. Reeves, E. P. *et al.* Intracellular secretory leukoprotease inhibitor modulates inositol 1,4,5-triphosphate generation and exerts an anti-inflammatory effect on neutrophils of individuals with cystic fibrosis and chronic obstructive pulmonary disease. *BioMed Res. Int.* **2013**, 560141 (2013).
231. Berton, G., Fumagalli, L., Laudanna, C. & Sorio, C. Beta 2 integrin-dependent protein tyrosine phosphorylation and activation of the FGR protein tyrosine kinase in human neutrophils. *J. Cell Biol.* **126**, 1111–1121 (1994).
232. Fuortes, M., Jin, W. W. & Nathan, C. Adhesion-dependent protein tyrosine phosphorylation in neutrophils treated with tumor necrosis factor. *J. Cell Biol.* **120**, 777–784 (1993).
233. Sengeløv, H., Kjeldsen, L., Diamond, M. S., Springer, T. A. & Borregaard, N. Subcellular localization and dynamics of Mac-1 (alpha m beta 2) in human neutrophils. *J. Clin. Invest.* **92**, 1467–1476 (1993).
234. Pinxteren, J. A., O’Sullivan, A. J., Larbi, K. Y., Tatham, P. E. & Gomperts, B. D. Thirty years of stimulus-secretion coupling: from Ca(2+) toGTP in the regulation of exocytosis. *Biochimie* **82**, 385–393 (2000).
235. Balla, T., Holló, Z., Várnai, P. & Spät, A. Angiotensin II inhibits K(+)-induced Ca2+ signal generation in rat adrenal glomerulosa cells. *Biochem. J.* **273(Pt 2)**, 399–404 (1991).
236. Bentwood, B. J. & Henson, P. M. The sequential release of granule constituents from human neutrophils. *J. Immunol. Baltim. Md 1950* **124**, 855–862 (1980).

237. Laudanna, C. *et al.* Sulfatides trigger increase of cytosolic free calcium and enhanced expression of tumor necrosis factor- α and interleukin-8 mRNA in human neutrophils. Evidence for a role of L-selectin as a signaling molecule. *J. Biol. Chem.* **269**, 4021–4026 (1994).
238. Ng-Sikorski, J., Andersson, R., Patarroyo, M. & Andersson, T. Calcium signaling capacity of the CD11b/CD18 integrin on human neutrophils. *Exp. Cell Res.* **195**, 504–508 (1991).
239. Sjölin, C., Stendahl, O. & Dahlgren, C. Calcium-induced translocation of annexins to subcellular organelles of human neutrophils. *Biochem. J.* **300 (Pt 2)**, 325–330 (1994).
240. Donnelly, S. R. & Moss, S. E. Annexins in the secretory pathway. *Cell. Mol. Life Sci. CMLS* **53**, 533–538 (1997).
241. Trilivas, I., McDonough, P. M. & Brown, J. H. Dissociation of protein kinase C redistribution from the phosphorylation of its substrates. *J. Biol. Chem.* **266**, 8431–8438 (1991).
242. Steadman, R., Petersen, M. M. & Williams, J. D. Human neutrophil secondary granule exocytosis is independent of protein kinase activation and is modified by calmodulin activity. *Int. J. Biochem. Cell Biol.* **28**, 777–786 (1996).
243. Nagaji, J. The role of protein kinase C and $[Ca^{2+}]_i$ in superoxide anion synthesis and myeloperoxidase degranulation of human neutrophils. *Kurume Med. J.* **46**, 157–162 (1999).
244. Blackwood, R. A. & Ernst, J. D. Characterization of Ca^{2+} -dependent phospholipid binding, vesicle aggregation and membrane fusion by annexins. *Biochem. J.* **266**, 195–200 (1990).
245. Francis, J. W., Balazovich, K. J., Smolen, J. E., Margolis, D. I. & Boxer, L. A. Human neutrophil annexin I promotes granule aggregation and modulates Ca^{2+} -dependent membrane fusion. *J. Clin. Invest.* **90**, 537–544 (1992).
246. Sjölin, C., Movitz, C., Lundqvist, H. & Dahlgren, C. Translocation of annexin XI to neutrophil subcellular organelles. *Biochim. Biophys. Acta* **1326**, 149–156 (1997).

247. Zou, W. *et al.* Store-operated Ca²⁺ entry (SOCE) plays a role in the polarization of neutrophil-like HL-60 cells by regulating the activation of Akt, Src, and Rho family GTPases. *Cell. Physiol. Biochem. Int. J. Exp. Cell. Physiol. Biochem. Pharmacol.* **30**, 221–237 (2012).
248. Mócsai, A. *et al.* Differential effects of tyrosine kinase inhibitors and an inhibitor of the mitogen-activated protein kinase cascade on degranulation and superoxide production of human neutrophil granulocytes. *Biochem. Pharmacol.* **54**, 781–789 (1997).
249. Mócsai, A. *et al.* Kinase pathways in chemoattractant-induced degranulation of neutrophils: the role of p38 mitogen-activated protein kinase activated by Src family kinases. *J. Immunol. Baltim. Md 1950* **164**, 4321–4331 (2000).
250. Mócsai, A., Ligeti, E., Lowell, C. A. & Berton, G. Adhesion-dependent degranulation of neutrophils requires the Src family kinases Fgr and Hck. *J. Immunol. Baltim. Md 1950* **162**, 1120–1126 (1999).
251. Fumagalli, L., Zhang, H., Baruzzi, A., Lowell, C. A. & Berton, G. The Src Family Kinases Hck and Fgr Regulate Neutrophil Responses to N-Formyl-Methionyl-Leucyl-Phenylalanine. *J. Immunol.* **178**, 3874–3885 (2007).
252. Gutkind, J. S. & Robbins, K. C. Translocation of the FGR protein-tyrosine kinase as a consequence of neutrophil activation. *Proc. Natl. Acad. Sci. U. S. A.* **86**, 8783–8787 (1989).
253. Möhn, H., Le Cabec, V., Fischer, S. & Maridonneau-Parini, I. The src-family protein-tyrosine kinase p59hck is located on the secretory granules in human neutrophils and translocates towards the phagosome during cell activation. *Biochem. J.* **309 (Pt 2)**, 657–665 (1995).
254. Mócsai, A. *et al.* Kinase pathways in chemoattractant-induced degranulation of neutrophils: the role of p38 mitogen-activated protein kinase activated by Src family kinases. *J. Immunol. Baltim. Md 1950* **164**, 4321–4331 (2000).
255. Simard, J.-C., Girard, D. & Tessier, P. A. Induction of neutrophil degranulation by S100A9 via a MAPK-dependent mechanism. *J. Leukoc. Biol.* **87**, 905–914 (2010).
256. Mócsai, A., Zhou, M., Meng, F., Tybulewicz, V. L. & Lowell, C. A. Syk is required for integrin signaling in neutrophils. *Immunity* **16**, 547–558 (2002).

257. Van Ziffle, J. A. & Lowell, C. A. Neutrophil-specific deletion of Syk kinase results in reduced host defense to bacterial infection. *Blood* **114**, 4871–4882 (2009).
258. Mitra, S. K., Hanson, D. A. & Schlaepfer, D. D. Focal adhesion kinase: in command and control of cell motility. *Nat. Rev. Mol. Cell Biol.* **6**, 56–68 (2005).
259. Kamen, L. A., Schlessinger, J. & Lowell, C. A. Pyk2 Is Required for Neutrophil Degranulation and Host Defense Responses to Bacterial Infection. *J. Immunol.* **186**, 1656–1665 (2011).
260. Luerman, G. C. *et al.* Identification of phosphoproteins associated with human neutrophil granules following chemotactic peptide stimulation. *Mol. Cell. Proteomics MCP* **10**, M110.001552 (2011).
261. Benard, V., Bohl, B. P. & Bokoch, G. M. Characterization of rac and cdc42 activation in chemoattractant-stimulated human neutrophils using a novel assay for active GTPases. *J. Biol. Chem.* **274**, 13198–13204 (1999).
262. Geijsen, N. *et al.* Regulation of p21rac activation in human neutrophils. *Blood* **94**, 1121–1130 (1999).
263. Heyworth, P. G. *et al.* Requirement for posttranslational processing of Rac GTP-binding proteins for activation of human neutrophil NADPH oxidase. *Mol. Biol. Cell* **4**, 261–269 (1993).
264. Lacy, P. Mechanisms of Degranulation in Neutrophils. *Allergy Asthma Clin. Immunol. Off. J. Can. Soc. Allergy Clin. Immunol.* **2**, 98–108 (2006).
265. Baier, A., Ndoh, V. N. E., Lacy, P. & Eitzen, G. Rac1 and Rac2 control distinct events during antigen-stimulated mast cell exocytosis. *J. Leukoc. Biol.* (2014).
doi:10.1189/jlb.0513281
266. Roberts, A. W. *et al.* Deficiency of the hematopoietic cell-specific Rho family GTPase Rac2 is characterized by abnormalities in neutrophil function and host defense. *Immunity* **10**, 183–196 (1999).
267. Mitchell, D. C. *et al.* GEFT, A Rho family guanine nucleotide exchange factor, regulates lens differentiation through a Rac1-mediated mechanism. *Curr. Mol. Med.* **11**, 465–480 (2011).

268. Welch, H. C. E. *et al.* P-Rex1, a PtdIns(3,4,5)P₃- and Gβγ-Regulated Guanine-Nucleotide Exchange Factor for Rac. *Cell* **108**, 809–821 (2002).
269. Damoulakis, G. *et al.* P-Rex1 directly activates RhoG to regulate GPCR-driven Rac signalling and actin polarity in neutrophils. *J. Cell Sci.* jcs.153049 (2014). doi:10.1242/jcs.153049
270. Welch, H. C. E. *et al.* P-Rex1 regulates neutrophil function. *Curr. Biol. CB* **15**, 1867–1873 (2005).
271. Sells, M. A. *et al.* Human p21-activated kinase (Pak1) regulates actin organization in mammalian cells. *Curr. Biol. CB* **7**, 202–210 (1997).
272. Itakura, A. *et al.* p21-Activated kinase (PAK) regulates cytoskeletal reorganization and directional migration in human neutrophils. *PLoS One* **8**, e73063 (2013).
273. Allen, J. D. *et al.* p21-activated kinase regulates mast cell degranulation via effects on calcium mobilization and cytoskeletal dynamics. *Blood* **113**, 2695–2705 (2009).
274. Vines, C. M. & Prossnitz, E. R. Mechanisms of G protein-coupled receptor-mediated degranulation. *FEMS Microbiol. Lett.* **236**, 1–6 (2004).
275. Mócsai, A. *et al.* G-protein-coupled receptor signaling in Syk-deficient neutrophils and mast cells. *Blood* **101**, 4155–4163 (2003).
276. Eitzen, G. *et al.* Proteomic analysis of secretagogue-stimulated neutrophils implicates a role for actin and actin-interacting proteins in Rac2-mediated granule exocytosis. *Proteome Sci.* **9**, 70 (2011).
277. Zerial, M. & McBride, H. Rab proteins as membrane organizers. *Nat. Rev. Mol. Cell Biol.* **2**, 107–117 (2001).
278. Deneka, M., Neeft, M. & van der Sluijs, P. Regulation of membrane transport by rab GTPases. *Crit. Rev. Biochem. Mol. Biol.* **38**, 121–142 (2003).
279. Chaudhuri, S., Kumar, A. & Berger, M. Association of ARF and Rabs with complement receptor type-1 storage vesicles in human neutrophils. *J. Leukoc. Biol.* **70**, 669–676 (2001).

280. Perskvist, N., Roberg, K., Kulyté, A. & Stendahl, O. Rab5a GTPase regulates fusion between pathogen-containing phagosomes and cytoplasmic organelles in human neutrophils. *J. Cell Sci.* **115**, 1321–1330 (2002).
281. Geppert, M., Goda, Y., Stevens, C. F. & Südhof, T. C. The small GTP-binding protein Rab3A regulates a late step in synaptic vesicle fusion. *Nature* **387**, 810–814 (1997).
282. Regazzi, R. *et al.* Expression, localization and functional role of small GTPases of the Rab3 family in insulin-secreting cells. *J. Cell Sci.* **109 (Pt 9)**, 2265–2273 (1996).
283. Stinchcombe, J. C. *et al.* Rab27a is required for regulated secretion in cytotoxic T lymphocytes. *J. Cell Biol.* **152**, 825–834 (2001).
284. Rothman, J. E. The protein machinery of vesicle budding and fusion. *Protein Sci. Publ. Protein Soc.* **5**, 185–194 (1996).
285. Söllner, T., Bennett, M. K., Whiteheart, S. W., Scheller, R. H. & Rothman, J. E. A protein assembly-disassembly pathway in vitro that may correspond to sequential steps of synaptic vesicle docking, activation, and fusion. *Cell* **75**, 409–418 (1993).
286. Brumell, J. H. *et al.* Subcellular distribution of docking/fusion proteins in neutrophils, secretory cells with multiple exocytic compartments. *J. Immunol. Baltim. Md 1950* **155**, 5750–5759 (1995).
287. Martín-Martín, B., Nabokina, S. M., Blasi, J., Lazo, P. A. & Mollinedo, F. Involvement of SNAP-23 and syntaxin 6 in human neutrophil exocytosis. *Blood* **96**, 2574–2583 (2000).
288. Martín-Martín, B., Nabokina, S. M., Blasi, J., Lazo, P. A. & Mollinedo, F. Involvement of SNAP-23 and syntaxin 6 in human neutrophil exocytosis. *Blood* **96**, 2574–2583 (2000).
289. Nabokina, S., Egea, G., Blasi, J. & Mollinedo, F. Intracellular location of SNAP-25 in human neutrophils. *Biochem. Biophys. Res. Commun.* **239**, 592–597 (1997).
290. Brochetta, C. *et al.* Involvement of Munc18 isoforms in the regulation of granule exocytosis in neutrophils. *Biochim. Biophys. Acta* **1783**, 1781–1791 (2008).

291. Zhao, X. W. *et al.* Defects in neutrophil granule mobilization and bactericidal activity in familial hemophagocytic lymphohistiocytosis type 5 (FHL-5) syndrome caused by STXBP2/Munc18-2 mutations. *Blood* **122**, 109–111 (2013).
292. Willemse, B., Lesman-Leegte, I., Timens, W., Postma, D. & ten Hacken, N. High cessation rates of cigarette smoking in subjects with and without COPD. *Chest* **128**, 3685–3687 (2005).
293. Takubo, Y. *et al.* Alpha1-antitrypsin determines the pattern of emphysema and function in tobacco smoke-exposed mice: parallels with human disease. *Am. J. Respir. Crit. Care Med.* **166**, 1596–1603 (2002).
294. Weissmann, N. *et al.* Stimulation of soluble guanylate cyclase prevents cigarette smoke-induced pulmonary hypertension and emphysema. *Am. J. Respir. Crit. Care Med.* **189**, 1359–1373 (2014).
295. Aggarwal, N. R. *et al.* Aquaporin 5 regulates cigarette smoke induced emphysema by modulating barrier and immune properties of the epithelium. *Tissue Barriers* **1**, e25248 (2013).
296. Koethe, S. M., Kuhnmuensch, J. R. & Becker, C. G. Neutrophil Priming by Cigarette Smoke Condensate and a Tobacco Anti-Idiotypic Antibody. *Am. J. Pathol.* **157**, 1735–1743 (2000).
297. Zappacosta, B. *et al.* Morpho-functional modifications of human neutrophils induced by aqueous cigarette smoke extract: comparison with chemiluminescence activity. *Lumin. J. Biol. Chem. Lumin.* (2010). doi:10.1002/bio.1233
298. Matthews, J. B. *et al.* Effect of nicotine, cotinine and cigarette smoke extract on the neutrophil respiratory burst. *J. Clin. Periodontol.* **38**, 208–218 (2011).
299. Mortaz, E. *et al.* Salmeterol with fluticasone enhances the suppression of IL-8 release and increases the translocation of glucocorticoid receptor by human neutrophils stimulated with cigarette smoke. *J. Mol. Med. Berl. Ger.* **86**, 1045–1056 (2008).
300. Overbeek, S. A. *et al.* Cigarette smoke-induced collagen destruction; key to chronic neutrophilic airway inflammation? *PloS One* **8**, e55612 (2013).

301. Caldwell, C. C. *et al.* Differential Effects of Physiologically Relevant Hypoxic Conditions on T Lymphocyte Development and Effector Functions. *J. Immunol.* **167**, 6140–6149 (2001).
302. Wang, W., Winlove, C. P. & Michel, C. C. Oxygen partial pressure in outer layers of skin of human finger nail folds. *J. Physiol.* **549**, 855–863 (2003).
303. Holm, S. & Bylund-Fellenius, A.-C. Continuous monitoring of oxygen tension in human gastrocnemius muscle during exercise. *Clin. Physiol.* **1**, 541–542 (1981).
304. Taylor, C. T. & Colgan, S. P. Hypoxia and gastrointestinal disease. *J. Mol. Med. Berl. Ger.* **85**, 1295–1300 (2007).
305. Sies, H. Oxygen gradients during hypoxic steady states in liver. Urate oxidase and cytochrome oxidase as intracellular O₂ indicators. *Hoppe-Seylers Z. Für Physiol. Chem.* **358**, 1021–1032 (1977).
306. De Groot, H., Noll, T. & Sies, H. Oxygen dependence and subcellular partitioning of hepatic menadione-mediated oxygen uptake. Studies with isolated hepatocytes, mitochondria, and microsomes from rat liver in an oxystat system. *Arch. Biochem. Biophys.* **243**, 556–562 (1985).
307. Gale, D. P. & Maxwell, P. H. The role of HIF in immunity. *Int. J. Biochem. Cell Biol.* **42**, 486–494 (2010).
308. Campbell, E. L. *et al.* Transmigrating Neutrophils Shape the Mucosal Microenvironment through Localized Oxygen Depletion to Influence Resolution of Inflammation. *Immunity* **40**, 66–77 (2014).
309. Peyssonnaud, C. *et al.* Critical role of HIF-1alpha in keratinocyte defense against bacterial infection. *J. Invest. Dermatol.* **128**, 1964–1968 (2008).
310. Botusan, I. R. *et al.* Stabilization of HIF-1alpha is critical to improve wound healing in diabetic mice. *Proc. Natl. Acad. Sci. U. S. A.* **105**, 19426–19431 (2008).
311. Cowburn, A. S. *et al.* Epidermal deletion of HIF-2 α stimulates wound closure. *J. Invest. Dermatol.* **134**, 801–808 (2014).
312. Amador, A. *et al.* Ischemic pre-conditioning in deceased donor liver transplantation: a prospective randomized clinical trial. *Am. J. Transplant. Off. J. Am. Soc. Transplant. Am. Soc. Transpl. Surg.* **7**, 2180–2189 (2007).

313. Moerida Belton *et al.* in *A16. TUBERCULOSIS: HOST DEFENSE* A1022–A1022 (American Thoracic Society, 2013). at http://www.atsjournals.org/doi/abs/10.1164/ajrccm-conference.2013.187.1_MeetingAbstracts.A1022
314. Grahl, N. *et al.* In vivo hypoxia and a fungal alcohol dehydrogenase influence the pathogenesis of invasive pulmonary aspergillosis. *PLoS Pathog.* **7**, e1002145 (2011).
315. Brooks, M. J. & Andrews, D. T. Molecular mechanisms of ischemic conditioning: translation into patient outcomes. *Future Cardiol.* **9**, 549–568 (2013).
316. Cai, Z., Luo, W., Zhan, H. & Semenza, G. L. Hypoxia-inducible factor 1 is required for remote ischemic preconditioning of the heart. *Proc. Natl. Acad. Sci. U. S. A.* **110**, 17462–17467 (2013).
317. Kalakech, H. *et al.* Role of hypoxia inducible factor-1 α in remote limb ischemic preconditioning. *J. Mol. Cell. Cardiol.* **65**, 98–104 (2013).
318. Meijer, T. W. H., Kaanders, J. H. A. M., Span, P. N. & Bussink, J. Targeting hypoxia, HIF-1, and tumor glucose metabolism to improve radiotherapy efficacy. *Clin. Cancer Res. Off. J. Am. Assoc. Cancer Res.* **18**, 5585–5594 (2012).
319. Iannitti, R. G. *et al.* Hypoxia Promotes Danger-mediated Inflammation via Receptor for Advanced Glycation End Products in Cystic Fibrosis. *Am. J. Respir. Crit. Care Med.* **188**, 1338–1350 (2013).
320. Shreeniwas, R. *et al.* Hypoxia-mediated induction of endothelial cell interleukin-1 alpha. An autocrine mechanism promoting expression of leukocyte adhesion molecules on the vessel surface. *J. Clin. Invest.* **90**, 2333–2339 (1992).
321. Yan, S. F. *et al.* Induction of interleukin 6 (IL-6) by hypoxia in vascular cells. Central role of the binding site for nuclear factor-IL-6. *J. Biol. Chem.* **270**, 11463–11471 (1995).
322. Karakurum, M. *et al.* Hypoxic induction of interleukin-8 gene expression in human endothelial cells. *J. Clin. Invest.* **93**, 1564–1570 (1994).
323. Arnould, T., Michiels, C. & Remacle, J. Increased PMN adherence on endothelial cells after hypoxia: involvement of PAF, CD18/CD11b, and ICAM-1. *Am. J. Physiol.* **264**, C1102–1110 (1993).

324. Milhoan, K. A., Lane, T. A. & Bloor, C. M. Hypoxia induces endothelial cells to increase their adherence for neutrophils: role of PAF. *Am. J. Physiol.* **263**, H956–962 (1992).
325. Niinikoski, J., Hunt, T. K. & Dunphy, J. E. Oxygen supply in healing tissue. *Am. J. Surg.* **123**, 247–252 (1972).
326. Rademakers, S. E., Lok, J., Kogel, A. J. van der, Bussink, J. & Kaanders, J. H. Metabolic markers in relation to hypoxia; staining patterns and colocalization of pimonidazole, HIF-1 α , CAIX, LDH-5, GLUT-1, MCT1 and MCT4. *BMC Cancer* **11**, 167 (2011).
327. McGovern, N. N. *et al.* Hypoxia selectively inhibits respiratory burst activity and killing of *Staphylococcus aureus* in human neutrophils. *J. Immunol. Baltim. Md 1950* **186**, 453–463 (2011).
328. Vince, R. V., Christmas, B., Midgley, A. W., McNaughton, L. R. & Madden, L. A. Hypoxia mediated release of endothelial microparticles and increased association of S100A12 with circulating neutrophils. *Oxid. Med. Cell. Longev.* **2**, 2–6 (2009).
329. Berg, J. M. *et al.* *Biochemistry.* (W H Freeman, 2002).
330. Steidle, C. & Huhn, D. [The ultrastructure of freeze etched neutrophil granulocytes]. *Blut* **20**, 90–104 (1970).
331. Murphy, B. M., O'Neill, A. J., Adrain, C., Watson, R. W. G. & Martin, S. J. The Apoptosome Pathway to Caspase Activation in Primary Human Neutrophils Exhibits Dramatically Reduced Requirements for Cytochrome c. *J. Exp. Med.* **197**, 625–632 (2003).
332. Borregaard, N. & Herlin, T. Energy metabolism of human neutrophils during phagocytosis. *J. Clin. Invest.* **70**, 550–557 (1982).
333. Graven, K. K., Yu, Q., Pan, D., Roncarati, J. S. & Farber, H. W. Identification of an oxygen responsive enhancer element in the glyceraldehyde-3-phosphate dehydrogenase gene. *Biochim. Biophys. Acta* **1447**, 208–218 (1999).
334. Lu, M., Holliday, L. S., Zhang, L., Dunn, W. A. & Gluck, S. L. Interaction between aldolase and vacuolar H⁺-ATPase: evidence for direct coupling of glycolysis to the ATP-hydrolyzing proton pump. *J. Biol. Chem.* **276**, 30407–30413 (2001).

335. Gess, B., Hofbauer, K.-H., Deutzmann, R. & Kurtz, A. Hypoxia up-regulates triosephosphate isomerase expression via a HIF-dependent pathway. *Pflüg. Arch. Eur. J. Physiol.* **448**, 175–180 (2004).
336. López-Barneo, J., Ortega-Sáenz, P., Pardal, R., Pascual, A. & Piruat, J. I. Carotid body oxygen sensing. *Eur. Respir. J.* **32**, 1386–1398 (2008).
337. Lahiri, S. *et al.* Oxygen sensing in the body. *Prog. Biophys. Mol. Biol.* **91**, 249–286 (2006).
338. Bruick, R. K. & McKnight, S. L. A conserved family of prolyl-4-hydroxylases that modify HIF. *Science* **294**, 1337–1340 (2001).
339. Kaelin, W. G. & Ratcliffe, P. J. Oxygen sensing by metazoans: the central role of the HIF hydroxylase pathway. *Mol. Cell* **30**, 393–402 (2008).
340. Paltoglou, S. & Roberts, B. J. HIF-1 α and EPAS ubiquitination mediated by the VHL tumour suppressor involves flexibility in the ubiquitination mechanism, similar to other RING E3 ligases. *Oncogene* **26**, 604–609 (2007).
341. Huang, L. E., Arany, Z., Livingston, D. M. & Bunn, H. F. Activation of hypoxia-inducible transcription factor depends primarily upon redox-sensitive stabilization of its alpha subunit. *J. Biol. Chem.* **271**, 32253–32259 (1996).
342. Semenza, G. L. Regulation of mammalian O₂ homeostasis by hypoxia-inducible factor 1. *Annu. Rev. Cell Dev. Biol.* **15**, 551–578 (1999).
343. Schofield, C. J. & Ratcliffe, P. J. Oxygen sensing by HIF hydroxylases. *Nat. Rev. Mol. Cell Biol.* **5**, 343–354 (2004).
344. Ryan, H. E., Lo, J. & Johnson, R. S. HIF-1 α is required for solid tumor formation and embryonic vascularization. *EMBO J.* **17**, 3005–3015 (1998).
345. Tian, H., Hammer, R. E., Matsumoto, A. M., Russell, D. W. & McKnight, S. L. The hypoxia-responsive transcription factor EPAS1 is essential for catecholamine homeostasis and protection against heart failure during embryonic development. *Genes Dev.* **12**, 3320–3324 (1998).
346. Maltepe, E., Schmidt, J. V., Baunoch, D., Bradfield, C. A. & Simon, M. C. Abnormal angiogenesis and responses to glucose and oxygen deprivation in mice lacking the protein ARNT. *Nature* **386**, 403–407 (1997).

347. Cai, Z. *et al.* Hearts from rodents exposed to intermittent hypoxia or erythropoietin are protected against ischemia-reperfusion injury. *Circulation* **108**, 79–85 (2003).
348. Kline, D. D., Peng, Y.-J., Manalo, D. J., Semenza, G. L. & Prabhakar, N. R. Defective carotid body function and impaired ventilatory responses to chronic hypoxia in mice partially deficient for hypoxia-inducible factor 1 alpha. *Proc. Natl. Acad. Sci. U. S. A.* **99**, 821–826 (2002).
349. Cramer, T. *et al.* HIF-1alpha is essential for myeloid cell-mediated inflammation. *Cell* **112**, 645–657 (2003).
350. Peyssonnaud, C. *et al.* HIF-1alpha expression regulates the bactericidal capacity of phagocytes. *J. Clin. Invest.* **115**, 1806–1815 (2005).
351. Walmsley, S. R. *et al.* Prolyl hydroxylase 3 (PHD3) is essential for hypoxic regulation of neutrophilic inflammation in humans and mice. *J. Clin. Invest.* **121**, 1053–1063 (2011).
352. Yuan, Y., Hilliard, G., Ferguson, T. & Millhorn, D. E. Cobalt inhibits the interaction between hypoxia-inducible factor-alpha and von Hippel-Lindau protein by direct binding to hypoxia-inducible factor-alpha. *J. Biol. Chem.* **278**, 15911–15916 (2003).
353. Baeuerle, P. A. & Henkel, T. Function and activation of NF-kappa B in the immune system. *Annu. Rev. Immunol.* **12**, 141–179 (1994).
354. Walmsley, S. R. *et al.* Hypoxia-induced neutrophil survival is mediated by HIF-1alpha-dependent NF-kappaB activity. *J. Exp. Med.* **201**, 105–115 (2005).
355. Cockman, M. E. *et al.* Posttranslational hydroxylation of ankyrin repeats in IkappaB proteins by the hypoxia-inducible factor (HIF) asparaginyl hydroxylase, factor inhibiting HIF (FIH). *Proc. Natl. Acad. Sci. U. S. A.* **103**, 14767–14772 (2006).
356. Dyugovskaya, L., Polyakov, A., Ginsberg, D., Lavie, P. & Lavie, L. Molecular pathways of spontaneous and TNF- α -mediated neutrophil apoptosis under intermittent hypoxia. *Am. J. Respir. Cell Mol. Biol.* **45**, 154–162 (2011).
357. Culver, C. *et al.* Mechanism of Hypoxia-Induced NF- κ B. *Mol. Cell. Biol.* **30**, 4901–4921 (2010).

358. Conrad, P. W., Rust, R. T., Han, J., Millhorn, D. E. & Beitner-Johnson, D. Selective activation of p38alpha and p38gamma by hypoxia. Role in regulation of cyclin D1 by hypoxia in PC12 cells. *J. Biol. Chem.* **274**, 23570–23576 (1999).
359. Seko, Y., Takahashi, N., Tobe, K., Kadowaki, T. & Yazaki, Y. Hypoxia and hypoxia/reoxygenation activate p65PAK, p38 mitogen-activated protein kinase (MAPK), and stress-activated protein kinase (SAPK) in cultured rat cardiac myocytes. *Biochem. Biophys. Res. Commun.* **239**, 840–844 (1997).
360. Misra, A., Pandey, C., Sze, S. K. & Thanabalu, T. Hypoxia Activated EGFR Signaling Induces Epithelial to Mesenchymal Transition (EMT). *PLOS ONE* **7**, e49766 (2012).
361. Stossel, T. P. *et al.* Filamins as integrators of cell mechanics and signalling. *Nat. Rev. Mol. Cell Biol.* **2**, 138–145 (2001).
362. Zheng, X. *et al.* Hypoxia-induced and calpain-dependent cleavage of filamin A regulates the hypoxic response. *Proc. Natl. Acad. Sci.* 201320815 (2014).
doi:10.1073/pnas.1320815111
363. Peyssonnaud, C. *et al.* Cutting edge: Essential role of hypoxia inducible factor-1alpha in development of lipopolysaccharide-induced sepsis. *J. Immunol. Baltim. Md 1950* **178**, 7516–7519 (2007).
364. Van Patot, M. C. T. & Gassmann, M. Hypoxia: adapting to high altitude by mutating EPAS-1, the gene encoding HIF-2 α . *High Alt. Med. Biol.* **12**, 157–167 (2011).
365. Flamme, I. *et al.* HRF, a putative basic helix-loop-helix-PAS-domain transcription factor is closely related to hypoxia-inducible factor-1 alpha and developmentally expressed in blood vessels. *Mech. Dev.* **63**, 51–60 (1997).
366. Tian, H., McKnight, S. L. & Russell, D. W. Endothelial PAS domain protein 1 (EPAS1), a transcription factor selectively expressed in endothelial cells. *Genes Dev.* **11**, 72–82 (1997).
367. Loboda, A., Jozkowicz, A. & Dulak, J. HIF-1 and HIF-2 transcription factors--similar but not identical. *Mol. Cells* **29**, 435–442 (2010).
368. Kapitsinou, P. P. *et al.* Hepatic HIF-2 regulates erythropoietic responses to hypoxia in renal anemia. *Blood* **116**, 3039–3048 (2010).

369. Shohet, R. V. & Garcia, J. A. Keeping the engine primed: HIF factors as key regulators of cardiac metabolism and angiogenesis during ischemia. *J. Mol. Med. Berl. Ger.* **85**, 1309–1315 (2007).
370. Tormos, K. V. & Chandel, N. S. Inter-connection between mitochondria and HIFs. *J. Cell. Mol. Med.* **14**, 795–804 (2010).
371. Biswas, S. *et al.* Effects of HIF-1alpha and HIF2alpha on Growth and Metabolism of Clear-Cell Renal Cell Carcinoma 786-0 Xenografts. *J. Oncol.* **2010**, 757908 (2010).
372. Rankin, E. B. *et al.* Hypoxia-inducible factor 2 regulates hepatic lipid metabolism. *Mol. Cell. Biol.* **29**, 4527–4538 (2009).
373. Tanaka, T. *et al.* Cobalt promotes angiogenesis via hypoxia-inducible factor and protects tubulointerstitium in the remnant kidney model. *Lab. Investig. J. Tech. Methods Pathol.* **85**, 1292–1307 (2005).
374. Keith, B., Johnson, R. S. & Simon, M. C. HIF1 α and HIF2 α : sibling rivalry in hypoxic tumour growth and progression. *Nat. Rev. Cancer* **12**, 9–22 (2012).
375. Elks, P. M. *et al.* Hypoxia inducible factor signaling modulates susceptibility to mycobacterial infection via a nitric oxide dependent mechanism. *PLoS Pathog.* **9**, e1003789 (2013).
376. Thompson, A. A. R. *et al.* Hypoxia-inducible factor 2 α regulates key neutrophil functions in humans, mice, and zebrafish. *Blood* **123**, 366–376 (2014).
377. Mecklenburgh, K. I. *et al.* Involvement of a ferroprotein sensor in hypoxia-mediated inhibition of neutrophil apoptosis. *Blood* **100**, 3008–3016 (2002).
378. Ma, S. *et al.* Store-operated Ca²⁺ entry mediated regulation of polarization in differentiated human neutrophil-like HL-60 cells under hypoxia. *Mol. Med. Rep.* (2014). doi:10.3892/mmr.2014.1894
379. Mc Govern, N. The effects of Hypoxia on Neutrophil biology. (University of Cambridge, 2010).
380. Fouret, P. *et al.* Expression of the neutrophil elastase gene during human bone marrow cell differentiation. *J. Exp. Med.* **169**, 833–845 (1989).
381. Takahashi, H. *et al.* Structure of the human neutrophil elastase gene. *J. Biol. Chem.* **263**, 14739–14747 (1988).

382. Haas, F. & Bergofsky, E. H. Role of the mast cell in the pulmonary pressor response to hypoxia. *J. Clin. Invest.* **51**, 3154–3162 (1972).
383. Steiner, D. R. S., Gonzalez, N. C. & Wood, J. G. Mast cells mediate the microvascular inflammatory response to systemic hypoxia. *J. Appl. Physiol. Bethesda Md* 1985 **94**, 325–334 (2003).
384. Chao, J., Wood, J. G. & Gonzalez, N. C. Alveolar macrophages initiate the systemic microvascular inflammatory response to alveolar hypoxia. *Respir. Physiol. Neurobiol.* **178**, 439–448 (2011).
385. Pinsky, D. J. *et al.* Hypoxia-induced exocytosis of endothelial cell Weibel-Palade bodies. A mechanism for rapid neutrophil recruitment after cardiac preservation. *J. Clin. Invest.* **97**, 493–500 (1996).
386. Goerge, T. *et al.* Secretion pores in human endothelial cells during acute hypoxia. *J. Membr. Biol.* **187**, 203–211 (2002).
387. Smith, P. K. *et al.* Measurement of protein using bicinchoninic acid. *Anal. Biochem.* **150**, 76–85 (1985).
388. Mitchell, T., Lo, A., Logan, M. R., Lacy, P. & Eitzen, G. Primary granule exocytosis in human neutrophils is regulated by Rac-dependent actin remodeling. *Am. J. Physiol. - Cell Physiol.* **295**, C1354–C1365 (2008).
389. Ramirez, R. D. *et al.* Immortalization of human bronchial epithelial cells in the absence of viral oncoproteins. *Cancer Res.* **64**, 9027–9034 (2004).
390. Gray, T. E., Guzman, K., Davis, C. W., Abdullah, L. H. & Nettekheim, P. Mucociliary differentiation of serially passaged normal human tracheobronchial epithelial cells. *Am. J. Respir. Cell Mol. Biol.* **14**, 104–112 (1996).
391. Vladar, E. K. & Stearns, T. Molecular characterization of centriole assembly in ciliated epithelial cells. *J. Cell Biol.* **178**, 31–42 (2007).
392. Hirst, R. A., Rutman, A., Williams, G. & O’Callaghan, C. Ciliated Air-Liquid Cultures as an Aid to Diagnostic Testing of Primary Ciliary Dyskinesia. *CHEST J.* **138**, 1441–1447 (2010).
393. Smith, C. M. *et al.* ciliaFA: a research tool for automated, high-throughput measurement of ciliary beat frequency using freely available software. *Cilia* **1**, 14 (2012).

394. Hannah, S. *et al.* Hypoxia prolongs neutrophil survival in vitro. *FEBS Lett.* **372**, 233–237 (1995).
395. Walmsley, S. R., McGovern, N. N., Whyte, M. K. B. & Chilvers, E. R. The HIF/VHL Pathway: From Oxygen Sensing to Innate Immunity. *Am J Respir Cell Mol Biol* **38**, 251–255 (2008).
396. Akhavani, M. A. *et al.* Hypoxia upregulates angiogenesis and synovial cell migration in rheumatoid arthritis. *Arthritis Res. Ther.* **11**, R64 (2009).
397. Taylor, J. L. *et al.* Role for Matrix Metalloproteinase 9 in Granuloma Formation during Pulmonary Mycobacterium tuberculosis Infection. *Infect. Immun.* **74**, 6135–6144 (2006).
398. O'Reilly, P. *et al.* N-alpha-PGP and PGP, potential biomarkers and therapeutic targets for COPD. *Respir. Res.* **10**, 38 (2009).
399. Carter, R. I. *et al.* The fibrinogen cleavage product A α -Val360, a specific marker of neutrophil elastase activity in vivo. *Thorax* **66**, 686–691 (2011).
400. Kothari, N. *et al.* Increased myeloperoxidase enzyme activity in plasma is an indicator of inflammation and onset of sepsis. *J. Crit. Care* **26**, 435.e1–7 (2011).
401. Johansson, L. *et al.* Neutrophil-derived hyperresistinemia in severe acute streptococcal infections. *J. Immunol. Baltim. Md 1950* **183**, 4047–4054 (2009).
402. Paone, G. *et al.* Analysis of sputum markers in the evaluation of lung inflammation and functional impairment in symptomatic smokers and COPD patients. *Dis. Markers* **31**, 91–100 (2011).
403. Fujimura, N. *et al.* Neutrophil elastase inhibitor improves survival rate after ischemia reperfusion injury caused by supravisceral aortic clamping in rats. *J. Surg. Res.* **180**, e31–36 (2013).
404. Clemmensen, S. N. *et al.* Alpha-1-antitrypsin is produced by human neutrophil granulocytes and their precursors and liberated during granule exocytosis. *Eur. J. Haematol.* **86**, 517–530 (2011).
405. Singh, P. K., Parsek, M. R., Greenberg, E. P. & Welsh, M. J. A component of innate immunity prevents bacterial biofilm development. *Nature* **417**, 552–555 (2002).

406. Kristof, A. S., Goldberg, P., Laubach, V. & Hussain, S. N. Role of inducible nitric oxide synthase in endotoxin-induced acute lung injury. *Am. J. Respir. Crit. Care Med.* **158**, 1883–1889 (1998).
407. Carnesecci, S. *et al.* NADPH oxidase-1 plays a crucial role in hyperoxia-induced acute lung injury in mice. *Am. J. Respir. Crit. Care Med.* **180**, 972–981 (2009).
408. Marriott, H. M., Hellewell, P. G., Whyte, M. K. B. & Dockrell, D. H. Contrasting roles for reactive oxygen species and nitric oxide in the innate response to pulmonary infection with *Streptococcus pneumoniae*. *Vaccine* **25**, 2485–2490 (2007).
409. Standish, A. J. & Weiser, J. N. Human Neutrophils Kill *Streptococcus pneumoniae* via Serine Proteases. *J. Immunol.* **183**, 2602–2609 (2009).
410. Nibbering, P. H. *et al.* Human lactoferrin and peptides derived from its N terminus are highly effective against infections with antibiotic-resistant bacteria. *Infect. Immun.* **69**, 1469–1476 (2001).
411. Weiss, S. J. & Regiani, S. Neutrophils degrade subendothelial matrices in the presence of alpha-1-proteinase inhibitor. Cooperative use of lysosomal proteinases and oxygen metabolites. *J. Clin. Invest.* **73**, 1297–1303 (1984).
412. Inauen, W. *et al.* Anoxia-reoxygenation-induced, neutrophil-mediated endothelial cell injury: role of elastase. *Am. J. Physiol.* **259**, H925–931 (1990).
413. Ishii, T. *et al.* Neutrophil Elastase Contributes to Acute Lung Injury Induced by Bilateral Nephrectomy. *Am. J. Pathol.* **177**, 1665–1673 (2010).
414. Hoffstein, S., Soberman, R., Goldstein, I. & Weissmann, G. Concanavalin A induces microtubule assembly and specific granule discharge in human polymorphonuclear leukocytes. *J. Cell Biol.* **68**, 781–787 (1976).
415. Serrander, L. *et al.* Selective inhibition of IgG-mediated phagocytosis in gelsolin-deficient murine neutrophils. *J. Immunol. Baltim. Md 1950* **165**, 2451–2457 (2000).
416. Pilette, C. *et al.* Increased galectin-3 expression and intra-epithelial neutrophils in small airways in severe COPD. *Eur. Respir. J. Off. J. Eur. Soc. Clin. Respir. Physiol.* **29**, 914–922 (2007).
417. Houghton, A. M. *et al.* Neutrophil elastase-mediated degradation of IRS-1 accelerates lung tumor growth. *Nat. Med.* **16**, 219–223 (2010).

418. Cools-Lartigue, J. *et al.* Neutrophil extracellular traps sequester circulating tumor cells and promote metastasis. *J. Clin. Invest.* (2013). doi:10.1172/JCI67484
419. Polosukhin, V. V. *et al.* Hypoxia-inducible factor-1 signalling promotes goblet cell hyperplasia in airway epithelium. *J. Pathol.* **224**, 203–211 (2011).
420. Lee, S. H. *et al.* Increased expression of vascular endothelial growth factor and hypoxia inducible factor-1 α in lung tissue of patients with chronic bronchitis. *Clin. Biochem.* **47**, 552–559 (2014).
421. Zinkernagel, A. S., Johnson, R. S. & Nizet, V. Hypoxia inducible factor (HIF) function in innate immunity and infection. *J. Mol. Med. Berl. Ger.* **85**, 1339–1346 (2007).
422. Rittner, H. L. *et al.* CXCR1/2 ligands induce p38 MAPK-dependent translocation and release of opioid peptides from primary granules in vitro and in vivo. *Brain. Behav. Immun.* **21**, 1021–1032 (2007).
423. Friedman, J. E., Chow, E. J. & Haddad, G. G. State of actin filaments is changed by anoxia in cultured rat neocortical neurons. *Neuroscience* **82**, 421–427 (1998).
424. Racusen, L. C. Alterations in human proximal tubule cell attachment in response to hypoxia: role of microfilaments. *J. Lab. Clin. Med.* **123**, 357–364 (1994).
425. Feldhaus, M. J., Weyrich, A. S., Zimmerman, G. A. & McIntyre, T. M. Ceramide generation in situ alters leukocyte cytoskeletal organization and beta 2-integrin function and causes complete degranulation. *J. Biol. Chem.* **277**, 4285–4293 (2002).
426. Hou, H. H. *et al.* Elastase induced lung epithelial cell apoptosis and emphysema through placenta growth factor. *Cell Death Dis.* **4**, e793 (2013).
427. Suzuki, K. *et al.* Impaired Toll-like Receptor 9 Expression in Alveolar Macrophages with No Sensitivity to CpG DNA. *Am. J. Respir. Crit. Care Med.* **171**, 707–713 (2005).
428. Xu, R., Li, Q., Zhou, X., Perelman, J. M. & Kolosov, V. P. Annexin II mediates the neutrophil elastase-stimulated exocytosis of mucin 5ac. *Mol. Med. Rep.* **9**, 299–304 (2014).
429. Smallman, L. A., Hill, S. L. & Stockley, R. A. Reduction of ciliary beat frequency in vitro by sputum from patients with bronchiectasis: a serine proteinase effect. *Thorax* **39**, 663–667 (1984).

430. Lukinskiene, L. *et al.* Antimicrobial activity of PLUNC protects against *Pseudomonas aeruginosa* infection. *J. Immunol. Baltim. Md 1950* **187**, 382–390 (2011).
431. De Vries, S. P. W., Eleveld, M. J., Hermans, P. W. M. & Bootsma, H. J. Characterization of the molecular interplay between *Moraxella catarrhalis* and human respiratory tract epithelial cells. *PloS One* **8**, e72193 (2013).
432. Li, Z. *et al.* Oxidized {alpha}1-antitrypsin stimulates the release of monocyte chemotactic protein-1 from lung epithelial cells: potential role in emphysema. *Am. J. Physiol. Lung Cell. Mol. Physiol.* **297**, L388–400 (2009).
433. Ho, W.-H. *et al.* Effects of areca nut extract on the apoptosis pathways in human neutrophils. *J. Periodontal Res.* **45**, 412–420 (2010).
434. Parlato, M. *et al.* CD24-triggered caspase-dependent apoptosis via mitochondrial membrane depolarization and reactive oxygen species production of human neutrophils is impaired in sepsis. *J. Immunol. Baltim. Md 1950* **192**, 2449–2459 (2014).
435. Nakajoh, M. *et al.* Retinoic acid inhibits elastase-induced injury in human lung epithelial cell lines. *Am. J. Respir. Cell Mol. Biol.* **28**, 296–304 (2003).
436. Greene, C. M. & McElvaney, N. G. Proteases and antiproteases in chronic neutrophilic lung disease - relevance to drug discovery. *Br. J. Pharmacol.* **158**, 1048–1058 (2009).
437. Stone, P. J. *et al.* Alpha 1-protease inhibitor moderates human neutrophil elastase-induced emphysema and secretory cell metaplasia in hamsters. *Eur. Respir. J.* **3**, 673–678 (1990).
438. Patel, I. S. *et al.* Relationship between bacterial colonisation and the frequency, character, and severity of COPD exacerbations. *Thorax* **57**, 759–764 (2002).
439. Murphy, T. F., Brauer, A. L., Schiffmacher, A. T. & Sethi, S. Persistent colonization by *Haemophilus influenzae* in chronic obstructive pulmonary disease. *Am. J. Respir. Crit. Care Med.* **170**, 266–272 (2004).
440. Parameswaran, G. I., Wrona, C. T., Murphy, T. F. & Sethi, S. *Moraxella catarrhalis* acquisition, airway inflammation and protease-antiprotease balance in chronic obstructive pulmonary disease. *BMC Infect. Dis.* **9**, 178 (2009).

441. Wilson, R., Dowling, R. B. & Jackson, A. D. The biology of bacterial colonization and invasion of the respiratory mucosa. *Eur. Respir. J.* **9**, 1523–1530 (1996).
442. Prescott, E., Lange, P. & Vestbo, J. Chronic mucus hypersecretion in COPD and death from pulmonary infection. *Eur. Respir. J.* **8**, 1333–1338 (1995).
443. Zariwala, M. A., Knowles, M. R. & Omran, H. Genetic defects in ciliary structure and function. *Annu. Rev. Physiol.* **69**, 423–450 (2007).
444. Fowler, C. J. *et al.* Abnormal nasal nitric oxide production, ciliary beat frequency, and Toll-like receptor response in pulmonary nontuberculous mycobacterial disease epithelium. *Am. J. Respir. Crit. Care Med.* **187**, 1374–1381 (2013).
445. Dvorak, A., Tilley, A. E., Shaykhiev, R., Wang, R. & Crystal, R. G. Do airway epithelium air-liquid cultures represent the in vivo airway epithelium transcriptome? *Am. J. Respir. Cell Mol. Biol.* **44**, 465–473 (2011).
446. Davis, E. E., Brueckner, M. & Katsanis, N. The emerging complexity of the vertebrate cilium: new functional roles for an ancient organelle. *Dev. Cell* **11**, 9–19 (2006).
447. Venaille, T. J., Ryan, G. & Robinson, B. W. Epithelial cell damage is induced by neutrophil-derived, not pseudomonas-derived, proteases in cystic fibrosis sputum. *Respir. Med.* **92**, 233–240 (1998).
448. Zhu, Y. *et al.* Collaborative interactions between neutrophil elastase and metalloproteinases in extracellular matrix degradation in three-dimensional collagen gels. *Respir. Res.* **2**, 300–305 (2001).
449. Salathe, M. Regulation of mammalian ciliary beating. *Annu. Rev. Physiol.* **69**, 401–422 (2007).
450. Clary-Meinesz, C. F., Cosson, J., Huitorel, P. & Blaive, B. Temperature effect on the ciliary beat frequency of human nasal and tracheal ciliated cells. *Biol. Cell Auspices Eur. Cell Biol. Organ.* **76**, 335–338 (1992).
451. Thomas, B. *et al.* Ciliary dysfunction and ultrastructural abnormalities are features of severe asthma. *J. Allergy Clin. Immunol.* **126**, 722–729.e2 (2010).
452. Vermeer, P. D. *et al.* MMP9 modulates tight junction integrity and cell viability in human airway epithelia. *Am. J. Physiol. Lung Cell. Mol. Physiol.* **296**, L751–762 (2009).

453. Wang, H., Zheng, Y. & He, S. Induction of release and up-regulated gene expression of interleukin (IL)-8 in A549 cells by serine proteinases. *BMC Cell Biol.* **7**, 22 (2006).
454. Nombela-Arrieta, C. *et al.* Quantitative imaging of haematopoietic stem and progenitor cell localization and hypoxic status in the bone marrow microenvironment. *Nat. Cell Biol.* **15**, 533–543 (2013).
455. L.M. Porter. Regulation of granulocyte apoptosis by hypoxia and glucocorticoids. (Cambridge, 2014).
456. Kaluz, S., Kaluzová, M. & Stanbridge, E. J. Regulation of gene expression by hypoxia: integration of the HIF-transduced hypoxic signal at the hypoxia-responsive element. *Clin. Chim. Acta Int. J. Clin. Chem.* **395**, 6–13 (2008).
457. Carmeliet, P. *et al.* Role of HIF-1alpha in hypoxia-mediated apoptosis, cell proliferation and tumour angiogenesis. *Nature* **394**, 485–490 (1998).
458. Tasiemski, A. *et al.* Presence of chromogranin-derived antimicrobial peptides in plasma during coronary artery bypass surgery and evidence of an immune origin of these peptides. *Blood* **100**, 553–559 (2002).
459. Wang, J. P. U-73122, an aminosteroid phospholipase C inhibitor, may also block Ca²⁺ influx through phospholipase C-independent mechanism in neutrophil activation. *Naunyn. Schmiedebergs Arch. Pharmacol.* **353**, 599–605 (1996).
460. Jackon, J. K., Tudan, C. & Burt, H. M. The involvement of phospholipase C in crystal induced human neutrophil activation. *J. Rheumatol.* **27**, 2877–2885 (2000).
461. Condliffe, A. M. *et al.* Sequential activation of class IB and class IA PI3K is important for the primed respiratory burst of human but not murine neutrophils. *Blood* **106**, 1432–1440 (2005).
462. Randis, T. M., Puri, K. D., Zhou, H. & Diacovo, T. G. Role of PI3Kdelta and PI3Kgamma in inflammatory arthritis and tissue localization of neutrophils. *Eur. J. Immunol.* **38**, 1215–1224 (2008).
463. Hirsch, E. *et al.* Central role for G protein-coupled phosphoinositide 3-kinase gamma in inflammation. *Science* **287**, 1049–1053 (2000).

464. J.K. Juss *et al.* Functional Redundancy of Class I Phosphoinositide 3-kinase (PI3K) Isoforms in Signaling Growth Factor-Mediated Human Neutrophil Survival. *PLoS One Press*
465. Cowburn, A. S., Cadwallader, K. A., Reed, B. J., Farahi, N. & Chilvers, E. R. Role of PI3-kinase-dependent Bad phosphorylation and altered transcription in cytokine-mediated neutrophil survival. *Blood* **100**, 2607–2616 (2002).
466. Sai, J., Raman, D., Liu, Y., Wikswo, J. & Richmond, A. Parallel Phosphatidylinositol 3-Kinase (PI3K)-Dependent and Src-Dependent Pathways Lead to CXCL8-Mediated Rac2 Activation and Chemotaxis. *J. Biol. Chem.* **283**, 26538–26547 (2008).
467. Lee, S.-M. *et al.* Hypoxia confers protection against apoptosis via PI3K/Akt and ERK pathways in lung cancer cells. *Cancer Lett.* **242**, 231–238 (2006).
468. Fan, C., Li, Q., Ross, D. & Engelhardt, J. F. Tyrosine Phosphorylation of I κ B α Activates NF κ B Through a Redox-Regulated and C-Src-Dependent Mechanism Following Hypoxia/Reoxygenation. *J. Biol. Chem.* **278**, 2072–2080 (2003).
469. Kim, K. S., Rajagopal, V., Gonsalves, C., Johnson, C. & Kalra, V. K. A Novel Role of Hypoxia-Inducible Factor in Cobalt Chloride- and Hypoxia-Mediated Expression of IL-8 Chemokine in Human Endothelial Cells. *J. Immunol.* **177**, 7211–7224 (2006).
470. Hwang, K. Y. *et al.* Baicalein suppresses hypoxia-induced HIF-1 α protein accumulation and activation through inhibition of reactive oxygen species and PI 3-kinase/Akt pathway in BV2 murine microglial cells. *Neurosci. Lett.* **444**, 264–269 (2008).
471. Mazure, N. M., Chen, E. Y., Laderoute, K. R. & Giaccia, A. J. Induction of vascular endothelial growth factor by hypoxia is modulated by a phosphatidylinositol 3-kinase/Akt signaling pathway in Ha-ras-transformed cells through a hypoxia inducible factor-1 transcriptional element. *Blood* **90**, 3322–3331 (1997).
472. Alvarez-Tejado, M. *et al.* Hypoxia induces the activation of the phosphatidylinositol 3-kinase/Akt cell survival pathway in PC12 cells: protective role in apoptosis. *J. Biol. Chem.* **276**, 22368–22374 (2001).
473. Alvarez-Tejado, M. *et al.* Lack of evidence for the involvement of the phosphoinositide 3-kinase/Akt pathway in the activation of hypoxia-inducible factors by low oxygen tension. *J. Biol. Chem.* **277**, 13508–13517 (2002).

474. Mottet, D. *et al.* Regulation of hypoxia-inducible factor-1alpha protein level during hypoxic conditions by the phosphatidylinositol 3-kinase/Akt/glycogen synthase kinase 3beta pathway in HepG2 cells. *J. Biol. Chem.* **278**, 31277–31285 (2003).
475. Kilic-Eren, M., Boylu, T. & Tabor, V. Targeting PI3K/Akt represses Hypoxia inducible factor-1 α activation and sensitizes Rhabdomyosarcoma and Ewing's sarcoma cells for apoptosis. *Cancer Cell Int.* **13**, 36 (2013).
476. Yadav, V. R. *et al.* Important role of PLC- γ 1 in hypoxic increase in intracellular calcium in pulmonary arterial smooth muscle cells. *Am. J. Physiol. Lung Cell. Mol. Physiol.* **304**, L143–151 (2013).
477. Geijsen, N. *et al.* Regulation of p21rac activation in human neutrophils. *Blood* **94**, 1121–1130 (1999).
478. Dooley, J. L. *et al.* Regulation of inflammation by Rac2 in immune complex-mediated acute lung injury. *Am. J. Physiol. - Lung Cell. Mol. Physiol.* **297**, L1091–L1102 (2009).
479. Yoon, S.-O., Shin, S. & Mercurio, A. M. Hypoxia stimulates carcinoma invasion by stabilizing microtubules and promoting the Rab11 trafficking of the α 6 β 4 integrin. *Cancer Res.* **65**, 2761–2769 (2005).
480. Hackenbeck, T. *et al.* The GTPase RAB20 is a HIF target with mitochondrial localization mediating apoptosis in hypoxia. *Biochim. Biophys. Acta* **1813**, 1–13 (2011).
481. Arsenault, D., Lucien, F. & Dubois, C. M. Hypoxia enhances cancer cell invasion through relocalization of the proprotein convertase furin from the trans-Golgi network to the cell surface. *J. Cell. Physiol.* **227**, 789–800 (2012).
482. Koelink, P. J. *et al.* Collagen degradation and neutrophilic infiltration: a vicious circle in inflammatory bowel disease. *Gut* **63**, 578–587 (2014).
483. Schofield, Z. V., Woodruff, T. M., Halai, R., Wu, M. C.-L. & Cooper, M. A. Neutrophils--a key component of ischemia-reperfusion injury. *Shock Augusta Ga* **40**, 463–470 (2013).
484. Martin, T. R., Raghu, G., Maunder, R. J. & Springmeyer, S. C. The effects of chronic bronchitis and chronic air-flow obstruction on lung cell populations recovered by bronchoalveolar lavage. *Am. Rev. Respir. Dis.* **132**, 254–260 (1985).

485. Baldi, S. *et al.* C-reactive protein correlates with tissue oxygen availability in patients with stable COPD. *Int. J. Chron. Obstruct. Pulmon. Dis.* **3**, 745–751 (2008).
486. Sabit, R., Thomas, P., Shale, D. J., Collins, P. & Linnane, S. J. The effects of hypoxia on markers of coagulation and systemic inflammation in patients with COPD. *Chest* **138**, 47–51 (2010).
487. Haslett, C., Guthrie, L. A., Kopaniak, M. M., Johnston, R. B., Jr & Henson, P. M. Modulation of multiple neutrophil functions by preparative methods or trace concentrations of bacterial lipopolysaccharide. *Am. J. Pathol.* **119**, 101–110 (1985).
488. Solomkin, J. S., Tindal, C. J., Cave, C. M. & Zemlan, F. Regulation of TNF-alpha receptor expression on human neutrophils by various cell activating factors. *J. Surg. Res.* **56**, 261–266 (1994).
489. Hitomi, Y. *et al.* Intermittent hypobaric hypoxia increases the ability of neutrophils to generate superoxide anion in humans. *Clin. Exp. Pharmacol. Physiol.* **30**, 659–664 (2003).
490. Schulz, R. *et al.* Enhanced release of superoxide from polymorphonuclear neutrophils in obstructive sleep apnea. Impact of continuous positive airway pressure therapy. *Am. J. Respir. Crit. Care Med.* **162**, 566–570 (2000).
491. Schmitz, K., Jennewein, M., Pohlemann, T., Seekamp, A. & Oberringer, M. Reoxygenation attenuates the adhesion of neutrophils to microvascular endothelial cells. *Angiology* **62**, 155–162 (2011).
492. Welch, H. C. E., Coadwell, W. J., Stephens, L. R. & Hawkins, P. T. Phosphoinositide 3-kinase-dependent activation of Rac. *FEBS Lett.* **546**, 93–97 (2003).
493. Akasaki, T., Koga, H. & Sumimoto, H. Phosphoinositide 3-kinase-dependent and -independent activation of the small GTPase Rac2 in human neutrophils. *J. Biol. Chem.* **274**, 18055–18059 (1999).
494. Weidemann, A. *et al.* HIF-1 α activation results in actin cytoskeleton reorganization and modulation of Rac-1 signaling in endothelial cells. *Cell Commun. Signal. CCS* **11**, 80 (2013).
495. Condliffe, A. M. *et al.* RhoG regulates the neutrophil NADPH oxidase. *J. Immunol. Baltim. Md 1950* **176**, 5314–5320 (2006).

496. Barnes, P. J. New therapies for chronic obstructive pulmonary disease. *Med. Princ. Pract. Int. J. Kuwait Univ. Health Sci. Cent.* **19**, 330–338 (2010).
497. Long term domiciliary oxygen therapy in chronic hypoxic cor pulmonale complicating chronic bronchitis and emphysema. Report of the Medical Research Council Working Party. *Lancet* **1**, 681–686 (1981).
498. Dirksen, A. *et al.* A randomized clinical trial of alpha(1)-antitrypsin augmentation therapy. *Am. J. Respir. Crit. Care Med.* **160**, 1468–1472 (1999).
499. Survival and FEV1 decline in individuals with severe deficiency of alpha1-antitrypsin. The Alpha-1-Antitrypsin Deficiency Registry Study Group. *Am. J. Respir. Crit. Care Med.* **158**, 49–59 (1998).
500. Dirksen, A. *et al.* Exploring the role of CT densitometry: a randomised study of augmentation therapy in alpha1-antitrypsin deficiency. *Eur. Respir. J.* **33**, 1345–1353 (2009).
501. Barros-Tizón, J. C., Torres, M. L., Blanco, I., Martínez, M. T. & Investigators of the rEXA study group. Reduction of severe exacerbations and hospitalization-derived costs in alpha-1-antitrypsin-deficient patients treated with alpha-1-antitrypsin augmentation therapy. *Ther. Adv. Respir. Dis.* **6**, 67–78 (2012).
502. Ma, S. *et al.* Alpha-1 antitrypsin augmentation therapy and biomarkers of elastin degradation. *COPD* **10**, 473–481 (2013).
503. Vogelmeier, C., Aquino, T. O., O'Brien, C. D., Perrett, J. & Gunawardena, K. A. A randomised, placebo-controlled, dose-finding study of AZD9668, an oral inhibitor of neutrophil elastase, in patients with chronic obstructive pulmonary disease treated with tiotropium. *COPD* **9**, 111–120 (2012).
504. Kuna, P., Jenkins, M., O'Brien, C. D. & Fahy, W. A. AZD9668, a neutrophil elastase inhibitor, plus ongoing budesonide/formoterol in patients with COPD. *Respir. Med.* **106**, 531–539 (2012).
505. Okayama, N. *et al.* Clinical effects of a neutrophil elastase inhibitor, sivelestat, in patients with acute respiratory distress syndrome. *J. Anesth.* **20**, 6–10 (2006).
506. Lupia, E. *et al.* Ablation of phosphoinositide 3-kinase-gamma reduces the severity of acute pancreatitis. *Am. J. Pathol.* **165**, 2003–2011 (2004).

507. Ong, E., Gao, X.-P., Predescu, D., Broman, M. & Malik, A. B. Role of phosphatidylinositol 3-kinase-gamma in mediating lung neutrophil sequestration and vascular injury induced by *E. coli* sepsis. *Am. J. Physiol. Lung Cell. Mol. Physiol.* **289**, L1094–1103 (2005).
508. Van Dop, W. A. *et al.* The absence of functional PI3Kgamma prevents leukocyte recruitment and ameliorates DSS-induced colitis in mice. *Immunol. Lett.* **131**, 33–39 (2010).
509. Ban, K. *et al.* Phosphatidylinositol 3-kinase gamma is a critical mediator of myocardial ischemic and adenosine-mediated preconditioning. *Circ. Res.* **103**, 643–653 (2008).
510. Jin, L., He, Z. & Peng, Z. [Protection of noninvasive limb ischemic preconditioning on myocardium in patients undergoing heart valve surgery under cardiopulmonary bypass]. *Zhong Nan Da Xue Xue Bao Yi Xue Ban* **36**, 768–775 (2011).
511. Mukhopadhyay, S., Xu, F. & Sehgal, P. B. Aberrant cytoplasmic sequestration of eNOS in endothelial cells after monocrotaline, hypoxia, and senescence: live-cell caveolar and cytoplasmic NO imaging. *Am. J. Physiol. Heart Circ. Physiol.* **292**, H1373–1389 (2007).
512. Valdez, S. R. *et al.* Acute sublethal global hypoxia induces transient increase of GAP-43 immunoreactivity in the striatum of neonatal rats. *Synap. N. Y. N* **61**, 124–137 (2007).
513. Noguera, A. *et al.* Enhanced neutrophil response in chronic obstructive pulmonary disease. *Thorax* **56**, 432–437 (2001).
514. Carter, R. I., Ungurs, M. J., Mumford, R. A. & Stockley, R. A. A α -Val360: A Marker of Neutrophil Elastase and COPD Disease Activity. *Eur. Respir. J. Off. J. Eur. Soc. Clin. Respir. Physiol.* (2012). doi:10.1183/09031936.00197411
515. Maclay, J. D. & MacNee, W. Cardiovascular disease in COPD: mechanisms. *Chest* **143**, 798–807 (2013).
516. Hoenderdos, K. & Condliffe, A. The neutrophil in chronic obstructive pulmonary disease. *Am. J. Respir. Cell Mol. Biol.* **48**, 531–539 (2013).